Planetary landscapes and the role of volatiles in their making

Susan J Conway

Habilitation à Diriger des Recherches

de Nantes Université

Laboratoire de Planétologie et Géosciences

par Susan J. Conway

Planetary landscapes and the role of volatiles in their making – Paysages planétaires et le rôle des composants volatils dans leur formation

présentée et soutenue publiquement

lundi 6 mars 2023 à 14 heures

devant le jury composé de :

Monsieur Nicolas MANGOLD, Directeur de recherche CNRS, Nantes Université - Président du jury

Madame Cathy QUANTIN-NATAF, Professeur, Université de Lyon Claude Bernard - Rapporteur

Madame Mary BOURKE, Associate professor, Trinity College Dublin - Rapporteur

Monsieur Sylvain BOULEY, Professeur, Université de Paris - Rapporteur

Monsieur Sébastien RODRIGUEZ, Maître de conférences HDR, Université Paris Cité - Examinateur

Contents

Abstract

This thesis concerns the study of planetary landscapes with the objective of understanding the role of volatiles in sculpting these landscapes which falls under the broad theme of planetary geomorphology. A general introduction to planetary geomorphology is followed by a summary of the research topics of the candidate since their PhD thesis. The primary focus of this research is on recent martian surface processes, followed by periglacial terrains on Earth and the evolution of the surface of Mercury. Two science questions emerge from this work. 1) What is the role of volatile loss in shaping planetary landscapes and how is that loss triggered/modulated? This thesis reveals that sublimation is an important process on modern Mars, yet the limits of this process are poorly understood. Volatile loss could also be an important contributor to slope processes on other bodies but has been largely overlooked. Equally melting ground ice can lead to catastrophic mass movements in places on Earth where permafrost was not suspected. 2) What are the limits of planetary comparison and in what contexts does insight prevail over misunderstanding? This thesis demonstrates that comparative planetology has been important in providing insight into surface processes on Mercury and on Mars yet studying gullies on Mars has revealed that equifinality can be problematic. Given this context how can planetary bodies be used to learn more about surface processes on Earth? The end of the thesis details the candidate's plans for future work to address these science questions, which entail simulations in the laboratory, analysis of orbital image and topographic data and fieldwork.

Résumé français

Cette thèse concerne l'étude des paysages planétaires avec l'objectif de comprendre le rôle des volatiles dans la formation de ces paysages - ce qui s'inscrit dans le thème général de la géomorphologie planétaire. Dans ce document, une introduction générale à la géomorphologie planétaire est suivie d'un résumé des sujets de recherche du candidat depuis son doctorat. Ils portent principalement sur les processus récents de la surface martienne, puis sur les terrains périglaciaires sur Terre et l'évolution de la surface de Mercure. Deux questions scientifiques émergent de ce travail. 1) Quel est le rôle de la perte des substances volatiles dans le façonnement des paysages planétaires ? Cette thèse révèle que la sublimation est un processus important sur Mars. La perte de substances volatiles pourrait contribuer de manière importante aux processus sur d'autres corps. De même, la fonte du pergélisol peut entraîner des mouvements de masse catastrophiques sur Terre où l'on ne soupçonnait pas la présence de pergélisol. 2) Quelles sont les limites de la planétologie comparée ? Cette thèse démontre que la planétologie comparée a joué un rôle important dans la compréhension des processus de surface sur Mercure et sur Mars, mais l'étude des ravines sur Mars a révélé que l'équifinalité peut être problématique. La fin de la thèse détaille les plans du candidat pour les travaux futurs visant à répondre à ces questions scientifiques, qui comprennent des simulations en laboratoire, l'analyse d'images orbitales et de données topographiques, et des travaux sur le terrain.

1 Introduction

This HDR thesis provides a summary of the research I have performed since starting my doctorate, which seeks to understand the influence of volatile substances, such as water and carbon dioxide, on landscape development on the terrestrial planets. It ties together the separate strands of research into a single thematic narrative, which aims to highlight my personal scientific motivation and the resulting driving research questions. The manuscript also provided me with an opportunity to highlight the aspects of my research I see as future research directions.

Water plays a vital role in shaping the surfaces of the terrestrial planets, notably Mars and the Earth. All three forms of water are found on Earth and it is one of the most important volatiles involved in geomorphic processes: physical, chemical and biological. However, as we move away from our planet, water's action becomes more subtle. The surface temperature and pressure conditions of other planetary bodies mean that other volatile species start to do more geomorphic work. For example, Mars' surface has an active carbon-dioxide (CO_2) condensation and sublimation cycle, which create landforms unique to this planet within the solar system (e.g., Thomas et al., 2011).

Knowledge of the water budget of a planetary body has implications for the composition and dynamics of the early Solar System and is a critical component in determining zones of habitability. Water changes the rheology of planetary mantles and is thought to be a pre-requisite for plate-tectonics (Albarede, 2009). The origin of water in the inner Solar System is poorly understood and the distribution of water in the interior, crust and atmosphere of a planetary body provide clues as to whether the water was incorporated during accretion and/or brought later by icy planetesimals from the outer asteroid belt and beyond (Albarede, 2009; Sarafian et al., 2014). A body's geological history records the evolution of its water-budget over time and the surface geomorphology forms part of that record. By studying the surface geomorphology of planetary bodies I aim to investigate their water budgets and more generally volatile budgets.

The recognition of process from the resulting shape of the landscape is the central tenant of observational geomorphology. The surfaces of the terrestrial planets are shaped by forces from within (e.g., tectonics and volcanism), from without (e.g., impacts) and by their own atmosphere (i.e., climate). Individual processes, such as water erosion, or micro-impacts, should leave characteristic topographic fingerprints and the balance of different processes can be untwined once an understanding these "fingerprints" is obtained. The application of geomorphology to the terrestrial planets is becoming increasingly relevant due to the quality and quantity of data from existing and upcoming missions. Obvious links have already been made - volcanoes are caused by volcanism and impact craters by impacts - but I intend to use a geomorphic approach to tease out the individual processes connected with volatile species, which are often embedded in more subtle signals. My research focuses on the exploitation of topographic data in all its forms: including detailed metre-scale study, which has only become possible in recent decades (even on Earth), integrated with a statistical approach using regional-scale medium- to low-resolution data (which is becoming of better quality).

The majority of my research focuses on Mars where there is abundant data and a large range of surface processes, however I also recognise the value of a broad outlook and therefore devote part of my research time to other bodies in the Solar System. Firstly and foremost, the Earth, where phase change of water ice to liquid in the context of degrading permafrost is becoming a pressing issue for evaluating hazard in a changing climate. Secondly, I have considered the influence of water and other volatiles on the surface geomorphology of airless rocky planets, moons and asteroids. It is only within the last 20 years that we have suspected that such volatile species were present near the surface of

the Moon and Mercury. Water-ice was recently found to be present inside the bowls of permanently shadowed impact craters on these two bodies and is thought to originate from exogenic (possibly cometary) delivery of water to their surfaces (e.g., Feldman et al., 1998; Harmon et al., 2001; Lawrence et al., 2013; Spudis et al., 2013). More subtle evidence for volatiles has been reported on the asteroid Vesta (Denevi et al., 2012).

The thesis is made up of a mixture of published and unpublished material. It begins in Chapter 2 with a general introduction to planetary geomorphology, which I wrote for volume five of the History of the Study of Landforms - an update for the key reference work published by the Geological Society of London (Conway, 2022). The heart of the thesis is found in Chapter 3, a modified version of a Chapter published in “Martian Enigmas” (brown text was added to provide additional details for this HDR), which concerns the action of water and CO_2 on sculpting the martian surface (Conway and Stillman, 2021). This chapter is the most substantive of the thesis as it represents the bulk of my published work. Chapter 4 discusses the role of ice to water phase transition in mass movements on Earth, encapsulating work on debris flows during my PhD thesis and on landslides in ground ice - a 5 year project supported by the French National Funding Agency (ANR). Chapter 5 summarises my work on landscapes on Mercury, which has been driven by co-supervision of PhD students at the Open University with Prof. David Rothery. Finally Chapter 6 provides a synthesis, with a summary of science questions emerging from my work to date and future work envisioned on Mars, the Earth, Mercury and other bodies.

2 Planetary Geomorphology

2.1 Abstract

With the advent of the space age, planetary geomorphology has become a stand-alone discipline. This contribution provides a summary of the different processes that have been identified to form landscapes and landforms on planetary bodies in our Solar System, including rocky planets, icy planets and moons, dwarf planets, comets and asteroids. I highlight the insights these landforms have provided into the workings of these bodies and how what has been learnt in space has often taught us new lessons about the Earth. Finally, I conclude that despite the limitations imposed by remote sensing, planetary geomorphology has a bright future in planning future missions to explore our Solar System as well as understanding the data that will be returned.

2.2 Introduction

This chapter is rather different from the rest of those in this book. First it is the only one that takes us away from our own planet. Secondly, it deals with a topic that was not covered, for obvious historical reasons, in the four previous volumes of the History of the Study of Landforms. Thirdly, it does not restrict itself to the temporal span of 1965-2000 which is the focus of this book. It reviews progress in the study of planetary geomorphology up until the present and shows the progress that has been made since the first successful missions were carried out from the mid-1960s onwards - It was in 1965 that Mariner 4 brought us back the first close-up photographs of another planet: Mars.

Planetary geomorphology is a branch of planetary science, which was born in the second half of the Twentieth Century from astronomy and has foundations in geology, meteorology, chemistry and biology. The rise of planetary geomorphology as a discipline goes hand in hand with an increasing use of satellite remote sensing data to study our own planet and the associated development of techniques to exploit these data.

The first remote sensing image of the Earth taken from space was in 1946. Only twenty years later, the NASA Mariner missions marked the first of a flurry of space missions that have only increased in number as the century progressed, bringing us images, topography and other data from all the major bodies in the Solar System and more. The objective of this chapter is not to provide a history of space exploration, which is done elsewhere (e.g., Burns, 2010), but to highlight the main discoveries and associated advances in the understanding of the processes and landforms of other worlds spanning the era of robotic and human exploration of space.

In order for landscapes and landforms to be studied the surface of the body has to be resolved at a sufficient resolution (in the author's opinion at least hundreds of metres per pixel). Hence to date, planetary geomorphology is restricted to solid bodies in our Solar System and relies on space probes sent to or near to the body of interest. We therefore have geomorphological information on (listed in approximate increasing solar distance):

- Mercury
- Venus*
- The Moon*
- Mars* and its moons Phobos and Deimos
- Dwarf planet Ceres in asteroid belt
- Asteroids (Bennu*, Ryugu *, Itokawa*, Vesta, Ida, Eros, Mathilde, Gaspra, Šteins, Toutatis)
- The satellites of Jupiter (Io, Europa, Ganymede, Callisto)

- The satellites of Saturn (Pan, Daphnis, Atlas, Prometheus, Pandora, Epimetheus, Janus, Mimas, Enceladus, Tethys, Telesto, Calypso, Dione, Helene, Rhea, Titan*,Hyperion, Iapetus, Phoebe)
- The satellites of Neptune (Proteus, Triton)
- The satellites of Uranus (Miranda, Ariel, Umbriel, Titania, Oberon)
- Dwarf planet Pluto and its moon Charon
- Trans-Neptunian Kuiper belt object "Arrokoth"
- Comets (Tempel 1*, Churyumov–Gerasimenko 67P*, Borrelly, Wild 2, Hartley 2)

(A * symbol indicates a landed mission)

This exploration has revealed a suite of familiar and unfamiliar processes and landforms compared to those found on Earth. This review will consider first processes and landforms already known from studying the Earth before the space exploration era and then move towards those processes and landforms less studied before Planetary Geomorphology became a distinct subdiscipline. Each section will highlight lesser-known landforms and knowledge gained from studying other worlds. For an exhaustive list of the landforms present on other worlds I refer the reader to the Encyclopaedia of Planetary Landforms (Hargitai and Kereszturi, 2015). For brevity only one or two references are cited per topic, with the intent that an interested reader can use them to access to the wider relevant literature on each topic.

2.3 Planetary aeolian landforms and processes

All bodies with an atmosphere have wind and aeolian landforms have been reported from: Mars, Venus, Titan and Pluto (Lorenz and Zimbelman, 2014; Telfer et al., 2018), as well as of course Earth. For a full review of planetary aeolian landforms and associated processes I refer interested readers to Bourke et al. (2019). The observation of aeolian bedforms including ripples, megaripples and dunes on other planetary bodies (Figure 2.1a,b) has been very important for understanding the basic physics underlying aeolian processes, because these planetary bodies provide different atmospheric densities and particle densities spanning a wider range of parameter space than accessible on Earth at the landscape-scale (Kok et al., 2012; Lapôtre et al., 2020). Martian aeolian bedforms have a wider diversity of form and size than their terrestrial equivalents (e.g., Bourke, 2010; Sullivan et al., 2020), which has led to researchers to question whether the basic physics underlying their formation are indeed the same. A prime example is the landform called a Transverse Aeolian Ridge (Figure 2.1c) which at < 1 m tall are thought to represent megaripples whose morphology is determined by grainsize sorting rather than reptation and creep and whose origin remains unknown at larger amplitudes (Zimbelman and Foroutan, 2020). Another example comes from radar images of longitudinal parallel and occasionally bifurcating ridges have been interpreted to be longitudinal dunes (Figure 2.1d) on Venus and Titan. Such dunes on Earth indicate strongly unimodal winds yet the "physics of saltation on Titan and Venus is fundamentally different from that on Earth and Mars […] dominated by direct fluid lifting" (Kok et al., 2012).

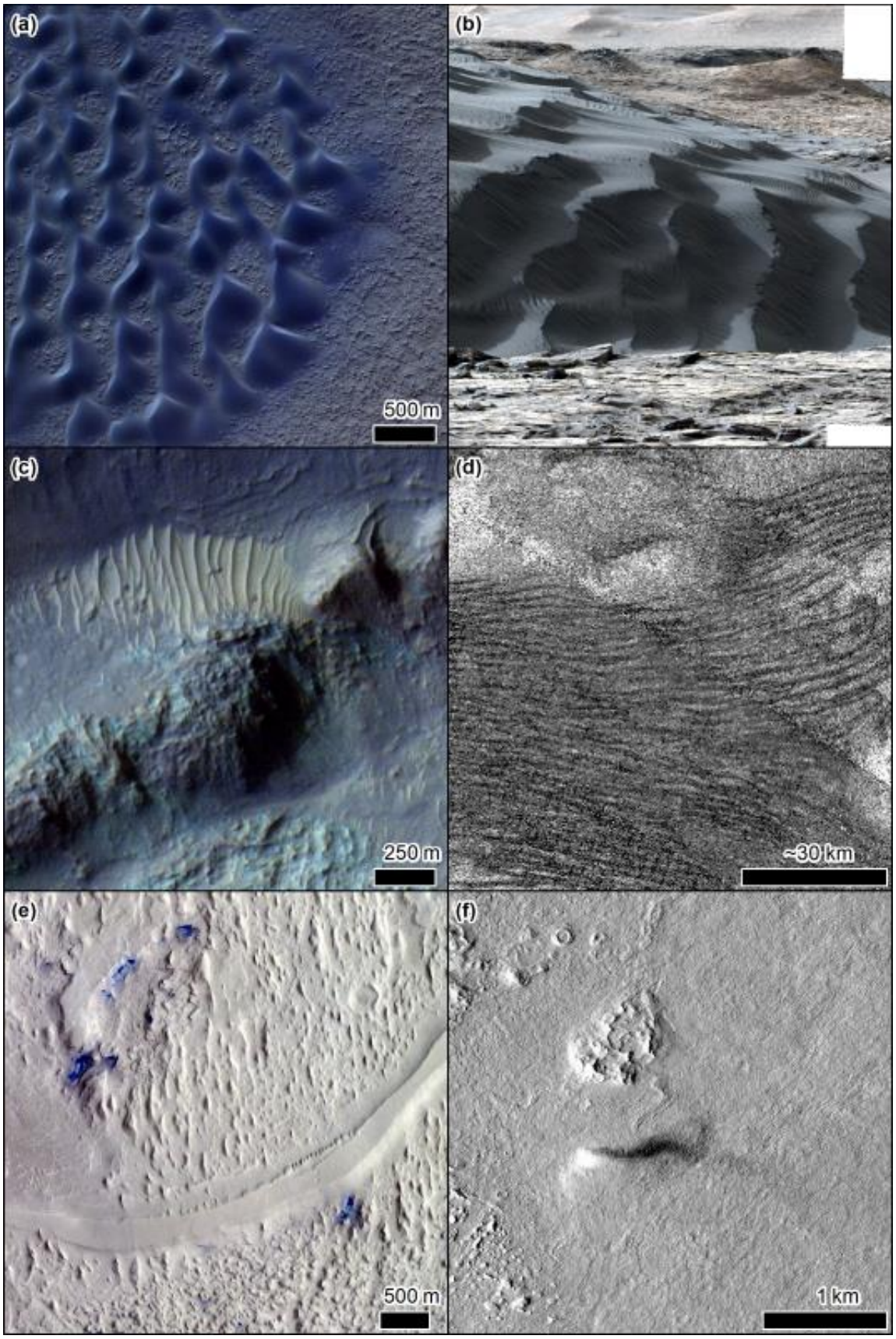

Figure 2.1: Aeolian planetary landforms. a) Dark Dunefield on the floor of a 35-km-diameter crater in Aonia Terra on Mars, CaSSIS image MY36_015406_006_0, credit ESA/Roscosmos/Unibe. b) Large ripples (spacing 2-2.5 m) superposed by smaller impact ripples on the secondary lee slope of Namib

Dune in Gale Crater on Mars. Mosaic of MSL Mastcam images from sol 1192 (Ewing et al., 2017), credit NASA/JPL-Caltech/Malin Space Science Systems. c) Transverse aeolian ridges (TARs) on the floor of a 17-km-diameter crater in Margaritifer Terra on Mars, CaSSIS image MY36_015406_006_0, credit ESA/Roscosmos/Unibe. (d) Cassini Synthetic Aperture radar image of the Shangri-La Sand Sea on Titan (PIA20710). Image credit NASA/JPL-Caltech/ASI. (e) Yardangs and an inverted channel in Aeolis Mensae region of Mars, CaSSIS image MY34_005683_188_2, credit ESA/Roscosmos/Unibe. (f) Dust Devil in Amazonis Planitia on Mars CTX image D02_028082_2155. Credit NASA/JPL/MSSS. North is up in all images apart from (b).

Hence, planetary observations have also revealed aeolian processes that are only experienced on extra-terrestrial environments resulting in potentially unique landforms. These include bedforms created by ablation (in the form of sublimation of ices – see also Section 2.11) rather than particle movements (Bordiec et al., 2020), which have so far only been studied in detail on the Antarctic ice cap (van den Broeke and Bintanja, 1995) or in ice caves (Obleitner and Spötl, 2011). Another surprising result was the discovery of dunes on the comet 67P Churyumov–Gerasimenko, which has no atmosphere (Jia et al., 2017; Thomas et al., 2015). These “dunes” are thought to form at times when the comet is close to the sun causing vigorous outgassing and strong winds being setup between sunlit and shadowed areas on the surface (Jia et al., 2017). Scouring “upwind” and build-up of sediment on the “downwind” of boulders supports this hypothesis (Mottola et al., 2015).

Abrasion by particles lofted by the wind results in erosional aeolian landforms, such as yardangs and the landscape-scale (Figure 2.1e) and ventifacts at the “field” scale (e.g., Wells and Zimbelman, 1997) – the orientation of these landforms is used as an important indicator of prevailing wind directions. Yardangs have been studied in most detail on Mars, but also have been suggested on Venus (Greeley et al., 1995), Titan (Paillou et al., 2016) and as an alternative interpretation of the “dunes” on Pluto (Moore et al., 2018).. The study of yardangs on Mars drove a renaissance for their study on Earth (Goudie, 2007) where their climate significance is still debated. Ventifacts have been observed at the surface of Mars and are remarkably similar to those found on Earth (Knight, 2008; Laity and Bridges, 2009) and most modern studies of terrestrial ventifacts refer to planetary-driven research on this topic.

Wind can also drive the formation of inverted landforms, which have been of particular importance in revealing ancient fluvial processes on Mars (Davis et al., 2016; Day and Kocurek, 2016)(Section 2.3). Wind is the agent that erodes and deflates the sediments surrounding the channel(s) which are more resistant to abrasion (Figure 2.1e). This additional resistance can come about from cementation, coarser grainsizes or lava capping (e.g., R. M. E. Williams et al., 2009).

Particular to Mars are landforms related to the copious dust at its surface, which also influences the atmospheric circulation on that body (e.g., Madeleine et al., 2011). Dust via airfall is incorporated in sedimentary deposits and ice-deposition landforms (e.g. the polar caps - Kieffer, 1990; or the ice-dust latitude dependant mantle - Mustard et al., 2001). Unique to Mars are “Slope Streaks” which are landforms associated with dust motion down steep slopes (e.g., Schorghofer et al., 2007; Sullivan et al., 2001), see Section 2.7 for further details. Dust Devils are atmospheric vortices which are common on Mars (Figure 2.1f) and have been observed by every landed mission (e.g., Ferri et al., 2003; Greeley et al., 2006b; Ryan and Lucich, 1983; Thomas and Gierasch, 1985). They can also be found in deserts on Earth (Balme and Greeley, 2006), yet on Mars they often remove the dust on the surface leaving a tortuous track in their wake which is clearly visible from orbit. Much recent research on terrestrial dust devils has been driven by the desire to better understand the phenomenon on Mars (e.g., Balme et al., 2012; Reiss et al., 2010).

2.4 Planetary fluvial landforms and processes

The possibility of extraterrestrial fluvial geomorphology was first revealed by the discovery of valley networks and channel systems on the surface of Mars (Masursky, 1973) (Figure 2.2a). On Saturn's satellite Titan fluvial landforms in the form of valley networks (Carolyn C. Porco et al., 2005; Tomasko et al., 2005) are thought to be formed by flowing liquid methane eroding the 'bedrock' of ice (Perron et al., 2006) (Figure 2.2b). Together with the observation of lakes (see Section 2.4), the existence of valley networks on Titan has led to the hypothesis of a hydrocarbon-cycle driven by the decade-long seasonal cycle and atmospheric synthesis of hydrocarbons. On Venus, the river-like canali could be lava channels or carved by, another as-yet unidentified, fluid (Jones and Pickering, 2003; Kargel et al., 1994; Komatsu and Baker, 1994). Equally dendritic valleys on Pluto have been proposed to be carved by flowing liquid nitrogen (Stern et al., 2017) - the favoured alternate interpretation as glacial in origin, is described in Section 2.8.

The observation of valley networks motivated the hypothesis that Mars had a full-hydrological cycle early in its history, when its atmospheric density was higher allowing surface liquid water to be stable (Pollack et al., 1987). This valley networks are visible in a degraded (Ansan et al., 2008) or inverted (Davis et al., 2016) state on the oldest visible surfaces of Mars (Figure 2.2a). Some of these valleys have low tributary order/number and by analogy with valleys with similar morphology on Earth have been interpreted to originate via groundwater sapping (Luo and Howard, 2008), hence revealing the potential presence of aquifers. Some have also been interpreted to originate from sub-icesheet drainage (Grau Galofre et al., 2020), attesting to potentially widespread glaciation early in Mars' history (Fastook and Head, 2015). The observation of meandering channel belts on Mars brought into question the hypothesis that vegetation was a prerequisite for developing meanders early in Earth's history (Ielpi and Lapôtre, 2020).

Outflow channels on Mars – thought to represent colossal outbursts of water (Baker and Kochel, 1979) from pressurised aquifers (W. A. Marra et al., 2015) - reach hundreds of kilometres in width and thousands in length (Figure 2.2c). They are characterised by streamlined obstacles and often multiple terrace levels indicating several pulses of activity (Warner et al., 2009). The outflow channels often originate at "Chaos Terrain" which also exists on Mercury (Rodriguez et al., 2020), Europa and Pluto (Skjetne et al., 2021) (Figure 2.2d), and hence is not a landform directly connected to fluvial processes. Chaos terrain is thought to form by the fracturing of a layer of crust sliding over a lower lubricated layer (water in the case of Mars and Europa and glacial flow of N_2 ice for Pluto). Alternatively, such outflow channels could be carved by very fluid lava (Leverington, 2011), as is thought to be the case for analogous channels found on Mercury (Byrne et al., 2013).

Mars' surface hosts many enigmatic discontinuous channel segments, some of which have been related to water release by impacts (Mangold, 2012). Others terminate in landforms that resemble alluvial fans on Earth, such as Peace Vallis and its fan that was explored by the Curiosity Rover and found to contain conglomerates (Williams et al., 2013). These observations, together with those of the outflow channels point to surface water occurring only episodically, which contrasts with the older valley networks which point to a full-hydrological cycle having existed on Mars. As surface liquid water is not thought to have been stable for the last 1 Ga due to low atmospheric pressure and humidity, all together this points to Mars's surface becoming more arid over time.

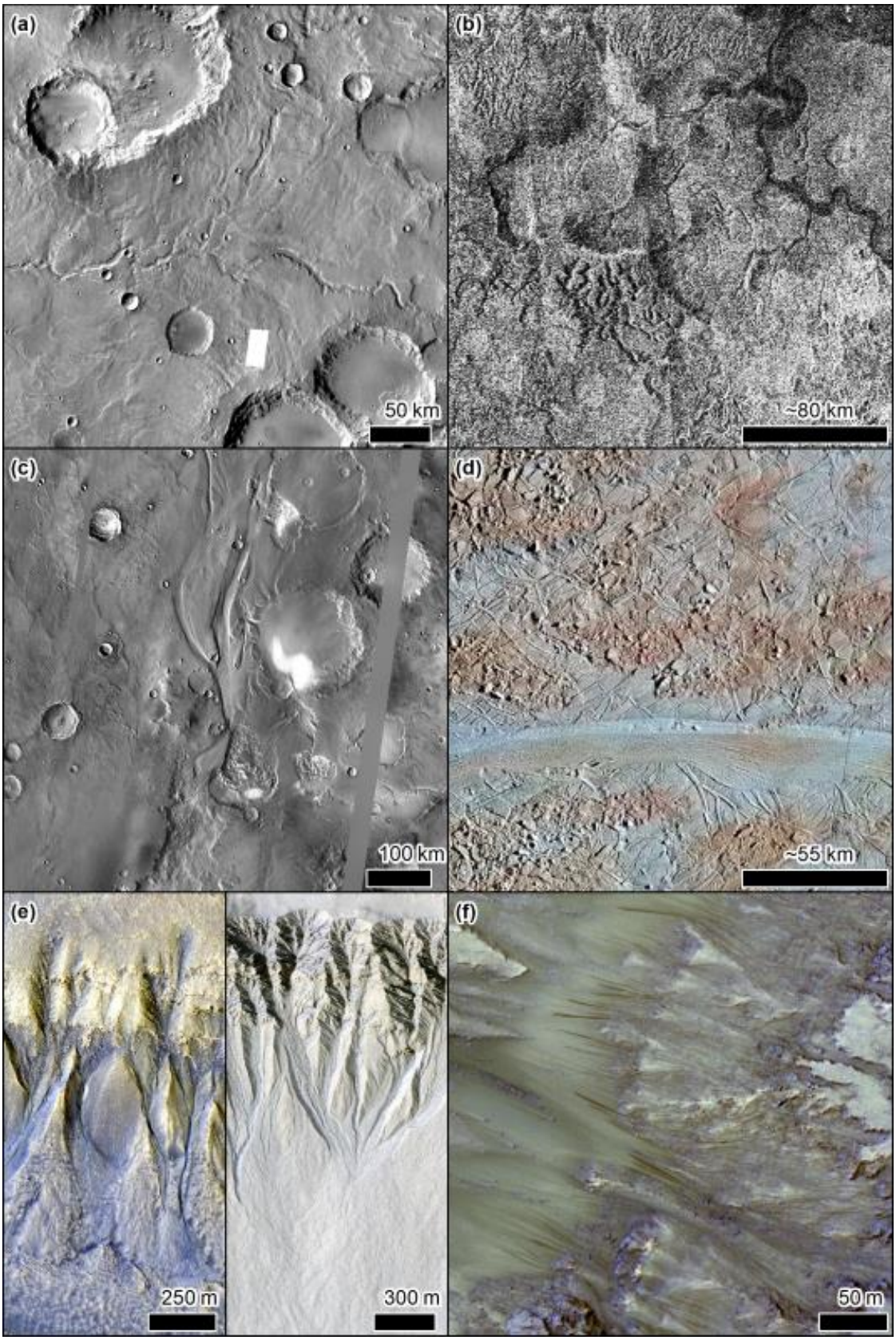

Figure 2.2: Fluvial planetary landforms. a) Evros Vallis, a valley network in Sinus Sabaeus region of Mars. The image is the Day IR THEMIS controlled mosaic available from the USGS. b) A synthetic aperture radar image of valleys near Titan's south pole taken by the Cassini spacecraft image reference PIA10219, credit NASA/JPL-Caltech/ASI. c) Baetis Chaos leading north into Maja Valles

outflow channel on Mars. The image is the Day IR THEMIS controlled mosaic available from the USGS. d) Chaos terrain on Europa near Agenor Linea taken by Galileo, image reference PIA23873, credit NASA/JPL-Caltech/SETI Institute. e) Two false-colour images of gullies on Mars: left Crater in Terra Cimmeria HiRISE image PSP_004019_1420 and right Gasa Crater, HiRISE image PSP_003939_1420, credit NASA/JPL/UofA. f) Recurring Slope Lineae in Palikir Crater, HiRISE image ESP_031102_1380, credit NASA/JPL/UofA. North is up in all images.

The smallest planetary landforms thought to be related to fluvial activity are kilometre-scale martian gullies (Figure 2.2e) (S. J. Conway et al., 2019; Malin and Edgett, 2000) and the metres-wide and up to hundreds of metres long Recurring Slope Lineae or "RSL" on Mars (Figure 2.2f) (McEwen et al., 2011). Martian gullies resemble first-order drainage systems dominated by debris flow processes on Earth, yet present-day flows in martian gullies during local winter argue against a completely fluvial origin (Diniega et al., 2010; Dundas et al., 2019a) – see Section 2.11. RSL are low albedo streaks that grow in the hottest times of year extending from rocky steep slopes (Ojha et al., 2014) and have been suggested to be water or brine seeps (Stillman et al., 2020), however the temporal and spatial limits of orbital observations mean their origin remains enigmatic and could represent a uniquely martian surface process and landform (F. Schmidt et al., 2017).

2.5 Coastal, lacustrine and kastic processes and landforms

Mars is the only planet besides Earth in the Solar System which is suspected to have had ocean-scale open bodies of standing liquid (in this case water). Mars' valley networks and outflow channels generally terminate in the northern lowlands and it is around these plains that two or more levels of putative shorelines have been identified (Carr and Head, 2019; Parker et al., 1993). These shorelines are characterised by a continuously traceable contact (expressed by albedo and/or topographic contrasts - Figure 2.3a) over thousands of kilometres and interpreted to represent wavecut platform(s). The lack of features typically associated with paleoshorelines on Earth, such as terraces, or barrier ridges (Ghatan and Zimbelman, 2006; Malin and Edgett, 1999), means this interpretation remains contentious. Variations in their altitude have been attributed to tectonic deformation post-formation (Citron et al., 2018), and are also used as evidence against the landforms representing shorelines (Sholes et al., 2021). The evidence for an ancient ocean is bolstered by the presence of deltas whose altitudes are consistent with the ocean levels represented by the shorelines (Di Achille and Hynek, 2010). Some of the shoreline landforms are alternately interpreted as the wash-up deposits of tsunamis (Figure 2.3b) (Costard et al., 2017; Rodriguez et al., 2016), which also implies the presence of an ocean.

Deltas are also one of the key lines of evidence in favour of the prevalence of paleolakes on ancient Mars (N. Mangold et al., 2012) (Figure 2.3c). Other lines of evidence include sedimentary and in situ observations by the Mars Science Laboratory rover Curiosity (Stein et al., 2018), spectral observations from orbit (Dehouck et al., 2010), and morphological arguments – e.g., channels ingress into depressions, but have no outlet or a higher elevation outlet (Cabrol and Grin, 1999; Fassett and Head III, 2008; Goudge et al., 2016, 2015). The only other body in the Solar System thought to host (or have hosted) seas or lakes is Saturn's Moon Titan (Figure 2.3d), whose 1.5 bar nitrogen-dominated atmosphere and -180°C surface temperature means that liquid methane is believed to be the main constituent of these lakes or seas, which are mainly located in polar regions. While some of these bodies are connected to drainage systems, others are thought to be the result of karstic-type dissolution processes (Mastrogiuseppe et al., 2019). Deposits interpreted to be evaporitic associated with basins located at Titan's tropics are inferred to be paleolakes or paleoseas (Moore and Howard, 2010), which could have resulted from seasonal (decadal timescales) or longer-term climatic changes on Titan (MacKenzie et al., 2014).

Numerous sulphate salt deposits exist on Mars and hundred-metre-scale depressions within them have been linked to karstic processes (Baioni and Sgavetti, 2013; Sefton-Nash et al., 2012) potentially related to groundwater circulation (Grindrod and Balme, 2010). Dissolution has been invoked to partly explain the collapse features associated with chaos terrain (described in Section 2.3). Pseudokarst is where material is lost by mechanisms other than dissolution e.g. thermokarst which in a planetary context has been employed to describe karst-like features caused by temperature induced volatile loss in contrast to the terrestrial definition which involves melting of ice-rich permafrost. These karstic landforms are described further in Section 2.11 and martian thermokarst initially also attributed to melting ice-rich permafrost are referred to in Section 2.8).

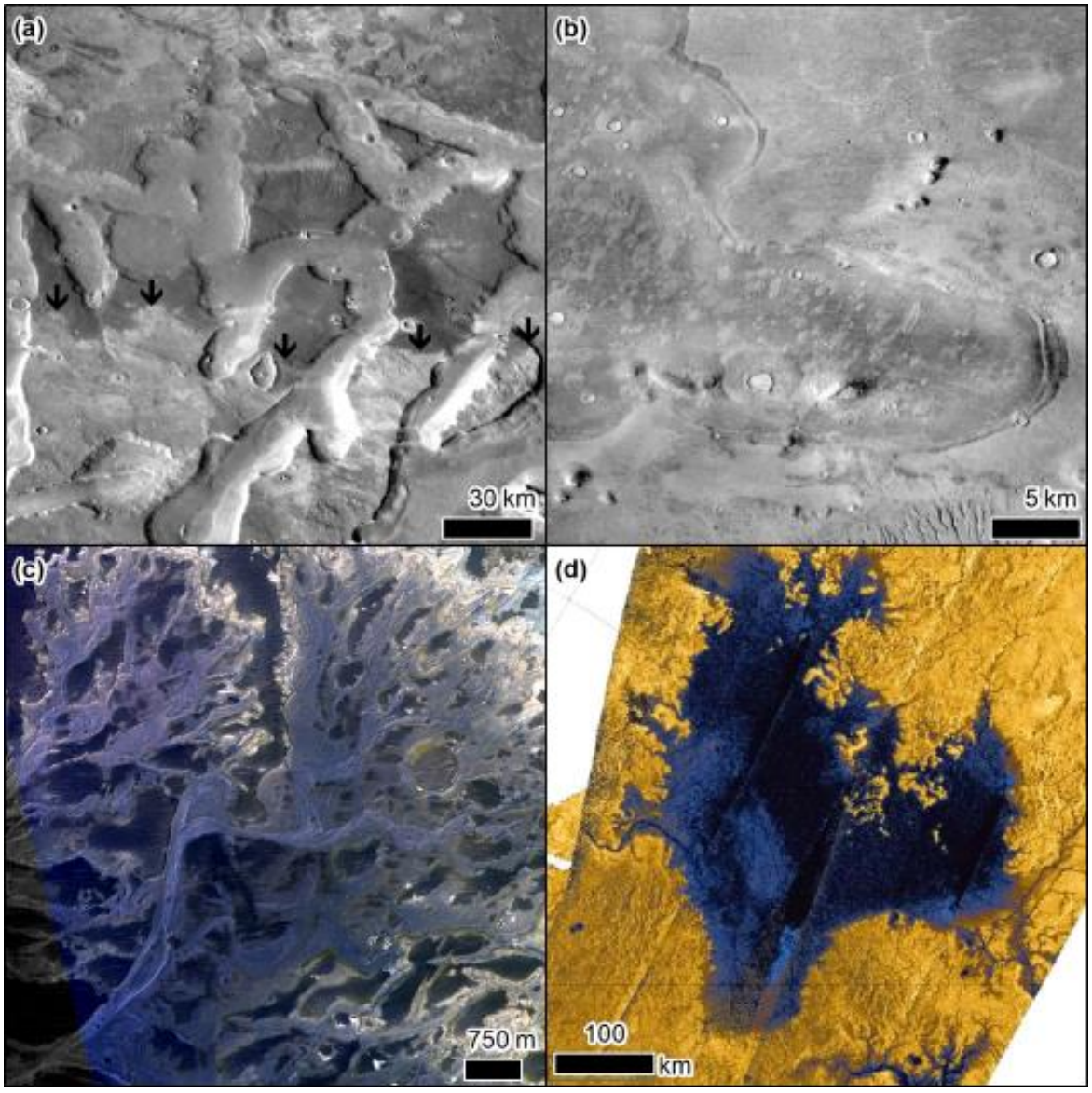

Figure 2.3: Coastal and lacustrine planetary landforms. a) Albedo contrast (black arrows) interpreted as a shoreline of a former northern ocean on Mars as seen in the Day IR THEMIS controlled mosaic available from the USGS. B) Lobate features interpreted to be tsunami runup deposits originating from an impact into a former northern ocean. CTX image P17_007835_2249, credit NASA/JPL/MSSS. c) CaSSIS false colour image of the inverted distributary channel systems within Eberswalde Crater on Mars, interpreted to be eroded remnants of a delta that formed within a lake in the crater. CaSSIS images MY34_004384_206_1 and MY34_004384_206_2, credit ESA/Roscosmos/Unibe. d) Cassini

false-colour radar image of Ligeia Mare, the second largest known sea of liquid hydrocarbons on Titan, credit: NASA/ESA/T. Cornet. North is up in all images.

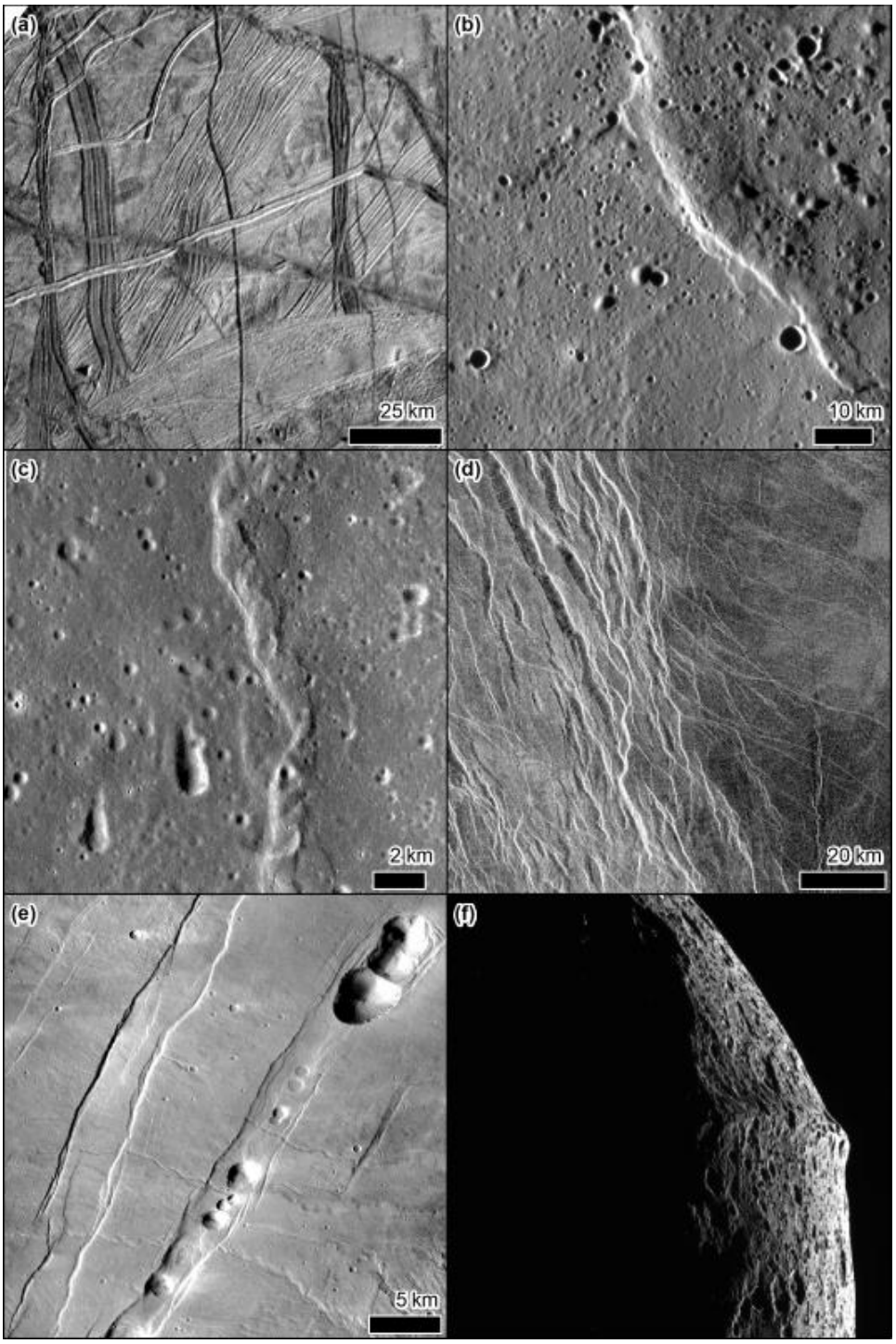

Figure 2.4: Tectonic planetary landforms. a) The surface of Europa divided into "plates" criss-crossed by fractures containing internal parallel ridges. Galileo SSI image 4700R, credit NASA/JPL-Caltech/SETI Institute. b) A lobate scarp on Mercury, MESSENGER MDIS NAC image EN1014447282M, credit NASA/Johns Hopkins University Applied Physics Laboratory/Carnegie Institution of Washington. c) Wrinkle ridge on the Moon, LROC NAC images M181023296 and M104376385, credit NASA/GSFC/ASU. d) Graben on Venus, extract of the Venus Magellan SAR FMAP Left Look Global Mosaic from the USGS. e) Graben and pit chains on Mars, CTX image B18_016700_2167, credit

NASA/JPL/MSSS. f) Limb image of Iapetus, showing the 20 km high equatorial ridge, taken by Cassini N1568094172_2. North is up in all images except f.

2.6 Planetary tectonic landforms and processes

Tectonic landforms are ubiquitous on planetary surfaces. Even the smallest bodies that have been explored, such as comets, show signs of fracturing which result from interior forces (El-Maarry et al., 2015). However, only the Earth has plate tectonics, whose action profoundly influences its landscapes, making it one of the most dynamic surfaces in the Solar System. Europa, which is an icy Moon of Jupiter, may have an analogous system of plates, but in this case the plates are made of water ice floating on a liquid water "mantle" (Kattenhorn and Prockter, 2014) (Figure 2.4a). The detailed morphology of Europa's plates was key in motivating the dynamic modelling that underpins our understanding of this planet's interior. A similar "jostling plates" model has been advanced for Venus based on analogy with deformational structures observed in actively deforming contents on Earth (Byrne et al., 2021). Typical compressional tectonic landforms include wrinkle ridges, high relief ridges and lobate scarps (Figure 2.4b, c), common on Mercury (Byrne et al., 2014), Mars (Herrero-Gil et al., 2019; Nahm and Schultz, 2011), and the Moon (Schleicher et al., 2019; Watters et al., 2010). They are thought to be compound landforms representing folds above faults, but not common on Earth (Crane, 2020) hampering their interpretation. Global mapping these compressional tectonic features on Mercury has provided an independent estimate of its global contraction (Byrne et al., 2014).

Typical extensional forms include graben (Figure 2.4d) and are found commonly throughout the solar system. Graben systems are sometimes associated with pit-chains, which are thought to be caused by fracture dilation (Ferrill et al., 2011) (Figure 2.4e) and whose origin is also interpreted to be magmatic (see Section 2.6):

Extensional tectonic features are very common on the icy moons of Jupiter, Saturn, and Neptune and their patterns have been vital in understanding the forces that influence these bodies including tidal stresses from their planets, crustal thickness, and mantle motions (Collins et al., 2009). Tectonic landforms on these icy satellites can be unique, for example the double ridges on Europa (Figure 2.4a), or the twisting double ridge-sets on Triton, or the prominent single equatorial ridge on Iapetus (Figure 2.4f).

2.7 Planetary volcanic landforms and processes

The definition of volcanism has been extended beyond magmatic volcanism in a planetary science context, to include also sedimentary volcanism and cryovolcanism and each are thought to produce somewhat distinct landforms. Magmatic volcanism requires interior heating and an availability of silicates to produce magma, so generally related volcanic landforms are found on terrestrial planets of the inner solar system, as well as the Earth's Moon and Jupiter's innermost moon Io. Volcanism at the largest scale (hundreds to thousands of kilometres) is recognised in the form of volcanic constructs, such as Tuulikki Mons on Venus (Basilevsky et al., 2012) (Figure 2.5a) or Olympus Mons on Mars (Morris, 1982) and/or volcanic plains, such as the Mare of the Moon (Figure 2.5b) (Stuart-Alexander and Howard, 1970) or the Northern Plains of Mercury (Denevi et al., 2013). Peculiar to Venus are coronae, arachnoids and novae, which are large patterns of fractures (concentric, concentric-radial and radial, respectively) believed to be volcanic in origin (Head et al., 1992). Io is the only planetary body in the Solar System where volcanic eruptions have actually been observed occurring (McEwen, 1998).

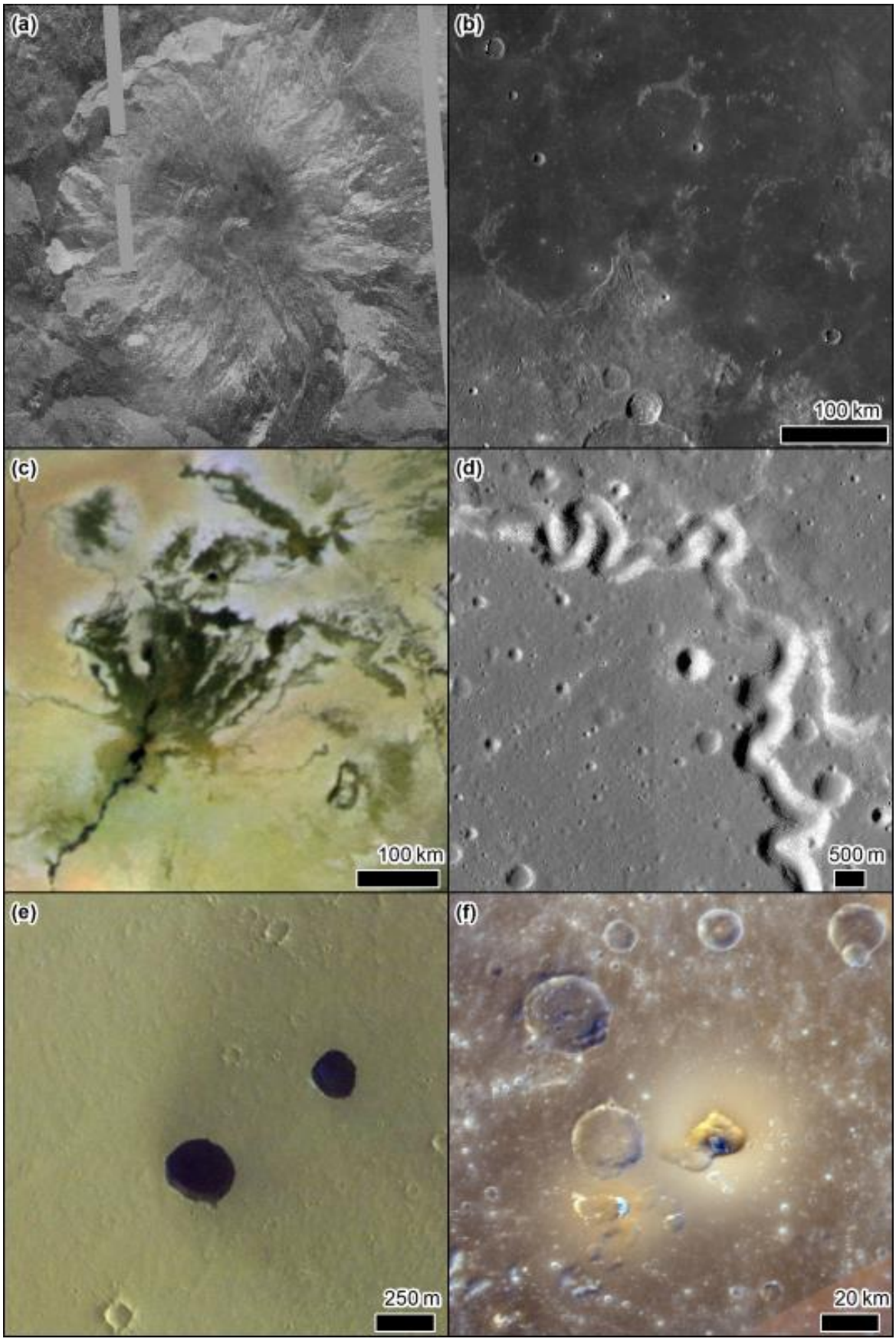

Figure 2.5: Volcanic planetary landforms. a) Tuulikki Mons a shield volcano on Venus, extract of the Venus Magellan SAR FMAP Left Look Global Mosaic from the USGS. b) The lunar maria with portions

of embayed impact crater rims visible and the contact with the highlands towards the bottom left. LORC WAC global mosaic made available by the USGS. c) Volund dark volcanic field on Io (Veeder et al., 2009)using the USGS Io basemap combining Voyager and Galileo images. d) Sinuous rilles on the Moon, LROC NAC image M1157998924, credit NASA/GSFC/ASU. e) Skylights on Mars, with the east-facing walls barely visible. CaSSIS false colour image MY36_015278_162_0, credit: ESA/Roscosmos/Unibe. f) Agwo Facula on Mercury, where the central vent is surrounded by smooth deposits with an orange coloration in the MDIS enhanced colour mosaic overlain by MDIS WAC image EW1012888774, credit NASA/Johns Hopkins University Applied Physics Laboratory/Carnegie Institution of Washington. North is up in all images.

Recognisable at the kilometre to tens of kilometre-scale on Mars, the Moon, Venus and Io are individual lava flows (Figure 2.5c – io "dark flow") and lava channels. On the Moon sinuous rilles (Figure 2.5d) – sinuous channels hundreds of metres to kilometres in width and up to 500 km long - were initially attributed to water (Peale et al., 1968), but are now generally acknowledged to be lava channels carved predominantly by thermal erosion (Hurwitz et al., 2013). "Skylights" (Figure 2.5e) – deep nearly vertically walled circular to elliptical depressions – on Mars and the Moon are interpreted to represent the collapse of the roof of lava tubes and present considerable interest as natural habitats which could be exploited for human exploration (Sauro et al., 2020). Larger pit chains are thought to represent collapse on the withdrawal of lava from dikes (Wyrick, 2004) but could also be tectonic in origin (see Section 2.5).

Evidence for explosive volcanism is usually smaller-scale (tens of kilometres) and more subtle in its surface expression, taking the form of pits with associated red-colouration on Mercury (Kerber et al., 2011) (Figure 2.5f), low-albedo markings on the Moon (Gustafson et al., 2012) and km-scale volcanic cones on Mars (Brož and Hauber, 2012).

Sedimentary volcanism (often called mud volcanism) is driven by the circulation of water through a planetary crust generally driven by tectonic forces or density contrasts and has been reported on Mars (Figure 2.6a). Here, movement of groundwater is thought to have remobilised ancient sedimentary deposits creating pitted cones and lobate-fronted flow features (Oehler and Allen, 2010). On Earth, mud volcanoes are the most commonly expressed landform resulting from sedimentary volcanism and differ from their volcanic counterparts in terms of morphology, however this distinction is harder to make on other bodies because of differences in environmental conditions are difficult to directly infer the potential morphologic impacts (Brož et al., 2020b).

Cryovolcanism is thought to be more abundant in the icy moons of the outer planets (Ahrens, 2020; Kargel, 1995), where liquid water and ice, are thought to substitute almost directly the more familiar lava and silicic rocks in the functioning of the volcanic plumbing system. On Ceres, brine driven cryovolcanism is thought to explain the bright faculae, such as Cerealia Facula in Occator Crater (Nathues et al., 2020) (Figure 2.6b). Inspired by planetary research cryovolcanic processes have been cited as a potential cause for explosive pits that occurred in continuous permafrost on the Yamal Peninsula in Russia (Buldovicz et al., 2018).

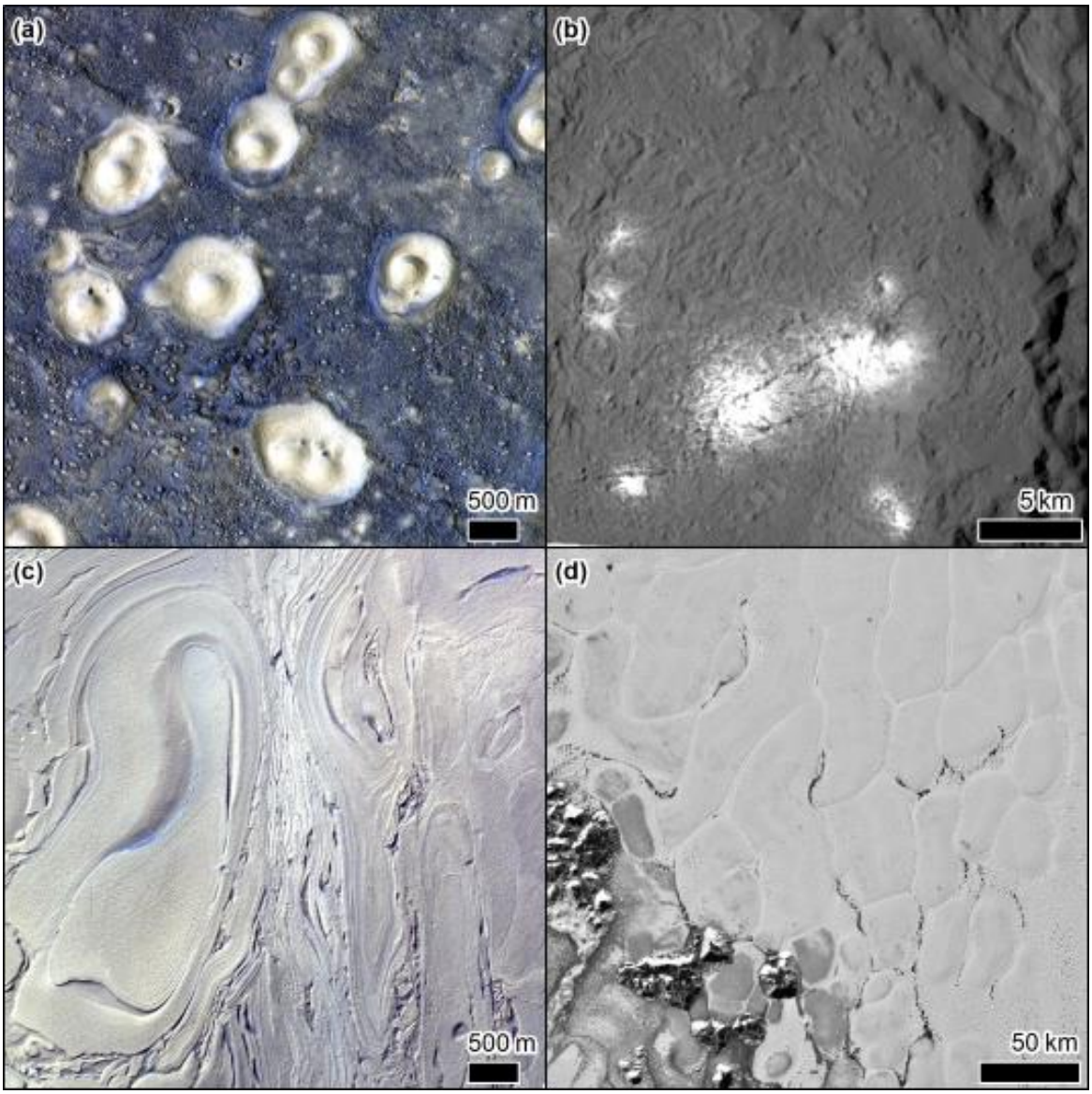

Figure 2.6: Sedimentary volcanism and cryo-volcanic landforms. a) Pitted cones interpreted to result from mud volcanism in Acidalia Planitia on Mars. CaSSIS image MY35_009227_048_0 credit: ESA/Roscosmos/Unibe. b) Bright faculae in Occator Crater on Ceres interpreted to be salt deposits resulting from cryovolcanism. DAWN framing camera image FC21B0070808_16169044543F6C, credit NASA/JPL-Caltech/UCLA/MPS/DLR/IDA. c) The enigmatic banded terrain on the floor of Hellas Basin on Mars. CaSSIS image MY36_015427_317_0 credit: ESA/Roscosmos/Unibe. d) The mysterious cellular structure of Sputnik Planitia on Pluto, image New Horizons global mosaic from the USGS. North is up in all images.

Diapirism (either compositional or thermal), where a less dense material rises through a denser one above it is often associated with sedimentary- or cryo-volcanism. The resulting landforms can be a result of tectonic deformation rather than extrusion at the surface. Several enigmatic terrains have been attributed to diapirism or associated convection: the honeycomb and banded terrain in Hellas basin on Mars (Figure 2.6c - cassis) (Bernhardt et al., 2016), Cantaloupe terrain on Triton (Schenk and Jackson, 1993) or the cellular structure of Sputnik Planitia on Pluto (Howard et al., 2017b) (Figure 2.6d).

ESA/Roscosmos/Unibe. e) Granular flows in Kepler Crater on the Moon, LROC NAC images credit: NASA/GSFC/ASU. f) Zoom in on the termini of the granular flows in panel e. North is up in all images.

2.8 Mass movements on planetary bodies

Landslides have been identified on nearly every solid planetary surface observed in the solar system. Notably the long runout landslides observed on bodies as diverse as Mars (Crosta et al., 2018; McEwen, 1989), Mercury (Brunetti et al., 2015), the Moon (Boyce et al., 2020), Iapetus (Singer et al., 2012), Callisto (Moore et al., 1999), Pluto's moon Charon (Beddingfield et al., 2020), Ceres (Duarte et al., 2019) and Comet 67P (Lucchetti et al., 2019) (Figure 2.7a-c) have inspired a comparative planetology approach seeking to understand the physical processes underlying the motion of the long-runout landslides. The role that volatiles do or do not play in the mobility of landslides is a key recurring theme. On one hand being used as an argument to support inclusion of volatiles on Iapetus (Singer et al., 2012) and on the other being used to refute their action on comet 67P (Lucchetti et al., 2019). For Ceres (Johnson and Sori, 2020; B. E. Schmidt et al., 2017) as for Mars, both cases have been presented and no consensus has yet been achieved (Harrison and Grimm, 2003; Johnson and Campbell, 2017).

Peculiar to Mars are a landform called "Slope Streaks" (Figure 2.7d) (Sullivan et al., 2001), which are thought to represent avalanches of dust-sized material, taking the form of contrasting albedo, downslope-widening streaks, up to several kilometres in length and hundreds of metres wide. Slope Streaks usually appear as relatively dark (and sometimes relatively light) downslope oriented streaks with barely detectable or negligible relief (Brusnikin et al., 2016; Chuang et al., 2007), which fade to the background albedo over time. They often widen from a point source and can be sinuous, overcome obstacles and have digitate margins. They can overtop small obstacles (Brusnikin et al., 2016) yet are generally diverted by topographic irregularities (Miyamoto, 2004), so can form complex bifurcating features. The involvement of liquid water has been invoked to explain their mobility on low slopes (Bhardwaj et al., 2017), but dry granular mechanisms seem to also provide an adequate explanation (Dundas, 2020).

Images at better than 1 m/pix on the Moon have revealed a diversity of mass movements on steep slopes, including lobate and digitate dry granular flows on Moon (Figure 2.7e,f) (Senthil Kumar et al., 2013; Xiao et al., 2013). The Moon and Mercury host unique surface textures hinting at slower downslope movement of the surface regolith, including "elephant hide texture" on the Moon and "chevron texture" on Mercury, whose precise origin is unknown (Zharkova et al., 2020). On Mars, tens to hundreds of metre-scale lobate forms on slopes have been associated with the existence of a solifluction-type movement on Mars (Gastineau et al., 2020; Johnsson et al., 2012) and are found in association with other landforms interpreted to be periglacial in origin (see Section 2.8).

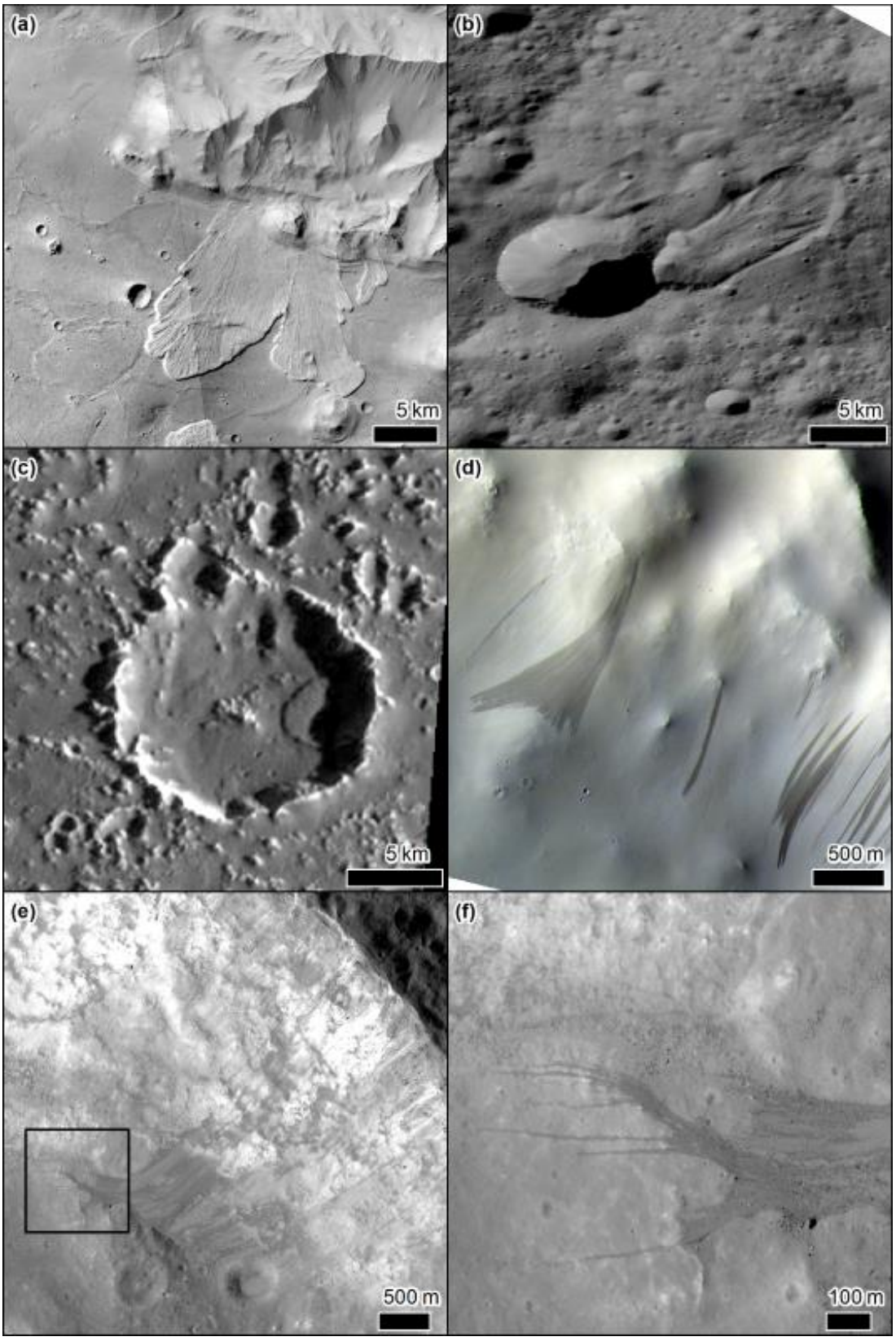

Figure 2.7: Planetary Mass Movements. a) Landslides in Valles Marineris on Mars, CTX images D20_034988_1669, G19_025850_1688, credit NASA/JPL/MSSS. b) Landslide on Ceres, DAWN FC FC21A0061028_16091125549F1D. c) Landslide on Callisto, Galileo SSI image 2840R, credit NASA/JPL-Caltech/SETI Institute. d) Slope Streaks on Mars, CaSSIS image MY36_015392_011_0 credit: ESA/Roscosmos/Unibe.

2.9 Planetary glacial and permafrost landforms and processes

Mars has an extensive suite of landforms at its mid-latitudes which are commonly accepted to be debris covered glaciers (Figure 2.8a) dating from the last 1 Ga of Mars' history. These glaciers can cover tens to hundreds of kilometres and reach hundreds of metres thick. Their water ice core has been revealed through orbital radar sounding (Petersen et al., 2018; Plaut et al., 2009), and their surface textures indicate slow viscous deformation. Modelling studies (Karlsson et al., 2015; Parsons et al., 2011) and the general lack of landforms associated with melt imply that the ice is likely perennially frozen to the glacier bed (cold-based glaciers). The rare discovery of ridges interpreted to be eskers connected to extant glaciers suggests that this constraint is only occasionally overcome (F. E. G. Butcher et al., 2020; Gallagher and Balme, 2015). Isolated eskers and moraine-like ridges have been interpreted to be signs of ancient glaciation and/or icesheets (Butcher et al., 2016; Head and Marchant, 2003).

On Pluto the existence of glaciers of N_2 ice has been reported (Howard et al., 2017a). These take the form of smooth material filling topographic lows in highland terrains with longitudinal albedo lineations indicating flow direction, which appear to flow out onto Sputnik Planum at lower elevation where the lineations blend into the plains materials (Figure 2.8b). These glaciers are hundreds of kilometres in length. The only other planetary body where debris covered glaciers have been proposed is the dwarf planet Ceres (B. E. Schmidt et al., 2017), but their ambiguous morphology means that landsliding could also be a viable interpretation.

Permafrost conditions exist on many bodies, particularly those in the outer solar system, yet landforms typically associated with permafrost on Earth generally imply the degradation of ground ice, or at least cycling of temperatures near water's triple point to produce terrain modifications e.g., periglacial landforms. One exception is the formation of polygon crack patterns in ice-rich soil by thermal contraction, which only requires temperature cycling – metre to decametre-scale examples of these landforms have been widely reported at latitudes greater than 50°N and S on Mars (Mangold, 2005; Mellon et al., 2009) where ground ice is thought to be prevalent (Feldman et al., 2011). Periglacial landforms have been reported on Mars, implying the action of freeze-thaw cycling in the planet's recent history and hence their interpretation as such remains a subject of debate. These landforms include:

- Gullies, which are alcove-channel-fan systems hundreds of metres to kilometres in length, which are found on steep slopes in the mid to high latitudes on Mars (Figure 2.2e) (Harrison et al., 2015; Malin and Edgett, 2000). Their resemblance at landscape and landform-scale to gullies carved by overland-flow and debris flow on Earth means that they have been widely interpreted to form by these processes (Balme et al., 2006; Conway and Balme, 2016; de Haas et al., 2015a), and the source of water is likely from snow and/or ground ice thaw. Yet their present activity has led to a re-evaluation of this interpretation (see Section 2.11 - Sublimation landforms and processes).
- Surface albedo and/or clast patterns that resemble, and have a similar-scale to, sorted patterned ground on Earth, including sorted circles on flat ground and stripes on sloping terrain (Gallagher et al., 2011; Soare et al., 2016) (Figure 2.8c).
- Lobate forms interpreted to be solifluction lobes (see Section 2.7) (Figure 2.8d).

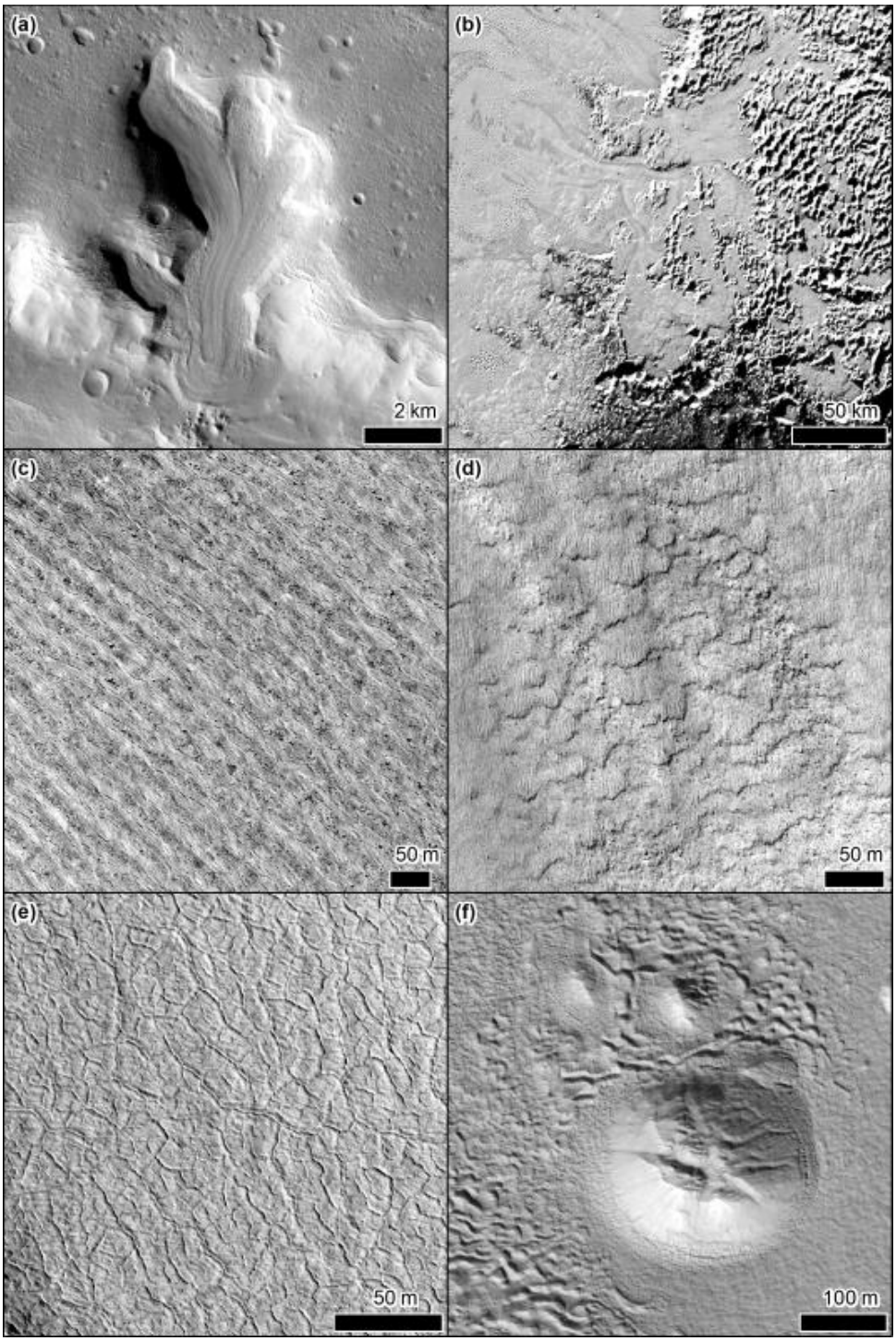

Figure 2.8: Planetary glacial and periglacial landforms. a) Debris covered glacier on Mars, CTX Image B05_011776_2208, credit NASA/JPL/MSSS. b) Glacial flows on Pluto imaged by New Horizons, taken from the Global Mosaic available from the USGS. c) Linear arrangements of boulder propagating downslope interpreted to be sorted patterned ground on an impact crater wall in the high northern latitudes on Mars, HiRISE image PSP_009580_2485, credit NASA/JPL/UofA. d) Lobate forms on the wall of an impact crater on Mars interpreted to be solifluction lobes, HiRISE image ESP_023679_1365, credit NASA/JPL/UofA. e) Polygonal fractured ground where the polygon boundaries are raised as single or double ridges, termed low centres polygons, HiRISE image PSP_005821_1095 credit NASA/JPL/UofA. f) A mound with a fractured summit near Moreaux Crater on Mars interpreted to be a pingo, HiRISE image ESP_058140_2225 credit NASA/JPL/UofA. North is up in all images.

- Polygonal patterned ground where the centres are lower than the margins and those margins form double-ridges implying the existence of ice wedges (Soare et al., 2014a; R.J. Soare et al., 2021) (Figure 2.8e).
- Scalloped depressions (Soare et al., 2008) and polygon junction pits (Costard et al., 2016) were initially interpreted to be true thermokarst (i.e. caused by thaw). However, together with expanded craters (Viola et al., 2015) are now thought to be caused by sublimation (Dundas et al., 2015a), see Section 2.11.
- Tens to hundreds of metre isolated hills or mounds with summit cracks/depressions interpreted to be caused by ice-heave, otherwise known as "pingos" (Burr et al., 2009b; Soare et al., 2005) (Figure 2.8f).

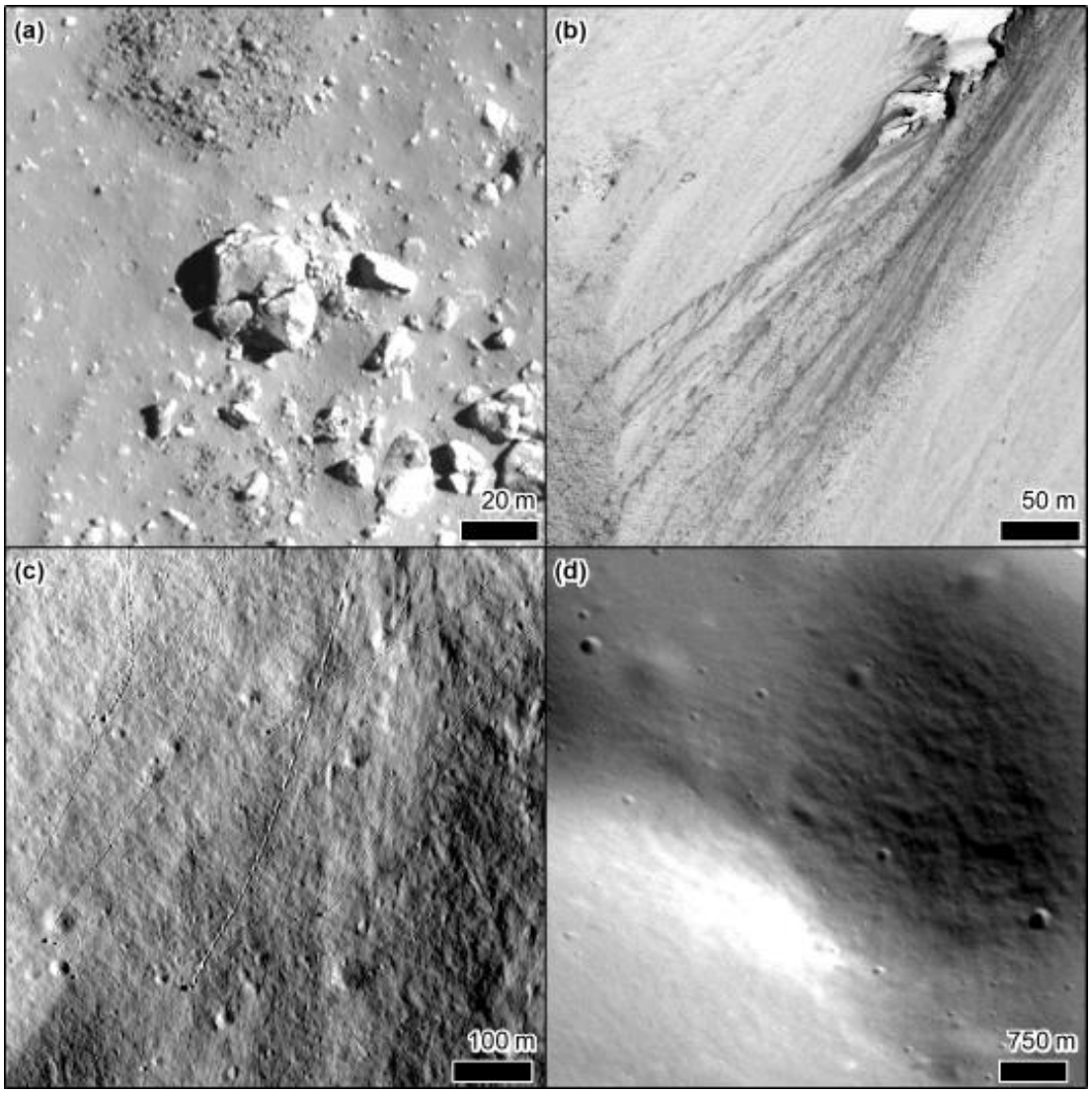

Figure 2.9: Weathering on planetary surfaces. a) Fractured rocks around Byrgius A Crater on the Moon, LROC NAC image M175698856LE, credit NASA/GSFC/ASU. b) Tracks and low albedo "ejecta" left by recent rockfalls on a crater wall on Mars, HiRISE image PSP_004110_1640, credit NASA/JPL/UofA. c) Multiple rocks which have left depressions behind them while rolling and bouncing over the lunar surface, LROC NAC image M1198659818LE, credit NASA/GSFC/ASU. d) Undulating, irregular surface texture on Mercury, termed "Elephant hide" (Zharkova et al., 2020) MDIS NAC image EN1042186062M, credit NASA/Johns Hopkins University Applied Physics Laboratory/Carnegie Institution of Washington. North is up in all images.

2.10 Weathering

Weathering on planetary bodies produces regolith from rock via a range of breakdown processes, some of them unknown on Earth. The landscape expression of these weathering processes includes softening of primary landforms, such as impact craters, following a generally diffusive trend (Fassett et al., 2017; Soderblom, 1970). Landforms directly linked to weathering processes, include regolith surface textures and rock shapes, which tend to be expressed at the metre-scale or less. Hence, *in situ* observations are best suited to inferring weathering processes are limited to the Moon, Mars, asteroids Bennu and Ryugu and comet 67P.

On bodies without an atmosphere the surface is subject to a range of processes not experienced at Earth's surface, including solar wind sputtering and micrometeorite impacts. In addition, thermal stress and fatigue are greatly accentuated by the high amplitude thermal variations experienced on many planetary surfaces compared to Earth (El Mir et al., 2019; Molaro and Byrne, 2012). Cracked rocks or "Puzzle rocks" observed on Bennu (Walsh et al., 2019), Ryugu (Sasaki et al., 2021), the Moon (Ruesch et al., 2020) and Mars (Eppes et al., 2015; Hörz et al., 1999) have been linked to thermal fatigue and/or micrometeorite impacts (Figure 2.9a). On Mars rocks can also be sculpted by the wind – producing ventifacts (Bridges et al., 1999; Greeley et al., 2006a; Thomson et al., 2008) (see also Section 2.2). Pitted boulder surfaces on Mars have been linked to transient melting of snow (Head et al., 2011) and volatile-related processes have been implicated in accelerating rock chute formation (Levin et al., 2022) and boulder breakdown (de Haas et al., 2013).

A consequence of rock breakdown is rockfalls, which have been observed to occur in repeat imaging of Mars (Grindrod et al., 2021; Vijayan et al., 2021) (Figure 2.9b). Roll/bounce marks left in the regolith in the wake of boulders (Figure 2.9c) have shown rockfall to be a recently active process on the Moon (Arvidson et al., 1975; Bickel et al., 2020a). Patterns in the distribution of rockfall tracks have been used to provide evidence for rock breakdown by thermal stress on Mars on the timescale of < 1Ma (Tesson et al., 2020), seismic activity on Mars (Roberts et al., 2012) and on the Moon (Senthil Kumar et al., 2016), as well as inform the regolith strength on the Moon (Bickel and Kring, 2020).

Some puzzling aspects of surface regolith appearance have been attributed to surface sintering caused by solar irradiation (Zharkova et al., 2020) (Figure 2.9d).

2.11 Impact Cratering

The process of impact cratering dominates most planetary surfaces apart from the Earth, Venus, Titan and Io which either have dense atmospheres reducing the incoming impactor population and/or surface processes that act to erase any crater landforms that are created. Impact craters create topographic relief that can serve as a catalyst for other surface processes and they expose materials from planetary interiors to active surface processes. For example, impacts can cause substantial seismic shaking (Schultz and Gault, 1975) and therefore can initiate mass movements (see Section 2.7).

The shape of an impact crater is primarily a function of the gravity, impactor size and the target surface composition (Melosh, 1989). Other factors, such as impact speed and angle, impactor composition, or target structure, also play a role in modulating the crater shape, but for the purposes of this review will not be considered in further detail. With increasing impactor sizes craters evolve from "simple" bowl-shapes towards more "complex", including flat-floored with a central peak up to multi-ringed basins (Figure 2.10a-c). The crater diameter at which the simple-to-complex transition occurs varies from planetary body to planetary body and is traditionally represented by plotting the population of craters on a logarithmic depth-diameter diagram. For example, on Mars the simple-to-

complex transition occurs at crater diameters of ~8 km, on Europa it occurs at ~1 km and Vesta at 28 km (Hiesinger et al., 2016).

Impact craters eject material from their cavity forming unique morphologies, such as ejecta blankets, secondary crater clusters/chains, and visible radial "rays" which can be global in extent (Figure 2.10d). Impact melt, found within the cavity and in the ejecta, shares many morphological characteristics with lava and in ancient terrains on the Moon and Mercury, the distinction between them can be challenging (Denevi et al., 2013). The outcrops located in crater walls and central peaks can provide relatively fresh exposures of subsurface materials providing insights into the subsurface composition of a body without having to drill *in situ* (Quantin et al., 2012).

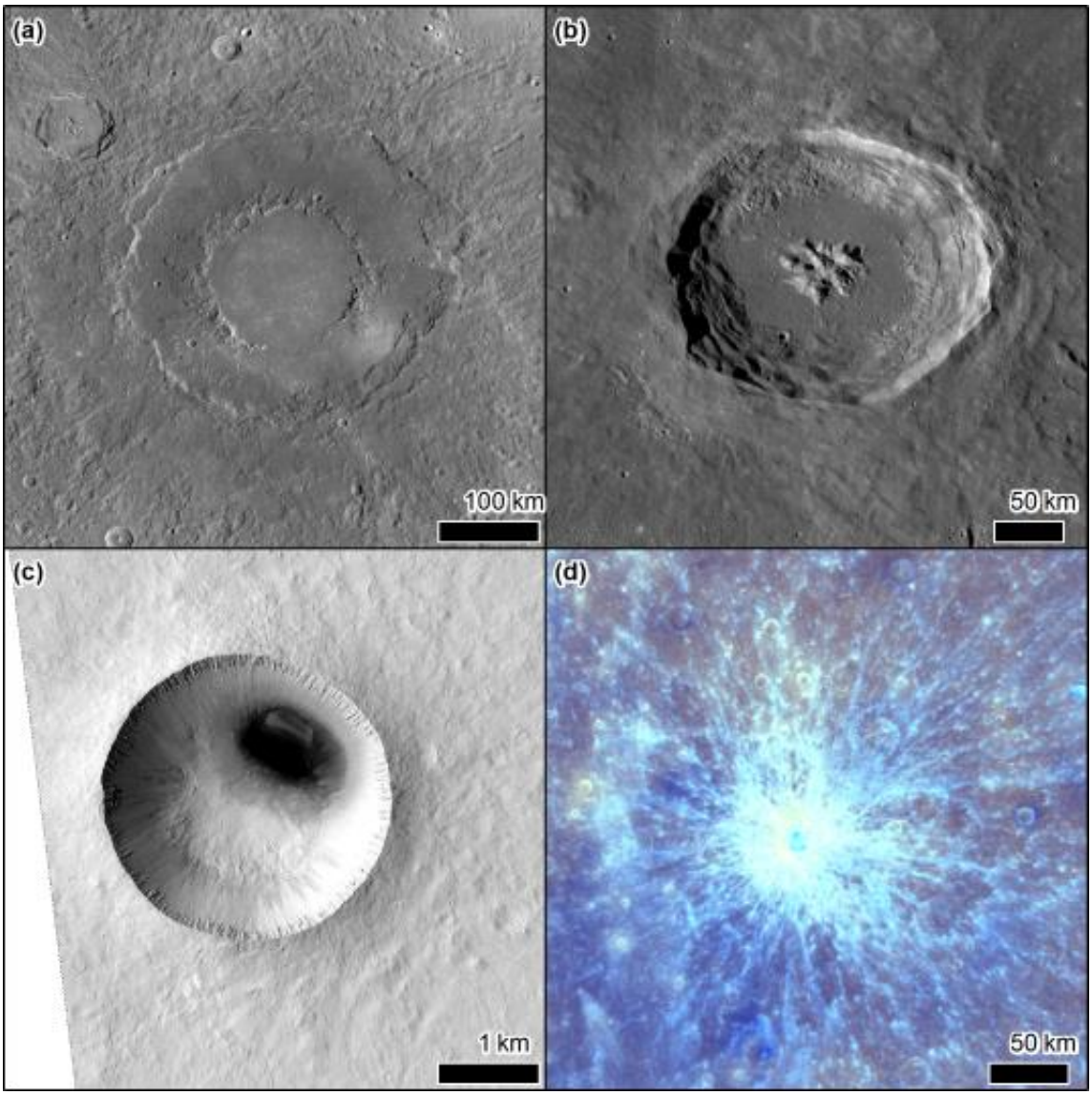

Figure 2.10: Impact craters on Planetary bodies. a) Rachmanioff, an impact basin on Mercury, with noticeable multiple rings, MDIS global BDR mosaic, credit NASA/Johns Hopkins University Applied Physics Laboratory/Carnegie Institution of Washington. b) Arstillus, a complex crater with central peak and wall terraces on the Moon, LRO global WAC mosaic, credit NASA/GSFC/Arizona State University. c) ~ 2km diameter simple crater on the floor of Pasteur Crater on Mars, HiRISE image ESP_045152_2000, credit NASA/JPL/UofA. d) Petipa, an impact crater with rayed ejecta on Mercury, MDIS global enhanced color mosaic, credit NASA/Johns Hopkins University Applied Physics Laboratory/Carnegie Institution of Washington. North is up in all images.

Impact craters substantially disturb the crust (Kenkmann et al., 2014) and as a result can form a structural conduit for endogenic processes that are then expressed at the surface, such as hydrothermal circulation (Osinski et al., 2013), explosive volcanism (Thomas et al., 2014a), or cryovolcanism (Nathues et al., 2020).

Impact craters are used as an essential dating tool in planetary science, as their size-frequency distribution is a function of the exposure age of a surface (Hartmann and Neukum, 2001). The degradation state of the craters, hence the ability to recognise the surface processes that have influenced them, is an important factor when interpreting the results of the crater size-frequency distribution (Michael and Neukum, 2010).

2.12 Sublimation landforms and processes

Environments dominated by sublimation are rare on Earth, hence entire landforms or landscapes dominated by this phase change are restricted to other planetary bodies. In particular the icy satellites of the outer Solar System have surfaces dominated by various ices and whose sublimation is thought to explain some of the most unusual landscapes (Mangold, 2011). For example, the entire surface of Jupiter's moon Callisto is thought to have been extensively modified by the sublimation of CO_2 and H_2O ices at its surface leaving a terrain dominated by dissected ridges and knobs (Figure 2.11a) (White et al., 2016). Helene, in the Saturn system, has a sculpted surface attributed to remobilisation of a thick layer of particles whose origin is sublimation from the plumes of Enceladus (Figure 2.11b) (Hirata et al., 2014).

Comets are another planetary body where sublimation is the dominant landscape forming process every time the comet approaches the sun. The first cometary orbital data from the Rosetta mission to comet 67P revealed astonishingly diverse landscapes, including dunes (see Section 2.2), retreating steep sided pits and cliffs (Figure 2.11c) (Vincent et al., 2015) and cracks and fissures(El-Maarry et al., 2015). The steep sided pits and cliffs are thought to be correlated to the plumes of outgassing (Vincent et al., 2016). Gassy outbursts were also noted to mobilise dust on asteroid Bennu, yet the geomorphic effect if any in this setting remains unclear (Lauretta et al., 2019).

On other bodies, depressions are the most common landform associated with sublimation and can be considered akin to karst on Earth. The perennial CO_2 ice found at the South Polar cap of Mars, undergoes retreat each year in the form of enlarging and coalescing circular to elliptical steep sided pits typically several hundred metres in diameter and metres deep, dubbed "swiss cheese" (Buhler et al., 2017) (Figure 2.11d). The loss of excess water ice from the ground via sublimation in the mid-latitudes of Mars results in "scalloped depressions" (Dundas et al., 2015a; Soare et al., 2007) – shallow-sloping depressions of hundreds of metres in extent, with an arcuate and steeper backwall. In the some of the same regions, sublimation expands polygonally patterned contraction cracks producing chains of pits and possibly cavities (Séjourné et al., 2011). Volatile loss has also been invoked to explain shallow, steep-sided depressions on Mercury which are surrounded by a relatively bright halo – "hollows" (Blewett et al., 2011) (Figure 2.11e). The discovery of these landforms was part of the realisation that Mercury's crust is not actually depleted in volatiles as once thought (Nittler and Weider, 2019).

The seasonal retreat of the CO_2 ice deposits across the surface of Mars results in a uniquely martian process caused by basal sublimation of the CO_2 ice (Kieffer et al., 2006). CO_2 ice is translucent to solar radiation, hence the increasing incoming solar radiation in late winter to early spring can heat the regolith under the CO_2 ice, causing it to sublimate and CO_2 gas to be trapped underneath it. The gas pressure builds until the ice above breaks, releasing the gas in a jet which deposits dark dust from under the ice onto the still bright icy surface. This phenomenon most commonly manifests itself as

dark fans or spots (Hansen et al., 2013) and on the steep slopes of dunes can even appear as digitate (Gardin et al., 2010). The sediment mobilised under the ice is thought to explain the observation of "spiders" – dendritic networks of channels leading to one or more "nodes" (Thomas et al., 2011) (Figure 2.11f). Individual spiders can be hundreds of metres in size and they can extend across many kilometres. Although spiders have not been observed to grow, similar branching networks have been observed to appear and grow on dunes ("furrows") (Portyankina et al., 2010). Sediment mobilisation by sublimating CO_2 is thought to explain ongoing sediment motions observed in martian gullies which only occur in winter (Dundas et al., 2019a). In particular, a uniquely martian morphology called "linear gullies" is thought to be formed by levitating blocks of CO_2 ice falling from icy dune crests (Diniega et al., 2013). Volatile loss is believed to drive the formation of gully-like-landforms on the asteroid Vesta (Scully et al., 2015) and on Mercury (Malliband et al., 2019).

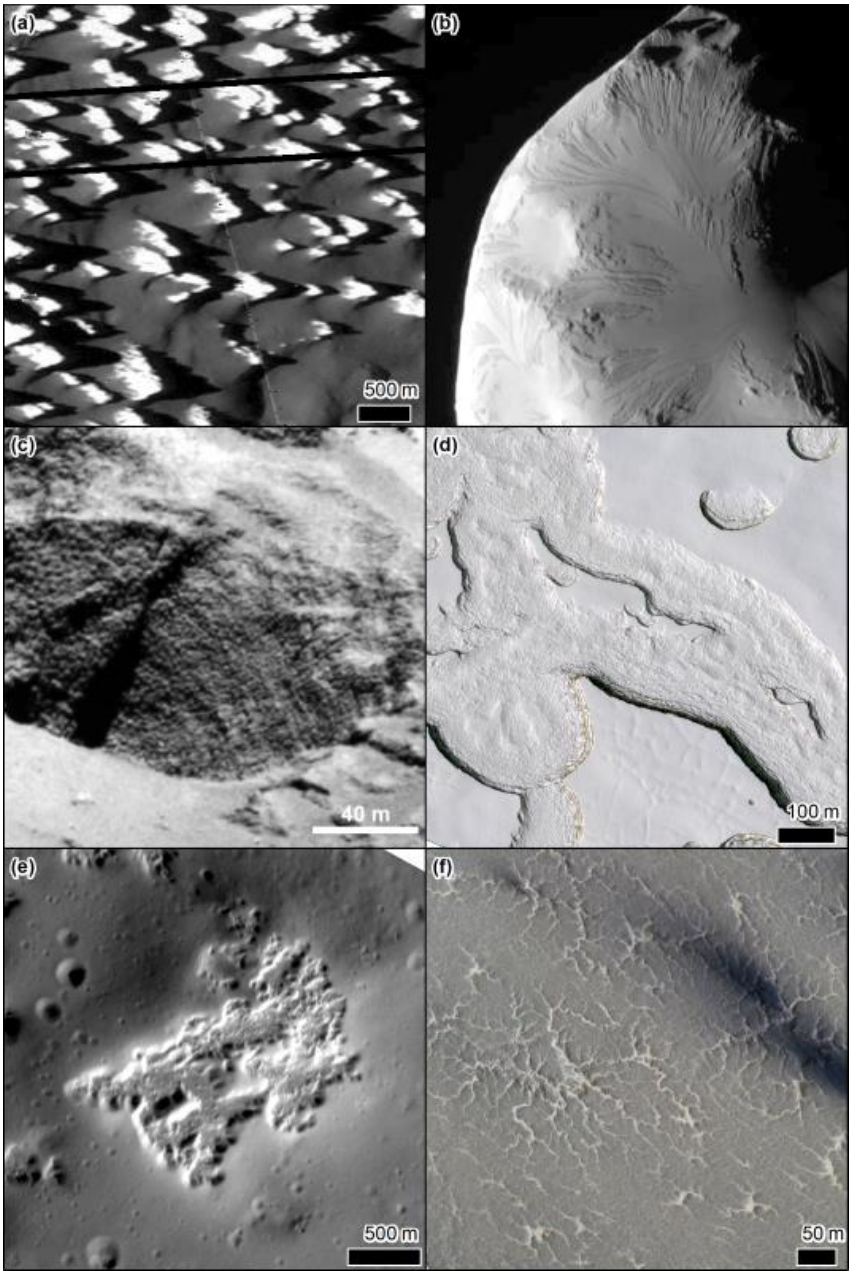

Figure 2.11: Sublimation dominated landscapes and landforms. a) Pinnacle terrain on Callisto Galileo SSI image 5214R, credit NASA/JPL-Caltech/SETI Institute. b) Image of the surface of Helene a moon of Saturn taken by the Cassini spacecraft image reference N1687119876_1, credit NASA/JPL-

Caltech/ASI, scene is about 30 km across. c) A steep pit revealing internal structure, on comet 67P/Churyumov–Gerasimenko taken by the OSIRIS narrow-angle camera, credit ESA/Rosetta/MPS for OSIRIS Team MPS/UPD/LAM/IAA/SSO/INTA/UPM/DASP/IDA. d) Siss cheese terrain in the co2 ice on the south polar cap of Mars, HiRISE image ESP_057828_0930, credit NASA/JPL/UofA. e) Hollows on Mercury, MDIS NAC image EN1042186062M, credit NASA/Johns Hopkins University Applied Physics Laboratory/Carnegie Institution of Washington. f) Spiders on Mars, where the dark marks are dust fans deposited by seasonal jets, HiRISE image ESP_055604_0930, credit NASA/JPL/UofA.

2.13 Discussion & Conclusions

Planetary geomorphology is distinctive from Earth-based geomorphology in that it is very reliant on remote sensing and often a more global-scale perspective is taken on unravelling the formation of landscapes and landforms. Satellite data of the Earth have spurred a number of studies taking a similar planetary-scale perspective on Earth (Chen et al., 2019; Poulos et al., 2012), but more often studies are local and/or regional in scale and scope. Planetary geomorphology is enticing to many, because of the aspect of exploration and the possibility of making unusual discoveries on alien worlds. Planetary geomorphology can drive key advances to better understand our own planet (Baker, 1993; Sharp, 1980).

One of the major limitations of planetary geomorphology is the problem of equifinality and the uncertainty of what landforms can be produced by processes unknown on Earth. To infer processes from landforms and landscapes is not an exact science and always open to interpretation. Access to the field can resolve many ambiguities on Earth, yet in a planetary context this is rarely an option and can lead to impasses where researchers just do not have enough data to disambiguate the leading hypotheses. Yet, as shown in this contribution, planetary geomorphology remains an essential tool in understanding the internal and external forces shaping bodies in the Solar System.

Planetary Geomorphology is likely to continue to grow, because the ability to interpret process from remote sensing data is key to planning future missions, for example deciding where to land or acquire certain types of data. Image and topographic data are the cornerstones of every new mission and future exploration will only add to our database of new and surprising planetary landforms and landscapes. Further, these landscapes have much to teach us about our own planet.

2.14 Acknowledgements

SJC is grateful to the CNES for financial support of her involvement in the ExoMars Trace Gas Orbiter CaSSIS, MRO HiRISE and BepiColombo missions. SJC received funding from the regional government Pays de la Loire scheme “Etoile Montantes” project METAFLOWS. The author thanks the spacecraft and instrument engineering teams for the successful completion and operation of CaSSIS. CaSSIS is a project of the University of Bern funded through the Swiss Space Office via ESA's PRODEX programme. The instrument hardware development was also supported by the Italian Space Agency (ASI) (ASI-INAF agreement no. I/018/12/0), INAF/ Astronomical Observatory of Padova, and the Space Research Center (CBK) in Warsaw. Support from SGF (Budapest), the University of Arizona (LPL) and NASA are also gratefully acknowledged. This study has been supported by the Italian Space Agency (ASI-INAF agreement no. 2020-17-HH.0).

3 The role of liquid water in recent surface processes on Mars

3.1 Introduction

This chapter is taken from Chapter 9 in the book "Mars Geological Enigmas – from the late Noachian to the present day" published in 2021 by Elsevier and edited by Richard J. Soare, myself, Jean-Pierre Williams and Dorothy Z. Oehler. The Chapter was led by myself and David Stillman assisted with the writing of Section 3.7.2 concerning Recurring Slope Lineae. In this modified version, I highlight at the end of each of the Sub-Sections of 3.7 in brown-coloured text my contributions to our understanding of the described landforms. Two additional sections have been added, Section 3.7.4 addresses the action of CO_2 on martian gullies, which in the book was dealt with in Chapter 10 by Colin Dundas (Dundas, 2021) and Section 3.7.7 addresses the role of water in landslides on Mars, which was not included in the original work.

Here, we provide an up-to-date review on the different landscapes and landforms that have been attributed to the action of liquid water in the Amazonian epoch on Mars and the current state-of-the-art regarding their interpretation. This chapter accompanies Dundas (2021) where the counterarguments are presented. The Amazonian epoch is thought to be dominated by hyper-arid climate conditions hostile to surface liquid water, and our review reveals that this steady-state is likely to be punctuated by episodic appearances of liquid water at the surface. The proposed sources of liquid water are varied: groundwater, thawing of surface-ice, deliquescence, ground-ice or glaciers, with triggers as variable as microclimates, climate-shifts, geothermal anomalies and impact cratering.

Our review covers recently active surface processes in the form of Slope Streaks, dark dune flows and Recurring Slope Lineae, all hypothesised at one point or another to be seeps of liquid water. We then cover landscapes and landforms which are proposed to be a result freeze-thaw cycles in the recent past, including gullies, lobate forms on hillslopes, pingo-like mounds, low-centred polygons, patterned ground and ice-loss landscapes. We present evidence that liquid water has been produced at the base of glacial landforms during the Amazonian, resulting in sinuous ridges (eskers) and enhanced crater-wall erosion. Liquid water brought up-from depth is thought to have produced mud-volcanos and other features related to sedimentary volcanism in the Amazonian and small fluvial channels amongst other features are thought to be related to melting induced by periodic impact events.

We end by summarising the importance of the search evidence of liquid water on Mars and by proposing solutions to the current impasses where progress is hindered due to limitations in data or our understanding.

3.2 Present-day and recent surface conditions on Mars

Of the planets of the Solar System Mars and Earth are the only two inner planets whose surfaces are thought to have hosted abundant liquid water early in their history (4.5-3.5 Ga). Liquid water is key for supporting life and seeking it out is a key tenet of astrobiology (Abrevaya et al., 2016). Hence, when searching for signs of extra-terrestrial life, space agencies have made Mars one of their principal targets. Mars is a rocky planet located outside Earth's orbit at a solar distance between 1.38 AU and 1.67 AU and has 1/3 the radius of the Earth (the mean martian radius is 3389.5 km). It orbits the sun in 687 earth days (~2 Earth years) and has a very similar day-length to the Earth (24hrs 37min). Its present-day axial tilt is close to the Earth's (25.19° compared to 23.44° on the Earth), giving rise to similar temporal and spatial patterns of insolation over a martian year. The eccentricity of the martian orbit is greater than the Earth (0.0935 compared to 0.0167), and the precession of its aphelion/perihelion through the seasons leads to greater seasonal amplitudes and asymmetries than

experienced on Earth. For example, with the current position of perihelion, the southern winters are relatively cold and short, compared to the southern winters which are less cold and longer. Mars lost its internally generated magnetic field approximately 3.6 Ga (Lillis et al., 2008; Milbury et al., 2012) that probably led to the loss of the majority of its atmosphere (Jakosky and Phillips, 2001). Surface geomorphology and sedimentary composition both point to declining activity of liquid water on Mars' surface over the last 3.5 Ga, which is strongly linked to the loss of Mars' atmosphere (Jakosky and Phillips, 2001). Mars' present-day atmospheric pressure ranges from 5-12 mbar (e.g., Hess et al., 1980; Ordonez-Etxeberria et al., 2019) and its main constituent gas is CO_2.

The low atmospheric pressure combined with the greater solar distance, mean that surface temperatures on Mars are on average much lower than on Earth (global mean is ~210K or -60°C) and the diurnal variation of temperature much greater. The lowest surface temperature is buffered around the condensation temperature of CO_2 at around 150K, while peak summer temperatures on and directly above favourable surface materials and orientations can exceed 300K (e.g., Stillman et al., 2014). The pressure and temperature conditions on present-day Mars mean that water should only be stable in solid or gaseous state. Atmospheric humidity on Mars is measured in precipitable microns, i.e. if the whole atmospheric column was condensed, only microns of water would result. Humidity typically ranges up to hundreds of precipitable microns (Smith, 2002), which is enough to generate, thin, yet visible surface frosts (Svitek and Murray, 1990). These general ranges of atmospheric pressure, humidity and temperature are below the triple point for liquid water, making this phase unlikely to occur in bulk.

However, there is theoretical and indirect evidence to support the possibility of thin films of water or brines developing within the martian soil at the present-day (e.g., Boxe et al., 2012; Jouglet et al., 2007; Kereszturi and Rivera-Valentin, 2012; Milliken et al., 2007; Möhlmann, 2008) or in the recent past (Sizemore et al., 2015). Pores within a regolith where water ice is also present can form microenvironments where the sublimation of the water ice can lead to increased humidity conditions (beyond those of the atmosphere). Under such conditions even at temperatures below the frost point transient liquid water films can form at the regolith or ice grain contacts and surfaces. Since data sent by the Phoenix mission (Hecht et al., 2009) perchlorate salts are now thought to be widespread on Mars (Glavin et al., 2013a; Navarro-González et al., 2010) and depress the freezing point and evaporation rate of water on Mars favouring the formation of thin liquid water films. Atmospheric humidity can increase to levels and beyond near the surface within the diurnal cycle (e.g., Maltagliati et al., 2011), and where the soil is in diffusive exchange with the atmosphere this could promote the formation of thin films of brine/water by deliquescence (Cull et al., 2014; Pál and Kereszturi, 2017). Additionally, even before a water saturated atmosphere is reached, perchlorate salts can adsorb water from the atmosphere via deliquesce and can form brines, which then have remarkable metastable properties (e.g., Gough et al., 2011; Nuding et al., 2015; Primm, 2018; Primm et al., 2018, 2019; Toner et al., 2014a). Whether or not such films constitute habitable environments has not reached consensus, but their water activity tends to be too low to support life (Jones and Lineweaver, 2012; Martín-Torres et al., 2015).

Some researchers have theorised that bulk transient liquid water could exist in the recent martian climate, either brought-up from underground aquifers (e.g., Gaidos, 2001; Goldspiel and Squyres, 2011; Malin and Edgett, 2000; Stillman et al., 2016) or melted from ice under extremely rare favourable combinations of temperature, and humidity conditions (e.g., Chevrier and Rivera-Valentin, 2012; Grimm et al., 2014; Hecht, 2002; Kossacki and Markiewicz, 2010). Melting from surficial ice is particularly difficult as there is a kinetic barrier to melting even if conditions are

conducive: because latent heat is consumed by sublimation at the surface of the ice which prevents the temperature from rising sufficiently to allow melting to occur (Mellon and Phillips, 2001).

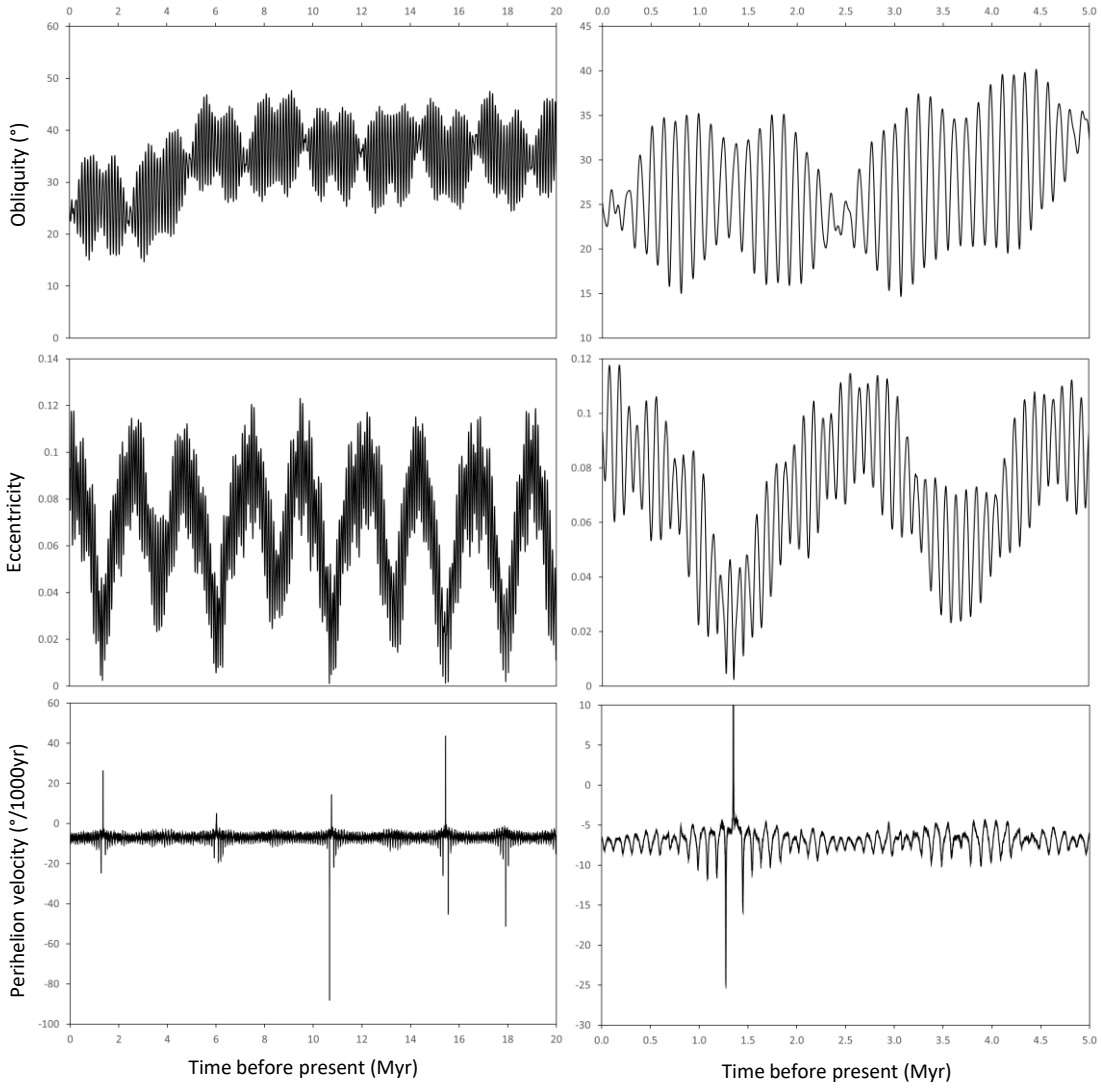

Figure 3.1: Secular changes in Mars orbital parameters for the last 20 Myr and 5 Myr as calculated by Lascar et al. (2004) *with initial conditions of Yoder et al.* (2003) *downloaded from: http://vo.imcce.fr/insola/earth/online/mars/La2003-04/index.html*

Many researchers have hypothesised that Mars' climate was substantially different in the recent past and may have been more conducive than at the present-day to the emergence and stability of liquid water (e.g., Costard et al., 2002; Richardson and Mischna, 2005). This is because Mars' orbital parameters (Figure 3.1) are much more variable than those of Earth and we already know that Earth's climate undergoes glacial-interglacial cycles as a result of periodic changes in orbital obliquity, eccentricity and the solar longitude L_s of perihelion – so called Milankovitch cycles – which change the amount and distribution of incoming solar radiation. Hence, the larger variations experienced by Mars should have more impact on the climate system than on Earth. Having a lower mass (i.e. moment of inertia) than the Earth and without a large Moon to stabilise the planet, Mars' axial tilt (obliquity) has varied between 15° and 40° in the last 5 Ma (compared to ±1.3° around the present value for Earth) with a period of 120 ka. Mars' eccentricity varies between 0 and 0.12 (compared to 0 to 0.068 for Earth) over 95 ka and L_s of perihelion takes ~51 ka years to return to its starting season

(Figure 3.1) (Ward, 1992, 1979, 1974). Global Climate Models (GCMs) have been used to try and predict the influence that these orbital changes should have on Mars' climate. Despite these large variations in incoming radiation, the low atmospheric pressure on Mars means that reaching the triple point of water is still challenging (Richardson and Mischna, 2005). Using current values for atmospheric pressure with obliquity at 35° Richardson and Mischna (2005) predict at most 100 days per year of transient liquid water (i.e. the time above the triple point) located at the base of Hellas Basin. It is hypothesised that at very high obliquities (>35°) sufficiently intense incoming solar radiation, at certain latitudes and times of year, means that ground ice could melt if it is protected from the low atmospheric pressure by an overburden slowing heat-loss by sublimation and impeding gas diffusion (e.g., K. E. Williams et al., 2009). At such obliquities, the two water ice polar caps are sublimated away due to the increased insolation at the poles. This significantly increases the atmospheric water vapour concentration (Mellon and Jakosky, 1995) and leads to a massive redistribution of water ice by cold trapping in the mid latitude region that is the coldest. It is also the region that experiences the most intense increases in solar radiation, so it is at the mid-latitudes where the most intense surface-atmosphere exchange of water is thought to occur. Conversely, at obliquities <17°, the atmospheric water vapour concentration decreases by more than an order of magnitude from the current value (Mellon and Jakosky, 1995) and prevents migration of any atmospheric water vapour. The recent discovery of large volumes of CO_2 ice sequestered in the south polar cap (Bierson et al., 2016; Manning et al., 2019; Phillips et al., 2011), opens up the possibility for a slightly higher atmospheric pressure (Buhler et al., 2019; Manning et al., 2006) than assumed by previous modelling studies, which would allow liquid water to be stable for a few more degrees above freezing before it boils.

These conditions – that of a hyper-arid cold desert – have thought to have reigned on Mars during the whole Amazonian period (since ~3 Ga) even if uncertainties in the orbital solutions do not allow us to predict the orbital parameters further than several tens of millions of years in a reliable way.

3.3 Present-day reservoirs of water on Mars

Even if surface conditions allow for the presence of liquid water, there must be a source of water (ice or vapour) for liquid water to be produced. Precipitation in the form of rain is generally accepted to be highly unlikely during the Amazonian (since ~3 Ga). There are three potential reservoirs for water: seasonally deposited ices/frosts from vapour in the atmosphere, surface ice reservoirs, or underground aquifers. Here, surface ice reservoirs are defined as those ices which can be reasonably considered to have exchanged with the atmosphere under Amazonian climate conditions. We discuss each of these sources in turn below and their likelihood for generating liquid water.

3.4 Seasonal ices and frosts

The most visible manifestation of Mars' seasonal cycle is the waxing and waning of the seasonal polar caps, which were noted even in early telescopic observations (Herschel, 1784). The seasonal polar caps comprise atmospherically deposited seasonal ices that brighten the surface. The majority of the ice is comprised of CO_2 and as a result the deposition of the seasonal ices causes a substantial fluctuation in the atmospheric pressure (Haberle et al., 2017). A minor component of water ice is included in these ices (Appéré et al., 2011; Brown et al., 2012, 2010). The ices are thought to originate as directly condensed frosts or fall as snow (e.g., Giuranna et al., 2008; Hayne et al., 2014), with direct observation being hindered by the polar hood (low lighting combined with a hazy atmosphere). The continuous seasonal polar caps, comprised of CO_2 and a minor component of H_2O, extend to 50-55° in both hemispheres (e.g., Piqueux et al., 2015) and are thought to reach a thickness of metres near the poles (e.g., Karatekin et al., 2006; Smith et al., 2001). Discontinuous deposits of ices are found down to latitudes of 30° in both hemispheres (Dundas et al., 2019a; Vincendon et al.,

2010b, 2010a), where water ice is found to lower latitudes than CO_2 ice. Discontinuous CO_2 extends to 35°S on steep pole-facing slopes in the southern hemisphere (Vincendon et al., 2010b), but its extent has not yet been measured in the northern hemisphere. Sublimation of the seasonal ices drives peaks in atmospheric water vapour to around tens of precipitable microns (Pankine et al., 2010; Pankine and Tamppari, 2019). Water ice frost forms an annulus around the retreating seasonal ices and as it sublimates is cold-trapped onto the retreating CO_2 ice before sublimating again later. Exchange of water vapour between hemispheres is strongest during the solstices (Haberle et al., 2017).

In general, water frosts and ices deposited seasonally are deemed to be unlikely sources of liquid water at the present-day and in the recent past, due to the very small quantities and the kinetic barrier to melting discussed in Section 3.2.

3.5 Surface Ice reservoirs

Surface ice reservoirs are our most accessible evidence that Mars has abundant water, and these can be split into:

- The polar caps (~10^6 km^3 each) (Plaut et al., 2007; Selvans et al., 2010)
- Mid-latitude glaciers (~10^5 km^3) (Levy et al., 2014)
- Ground ice (~10^4 km^3) (Conway and Balme, 2014; Kreslavsky and Head, 2002; Mustard et al., 2001)

Radar data have confirmed that the polar caps are almost exclusively water ice (Plaut et al., 2007; Selvans et al., 2010). The polar caps are the most voluminous reservoir of water on Mars and form upstanding broadly domal landforms with up to three kilometres of relief (Plaut et al., 2007; Selvans et al., 2010). The internal structure of the two caps is broadly similar, comprising layers of ice with variable dust-contents, visible in surface exposure at internal scarps and at depth via radar sounding (e.g., Becerra et al., 2017; Blasius et al., 1982; Fishbaugh and Hvidberg, 2006; Plaut et al., 2007; Selvans et al., 2010) and thus are generally accepted to form via atmospheric deposition of water ice. Both caps are dissected by spiral troughs which are thought to form during cap accumulation through a balance between sublimation and accumulation (Bramson et al., 2019; Smith et al., 2013; Smith and Holt, 2010) and they are more marked in the northern cap than in the southern cap. However, in the detail the two caps are quite different, likely as a result of the huge difference in altitude between the two hemispheres (base at -5000 m in the north and +1000 m in the south), which has a profound effect on atmospheric circulation (e.g., Haberle et al., 2017). The northern polar cap has a younger surface age than the southern cap (a few thousand compared to ~10 Ma; Herkenhoff and Plaut, 2000; Landis et al., 2016), and its bulk is estimated to have formed in the last few millions of years (Jakosky et al., 1995; Laskar et al., 2002; Levrard et al., 2007) even though its surface may be being continuously renewed (Herkenhoff and Plaut, 2000; Landis et al., 2016). It is thought to comprise a lower unit of ice-rich sands and an upper unit of polar layered deposits. It is broadly centred on the pole and is surrounded by outliers which formed separately (Bapst et al., 2018; Brothers and Holt, 2016; Brown et al., 2008; Conway et al., 2012). Hovius et al. (2008) suggested that some re-entrants into the cap represented channels carved by water released by volcanic heating, but later work showed these features were more consistent with wind erosion (Brothers et al., 2013). In contrast, the southern polar cap is located off-centre with respect to the southern pole and only a very small proportion of the cap has exposed water ice at the surface in summer (Hansen et al., 2005), compared to the complete exposure expressed by the northern cap.

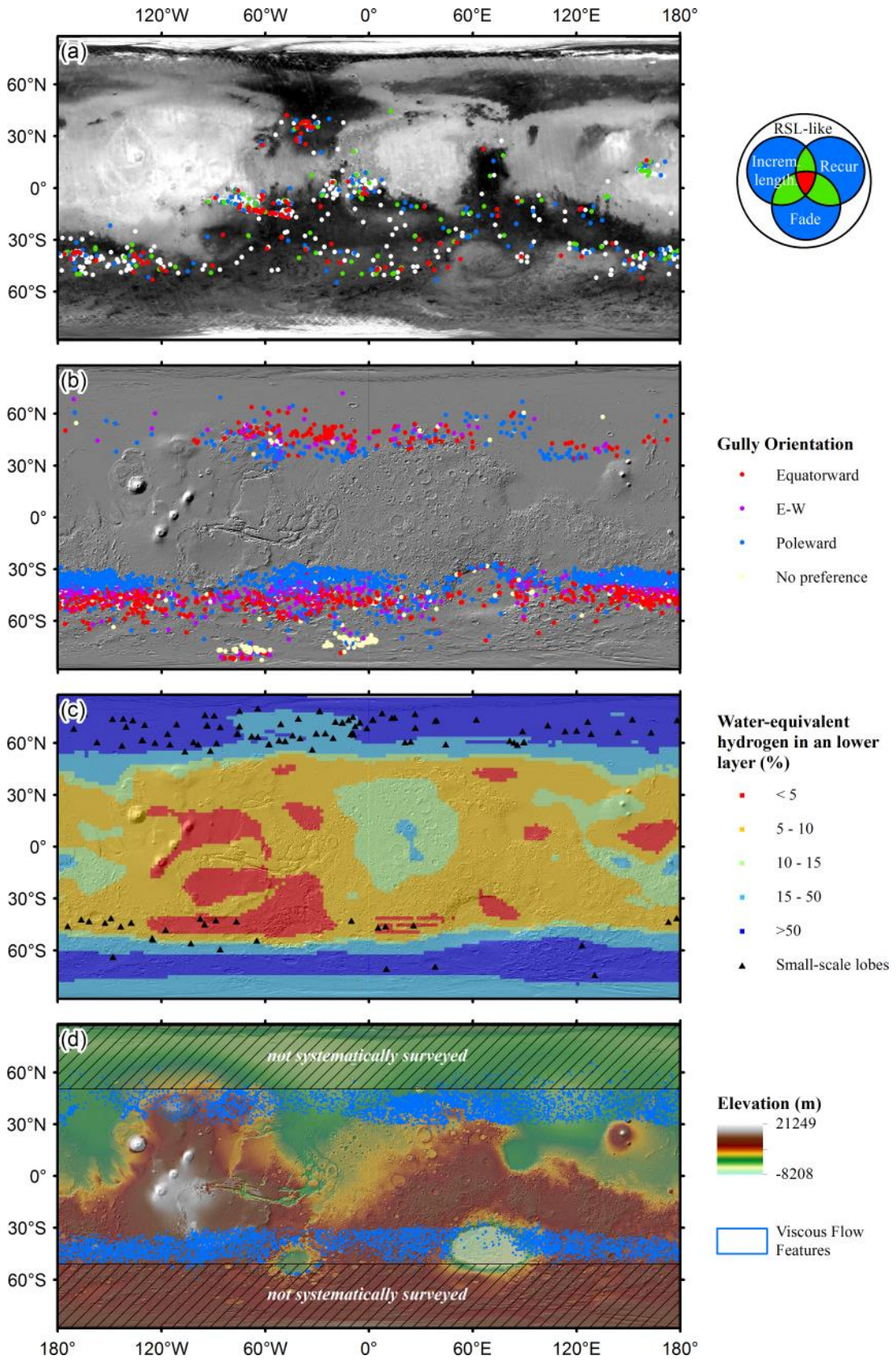

Figure 3.2: Global distribution of relevant landforms in the quest for evidence of liquid water on Mars. (a) Mars Odyssey Thermal Emission Spectrometer global albedo map overlain by the global distribution of Recurring Slope Lineae (RSL), where the legend to the right shows how many RSL attributes are displayed at each site, a confirmed RSL site being in red having evidence of incremental

lengthening, recurrence and fading. (b) Mars Orbiter Laser Altimeter (MOLA) derived shaded relief map overlain with the locations of gullies as published by Harrison et al. (2015)*. (c) Semi-transparent MOLA-derived shaded relief map with water equivalent hydrogen data from Pathare et al.* (2018) *overlain with locations of small-scale lobes from Johnsson et al.* (2018)*. (d) Semi-transparent MOLA-derived shaded relief map with colour-keyed MOLA-elevation overlain by the locations of glacial forms, or VFF as mapped by Levy et al.* (2014)*.*

The bright part of the cap is instead CO_2 ice. The deep structure of the polar cap has been harder to decode than for the northern cap because there are significantly fewer internal radar reflections. The cap is believed to have a series of packets of polar layered deposits with significant zones where CO_2 is thought to be sequestered (Bierson et al., 2016; Manning et al., 2019; Phillips et al., 2011). Much of the cap is covered by dust and hence has a lower albedo than exposed ice (Herkenhoff, 2001). The surface of the exposed cap is covered by a metres-thick layer of CO_2 ice which is currently retreating at metres per year (Buhler et al., 2017; Byrne, 2003; Thomas et al., 2009). There are numerous outliers of the southern cap and these might represent a more extensive cap in the past (Sori et al., 2019; Westbrook, 2009). Ancient units that surround the south polar cap (e.g., Fastook et al., 2012; Head and Pratt, 2001; Scott and Tanaka, 1987) are thought to represent water production at the base of the cap, which will be discussed in more detail in Section 3.7.6 in the context of a recent report of sub-glacial lakes found via radar sounding under the southern polar cap (Lauro et al., 2020; Orosei et al., 2018).

The mid-latitude glaciers are common and widespread across areas with topographic relief in the mid-latitudes (30-60°; Figure 3.2d) and have been classified by morphology and context into several groups including: viscous flow features (VFF), Concentric Crater Fill (CCF), Lobate Debris Aprons (LDA), Lineated Valley Fill (LVF) and Glacier-Like Forms (GLF). The glacial origin of all these features has now been generally accepted with the most convincing evidence coming from orbital sounding radar (Holt et al., 2008; Petersen et al., 2018; Plaut et al., 2009) and further conformed by their overall shape/form and surface textures (e.g., Baker and Carter, 2019a, 2019b; Head et al., 2010; Karlsson et al., 2015; Levy et al., 2009b; Mangold, 2003; Parsons et al., 2011). These glaciers are thought to comprise almost pure ice with a metres- to decametres-thick debris cover derived from the headwall and englacial materials. The present-day systems are believed to be out of equilibrium with the current climate and show extensive evidence for retreat and downwasting (Brough et al., 2016). Superposition relationships (Hepburn et al., 2019) and estimations of age derived from crater-size frequency distributions on their surfaces suggest that they formed during several “glacial maxima” over the last tens to hundreds of millions of years (Baker et al., 2010; Berman et al., 2015; Hartmann and Werner, 2010; Morgan et al., 2009). Each individual feature is likely to represent a series of ice-accumulation events (Fastook and Head, 2014; Weitz et al., 2018). As a general rule, martian glaciers are thought to be cold-based, i.e. no melting occurs near the base as is common in terrestrial glaciers, and they move via viscous deformation of the ice, rather than sliding over their bed (e.g., Parsons et al., 2011), which is consistent with their form. Possible exceptions to this general rule will be discussed in Section 3.7.6.

Ground ice is extensive on Mars and is spatially associated with surface deposits that tend to drape the topography, variously termed “mantling units”, “mantle”, latitude dependant mantle”, “pasted on terrain”, ”dust-ice mantle” amongst other terms. The main line of evidence for ground ice comes from the neutron spectrometer on Mars Odyssey (Boynton et al., 2002; Feldman et al., 2011, 2008, 2007, 2004; Maurice et al., 2011; Pathare et al., 2018; Wilson et al., 2018), where the content of ice in the top metre of the regolith is estimated to be 50-80% at latitudes >50°N/S (Figure 3.2c). These predictions were shown to be locally valid by the Phoenix lander, which found ice at depths of a few

centimetres both in the form of pore-filling ice and excess ice (Mellon et al., 2009). Surface temperature data from Mars Climate Sounder and Thermal Emission Imaging System indicate that ice occurs within centimetres to tens of centimetres of the surface at latitudes down to 35°N/45°S (Piqueux et al., 2019). In addition, high ice-contents from the neutron data correlation spatially with the observations of polygonally patterned ground (e.g., Levy et al., 2010b; Mangold, 2005), which is generally accepted to be a result of thermal contraction of ice-cemented ground (Mellon, 1997). Phoenix landed amongst such polygons and excavated and detected ground ice with a mean depth of 4.6 cm (Mellon et al., 2009). Additionally, Phoenix also detected segregated ice above the ground ice table. New impacts that reveal ice in their ejecta generally confirm this distribution (Byrne et al., 2009; Dundas et al., 2020, 2014), and even extend to lower latitudes (~40°) where the ice is predicted to be deeper than can be detected by the neutron spectrometer. At these latitudes, the surface mantling units become dissected, exposing layering and exhibiting pitting (Milliken et al., 2003; Schon et al., 2009b). These discontinuous mantles are found preferentially on pole-facing slopes at lower latitudes (e.g., Christensen, 2003). This latitude marks the boundary where the topography at scales of hundreds of metres becomes measurably smoother where these mantles are present (Kreslavsky and Head, 2002, 2000).

Ground ice is thought to be responsive to climate change and in diffusive equilibrium with the current climate (Aharonson and Schorghofer, 2006; Mellon and Jakosky, 1993; Schorghofer and Aharonson, 2005). The relationship between the near-surface ground ice detected by the neutron and thermal orbital data and the surface mantling units (with their ice content) is ambiguous. In some cases such surface mantling units can be locally decametres thick and have evidence for massive ice, from geomorphic and radar evidence (Bramson et al., 2015; Conway and Balme, 2014; Dundas et al., 2018; Stuurman et al., 2016). Such enrichments cannot come about from atmospheric diffusion into the regolith because of self-blocking, even if this can be bypassed by contraction cracking (Fisher, 2005) only tens of centimetres depths can be reached (see Section 3.7.5.4). The alternative is that these mantles represent units laid down under past high-obliquity climate conditions when snow/frost could be directly accumulated at the surface (Head et al., 2003; Madeleine et al., 2014, 2009) and protected from later sublimation by the accumulation of a sublimation lag of atmospherically derived dust centimetres in thickness. However, a universal composition of nearly pure ice for these units is not supported by the geomorphic evidence, which rather suggests development of the ground ice within a regolith matrix, i.e. excess ice (e.g., Levy et al., 2010b; Pathare et al., 2018; Soare et al., 2015). We discuss the development of excess ice further in the context of ice-loss landforms in Section 3.7.5.5.

Ground ice is generally considered to be an improbable, but still viable source for liquid water in the present and recent-past, as the soil above protects it from sublimation, removing some of the constraint of the kinetic barrier to melting.

3.6 Subsurface water reservoirs

Numerous authors have hypothesised the presence of aquifers on Mars (e.g., Abotalib and Heggy, 2019; De Toffoli et al., 2019; Gaidos, 2001; Goldspiel and Squyres, 2011; Salese et al., 2019), initially as a way to explain the fate of the large quantity of liquid water that is thought to have existed on Mars early in its history, as evidenced by the existence of the extensive valley networks (e.g., Craddock and Howard, 2002; Hynek et al., 2010; Hynek and Phillips, 2003; Kereszturi and Petrik, 2020; Luo et al., 2017; Penido et al., 2013; Williams and Phillips, 2001), the clay deposits found in Noachian terrains (e.g., Carter et al., 2015; Ehlmann et al., 2011b; Loizeau et al., 2007; Lowe et al., 2020, 2020; Milliken and Bish, 2010; Poulet et al., 2005), the outflow channels dated to the Hesperian or later (Andrews-Hanna and Phillips, 2007; Komar, 1979; Leask et al., 2007; Marra et al.,

2014; Max and Clifford, 2001; Montgomery and Gillespie, 2005; Vijayan and Sinha, 2017; Wilson, 2004) and the hypothesised northern ocean (e.g., Baker et al., 1991; Carr and Head, 2019; Clifford and Parker, 2001; Palumbo and Head, 2019). Mars is thought to possess a deep cryosphere (Carr, 1996; Clifford et al., 2010; Grimm et al., 2017; Lasue et al., 2019), where this cryosphere is impinged on by the geothermal heat flux, liquid water is thought to exist. Tectonic and surface temperature fluctuations perturbing the pressure state of this aquifer are thought to be responsible for the hundred-kilometre scale outflow channels which occurred in the Hesperian (Baker, 1979; Carr, 1979; Coleman, 2005; Harrison and Grimm, 2008; Marra et al., 2014). Smaller, yet similar perturbations have been proposed to explain gullies and RSL (Abotalib and Heggy, 2019; Gaidos, 2001), bringing up water from kilometres in depth. Shallower surface aquifers, including perched aquifers, have also been proposed (Goldspiel and Squyres, 2011; Marquez et al., 2005), but these are within reach of the orbital ground penetrating radars, such as the European Space Agency's MARSIS and NASA's ShaRAD, which have found no evidence for such bodies of water (Nunes et al., 2010). The non-detection of shallow aquifers by orbital radar is not definitive proof of their absence because the penetration of these radars into the martian crust is much lower than initially anticipated (Stillman and Grimm, 2011) and they are limited to detecting interfaces that aquifers may in fact not present (Farrell et al., 2009; Nunes et al., 2010).

Circulation of groundwater in the past has been hypothesised from in situ observation of post-digenetic alteration products, such as veins and nodules (e.g., Chan et al., 2004; L'Haridon et al., 2018; Stack et al., 2014) found within the sedimentary rocks deposited in impact craters and evidence from meteorite studies (Bridges et al., 2001; Gillet et al., 2002; Schwenzer et al., 2016), evidence for sedimentary volcanism (e.g., Brož et al., 2019; Gallagher et al., 2018; Oehler and Allen, 2010; Okubo, 2016; Skinner and Mazzini, 2009; Wheatley et al., 2019), and orbital detection of hydrothermal alteration products (e.g., Bishop et al., 2004; Ehlmann et al., 2011a; Viviano et al., 2013). Hence, present-day impingement of these hypothesised aquifers on the surface is hard to rule out and often relies on arguments based around Occam's razor – the simplest hypothesis is the most likely – as proving/disproving the presence of aquifers relies on knowledge of the subsurface that we do not have. So, unlike the other reservoirs of water discussed above, the presence of deep or shallow aquifers (and the cryosphere) remains purely hypothetical and would require considerable progress in our understanding of Mars to prove or disprove. Nevertheless liquid water sourced from aquifers is generally perceived to be unlikely to cause present-day or recent (last few millions of years) surface modifications, because of arguments based on structural and topographic context that will be discussed in Section 3.7.3 (e.g., Treiman, 2003). It is generally considered as a viable source of liquid water in the early Amazonian (Baker and Milton, 1974; Dohm et al., 2001; Rodriguez et al., 2015).

3.7 What is the evidence for recent liquid water on Mars?

As detailed above, our knowledge of the current surface temperature, pressure and humidity conditions on Mars and our expectations derived from Global Climate Models of the recent past, and lack of knowledge regarding the deep subsurface of Mars means that researchers believe that the production of surface liquid water is unlikely. Hence, evidence presented in favour of near-surface liquid water on Mars is, almost without exception, highly scrutinised. Despite this many surface features have been ascribed to the action of surface liquid water often in tight analogy with equivalent landforms found on Earth.

Below each of the major landscape elements that have been used to argue for recent surface water on Mars are described, the evidence supporting its generation by liquid water summarised and the

current assessment of the likelihood of the liquid water hypothesis described. The topics are addressed in a rough chronological order starting at the present-day and working towards the past.

3.7.1 Slope Streaks and dark dune flows

Three broad types of low albedo downslope-oriented "streaks" resembling a downslope flow have been observed to form at the present-day on Mars: Recurring Slope Lineae, Slope Streaks and dark dune flows. All three have been linked to liquid water occurrence at the present-day on Mars. Recurring Slope Lineae are detailed in the next section.

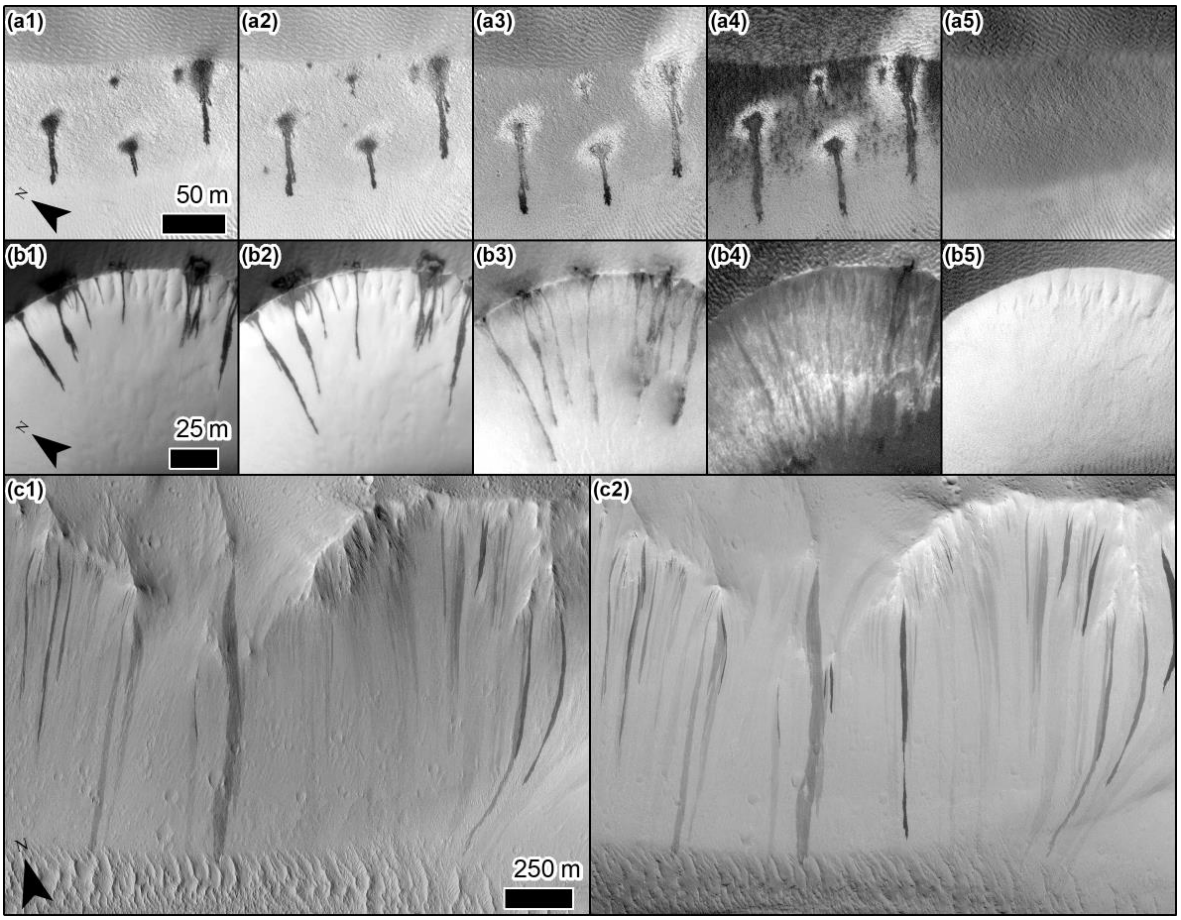

Figure 3.3: Examples of dark dune flows and slope streaks on Mars. Each letter represents a location while each number represents a different time of year. Please note each panel has been individually contrast-stretched to enhance visibility. Panels a1-5 show the evolution of a dark flows emanating from dark spots on the slip face of a linear dune in Richardson Crater (72.0°S, 179.4°E) in the southern hemisphere from MY27 Ls 210-340°. Note the development of the bright halo, the darker albedo at the tip of the flow and the lack of any morphological signature once the frost is removed. Panels b1-5 show the evolution of a dark flows located on the slip face of a barchan dune at a site informally named "buzzel" (84.0°N, 233.2°E) in the circum-polar erg in the norther hemisphere in MY 29 from Ls 029-087°. Again, note the lack of morphological signature once activity is over. Panels c1-2 show the appearance of new slope streaks on a slope located in the mid-latitude region of Mars (31.1°N, 226.0°E) in MY 31. HiRISE images: a1 PSP_003175_1080 Ls=210.6°, a2 PSP_003386_1080 Ls=220.7°, a3 PSP_003742_1080 Ls=238.1°, a4 PSP_003953_1080 Ls=248.5°, a5 PSP_005931_1080 Ls=340.4°, b1 PSP_007193_2640 Ls=28.8°, b2 PSP_007404_2640 Ls=36.3, b3 PSP_007905_2640 Ls=53.7°, b4 PSP_008248_2640 Ls=65.5°, b5 PSP_008867_2640 Ls=86.6°, c1 ESP_027092_2115 Ls=107° and c2 ESP_031971_2115 Ls=323°. Credit NASA/JPL/UofA.

Slope Streaks (Figure 3.3c) can be metres to kilometres in total length and they originate on steep slopes (e.g., Sullivan et al., 2001) in the equatorial regions of Mars. They often originate at a point, fan out to reach a maximum width, then terminate in a series of digitate lobes (e.g., Schorghofer et al., 2007) yet their detailed morphology seems to depend on the shape of the underlying slope (e.g., Dundas, 2020). Unlike RSL and dark dune flows, Slope Streaks show no incremental growth between images, but simply appear in any given image at their full extent (e.g., Schorghofer et al., 2007). Also, older streaks can appear bright compared to the surrounding terrain (e.g., Aharonson et al., 2003; Baratoux et al., 2006), which is unlike RSL and dark dune flows. Slope Streaks seem to remove a thin layer of material along their path and may push some material aside (Chuang et al., 2007; Phillips et al., 2007). Slope Streaks are found in dusty, low thermal inertia areas of Mars, so are generally assumed to be dry avalanches of dust (e.g., Dundas, 2020; Sullivan et al., 2001). The involvement of liquid water has been hypothesised, based on their occurrence on slopes whose temperatures can exceed 273K (Schorghofer et al., 2002), a bias in their occurrence towards warmer times of year (Heyer et al., 2019), interaction with topographic obstacles (Brusnikin et al., 2016; Kreslavsky and Head, 2009), extension onto low slopes and correspondence with terrains high in Cl and Fe (i.e. availability of salts to produce brines; Bhardwaj et al., 2017). None of these observations are completely diagnostic and dry dust avalanches could have a rheology that also satisfies these constraints (Bhardwaj et al., 2019a; Dundas, 2020; Miyamoto, 2004).

Dark dune flows (Figure 3.3a,b) are a strictly seasonal phenomena strongly linked to the defrosting phase during the retreat of the seasonal ices in spring and as the name suggests are only found on dark sand dunes (near the poles in both hemispheres). They are metres to hundreds of metres in overall length and develop from dark spots that appear on the seasonal ice cover. They grow incrementally as the seasonal progresses and are no longer visible once the seasonal ice cover has sublimated away, which contrasts with RSL which tend to gradually fade (e.g., McEwen et al., 2011) and slope streaks that can persist for decades (e.g., Schorghofer et al., 2007). Their development follows the same sequence of events: a) development of a dark spot, b) propagation of the flow away from the spot, c) development of bright halos in some cases and d) as propagation progresses the tip of the flow is darker than the source spot and terminates in a wider section. The general consensus is that the initial dark spots are formed by the “Kieffer model” (Kieffer et al., 2006) – this model describes the formation jets of CO_2 gas generated by basal sublimation of the seasonal translucent CO_2 slab ice. The basal sublimation builds pressure under the slab ice that when released by cracking entrains dust/sand that are then deposited around the crack forming a dark spot/fan at the surface. It is proposed that salt can also be included within these deposits and that the dark flows can be explained by the propagation of brines generated as interstitial water from cold-trapped water ice and preferential heating of the sediments forming the dark spot (Kereszturi et al., 2011b, 2011a, 2010, 2009; Kereszturi and Appéré, 2014; Kereszturi and Rivera-Valentin, 2016, 2012; Möhlmann and Kereszturi, 2010; Möhlmann, 2010, 2008, 2004). However, dry mass wasting phenomena driven by sublimation dynamics cannot be ruled out given the morphological, temperature and spectral constraints (Gardin et al., 2010; Hansen et al., 2013; Horvath et al., 2009).

Although water has been proposed for the formation of Slope Streaks and dark dune flows, the evidence presented to date favours dry avalanches and CO_2 ice sublimation mechanisms respectively.

My contribution to the state-of-the-art: Although I have not directly published on Slope Streaks and dark dune flows, both phenomena are found alongside other ongoing surface processes on Mars which I have studied. Slope Streaks associated with rockfalls are part of my ongoing work (Grindrod et al., 2021; Vijayan et al., 2021). These works suggest that Slope Streaks are more likely a dry phenomenon as they seem to be triggered by rockfall impacts and potentially the same seismic

shaking that leads to rockfalls themselves. Dark dune spots and flows occur alongside gullies on dunes, which will be discussed in Section 3.7.3. Our work shows that these spots and flows seem more likely to be promoted by the "Kieffer model", as their timing and evolution over time corresponds better with climate models predictions of when this effect should occur (Jouannic et al., 2019). How the spots transform into what appear to be ground-hugging flows remains a subject of ongoing research. Our work also suggests that dark flows may be part of the sediment transport cascade that promotes activity in gullies in general (Raack et al., 2020).

3.7.2 Recurring Slope Lineae (RSL)

Recurring slope lineae are a seasonal phenomenon characterised by downslope propagating relatively low albedo streaks up to hundreds of metres in length and generally metres to tens of metres in width (Figure 3.4). They were first identified thanks to repeated HiRISE images and are distinct from slope streaks and dark dune flows by growing at the warmest times of year (for a given slope and slope-orientation) and then fading until the pattern is repeated the following year (McEwen et al., 2011). It is this incremental downhill growth that led researchers to initially interpret these features as being driven by liquid water. This is because slope streaks and wind streaks, which are thought to be produced by dry granular flows (e.g., Chuang et al., 2007; Sullivan et al., 2001) or the removal of dust (Vincendon et al., 2015), respectively, do not grow, but are emplaced instantaneously (at the temporal scale of orbital observations). Although there may be mechanisms by which dry granular flows could mimic this behaviour (Dundas, 2021). RSL occur in exclusively areas that have a low abundance of surficial dust (unlike Slope Streaks which only occur on high albedo dusty slopes) and tend to originate at rocky outcrops towards the top of steep slopes. They are found in dense concentration in the Valles Marineris (VM; Chojnacki et al., 2016; McEwen et al., 2014; Stillman et al., 2017), but also on steep slopes in the northern (Stillman et al., 2016) and southern mid-latitudes (Stillman et al., 2014; Stillman and Grimm, 2018) (Figure 3.2b) and at tropical latitudes outside of VM (Stillman and Grimm, 2018). They often occur in association with mid-latitude or equatorial gullies (which are described further in Section 3.7.3): either on gully-interior slopes, or on slopes directly neighbouring the gullies.

RSL can be found individually or occur as dense concentrations and they tend to originate at the same place every year. Their overall length varies from year to year and neighbouring RSL can have different growth rates, and in certain locations an RSL can lengthen at the same time its neighbour is fading (Stillman et al., 2020, 2017). Their path downslope deviates around obstacles (Figure 3.4a-c, g-i) suggesting that they have little momentum and that the flow is thin compared to the obstacles visible at HiRISE resolution (~25 cm/pix). RSL can come together downslope (Figure 3.4c, f), split (Figure 3.4c, k) and have some limited sinuosity (Figure 3.4b, i). In Valles Marineris RSL are spatially and temporally associated with slumps in the loose materials over which they propagate (Chojnacki et al., 2016; Ojha et al., 2017) (Figure 3.5). Such slumps extend much further downslope than RSL, have similar albedos, fading timescale, and slopes (27.5° ± 2.7°; Stillman et al., 2020). RSL are most easily identified on materials that are generally smooth at the HiRISE scale (no grains >75 cm), but can be found on slopes covered in clasts (Figure 3.4d-f). They can propagate down pre-existing channels (Ojha et al., 2014), including gully channels. They tend to be restricted to slopes above the angle of repose (Dundas et al., 2017), but are found to extend to lower slopes (Schaefer et al., 2019; Stillman et al., 2020; Tebolt et al., 2020). However, RSL form on the upper reaches of scree slopes likely formed via mass wasting and are naturally at the angle of repose. Thus, just because RSL form on such a feature does not require that RSL be interpreted as a dry sediment flow (Tebolt et al., 2020). Isolated dark spots have been observed in rare cases immediately downslope of actively growing RSL, argued to be discontinuous RSL (Figure 3.4e) (Ojha et al., 2015; Tebolt et al., 2020). Stillman et al. (2017) interpreted such features as the "porpoising" of water flow,

where water flowing under the surface was only sucked to the surface via capillarity in locations of low albedo.

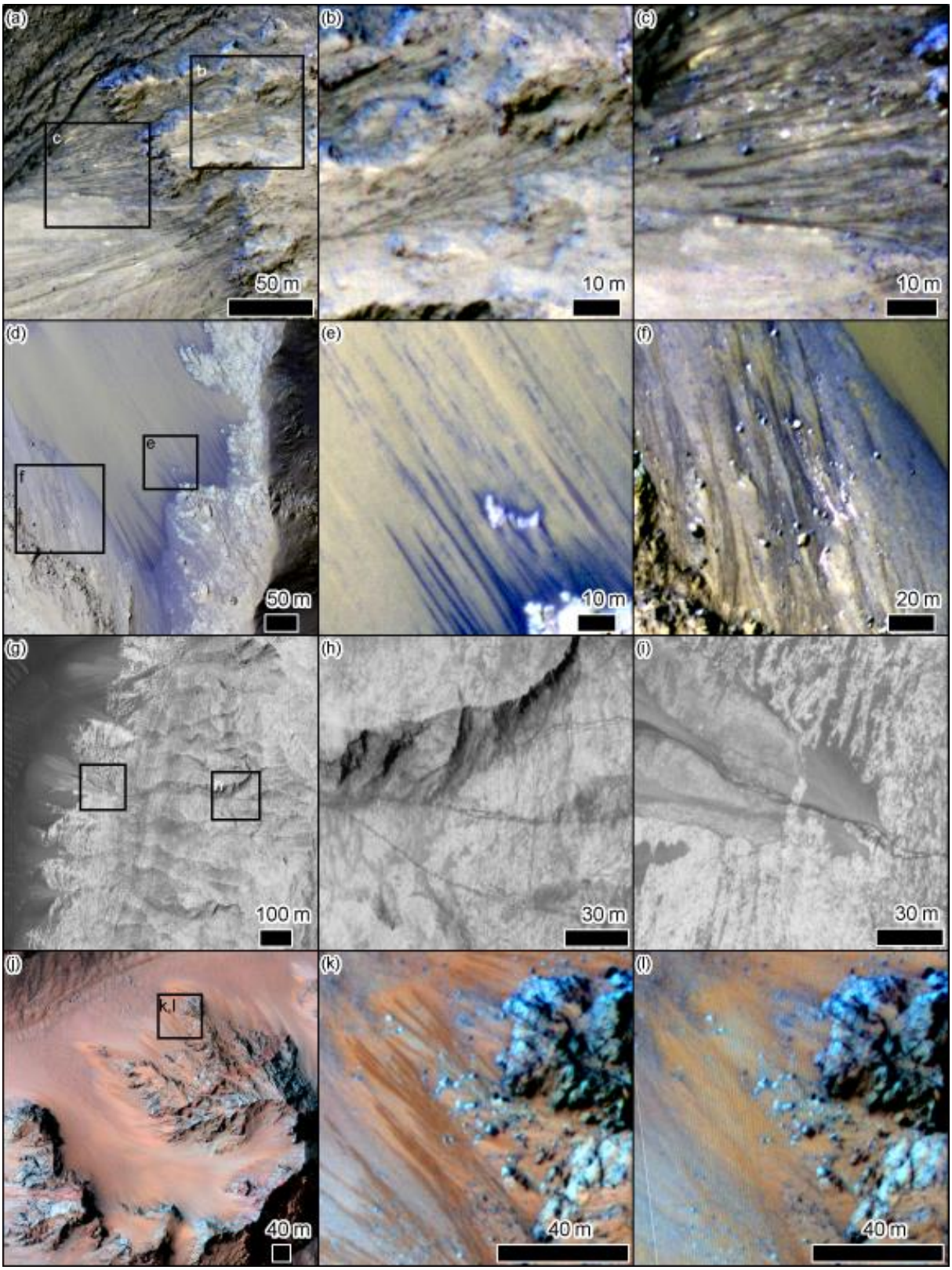

Figure 3.4: Examples of Recurring Slope Lineae (RSL), north is up in all panels. (a) RSL in the alcoves of gullies in Corozal Crater in the southern mid-latitudes with (b) showing multiple RSL coming together while deviating around obstacles and (c) showing their termini which often diverge. (a-c) False-colour

HiRISE image ESP_023218_1410 where colours have been stretched to best enhance the contrast. (d) RSL extending from rocky substrates onto sand on a ridge in Coprates Chasma in Valles Marineris at the equator with (e) showing their discontinuous downslope extensions and (f) their lower contrast on the upslope rocky materials. (d-f) False-colour HiRISE image ESP_043085_1670 where colours have been stretched to best enhance the contrast.(g) RSL on the interior light-toned layered deposits in Juventae Chasma in Valles Marineris at the equator with (h) showing their propagation over the bedrock with braided sections and (i) showing their extension onto the debris fans, again showing sinuosity and braiding. (g-i) HiRISE image PSP_006915_1760 where stretch has been chosen to best enhance the contrast.(j) RSL on the central peak of Hale Crater in the southern mid-latitudes in HiRISE image ESP_047172_1440 where (k) shows their extension onto lighter albedo "fans". (l) HiRISE image ESP_046605_1440 showing the same location as in panel k, but at a season when the RSL have faded. Image credits: NASA/JPL/UofA.

Concurrent observations of dust devil tracks, boulder tracks, and RSL suggest that the distinctive dark albedo of RSL is a result of the removal of dust (Schaefer et al., 2019) and that annual atmospheric dust deposition allows their reoccurrence the following year. The dust storm of Mars Year 28 and 34 resulted in many more candidate RSL being apparent and for RSL to be in general a lot longer than in previous years (McEwen et al., 2019; Stillman et al., 2014). An alternate hypothesis is that wicking of moisture to the surface or water absorbed into salts could be the cause of the darker albedo (Heinz et al., 2016; Massé et al., 2014). In any case it is agreed that RSL do not engender any significant downslope sediment transport at the HiRISE-scale. As no sediment transport is involved, they are generally thought to represent either subsurface percolation of water, or thin granular flows.

Apart from the various dry hypotheses for RSL formation, discussed further in Dundas (2021), water-based hypotheses require a mechanism to replenish the supply towards the top of the slope. They therefore focus around two potential mechanisms: i) atmospherically recharged source and ii) origin from aquifer seeps, which are discussed further below.

Mass balance arguments suggest that water ice frosts from the atmosphere are unlikely to be able to recharge RSL source areas, with RSL probably requiring metres cubed of water per metre of headwall, exceeding that which can be supplied from the dry martian atmosphere (Grimm et al., 2014). In addition, the kinetic barrier to melting, detailed in Section 3.2, would be particularly severe at the relatively warm locations of RSL occurrence in Valles Marineris – meaning the ices would need to somehow be protected by a lag in order to melt. Further, the melting of shallow subsurface ice is difficult as temperatures decrease with depth. If salt were present then melting could occur, but such melting would then flush these salts. This is unlikely because such a shallow subsurface ice would need a mechanism to recharge salt and significant amount of ice so that it could provide a source each year giving the recurrent behaviour of RSL (Stillman et al., 2014).

The surface temperature at which RSL start to grow argues that the water should be briny (i.e., have a depressed freezing point Grimm et al., 2014; Stillman et al., 2016) even though the near infra-red spectral detection of hydrated perchlorates associated with RSL from orbit (CRISM; Ojha et al., 2015) is now generally acknowledged to be due to instrument error (Leask et al., 2018; Vincendon et al., 2019) and no systematic detection has been made of chlorine bearing salts in thermal spectra (Mitchell and Christensen, 2016). The predicted abundance of salts on the martian surface is expected to be high, including chlorine-bearing species (Clark, 1981; Gellert, 2004; Keller et al., 2007; Kounaves et al., 2010; McSween and Keil, 2000) and notably perchlorates (Glavin et al., 2013b, 2013b; Hecht et al., 2009; Sutter et al., 2017; Toner et al., 2014b) which have remarkably large freezing point depression (e.g., Chevrier and Rivera-Valentin, 2012). This abundance has led researchers to propose that RSL could be produced by deliquescence of these salts, i.e. the

adsorption of water vapour (from the atmosphere or sublimated from ground ice) leading to the fluidisation of the salt (e.g., Bhardwaj et al., 2019b; Dickson et al., 2013). The relative humidity required for deliquescing Mars-relevant salts is on the order of >13% at 273 K (Gough et al., 2011; Heinz et al., 2016; Nuding et al., 2015; Primm et al., 2017), which for the same reasons as argued above seems high for the dry martian atmosphere. However, once these brines have formed they can form supersaturated and/or super cooled solutions with significant hysteresis prolonging their persistence in the environment (Gough et al., 2016; Primm et al., 2019; Toner et al., 2014a). Although temperatures are highest in the middle of the martian day, the relative humidity is at its lowest, so the early morning and late evening are more conducive to brine-formation by deliquesce (Gough et al., 2011; Primm et al., 2019). If RSL were caused by deliquescent salts, they should have different albedos at different times of day. This behaviour has not yet been observed with when comparing one morning CaSSIS image with an afternoon HiRISE image (Munaretto et al., 2020), but much more extensive analysis is required to substantiate this finding. Additionally, modelled water budgets using meso-scale atmospheric models coupled with deliquescence onto calcium perchlorate salts indicate an upper limit of 1 micron per sol, which is likely much too low to support any wet-dominated RSL formation mechanism (Leung et al., 2020).

Recharging sufficient salts into the source areas could be envisaged via atmospheric deposition, of notably perchlorate salts (Catling et al., 2010; Smith et al., 2014). If the brine comes from underground, there is no recharge problem for the salts, because the aquifer itself would be briny. However, repeating brine flows would be expected to continually deposit salts towards the ends of the RSL and within the subsurface. As no build-up has been detected from orbit there must be some unknown removal mechanism, if this hypothesis is true. The difficulty in recharging sufficient water (Stillman et al., 2016) and the proximity of RSL to fractures observed in the bedrock at which they originate (Abotalib and Heggy, 2019) have been used as arguments to support their origin via groundwater. As discussed in Section 3.7.3 for gullies, a groundwater origin is hard to substantiate with confidence as we have so little knowledge on the structure of the subsurface of Mars (e.g., heatflow, permeability, lithology, fractures, and cryosphere state/structure). Many of the most extensive RSL sites are found in locations that are advantageous for groundwater such as: the numerous RSL found within craters in the regional depression of Chyrse and Acidalia Planitia (Stillman et al., 2016), Garni crater on the floor of Melas Chasma (Stillman et al., 2017), and Palikir crater on the floor of the much larger Newton crater (Stillman et al., 2014). These sites could possess unconfined or confined/pressurized aquifers that could hydraulically connect to the surface via low permeability fractures. It should be noted that RSL are also found in places disadvantageous to groundwater access (Chojnacki et al., 2016). Nevertheless, such aquifers would need to possess a freezing depression that is greater than or equal to the mean annual surface temperature so that they could discharge to the surface only during the warmest part of the year (Stillman et al., 2016). Once the brine is discharged, it will then percolate downhill through the regolith. The regolith also must have an impermeable barrier to prevent the brine from seeping back into the subsurface before it shows a surface expression (Mellon and Phillips, 2001). Due to the large diurnal temperature variations, the brine is likely to completely or partially freeze at night, thus slowing its advance downhill. As discussed in Dundas (2021) there are also RSL locations that are not likely to be connected to an aquifer such as the numerous RSL sites found on Coprates Montes (Chojnacki et al., 2016).

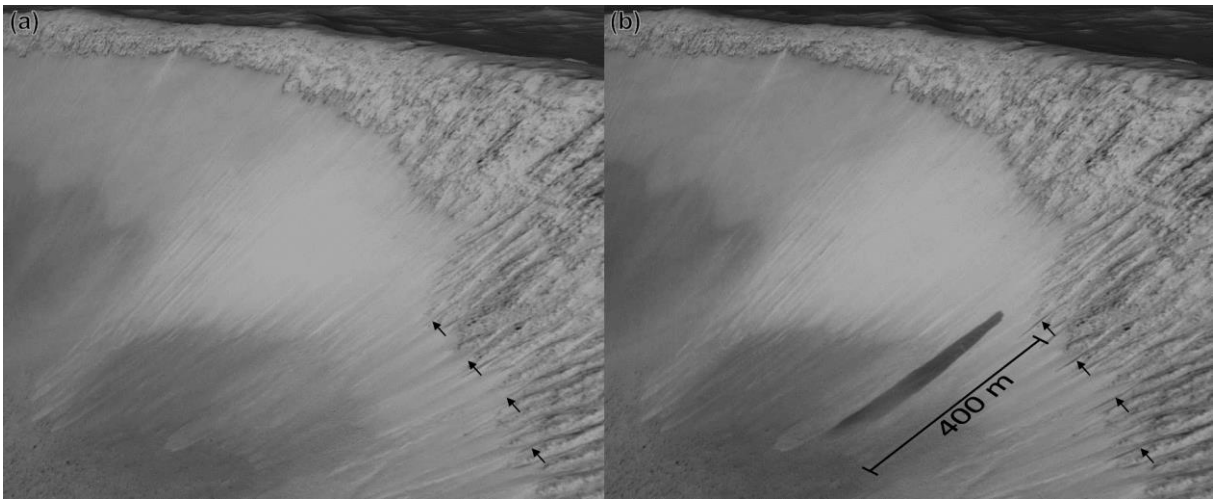

Figure 3.5: 3D rendering of a slump on the same slope as Recurring Slope Lineae (RSL) in Garni Crater. (a) Orthorectified HiRISE image ESP_034672_1685 showing the slope with RSL prior to the slump in MY32, Ls 65°. (a) Orthorectified HiRISE image ESP_035028_1685 showing the slope with RSL and the slump in MY32, Ls 77°, i.e. 26 sols after the image in panel a. Small black arrows point to the location of prominent RSL that grow between the two images. Image credits: NASA/JPL/UofA.

It is possible that liquid water is only the trigger for a motion that is then more granular, for example: the volume or weight change brought about by deliquescence could trigger a granular avalanche (Wang et al., 2019), or humidification-desiccation (water absorption-desorption) cycles could change the cohesive properties of the slope materials (Shoji et al., 2019). Experimental work has shown that boiling water or brines can cause grainflows, or eject pellets of damp material (Herny et al., 2019; Massé et al., 2016; Raack et al., 2017). These more "exotic" processes rely on the contact of liquid water with relatively warm substrates (>280K), as might be envisaged to happen at the edge of a propagating RSL flow-front, and vigorous boiling produces gas in the sediment pore-space capable of fluidising the granular bed, ejecting particles and even mobilising parts of the saturated mass. Such hybrid mechanisms would allow "dry" RSL to follow the seasonal patterns observed for RSL. However, similarly the purely dry mechanisms (Dundas et al., 2017; Schaefer et al., 2019; F. Schmidt et al., 2017; Vincendon et al., 2019), these granular flows would struggle to imitate the detailed growth histories of RSL (Dundas, 2021; Grimm et al., 2014; Huber et al., 2020).

In summary, the role of liquid water in Recurring Slope Lineae on Mars is supported by their temporal and spatial patterns of growth at the intra- and inter-seasonal scale, as well as their extension onto slopes lower than the angle of repose. The source of this water is problematic, either from the atmosphere or the subsurface. For brine-flows, a mechanism would be needed to remove the deposited salts. This outstanding problem for the "wet" hypothesis combined with new theories for the "dry" hypothesis has shifted the community's focus to resolving the issues regarding triggering and growth for the possible "dry" processes (e.g., Dundas, 2021). To date, no advanced modeling has been able to correlate the dry mechanism hypotheses with the observations.

My contribution to the state-of-the-art: I have contributed to understanding RSL by performing experimental work on the action of boiling water on sediment transport (Herny et al., 2019; Massé et al., 2016; Raack et al., 2017). These experiments were important to show that boiling water can in fact transport more sediment than stable water so for a given volume of water the transport capacity is increased from what we might expect from observing water or brine flows on Earth. I was involved in a UK Space Agency "Aurora" project led by Peter Muller to better understand RSL in Valles Marineris using machine learning techniques to improve the quality of topographic data. In

summary, existing stereo-derived elevation models paired with corresponding ortho-images are used to train a neural network to learn what topographic signal is expected based on the features observed in Mars images. The technique is applied to existing terrain models to improve their resolution and quality and is best applied in a pyramidal fashion, e.g. HRSC to improve MOLA, CTX/CaSSIS to improve HRSC, HiRISE to improve CTX/CaSSIS. Initial testing of the technique has been performed in Oxia Planum (Tao et al., 2021c, 2021c, 2021a, 2021d, 2021b) and is planned to be applied to Valles Marineris. Attempts to semi-automatically map RSL using image-differencing were successful on images which were less than several thousand pixels in any dimension but proved too computationally expensive to apply to stacks of HiRISE images, hence was abandoned. I am part of an ongoing effort within the CaSSIS team to capture an early morning image of RSL on the same day as HiRISE (which takes images around 3pm local Mars time) to reinforce the initial conclusions of our study in Hale Crater (Munaretto et al., 2020), which showed no albedo change consistent with dry rather than wet flows.

3.7.3 Gullies

The term "gully" for Mars encompass a huge variety of landforms, whose uniting attribute is the presence of a channel through which material is transported from the source alcove to the debris apron or fan (see review by S. J. Conway et al., 2019) (Figure 3.6). Gullies are not to be confused with "spur and gully" morphology which was originally reported on Mars in Valles Marineris (e.g., Lucchitta, 1987), but in this case the erosional and depositional parts are not connected by a channel. Spur and gully morphology with no channelisation is generally attributed to dry mass wasting processes which build talus cones in oversteepened landscapes (e.g., Thapa et al., 2017) and will not be discussed further here.

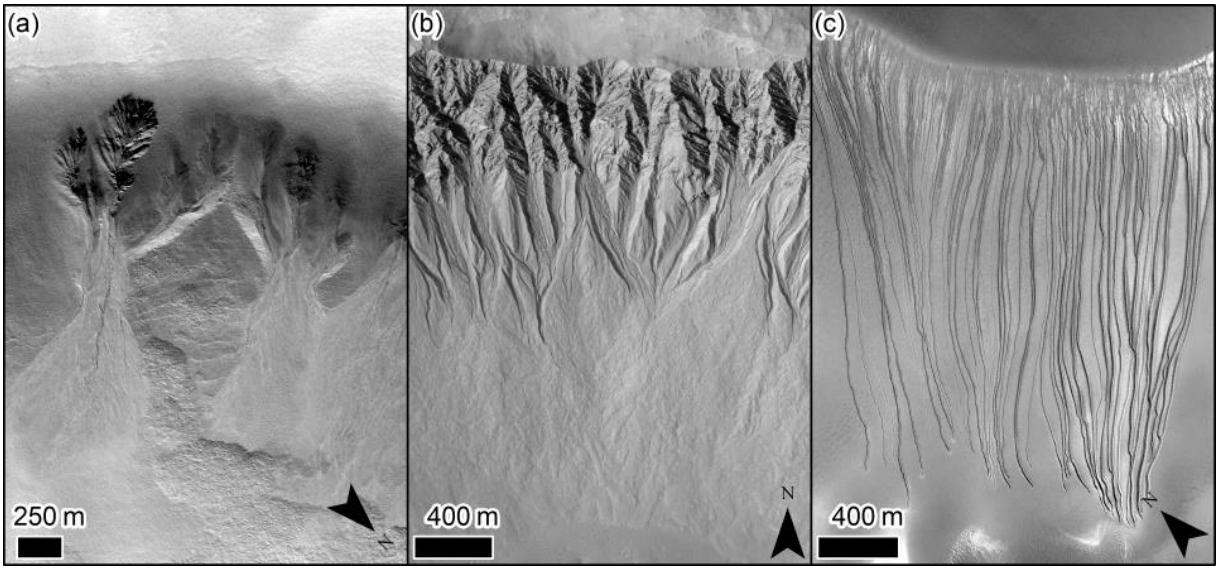

Figure 3.6: Examples of gullies on Mars. (a) Gullies incised into icy mantling materials on a crater wall in the northern hemisphere. Note the well-formed tributary networks, the abandoned alcoves and multiple generations of fan-deposits. HiRISE image ESP_018895_2410. (b) Gullies in Galap Crater in the southern hemisphere, where the alcoves are incised directly into the bedrock at the crater wall and no icy-mantling materials are present. HiRISE image PSP_003939_1420. (c) "Linear" gullies on the megadune located on the floor of Russell Crater in the southern hemisphere. HiRISE image ESP_038335_1255. Image credits: NASA/JPL/UofA.

Gullies, from the top of the alcove to base of the fan, are typically a kilometre in length (ranging from a hundred metres to several kilometres) and tens to hundreds of metres wide (ranging from decametres to ~kilometre). They were initially interpreted to be a result of liquid water flowing at the surface of Mars, because of their similarity to gullies carved by liquid-water on Earth and because of their latitude distribution and orientation preference (Malin and Edgett, 2000). Gullies are found primarily on steep slopes at latitudes polewards of 30° north and south (Balme et al., 2006; Bridges and Lackner, 2006; Dickson et al., 2007; Harrison et al., 2015; Heldmann et al., 2007; Heldmann and Mellon, 2004; Kneissl et al., 2010) (Figure 3.2b) and their variable spatial density in this latitude range is mainly a consequence of the availability of steep slopes (Conway et al., 2017). The sloping terrains where gullies are found comprise the relief-forming structures on Mars at kilometre-scales: impact craters (outer and inner walls, terraces, and central peaks/pits), valleys and graben, mesas, buttes, collapse pits and dark sand dunes. At latitudes between 30° and 40° gullies are found primarily on pole-facing slopes and >40° they have a preference for equator-facing slopes, but can be found on slopes with all orientations (e.g., Conway et al., 2017; Harrison et al., 2015; Heldmann and Mellon, 2004). Gullies can be found in the equatorial regions, but they are generally small (hundreds of metres long for metres in channel-width), rare and only reliably identified in HiRISE images (Auld and Dixon, 2016; Thomas et al., 2020), hence are not displayed with the larger landforms in Figure 3.2b. It should be noted that Auld and Dixon (2016) classified features with an alcove and an apron but no channel as gullies which deviates from the commonly used Malin and Edgett (2000) definition that requires the presence of a channel. The latitudinal pattern in distribution and orientation of gullies (Figure 3.2b) strongly suggests a climatic factor plays a role in conditioning their formation.

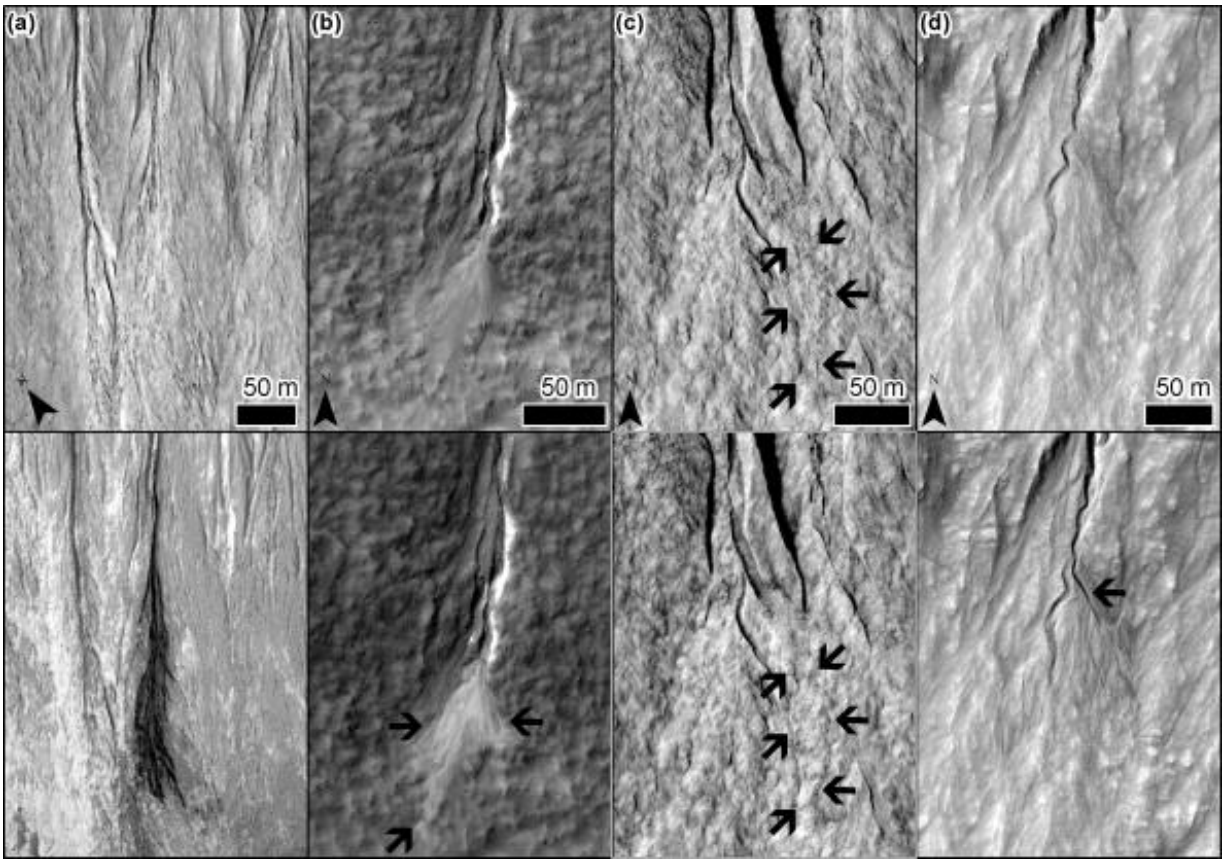

Figure 3.7: Examples of active martian gullies, where the top is the image before the change and at the bottom the image after the change. (a) Dark-toned deposit overlying frost in HiRISE image ESP_027567_1425 (before ESP_022688_1425). (b) Light toned deposit over an existing fan on HiRISE image ESP_031919_1435 (before ESP_014368_1435). (c) New high-relief deposit with no tonal

change in HiRISE image ESP_032078_1420 (before PSP_003939_1420). (d) New channel and deposit in HiRISE image ESP_032011_1425 (before ESP_013115_1420). Note, the before-after pairs are not necessarily the closest in time, but are chosen to best illustrate the changes. Image credits: NASA/JPL/UofA.

Worthy of particular attention are "linear gullies" (Figure 3.6c) which are a very unusual type of martian gully, lacking a terrestrial equivalent and is only found on steeply sloping dark sand substrates (e.g., Diniega, 2021; Diniega et al., 2013; Reiss and Jaumann, 2003). "Classic" gullies, as described above, are also found on dunes. Linear gullies comprise a long linear to sinuous parallel-walled groove flanked by levees, which trends downslope and does not change appreciably in width along its length. The source zone is often marked by many smaller tributary grooves and the terminus either blunt or with a series of disconnected pits, but with no obvious depositional fan/apron. They are often found near to other "classic" gullies and sometimes have morphologies that are transitional with other "classic" gullies (e.g. the channel part resembles a linear gully, whereas the source and deposit apron resembles a classic gully) (e.g., Pasquon et al., 2019b). They form a relatively small proportion of the overall gully population, but are one of the most active types of gully at the present-day (S. J. Conway et al., 2019).

Although gullies are too small to be dated directly via crater-size frequency distributions, their recent formation has been inferred by the lack of superposed impact craters. Dating of the terrains that gullies superpose has allowed authors to estimate maximum ages as 1-5 Ma (de Haas et al., 2019; Reiss et al., 2004; Schon et al., 2009a). Gullies are composite landforms where overlapping deposits demonstrate that gullies have many multiples of formative events (e.g., de Haas et al., 2015a; Johnsson et al., 2014; Levy et al., 2010a). Inverted gully fans/channels and re-incision into mantled alcoves provide further evidence that significant hiatuses occur between different active periods in gullies (e.g., Dickson et al., 2015).

Monitoring of gullies on Mars has revealed that downslope movements of material are ongoing and predominantly occur in local winter (Diniega et al., 2010; Dundas et al., 2012, 2015b, 2019a; Jouannic et al., 2019; Malin et al., 2006; McEwen et al., 2007; Pasquon et al., 2016, 2019a, 2019b; Raack et al., 2015). Gullies on sand dunes are particularly active and most sites show some kind of motion every year. Mass balance calculations on dune gullies has highlighted that these features can be formed entirely in as little as a few hundreds of years (Pasquon et al., 2019b). Only a few other sites show such cadences, with the majority of gullies showing activity having only one change within the last few decades of monitoring (e.g., Dundas et al., 2019a). Movements mostly take the form of relatively high or low albedo deposits on fans or within gully-channels (Figure 3.7b), with only some identifiable by their relief (Figure 3.7c,d). In a few cases the source of the sediment can be tracked back to an identifiable scarp (e.g., de Haas et al., 2019; Raack et al., 2020). Channels can be evacuated, or back-filled with sediment and new channels carved into fan-surfaces. Sites with gullies also often host RSL (Figure 3.4a-c) and often small-scale equatorial gullies are also found at RSL sites (Figure 3.4g-i).

Gullies have been proposed to form via both dry and wet processes, and a summary of the arguments in favour of the dry hypotheses can be found in Dundas (2021). Due to present-day activity occurring during local winter it is very unlikely that these motions are triggered by liquid water. The only exception is that the recent activity in linear gullies does occur at a time of year when water ice can be cold-trapped and surface temperatures are rapidly rising towards the melting point (Pasquon et al., 2016), but even in this case the link with CO_2 ices provides a simpler explanation and is more widely accepted (Dundas, 2021). It should be mentioned that some present-day activity characterised by the bright deposits, occur at times and places where CO_2 ices have not been

detected, but H_2O ices have (Vincendon, 2015), suggesting that water ice might be playing a role, although such deposits are found to be consistent with dry granular flows (Kolb et al., 2010; Pelletier et al., 2008). Whether the sediment transport observed at the present-day is representative of the processes that have formed the entire gully-landform still remains open to debate as gullies have a number of characteristics that are consistent with formation by flowing liquid water, as we detail below.

Martian gullies share many morphological characteristics with water-driven steepland erosional systems on Earth. Many of the detailed elements of martian gully morphology can be identified within larger terrestrial catchments, but also erosion-deposition systems that share a similar morphology can be found in permafrost to arid regions on Earth (Costard et al., 2007; Dickson et al., 2018; Hartmann et al., 2003; Hauber et al., 2018; Heldmann et al., 2010; Sinha et al., 2018). Sediment transport through such systems is typically via a cascade of different processes, including mass wasting or landsliding, debris flow and fluvial transport (e.g., Cavalli et al., 2013; Heckmann and Schwanghart, 2013; May and Gresswell, 2004). The upper part of martian gullies is often tributary in nature, forming an organised, hierarchical network, a typical organisation of fluvial systems on Earth. The lower part of martian gullies often comprises a fan, where multiple deposits overlap, a characteristic shared by alluvial fans on Earth (de Haas et al., 2018, 2016). Fresh individual deposits can be characterised by lobate margins and levees flanking the channel (Johnsson et al., 2014; Lanza et al., 2010; Levy et al., 2010a; Sinha et al., 2020), which are characteristic of debris flow processes on fans on Earth (e.g., Blair and McPherson, 2009; de Haas et al., 2015b). In-channel deposits can show braiding, streamlining, sinuosity, abandoned channel segments, terraces, all typical features of sediment-charged streams on Earth (e.g., Bakker et al., 2019). Topographically, both in terms of along-channel profiles and in terms of contributory-characteristics martian gullies are indistinguishable from terrestrial systems dominated by debris flow or fluvial processes (Conway et al., 2011b, 2015; Conway and Balme, 2016; Hobbs et al., 2017; Yue et al., 2014). Stratigraphic analysis has revealed that the deposits laid down in martian gully fans indicate a dominance of debris flow processes, even though typical debris flow surface morphologies, such as lobes and levees, are absent, probably as a result of surface erosion by wind (de Haas et al., 2015c).

Numerical models and experimental simulations both conclude that once liquid water is generated, it would be sufficiently stable to flow the whole length of the gullies and to transport sediment (Bargery and Gilbert, 2008; Conway et al., 2011a; Heldmann et al., 2005; Herny et al., 2019; Parsons and Nimmo, 2010; Raack et al., 2017). Its metastable state may result in some transport mechanisms that are rarely active on Earth, particularly those as a result of boiling, which can result in enhanced sediment transport for relatively limited quantities of water (Herny et al., 2019; Massé et al., 2016; Raack et al., 2017).

No matter the source for the liquid water, the proposed release mechanism is a result of the insolation conditions experienced by Mars under moderate to high obliquity conditions (>35°), when peak temperatures are experienced by steep pole-facing slopes in the mid-latitudes (Christensen, 2003; Costard et al., 2002; K. E. Williams et al., 2009; Williams et al., 2008). Three sources of water have been considered as possible: i) groundwater, ii) ground ice, or iii) surface ice precipitates (snow, or frost).

Groundwater: Both deep (Gaidos, 2001; Grasby et al., 2014) and shallow sources (Heldmann and Mellon, 2004; Marquez et al., 2005; Mellon and Phillips, 2001) have been proposed as the source for gullies, where in both scenarios seeps of water/brine occur when the incoming radiation is sufficient to melt the plug of ice formed where the aquifer reaches the surface, and falling winter temperatures reseal this plug. Where the radiation is too strong, water will evaporate rather than

flow and where the radiation is not strong enough, the plug will never melt – these factors explain the latitude orientation trends shown by gullies (Figure 3.2c). Both sources struggle to explain the emergence of gully alcoves at the top of isolated topography, where shallow aquifers would not be sufficiently voluminous to repeatedly supply sufficient water and deep aquifers would be improbable to emerge (e.g., Balme et al., 2006; S. J. Conway et al., 2019; Treiman, 2003). Although, recent arguments derived from RSL-research (Section 3.7.2) maintain that deep, pressurised aquifers could emerge at these elevated locations if a permeable pathway exists (Stillman et al., 2016).

Ground ice: Redistribution of the water ice from the polar caps to lower latitudes under conditions of high orbital obliquity is thought to explain the prevalence of ground ice down to 50° north and south (Jakosky and Carr, 1985; Madeleine et al., 2014; Mellon and Jakosky, 1995) and its discontinuous presence to 30°N and S (Kreslavsky and Head, 2000; Milliken et al., 2003; Mustard et al., 2001). The same high obliquity conditions could be conducive to its melting where peak temperatures are experienced in the subsurface on pole-facing slopes in the mid-latitudes (Costard et al., 2002; Kreslavsky and Head, 2003). In this scenario the distribution and orientation of gullies with latitude is a factor of both the availability of ground ice and the conditions required for its melting. Mass balance arguments show that ground ice is being lost during gully-formation (Conway and Balme, 2014), but gullies are found in zones without obvious presence of ground ice (de Haas et al., 2019; Johnsson et al., 2014), which argues against this hypothesis. Conversely, the abrupt absence of equator-facing gullies at 40° north and south matches surprisingly well with the anticipated absence of ground ice at these locations (Conway et al., 2018b).

Snow/frost: The formation scenario for snow and/or frost (de Haas et al., 2015a; Kossacki and Markiewicz, 2004; Williams et al., 2008) is similar to that for ground ice, but the source is seasonal surface deposits, rather than ice stored within the soil. For one particular site the debris flow cadence revealed by the deposit volumes and the age of the host crater is consistent with millimetres of snow over the catchment, which is broadly in accord with climate model predictions for snowfall at high obliquity (de Haas et al., 2015a). Whether atmospheric conditions in the past were conducive to melting at the surface, however, is a matter of debate.

In summary, although gullies on Mars strongly resemble terrestrial gullies carved by liquid water, it remains under debate as to whether the same processes were active on Mars. There is growing evidence that present-day activity almost certainly does not involve liquid water, but whether present-day processes are representative of the processes that have contributed to the construction of the whole gully-landform is still debated. If current modification processes of gullies cannot explain their entire formation, liquid water at high obliquity is the next most likely candidate to explain the formation of martian gullies.

My contribution to the state-of-the-art: My PhD thesis addressed the question of the processes at work in forming gullies on Mars and specifically dealt with the evidence for liquid water. I found that both the topographic long profiles and hydrological parameters (e.g., relation between the local slope and upslope drainage area in the watersheds) of martian gullies were more similar to debris flow and fluvial systems on Earth than pyroclastic flows, talus slopes or gully-like features on the Moon (Conway et al., 2015, 2011b; Conway and Balme, 2016). Later collaborative work revealed that debris flow like morphologies are relatively common in martian gullies (Sinha et al., 2020) and that secondary processes are probably accounting for the absence of these morphologies in a, as yet unknown, proportion of gully-fans (de Haas et al., 2015c). In one case we were able to estimate for the first time the recurrence interval of deposits in martian gullies and we found this cadence could be explained by Earth-like processes occurring only during periods of high orbital obliquity (de Haas et al., 2015a).

We found that the maturity of the gullies (as represented by their catchment size) has no relationship with the host-crater age (de Haas et al., 2019) and further that the reason for this was erasure by a glacial erosion "event" at ~5 Ma (see Section 3.7.6) (Conway et al., 2018a). We established that gullies and recent glacial landforms have a systematic spatial organisation suggesting that the ice in the glacial landforms could be promoting the formation of gullies, but also that gullies can be found without these landforms.

We undertook a re-analysis of the global database of martian gullies produced by Harrison et al. (2015) and found that the majority of the spatial distribution could be explained by the spatial distribution of the available steep slopes (Conway et al., 2017). We also found a remarkable transition from pole-facing to equator-facing/mixed at 40°, which can be used as a powerful constraint on future modelling. We used this constraint to show that freeze-thaw cycles can better explain the gully distribution than the past distribution of CO_2 ices (Conway et al., 2018b) using the results from a 1D climate model.

By examining the timing of morphological changes in linear gullies, combined with climate simulations we were able to show that liquid water could be produced via rapid heating caused by the final sublimation of the seasonal CO_2 ices (Pasquon et al., 2019b). Such water would be metastable and my experimental work has revealed that both freezing and boiling act to enhance the morphological expression of sediment transport, hence that less water would be needed than if stable water was considered (Conway et al., 2011a; Herny et al., 2019; Jouannic et al., 2015; Massé et al., 2016; Raack et al., 2017).

3.7.4 The role of CO_2 sublimation in gully formation

The present-day activity of gullies occurs at times of year when CO_2 is on the surface (Figure 3.8) and hence CO_2 sublimation is now the leading hypothesis for how sediment is transported in gullies at the present-day. However, because there is no terrestrial analogue for this sediment transport process, the precise mechanisms for transport remain to be defined. Five main hypotheses have been presented for how CO2 sublimation might transport sediment:

1. Cedillo-Flores et al. (2011) suggested that relatively warm sediment deposited atop a slab of CO2 ice would hover over the surface because it would cause sudden sublimation of the underlying CO_2. Their model was tuned to gullies found in the polar pits on Mars at 75°S, where CO_2 seasonal cover is known to be thick and hence might not be so applicable to gullies outside this region that are also known to be active. However, some flows have been observed to propagate over ice cover outside the polar regions (Dundas et al., 2019a).
2. Similarly for the polar gullies, Hoffman (2002) suggested that their activity could take the form of avalanches of CO_2 snow that entrain sediment, which are triggered by basal sublimation (see description of the "Kieffer" model below). Entrainment of warmer lithic material was proposed as a method to promote fluidisation in these mass movements.
3. Pilorget and Forget (2016) suggested that sediment could be transported by pressurised flows underneath a translucent slab of CO_2 ice. Inspired by the Kieffer et al. (2006) model for spiders. They based their investigation on the linear gullies in the Russell Crater dunefield (at 57°S), and extrapolated their findings to all gullies. However, slab ice is not found at every gully site and dune gullies are a rather special case. Their model makes a good prediction for periods where dark spots and flows appear (Section 3.7.1). However, most major movements occur at times when the ice-cover is discontinuous and hence do not fit with this model.

4. Diniega et al. (2013) suggested that blocks of CO_2 could detach from cornices and on contact with the warmer substrate downslope would sublimate vigorously at the base, carving a channel as they slid downslope. This hypothesis pertains to linear gullies in the effort to explain their unusual appearance. This mechanism has shown in experiments to be much more effective at low martian pressures (Mc Keown et al., 2017).
5. Dundas et al. (2019a) suggested CO_2 ice and sediment avalanches where sublimation is engendered by the release of potential energy and the entrainment (or contact) with warmer materials along the flow.

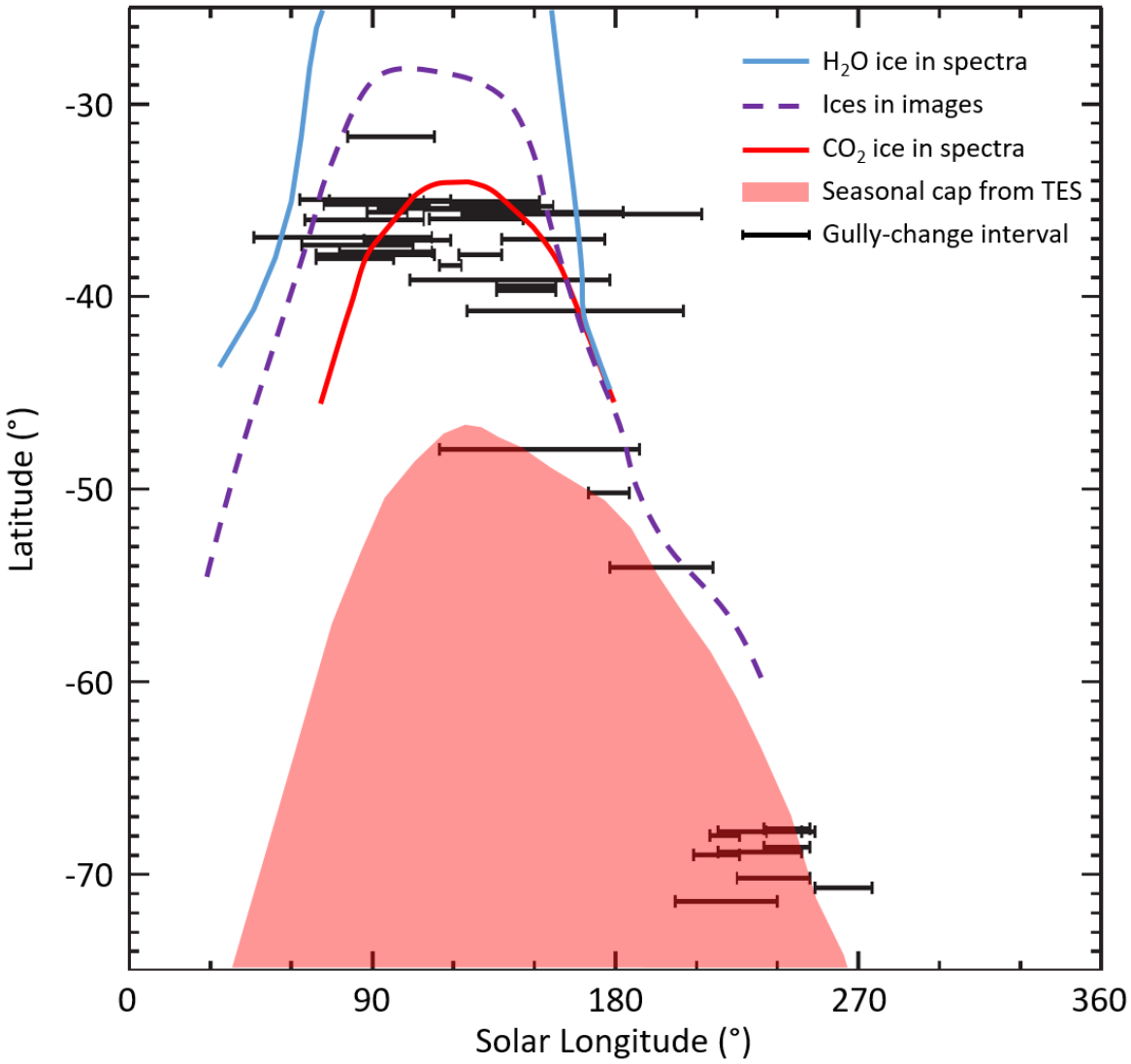

Figure 3.8: Activity of gullies plotted with evidence for seasonal ices obtained from the literature. The data on H_2O ice in spectra comes from OMEGA and CRISM data presented in Vincendon et al. (2010a)*, the data of ices in images on south-facing slopes comes from HiRISE data presented by Dundas et al.* (2019a)*, data for CO_2 ice in spectra come from CRISM data presented in Vincendon et al.* (2010b)*, the extent of the continuous seasonal CO_2 ice deposit come from TES data presented in Piqueux et al.* (2015) *and the gully-change intervals come from Dundas et al.* (2019a)*. Note: that the spectral and image observations represent discontinuous patches of ices as well as continuous and the lower latitude limit of the lines is determined by the latitude range of the relevant studies and not a non-observation.*

My contribution to the state-of-the-art: I co-supervised the PhD of Matthew Sylvest and we performed the first lab experiments where sediment transport by sublimating CO_2 was investigated under martian pressure conditions (Sylvest et al., 2019, 2016). In these experiments we condensed CO_2 into a sloping regolith and then sublimated the ice by top-down insolation. We found that CO_2 sublimation could trigger failures in these sloping regoliths. Further, highly permeable materials such as sand were only susceptible to sublimation triggered failure near the angle of repose. Failure was observed down to 15° in a Mars regolith simulant, containing more dust. Failures included single grain motions, granular avalanches and gradual downslope creep. These pioneering experiments left a number of open questions, including how CO_2 sublimation could fluidise a flow in motion. This question is being investigated by a PhD student I am co-supervising with Tjalling de Haas in Utrecht who performed flume experiments in October 2021 in the Open University Mars chamber where mixes of sediment and CO_2 ice grains were released down a chute onto an unconfined bed. This work has been supported by INSU's Programme Nationale de Planétologie and a regional grant "Etoiles Montantes" from Pays de la Loire. Analysis of the results is in progress but comparison with sediment-only experiments reveal significant fluidisation is possible. Further experiments to investigate the gas-permeability and heating rates required for this mechanism for comparison to climate model simulations is to be investigated in future work.

During the PhD of Kelly Pasquon (who was also my postdoc on the "Etoiles Montantes" project) and of Gwenael Jouannic (both at GEOPS), we investigated a number of gullies on dunes via repeat imaging using HiRISE allowing us to follow the seasonal evolution of the ices and what kinds of sediment motion were observed (Jouannic et al., 2019; Pasquon et al., 2019a, 2019b, 2016, 2016). These papers revealed that gullies on dunes are extremely active, and the masses moved each season mean that these gullies can be formed in tens to hundreds of years. The majority of motions in linear gullies occur at the very end of the defrosting season, however motions in classic gullies occur throughout winter. In classic gullies the motion seems to be triggered by abrupt failures of an icy flank, this material falls onto the already-defrosted floor (presumably hotter?), triggering sublimation-driven motion.

Finally, by using a 2.5D code designed to simulate debris flows over complex topography on Earth, we compared the simulation outputs with the real deposits observed in remote sensing data of martian gullies (de Haas et al., 2019). We input the topography derived from 1 m/pix HiRISE terrain models and compared the runout and distribution of erosion and deposition from model runs with different realistic friction parameters. This work revealed that new flows in martian gullies are similar to terrestrial debris flows in rheology. We estimate that less than 1% of CO_2 would be needed to achieve this level of fluidisation. An estimation that is presently being tested against lab data.

In collaboration with Colin Dundas, we have found that present-day flows observed in gullies are can explain the materials that form the fans of the gullies (Dundas et al., 2022) suggesting that CO_2 driven flows could explain the formation of the whole landform and not just present-day changes. Further the runout and topographic setting support this conclusion – with this result in consideration at Nature Geoscience.

In summary, my research has revealed that martian gullies bear the topographic signature of terrestrial debris flows and that CO_2 driven flows can produce such landforms without water. It remains to be explored how water and CO_2 driven debris flows can be distinguished.

3.7.5 Periglacial landforms

Many landforms tightly associated with periglacial conditions on Earth have also been reported on Mars, including: solifluction lobes, pingos, low-centred polygons, ice-loss depressions and sorted

patterned ground. For a in-depth review of these features on Mars, please refer to Balme et al. (2013). Periglacial conditions are those which are dominated by the action of freeze-thaw processes and do not necessarily imply permafrost or glacial conditions (French, 2013). Integral to periglacial conditions is the occurrence of freeze-thaw cycles and the formation of an active layer – that is a layer on top of the permafrost that undergoes annual thaw – hence in apparent contradiction with our understanding of the stability of liquid water on Mars. Implicit for the formation of periglacial landforms is the presence of ground ice, which as described in Section 3.5, which is a pre-requisite relatively easy to fulfil on Mars.

Below, we summarise the observations pertaining to each of these features and the way in which liquid water is thought to be involved in their generation and then introduce the concept of a landscape assemblage.

3.7.5.1 "Solifluction" lobes

Lobate forms found on hillslopes on Mars have a strong resemblance in form and scale to solifluction lobes on Earth (Gallagher et al., 2011; Johnsson et al., 2012, 2018; Soare et al., 2018a) (Figure 3.9). Like their terrestrial analogues they can be sheet-like or tongue-like, extending in the downslope direction and are bounded at their lower end by a scarp or "tread". Their margins can be picked out by relief or by clasts. The martian lobes can be larger in both width and length than solifluction lobes on Earth (generally up hundreds of metres), but their ranges of sizes do overlap and are typically tens of metres wide and long (Gastineau et al., 2020). Even though individual lobes are small, they occur in groups that can span hundreds of metres to kilometres across and downslope. Martian lobes have the peculiarity that they are found on slopes above 10° and on average ~25°, whereas terrestrial solifluction lobes can be found on all slopes up to 35° (Gastineau et al., 2020). They occur at latitudes poleward of 60° in the northern hemisphere and at latitudes of poleward of 40° in the southern hemisphere (Figure 3.2c) and are less common in the southern hemisphere (Johnsson et al., 2018).

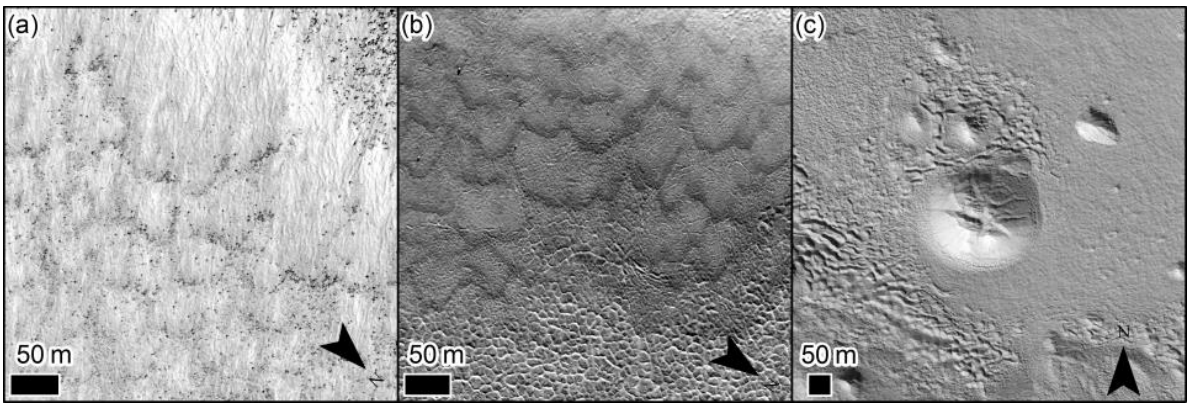

Figure 3.9: Examples of lobate forms and pingo-like mounds. (a) Lobate forms outlined by clasts on the wall of Heimdal Crater (Gallagher et al., 2011). Downslope is down-image. HiRISE image PSP_009580_2485. (b) Lobate forms marked by relief and overprinting polygonal terrain on an impact crater wall in the northern hemisphere (Johnsson et al., 2012). Downslope is down-image. HiRISE image PSP_010077_2520. (c) Pingo-like mound near Moreux Crater (R. J. Soare et al., 2021b) *with marked summit cracks. HiRISE image ESP_058140_2225. Credits: NASA/JPL/UofA.*

Solifluction lobes on Earth are sheets of material that move as a result of differential downslope movement caused by freeze-thaw cycling in the active layer (Matsuoka, 2001). A range of processes lead to the formation of solifluction lobes on Earth, including: gelifluction, plug flow, frost creep and retrograde movement (Matsuoka, 2001). The influence of each of these processes on the morphology of the lobes has not been isolated, but each requires extensive thaw and considering

martian lobes cover hundreds of metres of areal extent, this would require equivalently extensive thaw to prevail. The age of these features is uncertain, but is presumed to be late Amazonian as they are not overlain by any other feature and there is some evidence of motion today in the form of boulder motions on the same slopes (Dundas et al., 2019b). Alternatives to thaw for generating lobate forms have not yet yielded convincing results (Gastineau et al., 2020), but some kind of creep triggered by CO_2 ice-related processes has been suggested, but remains to be substantiated (Dundas et al., 2019b).

3.7.5.2 Pingo-like mounds

Mounds with spatial extents of tens to hundreds of metres are commonplace on Mars and have been attributed to the action of a range of processes, including differential erosion, volcanism (magmatic or sedimentary), inverted impact craters and pingos (e.g., Bruno et al., 2006; Burr et al., 2009a). Of particular interest for this discussion are those that have been identified as pingos (Figure 3.9) (Balme and Gallagher, 2009; Burr et al., 2009b; Dundas et al., 2008; Dundas and McEwen, 2010; R.J. Soare et al., 2021; Soare et al., 2014b, 2013a, 2013b, 2005). These landforms have been reported mainly in the mid-to-high-latitudes on Mars with the exception of one report near the equator (Balme and Gallagher, 2009).

Pingos on Earth can be formed by the impingement of permafrost upon a near-surface liquid water body (talik) generating hydrostatic pressure (closed system) or by artesian pressure developed in a talik connected to the surface (open system). Typically closed system pingos are developed when an alas, or thermokarst lake, catastrophically drains and the permafrost re-advances into the saturated sediments (e.g., Mackay, 2002). Open system pingos develop where sub-permafrost meltwater is pushed to the surface by an elevated hydrostatic gradient generated by surrounding topography, for example in the forefields of retreating glaciers (Christiansen, 1995; French, 2013). In both cases massive ice is formed in the core of the pingo which pushes up the surface above it, forming a mound. The mounds can be circular, elongate or form complexes in planform. On Earth, pingos can grow to heights of tens of metres with widths of hundreds of metres to nearly a kilometre (Gosse and Jones, 2011; Jones et al., 2012). As they grow via injection of water and deformation of the ground, they often display summit cracks where the deformation is greatest (e.g., Mackay, 1987). Their flanks slopes can increase beyond the angle of repose then causing mass wasting of the flanks. The cracks in the overburden can engender the destabilisation of the interior ice, forming a summit pit. If the ice at the core melts then the pingo can completely deflate leaving a shallow raised rim depression or pingo scar (Flemal, 1976).

Similarly, pingos on as Mars have been differentiated from other mounds, such as rootless cones, principally by their summit cracks (Figure 3.9) and pits, with some displaying flank mass wasting and irregular planforms. Such mounds have been reported in closed topographic environments, such as crater floors (Soare et al., 2013b), as well as at the base of slopes in more open topographic environments (Soare et al., 2014b). The implication of pingos on Mars is that there was sufficient melt to generate the talik, but no long-lived sub-surface water is required once they are formed. The age of the mounds on Mars is unknown, but they are not superposed by any other feature, so are presumably Late Amazonian in age. No alternative mechanism for ground-uplifting has been proposed as an alternative to the liquid water hypothesis, but the interpretation of these mounds as being a result of heave (and not one of the other potential and numerous mound-forming processes) remains under question, as liquid water is considered unlikely.

3.7.5.3 Patterned ground

Patterned grounds on Earth are characterised by the separation of the surface soils into relatively fine and clastic domains with regular, repeating patterns. These take the form of, sorted stone

circles, labyrinths, polygon-nets or piles, which can evolve into clastic stripes on sloping terrain. The ratio between the fines and clasts, the amount of confinement and the slope are all factors that play a role in determining the patterns that are expressed at the surface (Kessler and Werner, 2003). The mechanism that leads to the sorting is a feedback that involves frost heave combined with differing thermal inertias of saturated soil and stones (Hallet, 1990) and necessarily involves freeze-thaw cycles. On Mars surface patterns resembling those of sorted patterned ground on Earth have been identified at the equator (Balme and Gallagher, 2009), but more pervasively in the northern plains at >35 °N (Barrett et al., 2018, 2017; Gallagher et al., 2011; Gallagher and Balme, 2011; Soare et al., 2018b), but also in the southern hemisphere (Soare et al., 2016). The martian landforms include clastic polygons, stripes and boulder piles (Figure 3.10) and tend to be at the larger end of the scale of the sorted patterned grounds observed on Earth, with length-scales of tens of metres, as opposed to metres as usually seen on Earth (Barrett et al., 2018). The patterns follow the expected transition to stripes on sloping terrain on Mars as they do on Earth.

The presence of these landforms on Mars suggests a climatic episode where freeze-thaw cycles were common allowing the development of these landforms. An alternate CO_2 ice driven process is described in other papers (Dundas, 2021; Orloff et al., 2011, 2013), where CO_2 slab ice locks boulders in place while the ground contracts underneath them in winter, but no experimental or field evidence is available to test its efficacy, hence remains difficult to assess its likelihood. Whether these landforms are active at the present-day is unknown and their age is difficult to determine but given their uncratered and pristine appearance it is assumed to be late Amazonian.

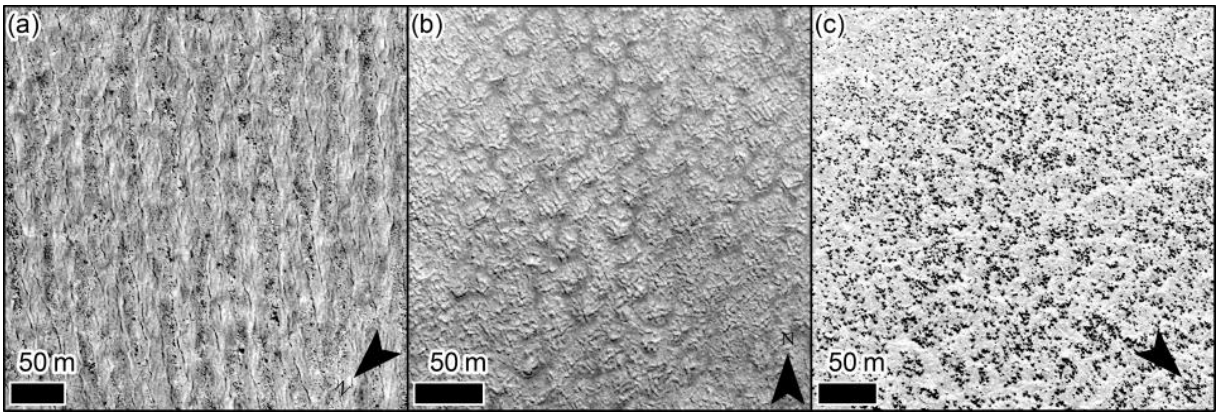

Figure 3.10: Examples of sorted forms on Mars. (a) Sorted stripes in Heimdal crater (Gallagher et al., 2011)*, where the stripes arepicked out by clasts, downslope is to the bottom of the image. HiRISE image PSP_009580_2485. (b) Sorted circles on the plains outside Heimdal Crater* (Gallagher et al., 2011)*. HiRISE image PSP_009580_2485. (c) Sorted nets near Lomonosov Crater* (Barrett et al., 2017)*, where clasts are arranged into polygonal patterns. HiRISE image ESP_017131_2485. Image credits: NASA/JPL/UofA.*

3.7.5.4 Low-centred polygons

In Section 3.5 we described the prevalence of polygonal patterns in the martian mid-to-high latitudes, which are believed to be a direct result of thermal contraction cracking of perennially frozen ground (Mellon, 1997). The polygons are generally metres to tens of metres in diameter (Mangold, 2005). In many areas the centres of these polygons are at lower elevations than their edge often with a double raised rim (Levy et al., 2009c, 2010b; Soare et al., 2014a, 2018a) (Figure 3.11d-f), "low-centred polygons", a phenomenon on Earth that is linked to active ice-wedge or sand-wedge polygons. Ice-wedge polygons form when liquid water penetrates cracks formed by thermal contraction and expands to both force the crack further apart and pushes up the material above it

(MacKay, 2002). Sand-wedges form when sand is repeatedly transported into the contraction crack and raised rims can be formed when the thermal re-expansion of the ground pushes against the additional material that has accumulated in the wedge causing the soil to be displaced upwards at the margin (Murton et al., 2000; Pewe, 1959). Without in situ investigation it remains unknown if the low centred polygons on Mars comprise ice or sand wedges and however, the presence of ice-wedges has been inferred by the landscape context of the low-centred polygons, a concept discussed further in Section 3.7.5.6. On their own low-centred polygons are ambiguous and have not been used to argue for the action of liquid water, but have been incorporated as part of a landscape assemblage that has been used to argue for the action of liquid water, see Section 3.7.5.6.

3.7.5.5 Ice-loss depressions

We refer readers Viola (2021) for a complete description of landforms interpreted to be a result of ice-loss collapse processes on Mars, but for completeness we provide an abridged description here as well. These landforms are often referred to as "thermokarst", which on Earth refers to landscapes created by collapse induced by thaw (increase in temperature), and on Mars this is likely not the case, so we do not use this term for Mars. "Cryokarst" is another term that has been used for these landforms (Costard, 2007), but is a term usually restricted to collapse features engendered by the loss of glacial ice via melting (e.g., Corbel and Gallo, 1970), hence we do not apply this term either. For collapse to occur the ground must contain ice in excess of the pore-space ("excess ice"), hence when it is lost a decrease in volume occurs. On Earth, ice-loss in thermokarst occurs via thaw, but on Mars ice-loss is more likely to occur by sublimation (e.g., Dundas et al., 2015a). This is in accord with observations, as no evidence of lakes or drainage channels have been observed. On Earth, thermokarst landforms are varied (e.g., Kokelj and Jorgenson, 2013), but of particular relevance to Mars are three features: terrain comprised of circular to oblate depressions often filled with water "alases" resulting from the degradation of excess ice, high centred polygons resulting from ice-loss at the polygon margins and beaded streams that are a result of the melting of ice in ice-wedge polygons. So called "scalloped depressions" are found on Mars (Figure 3.11b,c,e) and parallels have been drawn between these and alases on Earth (e.g., Lefort et al., 2010; Soare et al., 2008; Ulrich et al., 2010). These depressions are found polewards of 40°N (Orgel et al., 2018; Ramsdale et al., 2018; Séjourné et al., 2018) and poleward of 35°S (Voelker et al., 2017; Zanetti et al., 2010). A related feature is expanded craters (Figure 3.11a), which are circular resembling impact craters yet have an identifiable terrace (Viola et al., 2015; Viola and McEwen, 2018), and they have similar latitudinal distribution to scalloped depressions. High-centred polygons (Figure 3.11e) are found both in association with other ice-loss depressions on Mars and as isolated landforms, but as on Earth are associated with ice-loss at the polygon margins (e.g., Levy et al., 2009a; Soare et al., 2014a). On Earth, this loss can be from an ice-wedge (e.g., Ulrich et al., 2011), but also simply general loss of underlying massive or excess ice focused via the thermal contraction crack at the polygon margin (Marchant et al., 2002). Polygon junction pits (Figure 3.11b) are observed in Utopia Planitia (Costard et al., 2016; McGill, 1986; Soare et al., 2012, 2011) and parallels have been drawn between these expanded polygon margins and degraded ice-wedge polygons on Earth which form beaded-streams. All these ice-loss features are found in the mid-latitudes and also show concentrations at certain longitudes: Utopia and Acidalia Planitae in the northern hemisphere and Malea Planum in the southern hemisphere. The age of the ice-loss depressions is not easy to determine – they superpose all other landscape features, so are thought to be Late Amazonian (Viola, 2021).

Although it is likely that the ice-loss depressions on Mars do not involve the generation of liquid water, their presence is a strong indicator of excess ice and the generation of excess ice on Earth involves the presence of saturated ground (e.g., Rempel, 2007). Excess ice is differentiated from glacial or massive ice as it requires development of ice within the soil column, rather than deposition

of ice directly at the surface. Ice-loss terrain cannot develop in glacial ice as there would not be sufficient material left behind after thaw/sublimation to maintain the landform relief. Porous ice (analogous to firn) has been inferred to be present in areas with ice-loss terrain to depths of around a hundred metres from radar sounding data (Bramson et al., 2017, 2015; Stuurman et al., 2016), and could have up to 20% lithic material, however this is at odds with geomorphic evidence showing that ice could not have been precipitated from the atmosphere (e.g., boulders at the surface; Sizemore et al., 2015). Enriching the martian soil column to tens of metres of depth with ice in the absence liquid water is challenging because ice diffused into the pore-space tends to seal the underlying soil column from further deposition (Jakosky, 1983; Zent et al., 1986), even if migration through thermal contraction cracks is taken into account (Fisher, 2005). Segregation ice has been observed at the Phoenix landing site and can be generated without thaw (Mellon et al., 2009; Sizemore et al., 2015), but such diffusive processes are only thought to be able to produce excess ice in the first metre of the soil.

Note, that a porous medium with salt and ice in its pores will contain some residual liquid. The amount of unfrozen water depends on the temperature, salt concentration, salt type, and surface area of the medium. This water stays unfrozen due to freezing point depression due to the dissolved salts and because of the effects of surface energy along curved interfaces (Rempel, 2012; Sizemore et al., 2015). When a porous media with an appreciable amount of unfrozen water and permeability below freezing undergoes temperature cycling near 273 K, it can form segregated ice (i.e. ice lenses). This process is called cryosuction and occurs under a temperature gradient, where unfrozen water is suctioned to colder temperatures when the liquid veins in the colder soil constrict due to the colder temperature. This new water is then frozen and more water is drawn into the colder porous media. With the very cold temperatures of Mars, temperature cycling near 273 K only occurs within the first metre of the soil.

Hence, although ice-loss depressions are not thought to be engendered by melt, it is still an open question as to whether the generation of the terrain hosting these depressions implies enrichment of the ground in ice via migration of unfrozen water. The timing of the emplacement of the terrain hosting the ice-loss depressions is hard to determine, but is most likely to be during the Amazonian (Soare et al., 2015; R. J. Soare et al., 2021b; Viola, 2021; Willmes et al., 2012), although could be older.

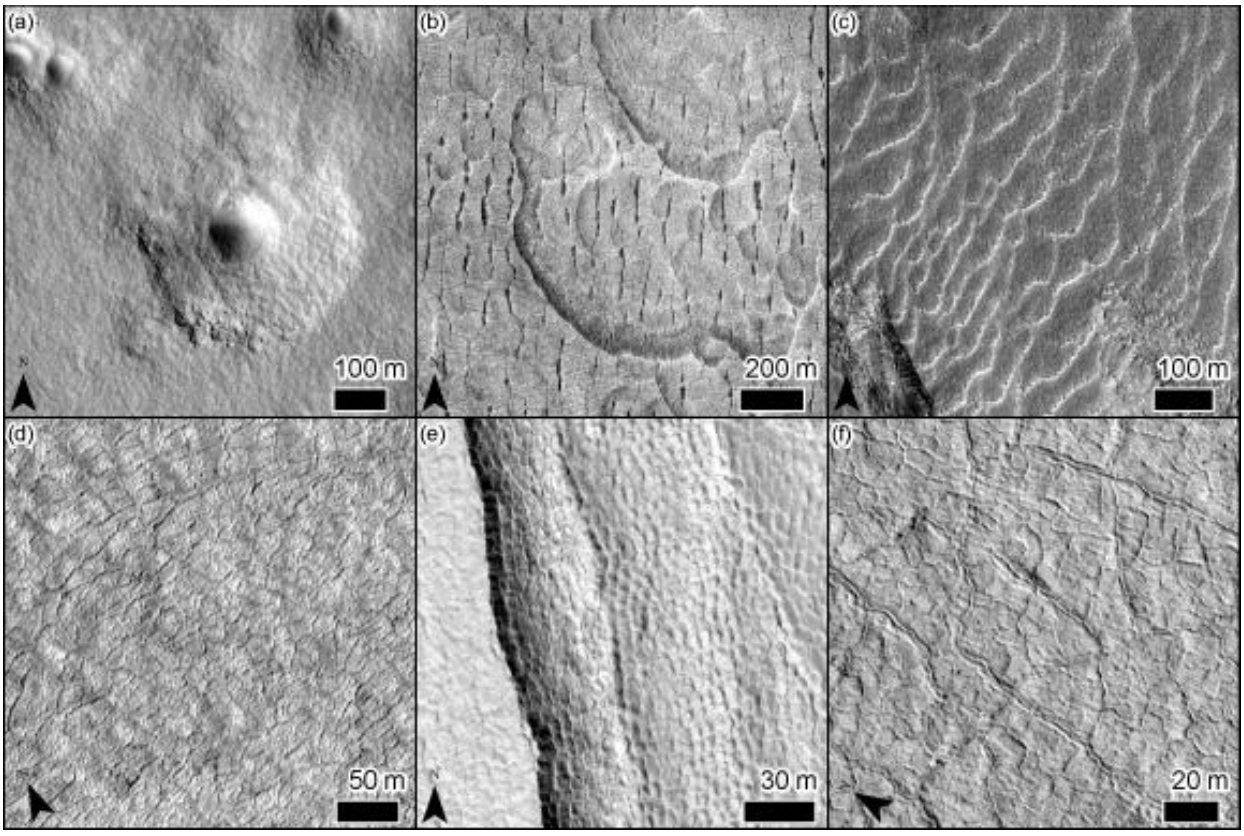

Figure 3.11: Examples of martian ice-loss depressions and different polygonal patterns. (a) Expanded secondary craters, where a polygonised basin can be seen extending away from the central bowl-shaped depression (REF). HiRISE image ESP_028411_2330. (b) "Scalloped" depressions in Utopia Planitia intersected by polygon-junction pits. HiRISE image PSP_007740_2250. (d) "Wavy" and polygonised depressions associated with gullies in the Argyre Basin. HiRISE image ESP_040974_1395. (e) Low-centred polygons on the inter-crater plains in the high southern latitudes. HiRSE image ESP_022381_1100. (e) Scalloped depression in Utopia Planitia with low-centred polygons near its wall and high-centred polygons on its floor. HiRISE image ESP_034164_2260. (f) Polygon margins marked by a double-raised rim. HiRISE image PSP_005821_1095. Image credits: NASA/JPL/UofA.

3.7.5.6 Landscape Assemblage

Above, we have examined each landform independently and examined the likelihood that each could be a result of processes involving liquid water. However, landforms do not occur in isolation and both the context and the association between landforms can favour one interpretation over another. This concept of a landscape assemblage (Figure 3.12) has been used to argue for the involvement of liquid water in the generation of landscapes on Mars (Balme et al., 2013; Gallagher and Balme, 2011; Hauber et al., 2011b, 2011a; Soare et al., 2005, 2014a, 2016, 2018a, 2018b; R. J. Soare et al., 2021b), where gullies, sorted patterned ground, lobate forms, low-centred polygons, pingos and/or ice-loss depressions are found in close proximity suggesting a common suite of processes in their origin. Figure 3.12 outlines such a scenario where freeze-thaw cycles within the materials in the crater wall, brings about sorting (to form stripes) and gelifluction to create solifluction lobes – extreme melting events lead to generation of gullies, whose melt water drives the formation of pingos at the base of the slope. The context of many of these assemblages is interpreted to be post-glacial, because of the following attributes: "washboard" texture on slopes (indicative of downslope deformation), polygonal surface textures and ice-loss-depressions (indicating high ice content), expanded fractures (which could be crevasses), all upslope of arcuate ridges with spatulate depressions (interpreted to

be moraines, e.g., Berman et al., 2005) and often stratigraphically above older glacial units (Head et al., 2008a; Jawin et al., 2018).

The fact that CO_2 ice processes and sublimation landscape assemblages are not found on Earth means an equivalent comparison cannot be made, a point that discussed further in Section 3.7.4.

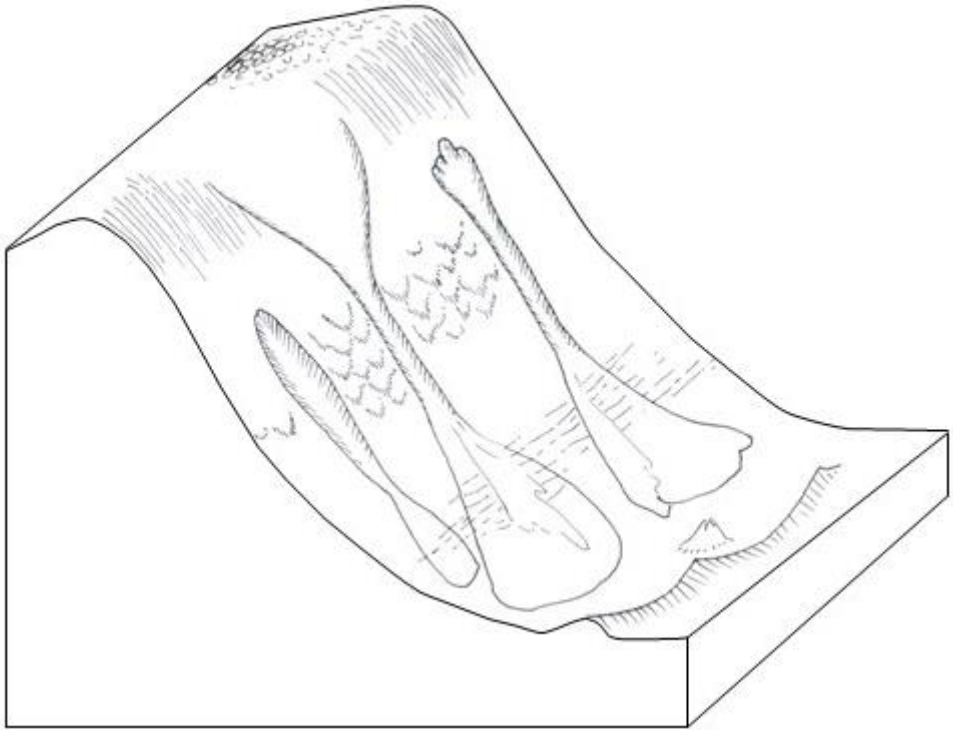

Figure 3.12: Sketch of landscape assemblage on a crater wall, with (from top to bottom), sorted circles leading into sorted stripes then solifluction lobes. Hillslope is incised by gullies, whose fans are partially overprinted by extensional fractures. At the base of the gullies are arcuate ridges and in the intervening basin, a pingo.

3.7.5.7 Periglacial contributions

My contribution to the state-of-the-art: With colleagues I have reported on periglacial landform assemblages from various regions of the planet, including Borealis Planitia (Gallagher et al., 2011) , Utopia Planitia (R.J. Soare et al., 2021; Soare et al., 2018b, 2013a, 2013b), Argyre Planitia (Soare et al., 2016, 2014a, 2014b), and Moreaux Crater in the northern plains (R. J. Soare et al., 2021b, 2021a). All these associations suggest that thaw has actively modified the top few metres of the ground on geologically recent timescales. Some of these periglacial landscapes may being revealed from lower strata meaning they represent a more ancient climate that was conducive to thaw (R. J. Soare et al., 2021a). Two papers specifically focused on lobate hillslope forms on Mars and we found close similarity in morphometry and geomorphology with solifluction lobes on Earth (Gastineau et al., 2020; Johnsson et al., 2018). In Gastineau et al. (2020) we specifically reported the dissimilarity between martian lobes and tiger stripes - patterns of stones formed in the hyperarid Atacama desert – an environment considered as one of the best Mars analogues. In Dundas et al. (2019b) we found evidence for recent boulder movement associated with some of the lobate forms , suggesting a possible formation by CO_2 ice driven processes. However, a lack of timing constraint and a definite link between the lobes and boulder movements means solifluction is still the leading hypothesis.

In Tesson et al. (2020) our initial hypothesis was that periglacial processes or at least thermal contraction/expansion cycles of ices could be one of the factors triggering rockfalls on Mars. This

work revealed that thermal stress was more important and slopes with ice deposits tended to produce fewer rockfalls, however latitudes polewards of 20° were not studied. We used this data to train a neural network to recognise rockfall tracks automatically in HiRISE images (Bickel et al., 2020b) and we have a NASA MDAP proposal accepted to use this trained neural network on the whole dataset, hence should be able to further examine this hypothesis.

3.7.6 Evidence for melting of martian icecaps or glaciers

Evidence for melting of martian icecaps or glaciers spans from the present-day, to contemporaneous with gullies (millions of years ago), contemporaneous with extant martian glaciers (hundreds of millions of years ago) to much earlier in martian history (billions of years ago). Orosei et al. (2018) and Lauro et al. (2020) reported radar evidence which suggested the presence of lakes of liquid brine underneath the south polar cap of Mars at the present-day. Recent modelling work has highlighted that the position of the proposed lake is not located in a local depression, but is connected to the hydrological system, hence is more likely a pocket of brine caused by locally elevated geothermal flux (Arnold et al., 2019). While MARSIS detects a significant radar return, it is unfortunate that the higher frequency radar sounder SHARAD has not detected this anomaly. SHARAD cannot always image the floor of the SPLD, however, given such a large signal one would expect a detection. Hence, although not substantiated by other evidence, it remains plausible that liquid water can be generated at the base of the martian polar caps, even under present-day conditions. Various lines of evidence already point to the fact that the south polar cap has undergone basal melting in the Early Hesperian – Late Noachian (e.g., Kress and Head, 2015). Sinuous ridges emanating away from the boundary of the south polar cap have been interpreted to be eskers – deposits laid down in sub-glacial channels (Butcher et al., 2016; Kress and Head, 2015; Scanlon et al., 2018, 2015). Scenarios in which elevated geothermal heat flux is required in the form of volcano-ice interaction (Ackiss and Wray, 2014; Ghatan and Head III, 2002; Wray et al., 2009) and passive climate-driven melting with a generally larger Noachian geothermal heat-flux (Fastook et al., 2012) have been explored and found to be plausible.

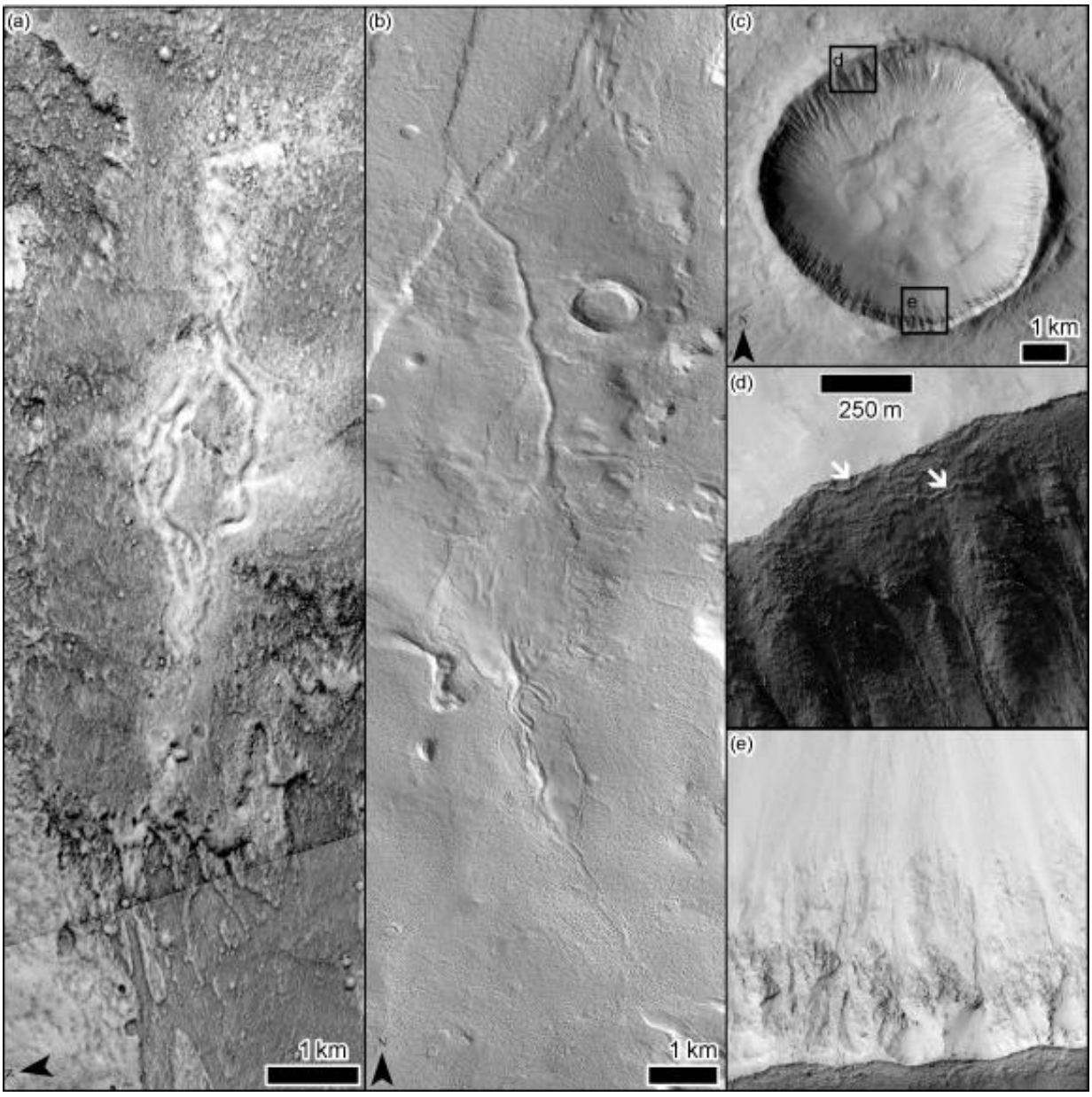

Figure 3.13: Evidence of basal melting of glaciers on Mars. (a) Sinuous ridge in Phlegra Montes (Gallagher and Balme, 2015) *interpreted as an esker, whose parent glacier is located off the bottom of the image. CTX Images G20_026224_2116 and P22_009583_2132. (b) Sinuous ridge emerging from parent glacier located in lower half of image in Tempe Terra* (Butcher et al., 2017)*. CTX image P05_002907_2258. (c) Crater in the southern mid-latitudes in CTX image G09_021563_1427 showing evidence of glacial erosion, where the glaciated pole-facing slope in (d) has a lower slope-angle with the bedrock spurs planed off (arrows) directly above arcuate ridges interpreted to be moraines, and the non-glaciated equator-facing slope in (e) has preserved bedrock spurs exhibiting a higher slope angle* (Conway et al., 2018a)*. (d-e) HiRISE image PSP_006663_1425. Image credits: NASA/JPL/UofA/MSSS.*

Sub-glacial or sub-ice-cap melting has also been proposed as an alternative to "the warm wet early Mars" explanation for the valley networks (Section 2.3) which are a global surface feature (e.g., Cassanelli and Head, 2015; Fastook and Head, 2015; Weiss and Head, 2015; Wordsworth et al., 2013). In contrast, the presently visible glaciers on Mars are generally believed to be cold-based, that is, their interior temperature never rises above the freezing point of water, hence their deformation

progresses via the plastic deformation of ice integrated over long time periods. As described in Section 3.5, the martian mid-latitudes are host to a huge number of glacial forms (Figure 3.2d), which are believed to be several tens to hundreds of million years old (see Hepburn et al., 2019 and references therein). Some evidence for surface melting of these features comes in the identification of tens of small supraglacial and pro-glacial channels (Fassett et al., 2010), but such channels do not imply the long-lived liquid water involved in basal melting. Recent work has overturned the cold-based paradigm for Amazonian glaciers in two ways: firstly examples of Amazonian debris covered glaciers directly associated with eskers have been reported (Butcher et al., 2017; Gallagher and Balme, 2015), and evidence has been found for enhanced erosion of mid-latitude crater walls which is consilient with wet-based glaciation in the last 5-10 Ma (Conway et al., 2018a).

In Phlegra Montes and Tempe Terra, sinuous ridges emerge from extant debris covered glaciers found within fault-bounded graben (Figure 3.13). These ridges are interpreted as being eskers, not just because of their intimate association with the glaciers, but because their morphological and topographic relationships are consistent with expectations from terrestrial glaciers/ice sheets (Butcher et al., 2017; F. E. G. Butcher et al., 2020; Gallagher and Balme, 2015). The formation of eskers requires substantial amounts of liquid water and its fate once it emerged from under the ice would have likely been quick evaporation and freezing, although no geomorphic evidence is apparent to support or refute this inference. It should be noted that on Earth catastrophic outbursts from sub-glacial conduits do not produce terminal deposits, in contrast to long-lived more stable flows (Burke et al., 2012; F. E. G. Butcher et al., 2020). As both systems are within fault-bounded graben, elevated geothermal heat flux associated with the crustal-thinning could be the reason that only these isolated individual esker systems have been found.

Analysis of high resolution digital elevation models has revealed systematic lowering of the slopes of pole-facing crater walls in the mid-latitudes intimately associated with the removal of bedrock spurs and transformation of the texture of the exposed bedrock (Conway et al., 2018a)(Figure 3.13). The amount of horizontal retreat required to explain the observed slope-lowering ranged up to 10^2 m/Myr and this elevated value is consistent with erosion rates of wet-based glaciers on Earth. Cold-based glaciers on Earth have erosion rates of tens of metres per million years and rates on Mars are expected to similar or lower because of the lower gravity and lower mean average temperature making the ice more rigid (Karlsson et al., 2015). The parts of the craters affected by the slope-lowering are intimately associated with the presence of a “pasted-on” mantling deposit located downslope of the removed bedrock, which can be interpreted to be an ice-rich till-like deposit due to the presence of downslope lineaments (striations). Where this mantle-deposit interacts with older glacial deposits (LDA or CCF) located on the crater floor there are arcuate ridges interpreted to be moraines (Arfstrom and Hartmann, 2005; Berman et al., 2005, 2008; Head et al., 2008a; Jawin et al., 2018; Whalley and Azizi, 2003). On Earth, terminal moraine ridges are formed by thrusting of the basal sediments towards the glacial surface, which is facilitated by the presence of liquid water (e.g., Benn and Evans, 2010), but recent research has revealed they can occur due to deceleration in entirely frozen cold-based glaciers (Fitzsimons and Howarth, 2020).

The implication of this work is that widespread, but limited melting occurred within the top decametres of the ground in the last 5-10 Ma on Mars. The exact trigger for this “event” is unknown, but seems to be related to the shift of Mars to lower average obliquity at 4.5 Ma (Laskar et al., 2004, 2002). Another possibility is that periglacial processes have caused the observed slope-lowering (which would still involve liquid water) or some other process driven by CO_2 frost-driven rock-breakdown, but at present no viable mechanism has been proposed. Given the close association of

this suite of landforms with gullies it is tempting to implicate melting for the whole suite of landforms, but whether this is reasonable is certainly debatable.

My contribution to the state-of-the-art: I co-supervised Frances Butcher's Undergraduate and PhD Dissertations where eskers were studied in detail. She reported on the morphometry of ridges in the Dorsa Argentea near the south polar cap and concluded they were similar to terrestrial eskers and thereby confirming previous interpretations of these representing drainage landforms of a former more extensive south polar cap (Butcher et al., 2016). She also studied ridges connected to extant glaciers on Mars and concluded that they were eskers resulting from melting of these ice bodies caused by exceptional conditions of elevated heat flux (Butcher et al., 2017; F. E. G. Butcher et al., 2020).

Modelling performed by collaborator Neil Arnold has revealed that the lakes under the south polar cap identified by radar could also be caused by elevated geothermal flux and further, be connected to the subglacial hydrological network (Arnold et al., 2019). In a recently accepted Nature Astronomy paper we show that subtle variations in the surface topography of the South Polar cap are consistent with topographic anomalies above subglacial lakes on Earth – supporting the possibility of basal water initially proposed from radar data (Lauro et al., 2020; Orosei et al., 2018), but widely contested.

Finally, I wrote the key paper describing the evidence for widespread glacial erosion associated with pasted-on terrain and the implication that this involves widespread melt (Conway et al., 2018a), described above.

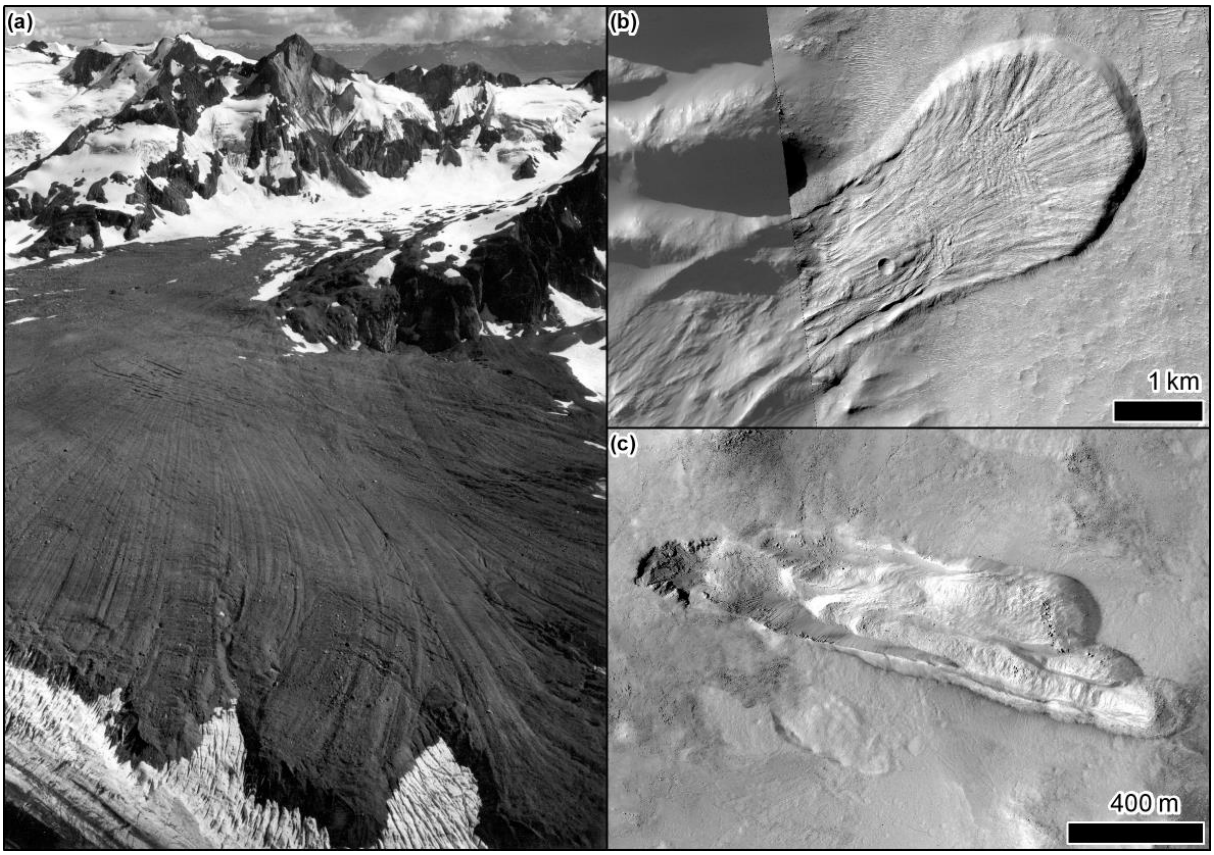

Figure 3.14 Landslides potentially influenced by water on Earth and Mars. (a) The 1964 Sherman Glacier long runout rock avalanche whose longitudinal ridge-and-furrow surface texture is attributed to its runout over an ice-body. Photo ID "ake00237" from the USGS photo library. (b) Landslide in a

26-km-diameter crater on Mars, whose deposits show a longitudinal ridge-and-furrow surface texture. North is up. HiRISE image ESP_043963_1550 overlain on CTX B01_010008_1554, credit NASA/JPL/UofA/MSSS. (c) Landslide part way down a 20° crater wall north of Nili Fossae showing evidence of viscous deformation (levees, compression ridges) attributed to the action of water.

3.7.7 Water in landslides

The potential role of water in landslides on Mars has been an ongoing issue since their discovery (De Blasio, 2011; Lucchitta, 1978), because of their extraordinary mobility, i.e. their long run out. In order to exceed the nominal run out distance predicted for a given rock mass there has to be a factor that reduces the fictional resistance. One possibility is liquid water or ice. In terms of volume only submarine landslides compare to the largest landslides on Mars which are found in the Solar System's largest canyon Valles Marineris (Legros, 2002). A recent survey (Crosta et al., 2018) revealed > 3000 landslides with areas > 1 km^2 found globally whose distribution cannot simply be attributed to the distribution of unstable slopes (Roback and Ehlmann, 2021). Only some of these landslides can be classified as being long run out. One of the remarkable characteristics of these long run out landslides is the presence of a series longitudinal ridges and furrows (e.g., Magnarini et al., 2021) (Figure 3.14). These features are also found in long run out landslides onto glaciers on Earth (Figure 3.12), which was one of the initial motivations for suggesting the involvement of water in these landslides (e.g., Lucchitta, 1978). These long runout landslides formed between 3.5 Gy and 50 My (Quantin et al., 2004b). Features of some of the smaller landslides, including a lobate terminus and lateral levees, also suggest the involvement of liquid water, because terrestrial debris flows involving water also show these features. Many of these smaller landslides are late Amazonian in age, so the presence of liquid water becomes more contentious.

My contribution to the state-of-the-art: I co-supervised Anthony Guimpier's Masters and PhD dissertations, where he found that four landslides (Figure 3.14) within a crater north of Nili Fossae had similarities with terrestrial earthflows, which necessarily involve liquid water to form (Guimpier et al., 2021; Pajola et al., 2022). These similarities included initiation on a slope around 20° inclination, presence of lateral levees, a steep lobate margin and compression ridges. Numerical modelling revealed that a dry granular flow could not reproduce this morphology. These landslides likely formed in the last few millions of years based on the lack of superposed craters, hence the origin of this water is puzzling. We suggest two possibilities: groundwater brought up by recent activity in the Nili Fossae system, or local melting of surface ice deposits, but we found no compelling evidence to support either hypothesis.

3.7.8 Sedimentary volcanism

Sedimentary volcanism is the mobilisation of sediments by groundwater circulation and is usually engendered on Earth pressurised aquifers caused by dense sediments overlying less-dense saturated sediments. Most eruptions are facilitated by gas production (usually methane) and/or tectonic activity. When this process involves clay-sized sediments it is referred to as mud-volcanism. Pitted cones interpreted to be mud-volcanoes have been reported in all three basins in the northern plains of Mars: Acidalia Planitia (e.g., Hemmi and Miyamoto, 2018; Oehler and Allen, 2010; Figure 3.15a), Chryse Planitia (e.g. Brož et al., 2019; Komatsu et al., 2016; Martínez-Alonso et al., 2011) and Utopia Planitia (e.g., McGowan, 2011; Skinner and Tanaka, 2007) (Figure 3.15b). These basins are at a lower elevation than the southern highlands (Figure 3.2d) and form a depositional trap for the sediments eroded from the highlands by the valley networks and outflow channels (e.g., Tanaka et al., 2005). At other sites, such as Candor and Coprates Chasmata (Okubo, 2016) and Terra Sirenum (Hemmi and Miyamoto, 2017) the pitted cones are located in sedimentary fill in other smaller basins. Sedimentary volcanism is thought to mobilise the sediments accumulated in these various basins to form cones

and flows. In Acidalia the mud-volcanoes are also associated with polygonal patterns tens of kilometres in diameter, which could represent fluid expulsion pathways (Allen et al., 2013). Fractures and spatially associated pitted cones are also interpreted to be a result of sedimentary volcanism in the Galaxias region (Figure 3.15c) (Gallagher et al., 2018) and sedimentary volcanism is a common interpretation of such enigmatic assemblages of km-scale polygonal fractures, ridges and aligned-cones (e.g., De Toffoli et al., 2018; Ivanov et al., 2014; Salvatore and Christensen, 2014; Skinner and Mazzini, 2009).

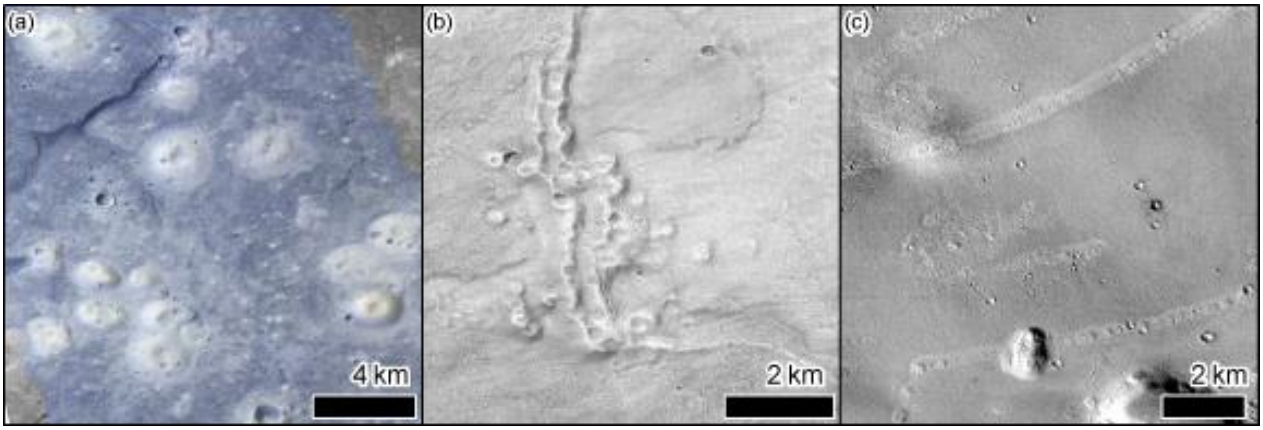

Figure 3.15: Examples of evidence for sedimentary volcanism on Mars. (a) Pitted cones in Acidalia Planitia with a fracture-junction visible top-left. CaSSIS image MY35_009369_141_0 with channels NIR, PAN and BLU mapped to RGB. (b) Pitted cones and ridges in southern Utopia Planitia. HiRSE image ESP_053364_2135. (c) Aligned cones in Galaxias region, CTX image B05_011746_2156. Image credits: NASA/JPL/UofA/MSSS/ESA/Unibe.

Present-day detections of methane in the martian atmosphere are still heavily debated (e.g., Webster et al., 2018 and references therein), but the discussion of methane has reignited interest in finding and analysing the surface expression of sedimentary volcanism on Mars, as methane gas can be a key driver of sedimentary volcanism on Earth. However, many of these features are estimated as being Amazonian in age or older (Ivanov et al., 2014; Komatsu et al., 2016; Oehler and Allen, 2010; Senthil Kumar et al., 2019), and in general are older than gullies and the most recent periglacial and glacial landforms, which means they cannot be *directly* linked to present-day atmospheric methane detections. Sedimentary volcanism implies a source of pressurised liquid water underground whose supply could be engendered by a wide-range of processes including: the impingement of the cryosphere on the hydrosphere due to long-term climate-shifts, destabilisation of clathrates (e.g., De Toffoli et al., 2019) via localised increases in geothermal heat flux or seismic/tectonic/magmatic activity, or simply diapirism of trapped saturated sediments (see summary in Skinner and Tanaka, 2007).

Sedimentary volcanism and by association liquid water, is not the only hypothesis for the generation of this suite landforms. Mud-volcanoes could easily be confused with magmatic cones, especially as the behaviour of mud is not well-constrained under martian surface conditions (Brož et al., 2020b) and similarly the associations of cones, ridges and fractures have been attributed to a range of processes, e.g. volcanic (e.g., Fagents et al., 2002; Frey and Jarosewich, 1982; Ghent et al., 2012), tsunamigenic (Costard et al., 2017) and glacial (e.g., Guidat et al., 2015; Kargel et al., 1995; Rossbacher and Judson, 1981). These alternates also imply liquid water, as the volcanic hypothesis requires volatile enrichment to cause the explosive eruptions making the cones (lava-ice or lava-water interaction). The alternates generally imply short-lived episodes of water generation, as opposed to the long-lived aquifer implied in sedimentary volcanism. Liquid water is consistent with

the morphology of these features and it is difficult to assess if the sub-surface conditions of Mars could have been conducive to their formation via sedimentary volcanism, as we know so little about the internal structure of Mars (cf. Section 3.6).

My contribution to the state-of-the-art: Czech collaborators performed the first experimental exploration of the effects of the martian environment on the behaviour of mud flows (Brož et al., 2020a, 2020b). These experiments revealed that boiling and freezing combine to produce features analogous to those found in terrestrial lava flows. This has two implications: first diagnostic morphologies of mudflows and mud volcanism on Earth cannot necessarily be used to identify their analogues on Mars; second many Martian features initially interpreted as resulting from magmatic volcanism may result from sedimentary volcanism. In Brož et al. (2022) , we report on a series of subtle topographic landforms associated with mud volcanism in Chryse Planitia on Mars. These new landforms were only identifiable in elevation data at 1 m/pix derived from HiRISE images. We also revealed a complex suite of landforms in Galaxias Chaos (Gallagher et al., 2018), comprised of disaggregated landscape when fractures transition to ridges, pits chains to mound-chains and divided mesas. These landforms represent fracturing and sliding of blocks of more coherent material over a mobile saturated sedimentary layer that in places descended between the blocks and in other places was extruded onto the surface. Downslope of this assemblage lies a series of drainage channels leading to the northern plains.

3.7.9 Liquid water morphologies associated with impacts

Hypervelocity impacts by bolides into planetary surfaces deposit huge amounts of energy into the target body, of which most is converted into heat (Melosh, 1989). The lack of substantial atmosphere on Mars means that bolides reach the surface with greater energy than they do on Earth. As discussed in Section 3.3 we know that there are substantial amounts of water ice in the near-surface of the martian crust and potentially a deep cryosphere, and so the heat deposited into the crust by impacts could generate liquid water by melting. This could be melting immediately during the impact in the cavity and the ejecta (e.g., Boyce et al., 2012; Newsom, 1980; Weiss and Head, 2016), vaporisation of the ice could inject vapour into the surrounding atmosphere and create a transient and localised hydrological cycle (e.g., Kite et al., 2011; Segura, 2002; Segura et al., 2008; Steakley et al., 2019) and finally the thermal anomaly could maintain hydrothermal circulation within the crust for thousand or millions of years post impact (e.g., Abramov and Kring, 2005; Barnhart et al., 2010; Osinski et al., 2013; Rathbun and Squyres, 2002).

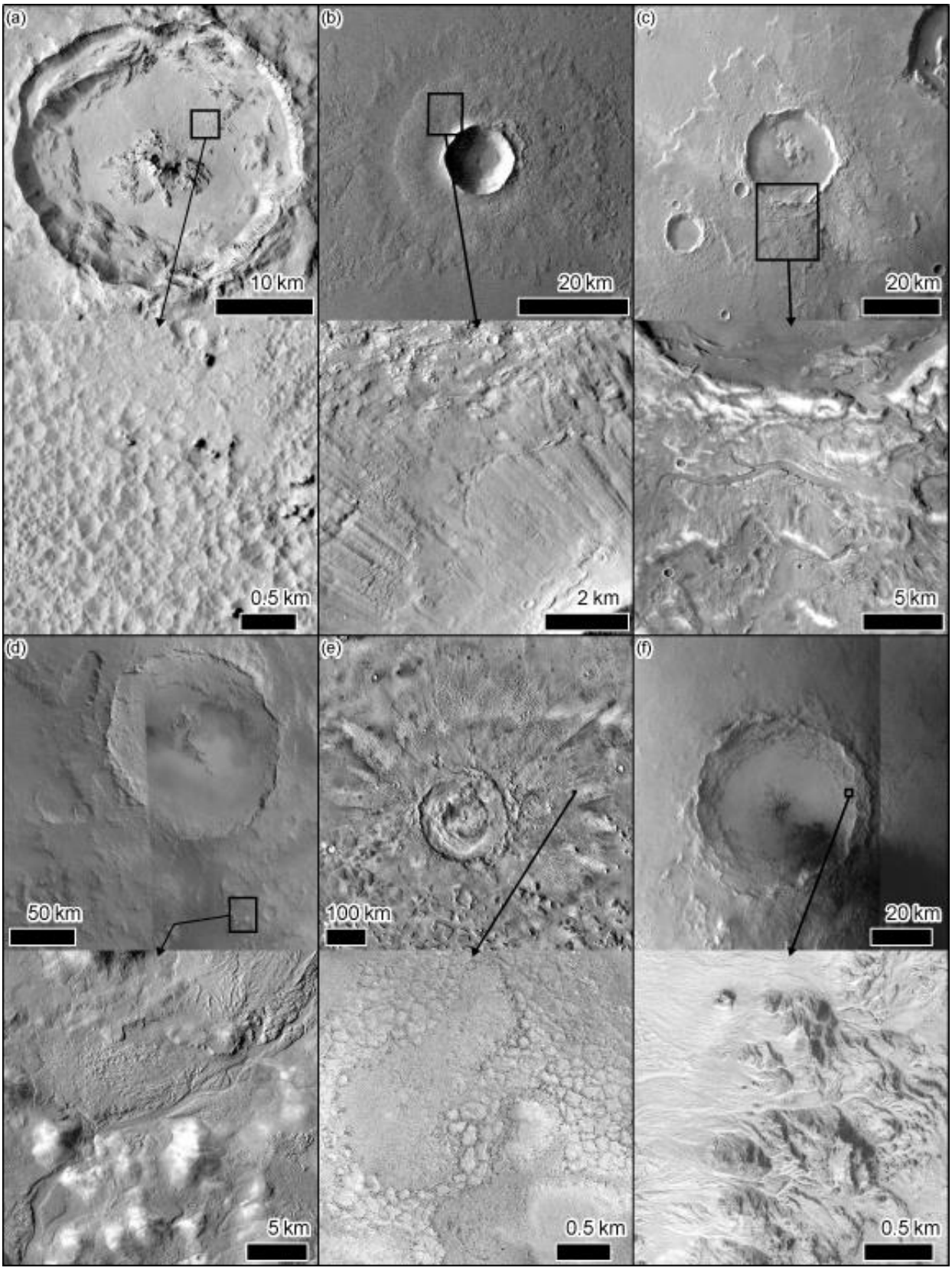

Figure 3.16: Crater-related liquid water morphologies. (a) Pits on the floor of <10 Ma Tooting Crater (Mouginis-Mark and Boyce, 2012)*. CTX image P01_001538_2035. (b) Double-layered ejecta crater in northern plains, with lobate margins and radiating grooves* (Weiss and Head, 2014)*. Top HRSC image h2878_0000 and bottom CTX image P20_008833_2149. (c) Multilayer ejecta crater in southern hemisphere with channels incised into its ejecta blanket* (Mangold, 2012)*. Top, HRSC image*

ha313_0000, bottom CTX image B16_015984_2149. (d) Hale Crater with channels incising the ejecta. Top HRSC images h2526_0001 and h0533_0000, bottom CTX image P03_002220_1418. (e) Lyot Crater with clastic polygonal networks in the ejecta. Top THEMIS day IR controlled mosaic image from the USGS and bottom HiRISE image ESP_016985_2315. (f) Mojave Crater with alluvial fans on the inner craters slopes. Top HRSC images hd605_0000 and h1991_0000 and bottom HiRISE image ESP_012834_1875. Image credits: NASA/JPL/MSSS/ESA/DLR/UofA.

Geomorphological evidence for these processes in the Amazonian epoch is abundant. Craters only a few million years old display pits on their floors (Figure 3.16a) and within their ejecta materials interpreted to be a result of volatile-release as steam (Boyce et al., 2012; Morris et al., 2010; Mouginis-Mark and Boyce, 2012; Tornabene et al., 2012). These pits can be associated with incised channels, alluvial fans (Figure 3.16f) and debris lobes emanating from high points inside the crater cavity, thought to represent the flow of water-rich materials immediately post-impact, e.g. alluvial fans in Tooting and Mojave Craters both dated to < 10 Ma (Goddard et al., 2014; Morris et al., 2010; Williams and Malin, 2008). Channels incising into and emanating from ejecta blankets are used as evidence for water escaping from the melting cryosphere beneath (Figure 3.16c,d) (El-Maarry et al., 2013; Harrison et al., 2010; Jones et al., 2011; Mangold, 2012; Weiss et al., 2017). Clastic polygonal networks in the ejecta of Lyot Crater (Figure 3.16e) even suggest that water in the ejecta blanket could result in longer-term ice-segregation processes (Brooker et al., 2018) and conical landforms in the ejecta flows at Hale Crater may also be suggestive of longer-term ice-loss processes (S. Conway et al., 2019).

Lobate ejecta morphologies (e.g., multi-layer ejecta, double-layer ejecta - Figure 3.16b) are interpreted to be the result of fluidisation and are observed almost exclusively at the mid- to high-latitudes (e.g., Barlow, 2006, 2005; Barlow and Perez, 2003; Costard, 1989; Mouginis-Mark, 1981, 1979). Numerical models generally find this morphology to be consistent with either melting or a volatile-rich layer (e.g., Baratoux et al., 2002; Oberbeck, 2009; Weiss and Head, 2014, 2013). However, other modelling studies find that the fluidisation is unrelated to water and could be due to increased fragmentation (Rager et al., 2014) or the presence of an erodible surface (Wada and Barnouin-Jha, 2006) –yet both require preconditioning of the surface by water or water ice to explain the latitudinal distribution.

Spectral evidence for hydrothermal alteration is common in craters prior the Amazonian, but is lacking in Amazonian craters (Turner et al., 2016). Similarly, evidence for crater-bound paelolakes, which could result from hydrothermal circulation are lacking particularly from the late Amazonian epoch (e.g., Cabrol and Grin, 1999).

Craters also host numerous fluvial channels or fans that cannot necessarily directly be linked to the impact event itself but could be formed as a result of the impact's topography (microclimate, and/or sink) or its interaction with groundwater. Examples include: regional drainage networks of Lyot Crater linked to surface ice accumulation and melt in a climatic microenvironment (Dickson et al., 2009), valleys draining into craters' central pit (Peel and Fassett, 2013), and alluvial fans dated to around ~1 Ga resulting from prolonged runoff (e.g., Grant and Wilson, 2011; Kite et al., 2019, 2017; Nicolas Mangold et al., 2012).

In summary, impact crater related morphologies in the late Amazonian represent very transient melting of ground ice mobilised by the impact event, with more substantial evidence for sustained liquid water environments tending to come from the early Amazonian. In essence, most of these landform interpretations are consistent with our expectations for the existence of liquid water on

Mars, as impacts are almost intuitively expected to cause melting if they interact with ice, but some of the details of exactly how much water and its origin are more the focus of debate.

My contribution to the state-of-the-art: In Brooker et al. (2018), we examined the hundred metre scale polygonal network found in amongst the ejecta deposits of Lyot Crater, the impact that penetrates the deepest into the northern plains. These polygons are formed by metre-scale clasts that are often aligned along the polygon margins, they are found at a consistent range from the crater centre and only in the ejecta to the E and NE of the crater. They are found in the hollows of the ejecta. We hypothesized that these polygons could represent post emplacement freeze-thaw cycling of parts of the ejecta particularly enriched in water. We found no evidence to support periglacial process at work, nor desiccation cracking but rather that these polygons are large thermal contraction polygons filled by cementing material that later broke up.

In a further paper under consideration (see abstract - Conway et al., 2020), we examine the ejecta deposits of Hale crater (Masters project of Coralie Peignaux), which have evidence for fluidisation and dewatering reported in other papers (Collins-May et al., 2020; El-Maarry et al., 2013; Jones et al., 2011). Here, we report on fields of cones associated with these fluidised ejecta and we make an analogy with molards on Earth (Section 4.3) to suggest that the Hale impact ejected blocks of ice cemented sediment several to tens of decametres in size that were subsequently transported in the more viscous part of the fluidised ejecta.

3.7.10 Other evidence for liquid water in the Amazonian

Other morphological evidence for liquid water dates to the early Amazonian with both valley networks and outflow channels having been reported to have been active at this time. It is generally acknowledged that water in such systems was short-lived and ephemeral in contrast to the Noachian valley networks (e.g., Hauber et al., 2013; Wilson et al., 2016). For example, shallow snowmelt has been proposed to explain valleys in Gorgonum and Newton basins (Howard and Moore, 2011), for Kārūn Valles (Adeli et al., 2016) and valley networks on the flanks of martian volcanos (Fassett and Head III, 2008). A liquid water origin for these landforms represents the consensus even if its source is debated and varied.

Some of the martian outflow channels are also dated to the Amazonian (particularly those on the flanks of the martian volcanos) and their interpretation is less consensual. A detailed discussion of the competing hypotheses can be found in Levington (2021) and Gallagher and Bahia (2021). In brief the crux of the debate is whether these outflow morphologies can be ascribed to outpourings of water or mud triggered by lava-ice interaction (e.g., Balme et al., 2011; Burr, 2002; Vijayan and Sinha, 2017; Wilson and Head, 2002) or deep aquifer sources (e.g., Hanna and Phillips, 2006; Marra et al., 2014; Wouter A. Marra et al., 2015), or low viscosity lava (Leverington, 2011, 2009). The debate arises from the observation that these outflow channels are covered in basalt and are not apparently covered by sedimentary facies, as might be expected from outpourings of liquid water.

3.8 Synthesis and outlook

The reason that the debate around the evidence for liquid water in Mars is still a hot topic is because the search is motivated by not only scientific curiosity, but can be framed in the larger question of whether life exists or arose elsewhere in the Solar System. In the search for present or past life beyond our planet, finding evidence of present or past liquid water on Mars has been a preoccupation of planetary scientists since the beginning of orbital observations and has been the reason that various space agencies have sent missions to Mars (and NASA's motto "follow the water"; Hubbard et al., 2002; e.g., ESA's ExoMars missions; Kereszturi et al., 2016; Vago et al., 2017). Without a protective atmosphere the surface of Mars is bathed in ionising radiation and solar

particles, making it a particularly challenging surface environment for life at the present-day (e.g., Teodoro et al., 2018). However, finding evidence that liquid water has appeared periodically at the surface could indicate that Mars has subsurface water reservoirs that could be harbours for extant life. Recent activity of liquid water also bolsters the probability of liquid water activity in the past and the longevity of habitable conditions. The presence of habitable conditions also increases the chance that the space probes we send to Mars could contaminate these likely uninhabited habitats (Cockell et al., 2012) and out of this concern have arisen planetary protection regulations (National Aeronautics and Space Administration, 2005). These regulations determine the level of sterilisation to which a spacecraft must be submitted to reduce the likelihood of cross-contamination. This effectively prohibits the direct exploration of zones that could have liquid water, for example sites with RSL and gullies are subject to these rules (Kminek et al., 2010; Rummel et al., 2014). Water is also an important resource for future human investigations, even in its solid state (e.g., Heldmann et al., 2014) and hence finding zones where relatively pure water ice would be easily accessible has attracted some recent attention (e.g. SWIM project; Perry et al., 2019).

While none of the features described here have been proven beyond all doubt to require the activity of liquid water, in the aggregate it is challenging to explain all of them without any liquid water on an ice-rich planet that has straddled the triple point of water for all of the Amazonian. Liquid water is more generally agreed to be responsible for early Amazonian features including valleys, channels, alluvial fans and deltas, most of which are thought to originate from punctual or rare events. However, a consensus view has not been reached over the role, or not, of sedimentary volcanism in building landforms over this period. In the late Amazonian to present-day, the role of water is much less certain, with practically all landforms interpreted as being linked to liquid water having substantial alternate hypotheses. The exceptions are solifluction lobes and pingos where to-date there is no alternate hypothesis to those involving liquid water has been proposed. The evidence for sub-glacial melting in the Late Amazonian is a topic that has only recently been opened and will likely receive more attention as more observations are collected. For presently active features, the focus is currently on processes that do not involve liquid water, but the behaviour of certain downslope flows means that liquid water has not been entirely ruled out. RSL continue to be the most likely of presently active surface features to be linked to liquid water. For the reasons outlined above it is important to continue studying these landforms and continually assess the balance of evidence as new data are collected.

The long-lived and ongoing debate over the presence of recent liquid water at the martian surface raises a couple of important questions for planetary science:

- What level of knowledge do we need to determine (with a reasonable level of confidence) whether liquid water could be present at the surface?
- Are we being misled by Earth analogues and our *a priori* knowledge of terrestrial geomorphology?

For the existence of present-day liquid water, RSL are the primary focus of debate, although periodically other features are proposed (Bhardwaj et al., 2017; Heyer et al., 2019; Kossacki and Markiewicz, 2010; Kreslavsky and Head, 2009). Progress on RSL is being hindered by:

- Lack of high temporal resolution monitoring (imaging, SAR, IR and VIS-NIR spectral) at the spatial resolution of CaSSIS-HiRISE, observations at different times of day or even better continuous monitoring

- Lack of knowledge of the near-surface atmosphere apart from the handful of places where we have landed missions with meteorology instruments. This limits our knowledge on the influence of micro-environments in the steep topography where RSL are found.
- Lack of knowledge of the basic attributes of the martian subsurface, including the crustal heat flow, porosity, permeability of the regolith with depth, the presence and structure of a potential cryo-hydro-sphere.

Debates over water in the recent past also depend on the above lacunae and we can also add:

- Limits/uncertainties in our ability to model the martian climate at the present-day are magnified when applied to the past and limit our ability to understand past environments. Hence, we are reliant on geomorphic evidence for informing us about the activity of liquid water at the surface, which in and of itself is reliant on our knowledge of what processes form landscapes on Earth.

The existing hardware in orbit around Mars and on its surface combined with their operational constraints and observational modes cannot resolve these problems. New hardware could address some of these issues, for example in orbit: a CaSSIS-HiRISE imager on a spacecraft with a lower orbital inclination to provide higher frequency imaging and time of day coverage (McEwen et al., 2012) , high-resolution (10 m/pix) thermal imager to better constrain thermal inertia and possibly the temperature of shallow brine, Synthetic Aperture Radar (SAR) with high resolution (18 m/pix) orbital radar to detect shallow ice or liquid water, or an imaging spectrometer capable of distinguishing ices and their structure at high resolution. Surface measurements could include: a network of heat flow probes to determine how heat flow varies over Mars and better constrain its value, to measure the volume of subsurface ice (Grimm and Stillman, 2015), ground penetrating radar (GPR) to detect the structure of segregated ice and possibly any shallow aquifers, a transient electromagnetic sounder (TEM) capable of detecting aquifers to a depth of a few kilometres (e.g., Stamenkovic et al., 2020), or use of the magnetotelluric (MT) method to passively sense deep conductive bodies and is capable of detecting a subsurface aquifer within the first 5 km of the crust (Grimm, 2002; e.g., Grimm et al., 2020).

Our knowledge from terrestrial geomorphology inevitably leaves us with a biased view of the landscapes and landforms we find on Mars. Not only that, but even on Earth multiple processes can lead to similar looking landforms “equifinatlity” – a problem usually resolved on Earth by employing a multidisciplinary investigation. For example, hummocky landforms can be the result of rock avalanches or be the vestiges of glacial terminal moraines (e.g., McColl et al., 2019; McColl and Davies, 2011). These conundra are resolved using sedimentology, stratigraphy, geophysical techniques and cosmogenic or other dating techniques, in combination with field and remote sensing observations (e.g., images, digital terrain models). On Mars we only have remote sensing data to rely on and sometimes even with images, spectral data, radar and digital terrain models the interpretation can remain ambiguous. We are also confronted with an environment where the processes acting on it could, and should, be quite different to those on Earth. For example, the lack of plate tectonics on Mars means that evidence of surface processes is preserved longer at the surface than we are used to on Earth, meaning landforms with a “fresh” appearance could date to hundreds of thousands if not millions of years. The generation of relief on Earth is dominated by the continuous action of plate tectonics and its associated volcanism, whereas on Mars the relief is created by stochastic impact events and in the past the development of outsized volcanoes and fault-systems. This means the overall structure of the landscapes of the two planets is fundamentally different starting at the continental scale.

Despite these differences, as demonstrated in Section 3.3, remarkably similar landscapes and landforms are found on the two planets at scales of kilometres to metres. Terrestrial analogues have therefore helped us to deduce what kinds of processes are active to produce these landscapes. A philosophical analysis of the utility of Earth analogues for informing planetary investigations is beyond the scope of this work, but interested readers are referred to the analyses of Baker (2014). Nevertheless, whether or not "something else" can produce the same landscapes and landforms as liquid water is unknown and is one of the core uncertainties stemming from our use of terrestrial analogues. For example, for martian gullies we know the flows at the present-day are fluidised to the same degree as water-saturated debris flows on Earth (de Haas et al., 2019), but we do not know if sublimating CO_2 could mimic this fluidisation despite being controlled by different physics (de Haas et al., 2019).

Another method of addressing the range of environmental conditions under which water (or brine) can result in landform development is to perform controlled laboratory experiments. Such experiments need to have two complementary outlooks. Firstly, experiments to address basic physical questions (how fast can brines form by deliquesce in presence of Mars sediments?) in order to test our parameterisation and understanding of the physical laws underpinning the kinetics of individual processes. The aim is to understand the basis physics in a realistic transient environmental setting for Mars. Additionally, understand the metastability of brine can be very important as brine can remain liquid for an extended period of time (e.g., Gough et al., 2011; Primm et al., 2019, 2017; Toner et al., 2014a). Secondly, more complex simulations, analogous to flume experiments, where processes can be transient and interlinked in order to address the open questions in an empirical fashion. For example, laboratory work can be used to compare the action of water as a fluidising agent to that of gas supported flows. Particularly in this second case, care needs to be taken to appropriately scale the experiments and consider the limits of their application to Mars (Paola et al., 2009).

3.9 Conclusions

If we used geomorphological arguments in isolation the case for liquid water on Mars would be hard to counter. The main argument against liquid water is that martian environmental conditions should not allow its production, so either we have some fundamental misunderstanding of the martian surface/subsurface conditions at the present and/or in the recent past, or some other agent(s) is(are) acting like liquid water does on Earth. For some of the landforms examined in this chapter alternative processes have been identified, but for others, namely "solifluction" lobes and pingo-like mounds, liquid water remains the only suggested agent. The lack of agent does not imply one does not exist, but it could remain to be elucidated. We maintain that liquid water is a viable contender to explain the present-day activity of RSL, the recent formation of gullies, periglacial landforms and subglacial landforms and the formation of certain impact-related features and sedimentary volcanism in the deeper past. The implication being that, although a lot less active than in the past, liquid water remains an active geomorphological agent on Amazonian Mars. In order to consolidate this position, we argue that the most progress can be made in the short-term by focussing research efforts on experimental work informed by remote sensing observations and in the long-term by better equipped Mars-missions in the future. Additionally, sending a small mission to determine, if Mars still possesses deep groundwater would be greatly beneficial as it can serve as an end member for the likelihood of water to have survived in the ground for 100 Ma to Ga.

3.10 Acknowledgements

The authors would like to thank Jay Dickson and an anonymous reviewer for their helpful comments on the manuscript, which improved its quality. SJC is grateful to the French Space Agency CNES for

supporting her HiRISE and CaSSIS related work. DS was supported by NASA MDAP grant number 80NSSC19K1225. The authors thank the spacecraft and instrument engineering teams for the successful completion and operation of CaSSIS. CaSSIS is a project of the University of Bern funded through the Swiss Space Office via ESA's PRODEX programme. The instrument hardware development was also supported by the Italian Space Agency (ASI) (ASI-INAF agreement no. I/018/12/0), INAF/ Astronomical Observatory of Padova, and the Space Research Center (CBK) in Warsaw. Support from SGF (Budapest), the University of Arizona (LPL) and NASA are also gratefully acknowledged.

4 Mass movements in periglacial terrains on Earth

4.1 Introduction

Mass movements occur when the balance between resistive forces (cohesion, friction) and gravitational forces within surface materials are disturbed. In this chapter we will only discuss mass movements in surficial materials and not those that are rooted in bedrock. Periglacial terrains can be particularly susceptible to mass wasting of surficial materials, because of the frequent phase changes of water which cause large variations and strong gradients in saturation which directly influences their cohesion. In particular, periglacial conditions in post-glacial landscapes, which have high relief, discontinuous permafrost and abundant fine and coarse sediments (moraine, scree, etc), can lead to both rapid and slow mass movements. Please note that in this chapter "permafrost" refers to the thermal condition where the ground is below freezing for two or more years and so does not refer to the presence or absence of ice, although permafrost is often used to refer to terrain containing ground ice. Slow mass movements involve slow creeping movements and in periglacial environments often develop into solifluction lobes or sheets (which are dealt with elsewhere, see Section 3.7.5.1). Rapid mass movements in surficial materials include debris flows and landslides, which will be the two foci of this chapter.

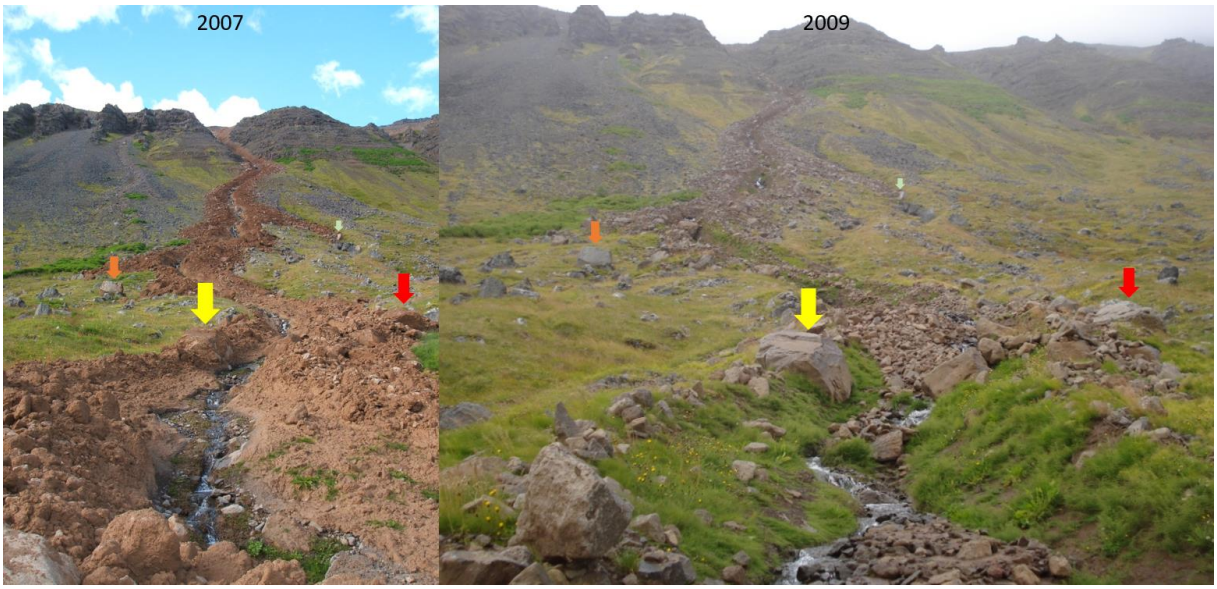

Figure 4.1: A debris flow that occurred above the town of Ísafjörður in 2006. Photo on the left taken by Armelle Decaulne and on the right by Nicolas Mangold. The coloured arrows indicate the location of the same boulders in each image. They were transported in the flow and are 0.5-1 m in size. The abundant fines that initially coated the boulders have been quickly removed by subsequent rainfall.

4.2 Debris flows

Debris flows are mixtures of sediment and water (usually up to ~ 40 %) that surge downhill in response to gravity (Iverson, 1997). They occur in steep terrain and either propagate over hillslopes or through pre-existing channel networks (torrents). They produce characteristic deposits including lobate snouts and lateral levees. They are triggered, and their motion is maintained by, excess pore-pressure in the sediments. This can be brought about in nominally stable hillslope (or torrent) materials by unusual precipitation events (e.g., prolonged and /or intense rainfall or snowmelt), or disturbances in the upslope hydrology (e.g., forest fire, infrastructure or land use changes). In torrent systems the cadence of debris flow events is also conditioned by the supply of material to the system which depends on local climate and geology and can be slow and continuous (e.g., frost shattering) or sudden (e.g., a landslide). The complex interaction between granular material (which can be

metres in size) , fines (silt, clay) and water, leads to dynamic, transient and difficult to predict behaviour, such as surging, granular flow fronts, self-blocking, etc. (Ancey, 2007; Iverson, 2014). The fact that debris flows can transport large granular debris (Figure 4.1) makes them dangerous and they pose a risk because they are hard to predict, in terms of when/where they might occur and how big they could be (volume and travel distance). Debris flows also play a role in landscape evolution, as part of the sediment cascade, and their long term influence leaves a detectable mark in the morphology of upland first order catchments (e.g., Lague and Davy, 2003) and on alluvial fans (e.g., Blair, 1999).

Debris flow torrents give rise to alluvial fans where they emerge onto the plains or valley floor. These are often sites of human construction as they are raised above the flood level of the main river, yet present relatively level terrain in mountain environments. Debris flows on the fan are infrequent enough to be forgotten or controlled. Alluvial fans can also be constructed by fluvial processes, but differences in the sediment transport mechanisms leads to significant differences between debris flow dominated and fluvial-dominated fans in their internal architecture and surface morphology. Debris flow fans tend to be steeper (>15°) and have little internal structure compared to fluvial fans (Blair, 1999; de Scally and Owens, 2004; Wilford et al., 2004).

Hillslope debris flows tend to be smaller in volume than torrent-based debris because they are less likely to erode and incorporate additional sediment along their path than torrent debris flows. Debris flows can bulk up to several times their original volume in this way (e.g., de Haas et al., 2022; Santi et al., 2008). Hillslope debris flows deposit at much higher slope angles (Fannin and Wise, 2001) than those confined to torrents attesting to the high losses of energy in hillslope systems compared to torrent systems. Hence, the generally lower volume, lower energy hillslope debris flows pose less risk to human lives and habitation than debris flows in torrent systems and are subsequently less studied.

Efforts to understand the risk posed by debris flows and assist local authorities in planning take two main approaches:

- Susceptibility analysis on a regional scale. Such studies typically use records of debris flow events and relate them to spatial variations in geology, steepness, vegetation cover, etc. to determine which catchments are most susceptible (e.g., Blais-Stevens and Behnia, 2016; Kneisel et al., 2007; Kritikos and Davies, 2015; Xu et al., 2013). Meteorological conditions can also be included in such analyses and can then be used to estimate threshold conditions (rainfall intensity and location). Such assessments are commonly undertaken by institutes such as geological surveys.
- Modelling individual flows in known debris flow catchments. Such models use a stream profile or full 3D representation of the terrain and an input volume or hydrograph to predict the run out and deposit thickness of a debris flow event (e.g., Calligaris et al., 2008; Christen et al., 2007; Pudasaini, 2012). Debris flows are usually considered as a Bingham type fluid, but models can include more complex rheologies, such as considering the fluid and solid phases separately. These models open require an expert practitioner to obtain robust results and this can discourage use by local authorities.

An alternative version of the second approach is to use data on previous events to establish empirical laws for debris flow propagation over topography (e.g., Fannin and Wise, 2001). These empirical models are easier for non-expert uses to implement and require little or no specialist software. My PhD thesis was entitled “Debris flows on Earth and Mars” and the first published contribution was a paper that established an empirical propagation “law” for debris flows above the town of Ísafjörður in NW Iceland (Conway et al., 2010). Using detailed topographic data from LiDAR and differential GPS

we were able to accurately track patterns in erosion and deposition along the debris flow track and relate them to the slopes experienced along those tracks. We could then run this relation to simulate a realistic range of debris flow sizes and behaviours to establish which parts of the town were most at risk (Figure 4.2). Since this work was published the defensive barriers have been increased in height and they also protect from snow avalanches.

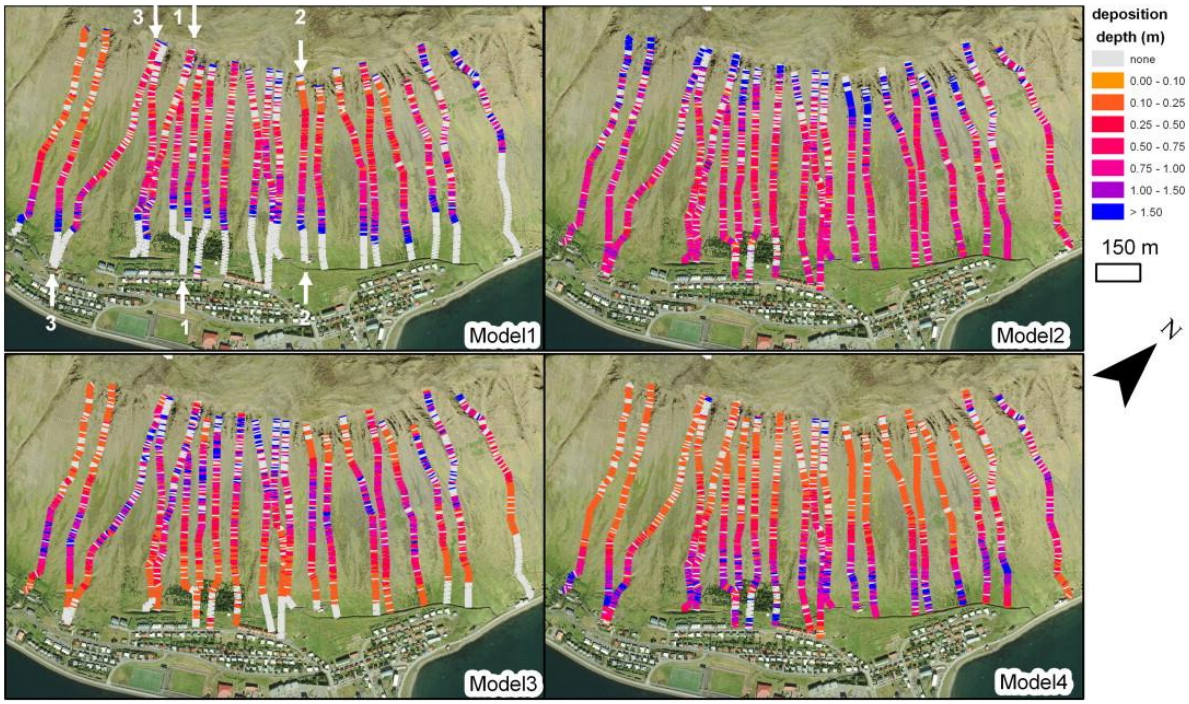

Figure 4.2: Model debris flow paths derived from different relations between the normalised cumulative deposition thickness and cumulative average slope derived in Conway et al. (2010) *overlain on the air photo mosaic of Ísafjörður taken by NERC ARSF.*

By differencing of LiDAR data taken in 2007 and 2012 we were able to establish two modes of debris flow triggering above Ísafjörður (Morino et al., 2018): the firehose effect – where debris accumulates within the bedrock chutes before being remobilised as a debris flow – this produced larger events, and hillslope triggered debris flows, smaller flows which were entirely confined to the talus slope. This work highlighted how repeat high resolutions topographic surveys can highlight processes that contribute to debris flows before they occur.

4.3 Landslides involving ground ice

Landslide is a general term for a large collection of mass movement features, which sometimes also includes debris flows. Many systems have been used to organise these mass movements into logical categories but often the terminology applied is confused and sometimes contradictory. The most widely applied is the updated Varnes classification (Hungr et al., 2014) which divides mass movements by type of motion and material involved where different morphological characteristics can be assigned to failures in each class – I will adhere to this system here.

This section will touch on (rotational) debris slides, and debris avalanches which are the types of landslide where involvement of ground ice has been reported. It should be noted that the interaction between landslides and glacial ice (rather than ground ice) has been more extensively studied, from the point of view of their influence on glacial dynamics and glacial sediment transport (e.g., Dunning et al., 2015; Hewitt, 2009), as well as from the point of view of increased mobility/hazard of such landslides (e.g., Dufresne et al., 2019; Sosio et al., 2012).

Retrogressive thaw slumps are a common type of mass movement in continuous permafrost environments with extensive excess ground ice, where wholescale detachment of the active layer results in large-scale mudflows/slides, which can be active for decades (e.g., Burn and Friele, 1989; Swanson and Nolan, 2018). Retrogressive thaw slumps have received much attention as they are a very visible sign of the degradation of the arctic permafrost due to increased global surface temperatures over the last decades (e.g., Lacelle et al., 2010; Lantz and Kokelj, 2008). Their impact on human population remains low at the moment, but do pose risk to roads, pipelines and other infrastructure.

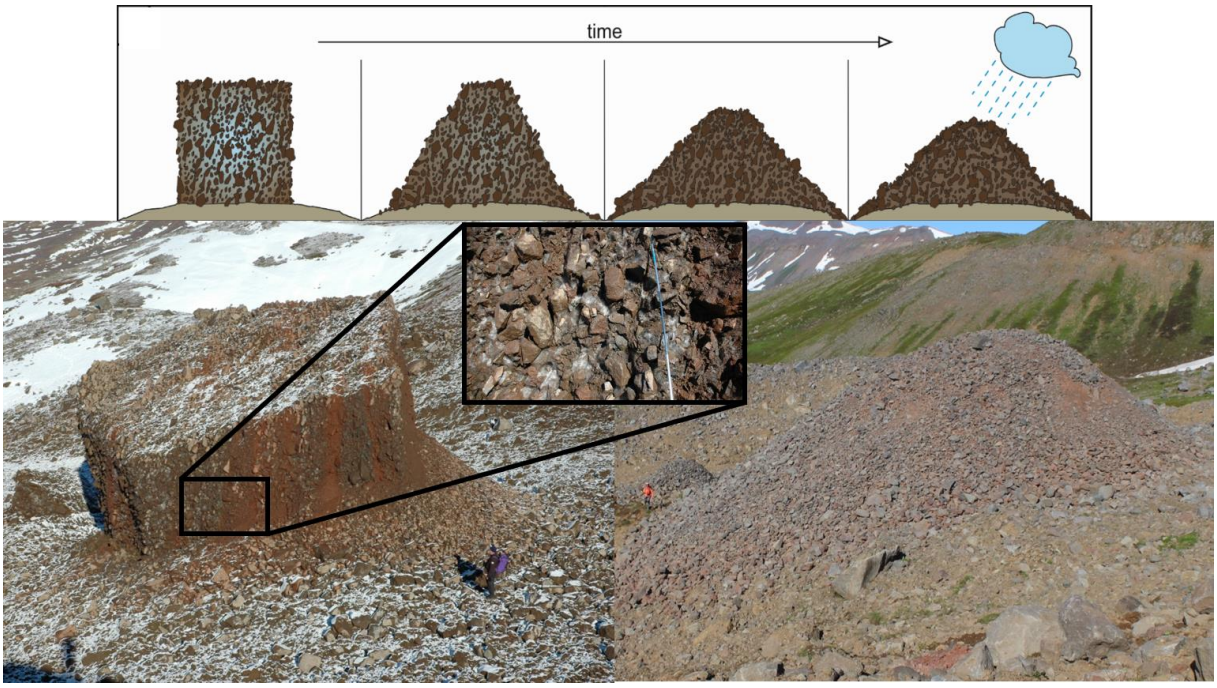

Figure 4.3: Formation of a molard, modified from Morino et al. (2019) *. Top: Side-view schematic evolution of a molard, from the block of clast-supported imbricated talus deposits cemented by ground-ice (bluish colour) to the collapsed conical mound of debris, preserving sorted gravel deposits on its surface (dark brown), with fine deposits (light brown) being leached out. The inset shows the ice cement between the grains (walking pole for scale). Bottom-left: the largest block of ice-rich sediments that fell during the Móafellshyrna event. The deposits are composed of imbricated boulders, cobbles, and pebbles embedded in brown to red sandy to silty clay Note the person as a scale on the right. Bottom-right: the resulting molard three years after the failure, note the person as a scale on the left.*

In contrast, the involvement of ground ice in landslides occurring in areas of discontinuous permafrost in periglacial environments and post-glacial landscapes, is harder to identify. Such zones often have habitation because the valley floors are the only places to build even if populations are sparse. Discontinuous mountain permafrost can occur in a wide range of physiographic settings, including: fjordlands (Norway, Iceland), mountain chains (Alps, Rockies, Himalaya), and volcanic edifices (Rockies in North America, Kamchatka).

Discontinuous permafrost can form in a wide variety of materials and have different configurations – favourable settings include pole-facing rockwalls (Magnin et al., 2015). The release of rock avalanches and rockfalls caused by the melting of structurally important ice in steep and/or sub-vertical rockwalls has been receiving increasing attention in the Alps, as it visibly affects tourist sites and can be destructive to infrastructure (e.g., Deline et al., 2013; Draebing et al., 2017). The

involvement of melting ice in these failures can only be ascertained by examination of their source areas and has not been reported to influence the dynamics of the mass movement (ice only makes up a minor component of the overall mass). Ice can be present in larger fractions in debris or soils in permafrost areas, compared to bedrock. Yet, because there is little existing knowledge of which landslides in zones of discontinuous permafrost contain ground ice it is challenging to assess the influence of ground ice on the behaviour of the mass movement – hence an important knowledge gap exists.

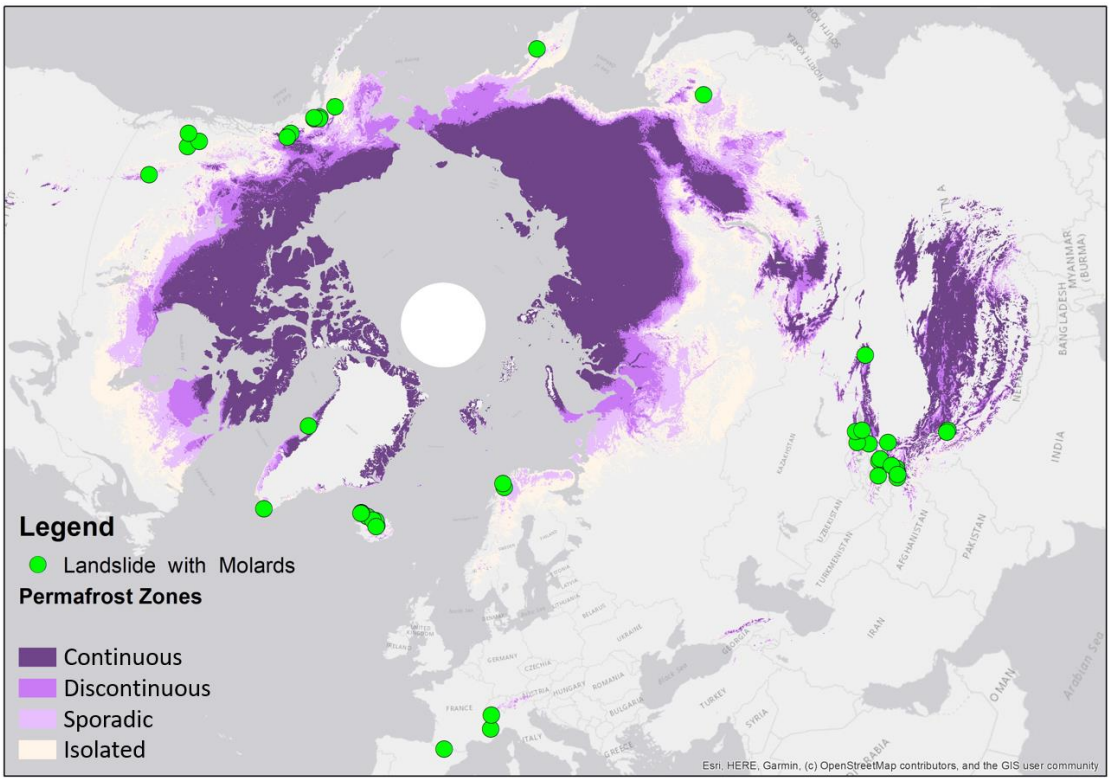

Figure 4.4: Northern hemisphere permafrost map from Obu et al. (2019) *overlain by locations of landslides with molards collated during the PERMOLARDS project. Landslides located in the southern hemisphere, notably the Andes, are omitted.*

Ground ice in talus and moraine materials is often located in perched positions and have no outwardly visible signs of their internal ice content (Morino et al., 2019), researchers therefore often rely on geophysical techniques to determine the ice content and its distribution (e.g., Langston et al., 2011; Scapozza et al., 2011). Finding examples of landslides occurring in ice cemented sediments is challenging in the literature, with only a few cases directly reporting the involvement of such materials (Brideau et al., 2009; Milana, 2015). However, such landslides can show a distinctive landform that indicates the presence of ground ice within the mobilised materials – these are called "molards". Molards are cones of debris which represent the former location of ice cemented blocks of sediments that collapsed once the supporting ice melted (Figure 4.3). Molards have been reported in landslides in only a handful of locations, including Argentina, Canada and Tibet and in only two cases was the presence of ground ice linked directly to their occurrence (Brideau et al., 2009; Milana, 2015). We published a recent key paper (Morino et al., 2019) which brought these landforms back into the spotlight as potential harbingers of a hidden hazard linked to climate change in zones of discontinuous permafrost, but also as landforms that could indicate the past distribution of discontinuous permafrost conditions.

Hence, these newly "rediscovered" landforms are the subject of an accepted ANR project PERMOLARDS, of which I am PI running from 2019 to 2024. We have already catalogued 51 sites where molards are found in landslide deposits in practically every area of discontinuous permafrost in the world (Figure 4.4). This catalogue was established from personal communication from other researchers who saw presentations of our work and a small number from serendipitous finds on Google Earth.

We are currently working on understanding if certain source lithologies are prone to molard formation and if any other systematic factors link the molard bearing landslides other than the occurrence of ice cemented ground. In parallel we are establishing criteria to differentiate these landforms from hummocks which occur in rock avalanches. To perform these tasks, we are using satellite remote sensing data to examine the distribution of molards in the landslide deposits, to estimate the landslide volume, and to establish the topographic setting (e.g., orientation of source area, hydrological connectivity, hillslope gradient, etc.).

4.4 Ongoing work

Using recent InSAR data we have been able to study in more detail the perched debris on top of the bench above Ísafjörður and in concordance with the geomorphological evidence those materials are creeping. We do not know if this site will have more frequent debris flows or if such a setting could experience a mass decollement and release a landslide. However, there is other evidence for detachments of rock glaciers (i.e. creeping masses of ice cemented sediment), so we think this is an urgent area of future research. Some molard-forming landslides have originated as detachments of rock glaciers (Milana, 2015; Ravanel, 2009). We aim to publish this discovery in the first half of 2023. We are exploring the possible parallels between glacier and rock glacier detachments that lead to landslides and this could lead to a further publication.

The PERMOLARDS project is at its midpoint, and three main tasks remain. First, analogue experiments simulating the development of molards from the initial blocks of ice commented sediments. This is the PhD project of Calvin Beck who started at the University of Caen in November 2021. He benefits from preliminary experiments done by PhD student Meven Philippe and three interns, who showed gravel sized materials were more conducive to molard formation than sand-sized, molards formed underwater are shorter and that both individual grain fall and grain avalanches are important. Calvin is preparing these initial results for publication in 2022. He will continue to study the effect of grainsize and will monitor the temperature as well as shape during molard formation. The novel apparatus consisting of an array of Raspberry Pi and cameras to capture time lapse images to then create time lapse photogrammetric 3D models of the analogue molards will be written up as a technical contribution by Meven Philippe.

Second, reduced access to the field means that we have not been able to gain insight into the longevity of molards in the landscape by cosmogenic dating. This is one of the main objectives for the 2022 field season. Third, we were able to place temperature sensors in Iceland which will enable us to model the permafrost conditions around recent molard bearing landslides. These data were retrieved in June 2022 and are pending analysis.

Finally, it is clear that the PERMOLARDS project will leave many questions unanswered. One of the most important is the configuration of the ground ice within the source areas of these landslides. The effort and cost associated with simply reaching these areas (helicopter) makes deploying the usual geophysical methods challenging (e.g., GPR, ERT). This aspect of the project will form the basis for future applications for funding.

5 Volatiles on Mercury

5.1 Introduction

Mercury is the innermost planet in the solar system. It has a higher average density than the other terrestrial planets, which is a result of a much larger iron core compared to its mantle/crust compared to the other planets. Models to explain this anomaly include high-temperature processes that would also remove volatile elements, e.g. stripping by an early active Sun (e.g., Cameron, 1985), or giant impacts (e.g., Benz et al., 1988). Hence, the expectation prior to the arrival of NASA's MESSENGER spacecraft in orbit around Mercury in 2011 was that the planet would be volatile depleted in composition, which turned out not to be the case (e.g., Nittler et al., 2018). In parallel to these geochemical discoveries, the images returned by MESSENGER also revealed a number of geomorphological signs of these volatile elements, including numerous hollows (e.g., Blewett et al., 2011), and explosive volcanic vents and associated faculae (e.g., Head et al., 2008b; Kerber et al., 2009) found across the whole planet. The permanently shadowed areas at Mercury's poles are host deposits of water ice and organics, cold-trapped volatiles which may be partially endogenic in origin (e.g., Chabot et al., 2013; Lawrence et al., 2013). We have also interpreted conical landforms in the Caloris impact basin as a consequence of the volatile enrichment of the crust (Wright et al., 2020). Finally "slope lineae", as yet unreported in the peer-reviewed literature may also result from volatile driven processes (Malliband et al., 2019). These surface features have been the focus of ongoing collaborative work with Open University through co-supervision of 7 PhD students with David Rothery and other collaborators (see detailed CV in the Annex). Each of these science themes will be briefly described in the following sections, with a focus on the advances made by these students. Five of these students also prepared a quadrangle geological map using MESSENGER data as part of their thesis as part of an ongoing effort to prepare for the arrival of BepiColombo in orbit in December 2025 (Figure 6.1). These maps provide context for the observations of BepiColombo and will be an integral part of planning the observations.

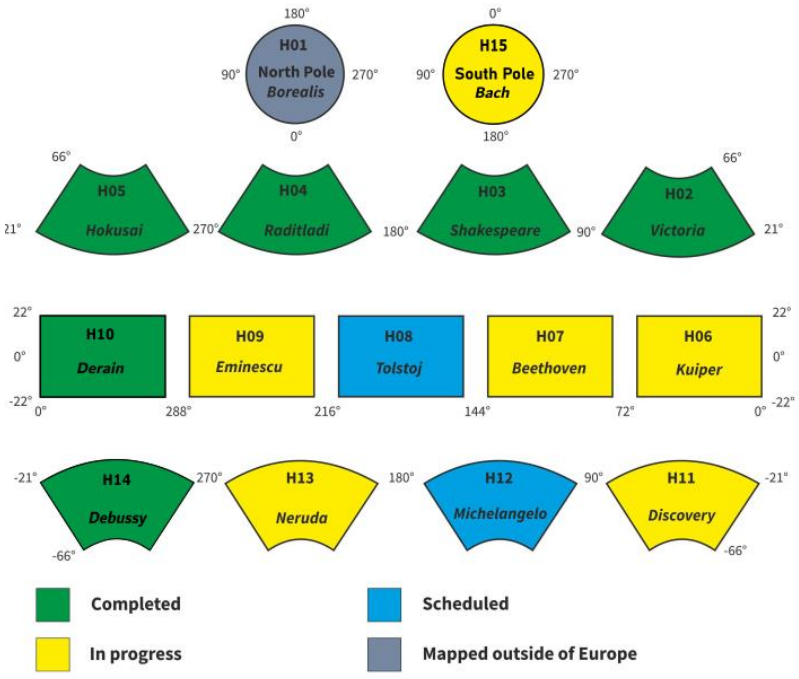

Figure 6.1: The Mercury quadrangles coloured by status as of November 2021. Credit: Annie Lennox.

5.2 Hollows

One of the most remarkable geomorphological discoveries of the MESSENGER mission was that of "hollows" (see also Section 2.12; Figure 2.11e): steep-sided, flat-bottomed depressions usually surrounded by a relatively bright and blue halo. Hollows can occur individually or in groups. Individual hollows can have a diameter up to several kilometres and have been observed in the highest resolution images of Mercury at ~1.5 m/pix so seem to have no smallest size (Zharkova et al., 2020). Depths are generally Limited to several decametres independent of their diameter (Blewett et al., 2016; Fassett, 2016; Thomas et al., 2014b). Fields of hollows can span many tens of kilometres. In plan-view hollows have irregular shapes with cuspate edges and where many hollows are tightly clustered they give the surface an etched appearance. Hollows surrounded by a halo are interpreted to active and those without a halo, as inactive (Blewett et al., 2011), but no growth has actually been observed.

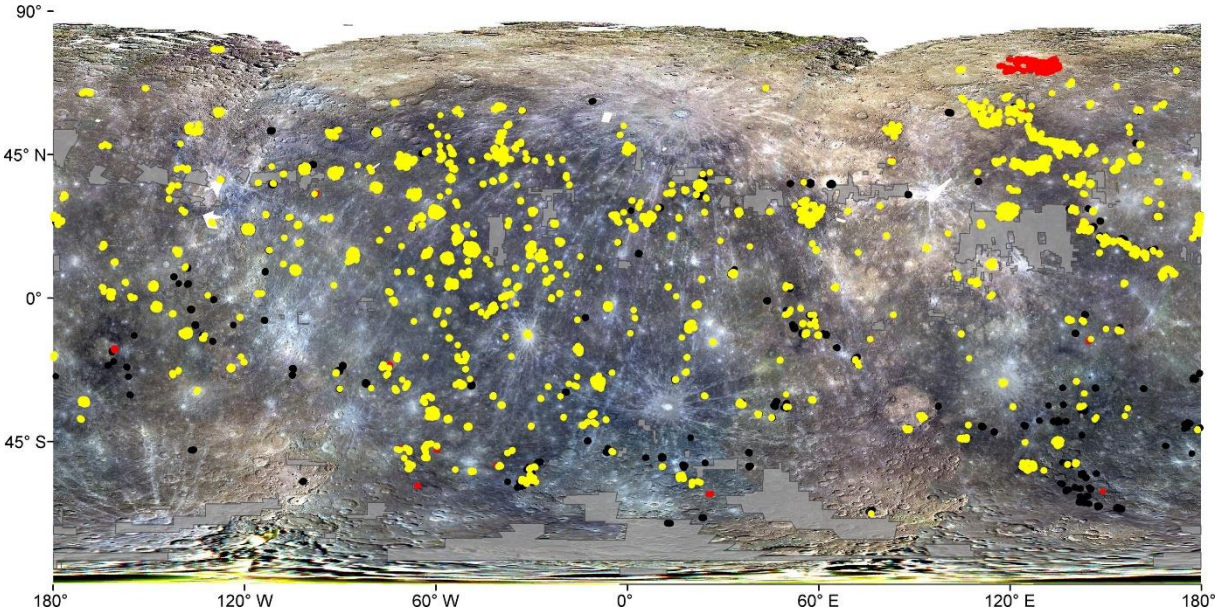

Figure 6.2: Taken from Thomas et al. (2014b)*, global occurrence of hollows, vents with facula and spectrally red pitted ground. Yellow: hollows; black: vents with facula; red: spectrally red pitted ground; grey: area not imaged at <180 m/px. (Base mosaic: MESSENGER global colour v3.)*

The relatively small relief of hollows and the inferred fast resurfacing rates on Mercury (Fassett et al., 2017) suggest these features are young, which is further supported by the fact they can occur in rayed craters whose age is thought to be <1 Ga (Blewett et al., 2018) and do not have superposed impact craters (Blewett et al., 2016). Recent analyses suggest they could be as young as 100 ka (Wang et al., 2020). The formation of hollows by scarp retreat supported by their morphology (Blewett et al., 2011) and correlated patterns in spectral properties (Barraud et al., 2020).

Our mapping (Thomas et al., 2014b) confirmed that of Blewett et al. (2011) that hollows are found globally (Figure 6.2), yet seem to have an association with the so-called "Low Reflectance Material". LRM has a darker than average albedo and its distribution indicates that it has been emplaced at the surface by huge impact events and then redistributed by smaller ones (Rivera-Valentin and Barr, 2014) – it is thought to represent a near-global subsurface layer enriched in a dark component, likely graphite (Peplowski et al., 2016). Our work on the spectral properties of hollows in Eminescu crater (Thomas et al., 2016) provide supporting evidence that the LRM is graphite-rich and in addition suggest (Ca- or Mg-) sulphides are a component of the volatile material lost in the hollow-forming process. However, other studies point to elemental sulphur as the lost-volatile (Phillips et al., 2021),

others to chloride (Lucchetti et al., 2021) and yet others to carbon (Wang et al., 2020). The bright halos around hollows have diffuse boundaries and our work suggested that they are likely composed of finer grained materials than the regolith in general (Thomas et al., 2016).

5.3 Vents

Mercury's surface is dominated by effusive lava plains of various ages as confirmed by our mapping (e.g., Wright et al., 2019). This effusive activity is thought to have stopped around 3.5 Ga because of the onset of global contraction of the planet as it cooled (e.g., Byrne et al., 2014) which leads to magma ascent being blocked. As shown by our work (Figure 6.2), hundreds of volcanic vents resulting from explosive eruptions are found globally (Thomas et al., 2014b, 2014c). These vents are circular to irregularly shaped depressions without a substantially raised rim which are in general around tens of kilometres in diameter. Many are associated with facula – red-coloured spectral anomalies with diffuse margins – interpreted to be pyroclastic deposits (Goudge et al., 2014; Kerber et al., 2011). These deposits mantle the surrounding terrain (Figure 2.5). The lack of atmosphere and low gravity mean that explosive eruptive products are not expected to build relief, but instead spread fine particles in a blanket across the surface (Barraud et al., 2021; Besse et al., 2020; Brož et al., 2018). Our work has revealed only one possible exception – two possible volcanic cones with a summit pits (Wright et al., 2018). However, the possibility that these are a fortuitous alignments between a hill and a smaller impact crater cannot be ruled out with current data.

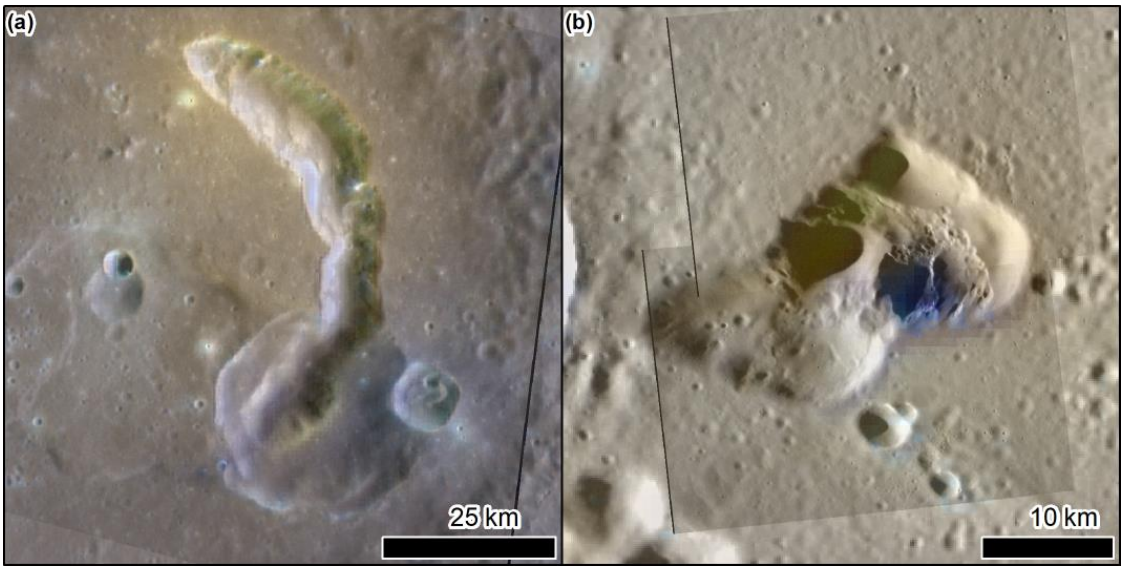

Figure 6.3 Vents that show evidence for multiple events. (a) MDIS NAC image EN0219817290M (b) MDIS NAC images EN0220591242M and EN0220591249M. For both panels the MESSENGER MDIS Enhanced Color Mosaic at 665 m/pix is in semi-transparent.

Our work has revealed that these vents have been active repeatedly as shown by their compound internal structure (Figure 6.3) (Pegg et al., 2021a; Rothery et al., 2014). The fact that different sub-vents have different degradation states attests to the longevity of this eruptive style on Mercury. Our observations of superposition with young craters and by using crater-size frequency distributions revealed that the most recent events could be as little as 1 Ga (Thomas et al., 2014a). The fact that explosive eruptions can occur on Mercury, that this style of eruption has been ongoing throughout the planet's history and that the most recent activity is so young are three discoveries that changed the way we think about Mercury's history and structure. Explosive eruptions require a volatile component in the rising magma to form the gases that drive the eruption – exactly what form this volatile takes is

currently unknown, but is thought to be distinct from the volatile that is lost in hollow-formation (Lucchetti et al., 2021).

Our finding that that vents occur on faults or crater-related structures suggests that the path taken by magma exploits crustal weaknesses (Rothery et al., 2014; Thomas et al., 2014c) and it is possibly the volatile component to the eruption that can overcome compressive crustal stresses caused by global contraction.

5.4 Cones and slope lineae

Caloris basin is over 1500 km in diameter making it one of the largest impact basins in the Solar System and dates to 3.8-3.9 Ga. The basin itself is floored with lava plains which are cut by radial graben whose origin is unknown. The rim materials have around 2 km of relief and the ejecta deposits have a number of unique features. One of these features is the occurrence of conical mounds inside the Odin Formation. We found that these mounds share traits with molards on Earth (Chapter 5), although larger in size, they have similar flank slopes and overall shape (Wright et al., 2020). We also found evidence that they had spread over time, covering small impact craters (Figure 6.4a,b). We concluded that they likely formed from initially blocky ejecta material that on losing a volatile component degraded into cones. This suggests that the crustal material ejected by the Caloris impact was enriched in volatiles and therefore is in agreement with the findings of other studies showing that the crust of Mercury is volatile enriched.

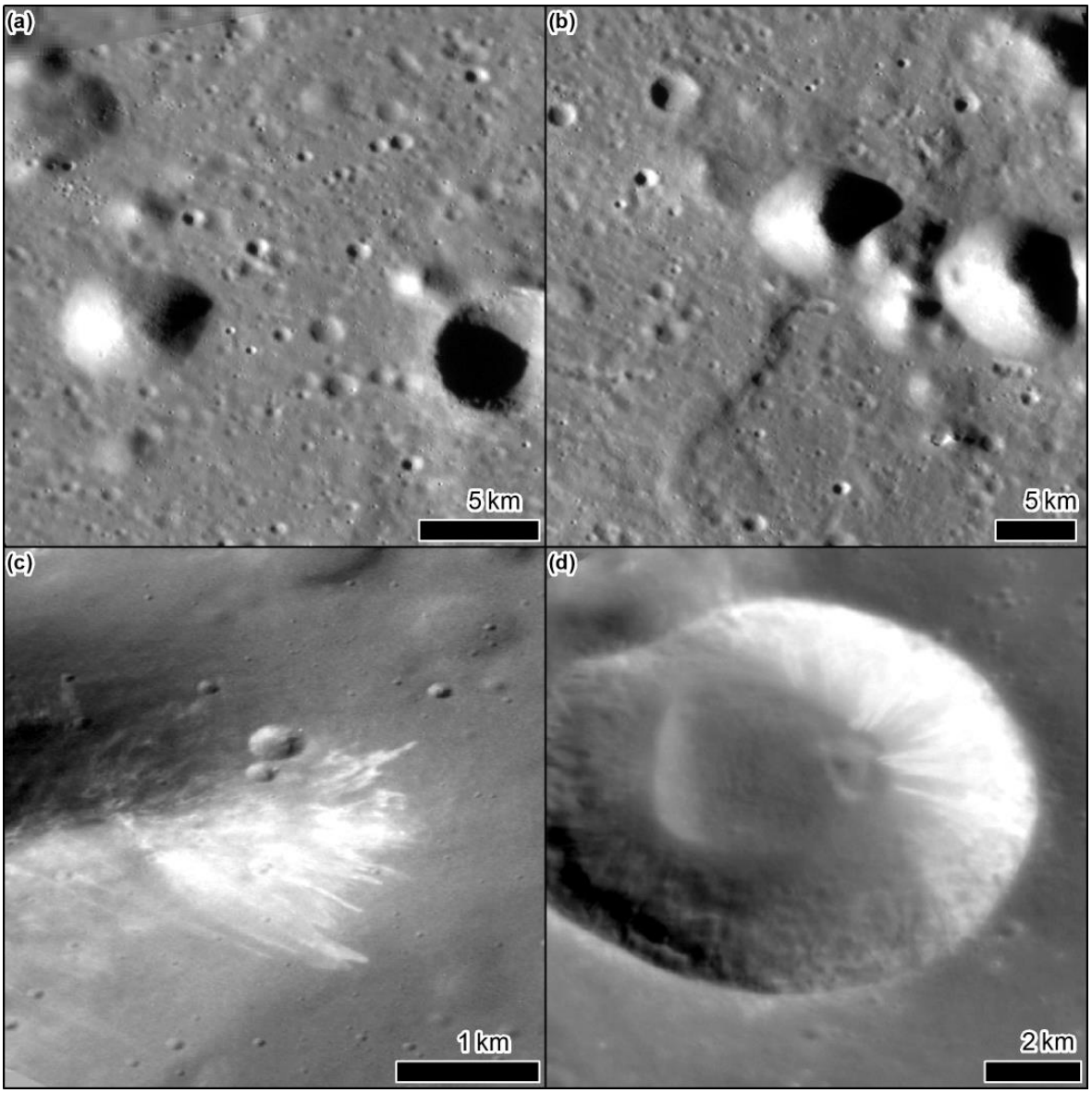

Figure 6.4: Examples of conical mounds (a,b) and slope lineae (c,d) on Mercury. (a) MDIS NAC image EN1045703411M, (b) MDIS NAC images EN1045674609M and EN1045674594M. (c) MDIS NAC image EN1044173928M. (d) MDIS NAC image EN1004160887M.

Slope lineae were first noted as associated with hollows by Blewett et al. (2018). They downslope oriented features generally picked out as higher relative albedo, but also picked out as alcove-channel, systems in relief (Malliband et al., 2019). First studied in the Derain Quadrangle by PhD student Chris Malliband, undergraduate intern Camile Aubry performed a global-scale survey in 2019 (Aubry et al., 2021) where we found no specific spatial pattern to their distribution (Figure 6.5). In addition, although they are often found with hollows, this is not systematic and the same can be said for spur and gully terrain. Spur and gully terrain is typically caused by bedrock outcropping near a crater rim (Levin et al., 2022). Mercury's regolith is thought to be very thick (Kreslavsky et al., 2014), so finding even tens of examples is unexpected given they do not correlate with recent volcanic plains. On the Moon spur and gully features are extremely rare despite the regolith being approximately three times thinner (up to tens of metres). These results are being prepared for a publication in 2022.

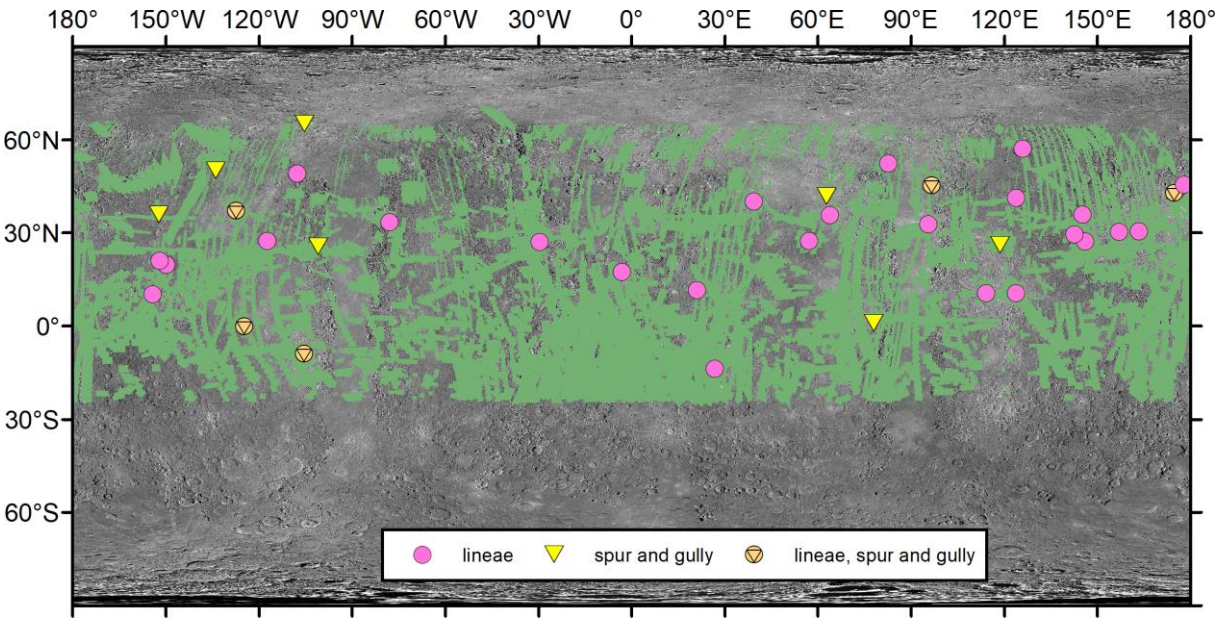

Figure 6.5: Global map of Mercury using the MESSENGER WAC image mosaic overlain in green by the distribution of NAC image better than 100 m/pix available in the survey area (-25 to 65° N) and the locations of lineae and/or spur and gully morphology.

5.5 Lobate ejecta and permanently shadowed areas

On Mars and icy satellites impact crater ejecta with lobate margins is interpreted to represent fluidisation of the ejecta blanket by volatiles (e.g., Barlow and Perez, 2003; Boyce et al., 2010). Such ejecta deposits are not generally found on the Moon. Similar lobate ejecta have been reported on Mercury (Xiao and Komatsu, 2013) and are being investigated by Annie Lennox, a PhD student I am co-supervising at the Open University. She has already found several additional examples not reported in Xiao and Komatsu (2013) (Figure 6.6) and all examples seem to be a result of the influence of topography, so perhaps an impact induced landslide fluidised by the crater-forming process, similar to acoustic fluidisation (Collins and Melosh, 2003; Melosh, 1979). The involvement of volatiles does not seem to be necessary and requires further analysis to rule out.

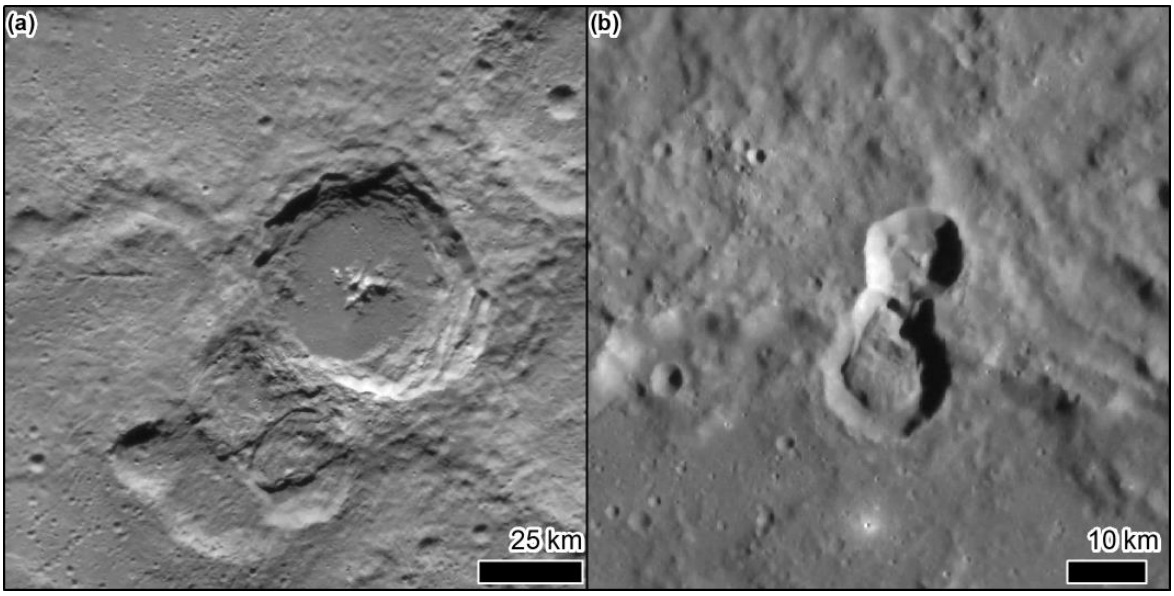

Figure 6.6: Examples of lobate ejecta on Mercury. (a) 'Brooksbank' crater is located near the South Pole at 70.4°S, 1.5°E. (b) A small unnamed crater near the equator at 12.7°S, 56.0°E.Basemap is the MESSENGER MDIS Global 166m/pix monochrome mosaic.

Recent discoveries have highlighted water's presence in permanently shadowed impact craters on the surface of Mercury and the Moon using combined evidence from radar and neutron flux data (Chabot et al., 2013; Feldman et al., 1998; Harmon et al., 2001; Lawrence et al., 2013; Spudis et al., 2013). The deposits on Mercury are thought to be thicker than those on the Moon and images from MESSENGER show these deposits in the north have a distinct albedo and smooth texture meaning they are geologically young (Chabot et al., 2016, 2014). This is supported by timescales of impact gardening which estimate the ice cannot be more than 200 Ma old (Costello et al., 2020). Hence, the favoured origin is delivery by a comet impactor and cold trapping in the permanently shadowed regions, but an endogenic source cannot be ruled out. The permanently shadowed area in the south polar area is approximately twice as large as in the north (Chabot et al., 2018), yet MESSENGER data from this hemisphere is sparse and of lower resolution due to the spacecraft's elliptical orbit. These south polar permanently shadowed regions fall within the mapping quadrangle of Annie Lennox currently under my co-supervision as a PhD student at the Open University. Her work on the geomorphology of the area will help to plan detailed observations of these zones for BepiColombo.

5.6 Catenae, faults, and graben

Catenae are alignments of circular-overlapping to irregular elongate pits, which can form semi-continuous troughs, usually without a significant raised rim. Most catenae on Mercury are aligned radially to large impacts and hence can be most readily interpreted as chains of secondary impacts. However, many orphan catenae exist and were investigated during the PhD of Emma Fegan who I co-supervised (Figure 6.7a,b). On the Galilean satellites isolated catenae have been attributed to comet impacts, where the comet was tidally disrupted into a string of small impacting bodes just prior to collision (Melosh and Schenk, 1993). We surmised that this is a plausible explanation for catenae on Mercury which have a linear alignment but could not be associated with a primary impact site. Pit chains are found on the flanks of the martian volcanoes and are thought to be related to collapse above evacuated dikes (e.g., Mège, 2003), or a result of collapse in a purely tectonic (graben, or normal faults) context (e.g., Ferrill et al., 2011, 2004), or collapse of lava tubes (e.g., Sauro et al., 2020). Extensional stresses are believed to explain the existence of orphan catenae on Ceres (Scully et al., 2017). We attributed catenae on Mercury that curved around craters or other features to be volcano-tectonic in origin, but without being able to conclude on the precise mechanism.

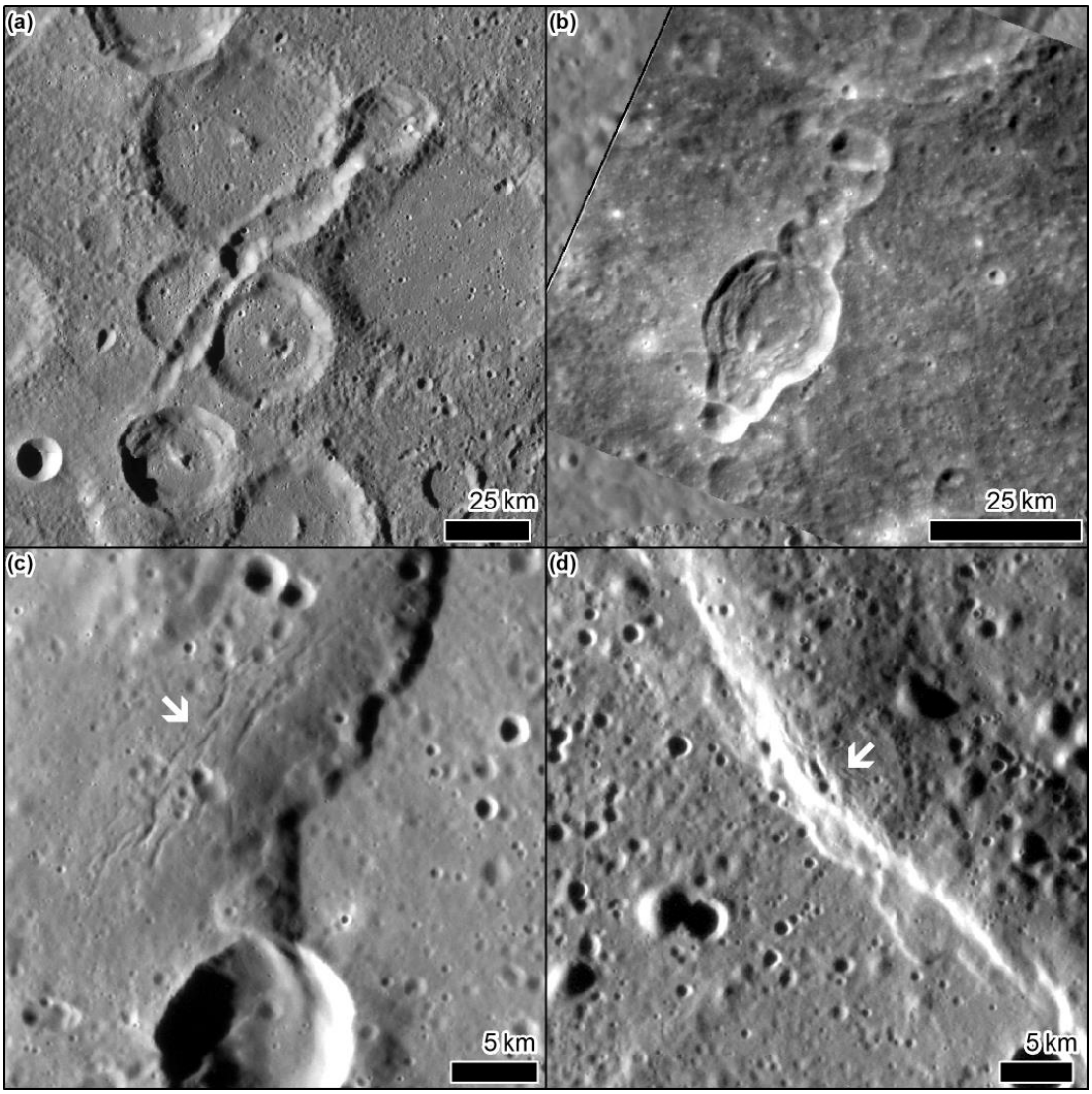

Figure 6.7: Example catenae and graben on lobate scarps. (a) Catena in the MESSENGER MDIS Global 166m/pix mosaic. (b) Catena in MDIS WAC image EN1004216498M. (c) Graben (white arrow) on a lobate scarp in MDIS NAC image EN1014965470M. (c) Graben (white arrow) on a lobate scarp in MDIS NAC image EN1014447282M.

Tectonic forces are a major geomorphic agent on Mercury, which is thought to have contracted by up to 7 km in diameter (0.1%) since its formation (Byrne et al., 2014). This global contraction manifests itself as lobate scarps and high relief ridges – surface folds located over a thrust fault tip. Wrinkle ridges are another common tectonic feature but are only thought to affect the volcanic plains which they deform. The estimate of the shortening represented by lobate scarps is the method by which global contraction is estimated and is therefore sensitive to the assumptions made about the geometry of these structures, including their dip-angle (Byrne et al., 2014; Watters, 2021). David Pegg, a PhD student I co-supervised at the Open University, discovered an example of a lobate scarp crossing a volcanic vent, meaning for the first time the 3D geometry of the fault under the lobate scarp could be directly measured (Pegg et al., 2021b). We found the dip angle to be 28° ± 5, consistent, but with the higher end for previous estimates favouring higher estimates for global contraction. Ben Man, another PhD student I co-supervise at the Open University, discovered the existence of small graben on the backs of lobate scarps (Figure 6.7c,d) and is currently mapping their global distribution. These small graben have little relief and are not superposed by craters meaning

that the host lobate scarp must have had geologically recent displacement, due to the rapid erasure of surface topography (Fassett et al., 2017), which somewhat contradicts models predicting slowing of global contraction towards the present day (Crane and Klimczak, 2017).

5.7 Synthesis and outlook

MESSENGER data have revealed a surprising geomorphological diversity on Mercury's surface- in turn revealing a planet with an unsuspected active or recently active surface processes, as highlighted by the small sampling of the discoveries summarised in this chapter. The sparse low altitude MDIS images gave an enticing glimpse of what surprises may he revealed by the higher resolution images of the SIMBIO-SYS cameras aboard BepiColombo which will start collecting data in late 2025. SIMBIO-SYS comprises:

- STC – Stereo Channel: global colour coverage of the surface in full stereo at 50-100 m/pixel resolution with four spectral channels (panchromatic (650) + 550, 700, 880 nm).
- HRIC – High spatial Resolution Imaging Channel at 5 m/pixel covering ~10% of the surface, with the same four bands as STC.
- VIHI – Visible Infrared Hyperspectral Imager Channel at 100-400 m/pix with a wavelength range of 400 – 2000 nm with possible extension to 2200 nm and a spectral sampling every 6.25 nm).

The discoveries and mapping performed by the students I supervise are being used as integral datasets in planning the acquisition of data by the science team of SIMBIO-SYS, specifically for the targeting of HRIC and high resolution VIHI images. My experience in martian exploration tells me that higher resolution images will reveal features that are as yet unsuspected on the surface of Mercury. Hence, in the coming decade I aim to continue to explore MESSENGER data to its full until BepiColombo arrives, when a new era of Mercury exploration will begin.

6 Synthesis and future work

6.1 Synthesis

Over the last 15 years I have sought to understand the workings of our planet and other worlds by studying their landscapes to deduce the processes that shape them.

An issue that I have confronted during my research has been the issue of equifinality – the formation of similar landforms by different processes – an important confounding factor when trying to use landscapes to infer formation process. I initially started with the conviction that gullies on Mars were carved by liquid water, mainly because their 3D morphology resembles so closely debris flow systems on Earth (Conway et al., 2011b; Conway and Balme, 2016). However, recent monitoring shows martian gullies are active when the ground is too cold for liquid water (e.g. Dundas et al., 2019a) and our experiments with sublimation driven flows show that this process can resemble a wet debris flow (results in preparation for publication). Detailed examination of the topography and morphology of recent flows with collaborator Colin Dundas has revealed present-day flows can do sufficient geomorphic work to explain the development of whole gully-systems in reasonable timescales (Dundas et al., 2022). This realisation means that my future work on gullies will focus on sublimation driven processes and understanding how they do geomorphic work. I will seek to understand whether wet debris flows can be distinguished from gas-fluidised flow using remote sensing data alone. It still remains possible that liquid water was at the origin of the gully-landform, and CO_2 sublimation is only remodelling the landform today – a possibility that must be kept in the back of one's mind. Equally it is intriguing and exciting to explore the possibility that a gas-supported flow could entirely produce landforms so similar to those created by wet debris flows on Earth. Are wet debris flows on Earth and CO_2 sublimation driven flows on Mars truly equifinal? The fact that these flows are governed by different fundamental physics argues this should not be the case. On one hand water is an incompressible fluid, and on the other CO_2 gas is compressible and being produced during the flow – this should result in distinct behaviours of the flows and in the resulting deposits. Granular flows are challenging to simulate numerically, and even more so when other phases are introduced and changes in phase, which require an inclusion of thermal exchange in the model. To date we have used single-rheology models to simulate flows observed in Martian gullies (de Haas et al., 2019). These models use friction parameters combined with empirical parameters, which describe the flow behaviour in sufficient detail to explain the observed run out lengths and pattern of erosion and deposition. However, these parameters are an abstraction allowing efficient calculation, and have limited physical meaning. It seems that in the short term numerical modelling of granular flows will not allow us to distinguish wet and gas-driven flows. A deeper knowledge of the driving physical processes, which in my opinion can only come from laboratory simulation, is a prerequisite for progress in this area – see next section for ideas on future work.

Exploring the geomorphic work that can be done by gas-supported flows also contributes knowledge to the wider field of geophysical granular flows. An example is pyroclastic density currents which are challenging to study in situ, because of their extreme temperature and speed. A flow driven by sublimating particles could be used as an analogue for the gas production in pyroclastic density currents which lead to high pore pressures and velocities (e.g., Brosch et al., 2021). Equally, it is thought that phase changes are important during snow avalanches (e.g., Bartelt and Lehning, 2002). Hence, sublimation driven flows could be used as an analogue to gain insight into other geophysical granular flows.

Considering now the landscape-scale influence of punctual gas-driven flows, one point of contention is the question of how such flows could result in tributary networks, which are generally

acknowledged to be the result of a distributed input (e.g. precipitation; Gulick et al., 2019). Water flowing over the landscape naturally flows and collects downslope, whereas single mass flows do not collect downslope. Shelef and Hilley (2016) found that discrete flows released stochastically with variable size could form tributary networks, as they collect downslope over long averaging timescales. Implementing such flows into a landscape evolution model could give insights into the size-frequency distribution required to construct fluvial-like tributary networks by gas-driven flows.

Other landforms on Mars remain enigmatic and to me it seems most likely that periglacial landforms, such as solifluction lobes, and sorted patterned ground will prove to be the key evidence for liquid water – especially because we now know perchlorates are common on Mars and have substantial freezing point depression (Chevrier et al., 2009; Primm et al., 2017) favouring the formation of melt-water. Such landforms probably only require thin films of liquid water to form episodically (Sizemore et al., 2015) and perhaps take many millennia to form. The processes underlying solifluction and sorted patterned ground are not completely understood on Earth and the influence of salts on these process is totally unknown. This is an area of fundamental research which would require considerable resources in order to explore these processes experimentally. There are challenges related to precise temperature control and measuring and characterising thin films of water in granular media. We cannot try to numerically model these processes, which would enable us to scale the process to Mars, until these basic experimental results have been obtained.

In general, a better understanding of the deposition, migration and sublimation of ice that results in ice-related landforms is needed to unlock the potential for liquid water and also to better prepare for future robotic missions, such as Mars Ice Mapper. Such knowledge has important knock-on implications for future human exploration, because water ice is key to sustaining humans and generating the fuel needed to return to Earth. Identifying the locations of easily accessible clean ice at latitudes where astronauts would not be subject extreme environmental conditions (e.g. extremes of temperatures at the poles) was one of the motivations for the Mars Ice Mapper mission (Davis et al., 2021).

My work to-date has highlighted the important role of debris covered glaciers on shaping the surface of Mars. In Conway et al. (2018a) we highlighted the potential for glacial erosion to have modified large portions of the martian mid-latitudes. However, we did not explore whether the amount of erosion varied with latitude, which is a key variable to understand the processes underlying the erosion. We might expect water production, that we posit drives the sub-glacial erosion, to be sensitive to average surface temperature, which varies systematically with latitude. We are preparing a paper for publication that reports on the discovery of the first vertical section into a debris covered glacier revealed by a gully-incision (Frances E. G. Butcher et al., 2020). Yet, the exact relation between gullies and debris covered glaciers remains ambiguous. In Conway et al. (2018a) we found that the glacial erosion was sufficient to erase any previously existing gullies. Gullies that erode into debris covered glaciers themselves make little impact on the underlying terrain meaning once the ice is removed then their signal would be lost. Hence gullying is only an effective landscape modifying process on slopes without ice deposits. Otherwise the morphology of the ice deposits dominate over that of the gullies over long time-scales. If gullies are indeed formed by CO_2 sublimation processes and we also know that ground-ice modulates its deposition/condensation (Vincendon et al., 2010b), but we do not know how water ice modulates the action of this CO_2 sublimation processes at the hillslope scale. Recent work by Khuller and Christensen (2021) revealed that new erosional scarps in the walls of gullies might be exposing heavily dust-contaminated ice. Such scarps could reveal ice that is relatively easy to access for human explorers compared to that buried in debris covered glaciers.

In summary, the integration of Mars' glacial history with that of its gully-systems and other potentially periglacial landforms is an important area requiring further work to clarify the potential for liquid water associated with these landforms and also to better understand the ice distribution and its nature at the martian mid-latitudes.

On Earth, I have sought to better understand hazard from mass movements in periglacial environments, which led to studying the role of ground ice in mass movements. In the current context of rising average global temperatures, understanding how ice-degradation leads to mass movements is of increasing importance. Periglacial terrains are often characterised by discontinuous permafrost and surface materials can show little or no surface indication that there is ground ice. Discontinuous permafrost environments are by definition at the limits of permafrost stability and are most sensitive to degradation. These characteristics make these terrains both challenging to study and at the same time an urgent area of research. This difficulty in detecting ground ice and its sometimes subtle action is illustrated by the debris flows I have investigated since my PhD in Ísafjörður in NW Iceland. We have realised that the debris flows that I initially studied during my PhD may be a result of the motion of a rock-glacier like mass of ice cemented sediment perched on a topographic bench – this provides a good explanation for the unusually high cadence of debris flows at this location. In compiling the global inventory of molard-hosting landslides for the PERMOLARDS project, we have realised that mass movements involving ground ice are more diverse than we initially expected. Further, techniques I have developed for use in studying gullies and landslides on planetary bodies, we are now using to study these terrestrial landslides. Hence, in my future work I aim to take this approach one step further and use planets as a test-bed for understanding terrestrial hazards – see the next section. The question of the precise mechanism(s) that trigger the landslides that generate molards has so far been left open in the PERMOLARDS project because of the difficulty in accessing the source areas of these landslides. This remains an important open question because it is this knowledge that permits the prediction of where and when future landslides could occur. The PERMOLARDS project is providing us with the necessary background knowledge on the types of terrain (lithology, soil, topographic setting) susceptible to such landslides, but only the most basic information on the state of the local cryosphere in these locations. The fact that portions of ground ice are mobilised by these mass movements and their often high water content is highly suggestive of the role of permafrost melting in the triggering and dynamics of these mass movements, but remains speculative.

One of the aims of the PERMOLARDS project was to determine the longevity of the molards in the landscape with the aim of using paleo-molards as a marker of past permafrost and its degradation. The influence of glacial retreat on mass movements has been the topic of much research (see McColl, 2012 and references therein) – it falls within the general envelope of paraglacial processes. According to Ballantyne (2002) paraglacial processes are those "directly conditioned by former glaciation and deglaciation". The effect of retreating permafrost could be considered part of the paraglacial paradigm, and its effect on rockwalls in generating rock avalanches has been studied (e.g., Bottino et al., 2002; Deline, 2009), yet less so the degradation of ice-cemented ground to form debris avalanches. Our research during the PERMOLARDS project has revealed that landslides in Iceland have very diverse morphologies (Jónsson et al., 1957) compared to those located in other countries e.g. they often have multiple lobes/tongues, longitudinal ridges, levees and complex surface textures. The influence of the soil/rock conditions in creating these morphologies has not been explored in detail and could be a consequence of the paraglacial conditions in Iceland. Hence, studying these landslides may help us to better understand landslides on Mars, where the influence of liquid water is under much debate – see next section.

On Mercury, the work of the PhD students I have supervised has revealed a more diverse and recently active surface than could have been anticipated prior to the MESSENGER mission. From these discoveries that of the hillslope lineae (Section 6.4, Figure 6.4) reinforces the outcomes of my work on martian gullies – that of equifinality. Many of these downslope features could be explained by differential mass wasting of slope materials with different compositions resulting in different colours. Others are more intriguing: notable those with notable alcoves and lobes in Nathair facula and those on low slopes (e.g. Figure 6.4). No easy explanation can be found for these landforms without invoking additional fluidisation of the downslope movement, which on Mercury could be brought about by sudden volatile loss invoked previously for the formation of hollows (Section 6.2; Blewett et al., 2011). A liquid as a fluidising agent is extremely unlikely to explain the formation of these gully-like landforms on Mercury and my research on Mars (Section 3.7.4) has revealed gas supported flows can mimic attributes of liquid-supported flows. What exactly this volatile species is on Mercury and how it is lost (sublimation or another solar-wind driven mechanism) will probably have to await further data to be gathered by BepiColombo. The discovery of downslope lineae or gullies on Mercury opens up other landforms on other bodies for reinterpretation – for example the "gullies" on Vesta interpreted to be caused by transient liquid water (Scully et al., 2015) may be more likely explained by explosive sublimation of water ice. Downslope lineae have been reported on numerous other bodies (e.g., Phoebe - C. C. Porco et al., 2005; Ceres - Sam and Bhardwaj, 2022; Phobos - Shi et al., 2016) and the lineae on Mercury may form a template for their interpretation.

In summary, the main science questions that have emerged and evolved from my ongoing work are:

- What is the role of volatile loss in shaping planetary landscapes and how is that loss triggered/modulated? Sublimation is an important process on modern Mars, yet the limits of this process are poorly understood. Volatile loss could also be an important contributor to slope processes on other bodies, but has been largely overlooked. Equally melting ground ice can lead to catastrophic mass movements in places on Earth where permafrost was not suspected and requires more investigation.
- Comparative planetology has been important in providing insight into surface processes on Mercury and on Mars, yet my experience in studying gullies on Mars has revealed that equifinality can be problematic. What are the limits of planetary comparison? Where does insight prevail over misunderstanding? Over what temporal and spatial timescales are comparisons useful and/or valid? How can we combat subjectivity (one person's "looks-like" can be "completely different" to another person) using quantitative measures? Can planetary bodies be used to learn more about surface processes on Earth?

6.2 Future work

In the immediate future, I envision two projects as PI to further pursue my research in planetary geomorphology. The first is a project submitted to the French National Funding Agency (ANR) for the 2021 call but was rejected after round 2 despite positive reviews and in 2022 did not pass round 1. The project acronym was "HowDryisMars" and work will continue on this topic without the support of the ANR at a slower cadence, while reapplying. Part of this project is being pushed forward by PhD student Lonneke Roelofs at Utrecht who I co-supervise with Tjalling de Haas funded by NWO.

This project was entitled "How does dry ice sublimation modify gullies on Mars: can it mimic flowing water?" and would aim to shed light on landscape evolution on extra-terrestrial bodies caused by sublimation of ices. It is challenging to study the effects of sublimation on slope processes directly in the field on Earth as it is a marginal process. Yet, a better understanding of this process could lead to fundamental reinterpretations of extra-terrestrial landforms, such as gullies on Mars. We may be

mistakenly interpreting martian gullies as derived from liquid water, because processes driven by sublimation may be able to mimic flowing water, with a knock-on impact on our understanding of the planet's recent habitability and potential resources available for future (human) exploration. More widely, understanding sublimation's landscape signature will result in better planning of future observations on Mars and other Solar System bodies. The objectives would be to:

- Define the processes underlying, and the limits of, sediment transport by CO_2 ice sublimation in the laboratory. Including both limits of material properties and environmental parameters.
- Make the first spatially resolved measurements of the volumes mobilised of recent slope movements in gullies on Mars using new photogrammetry methods developed in the consortium (Figure 7.1). Combined with observations of the timing, topographic/geologic setting and amount of CO_2 and H_2O ice present we aim to quantify the landscape impact of the sublimation-driven transport.
- Bridge the gap in spatial and temporal scales and environment between the sediment motions observed in the laboratory and the observations on Mars using numerical modelling combining 2.5D flow dynamics models with an advanced global climate model for Mars.

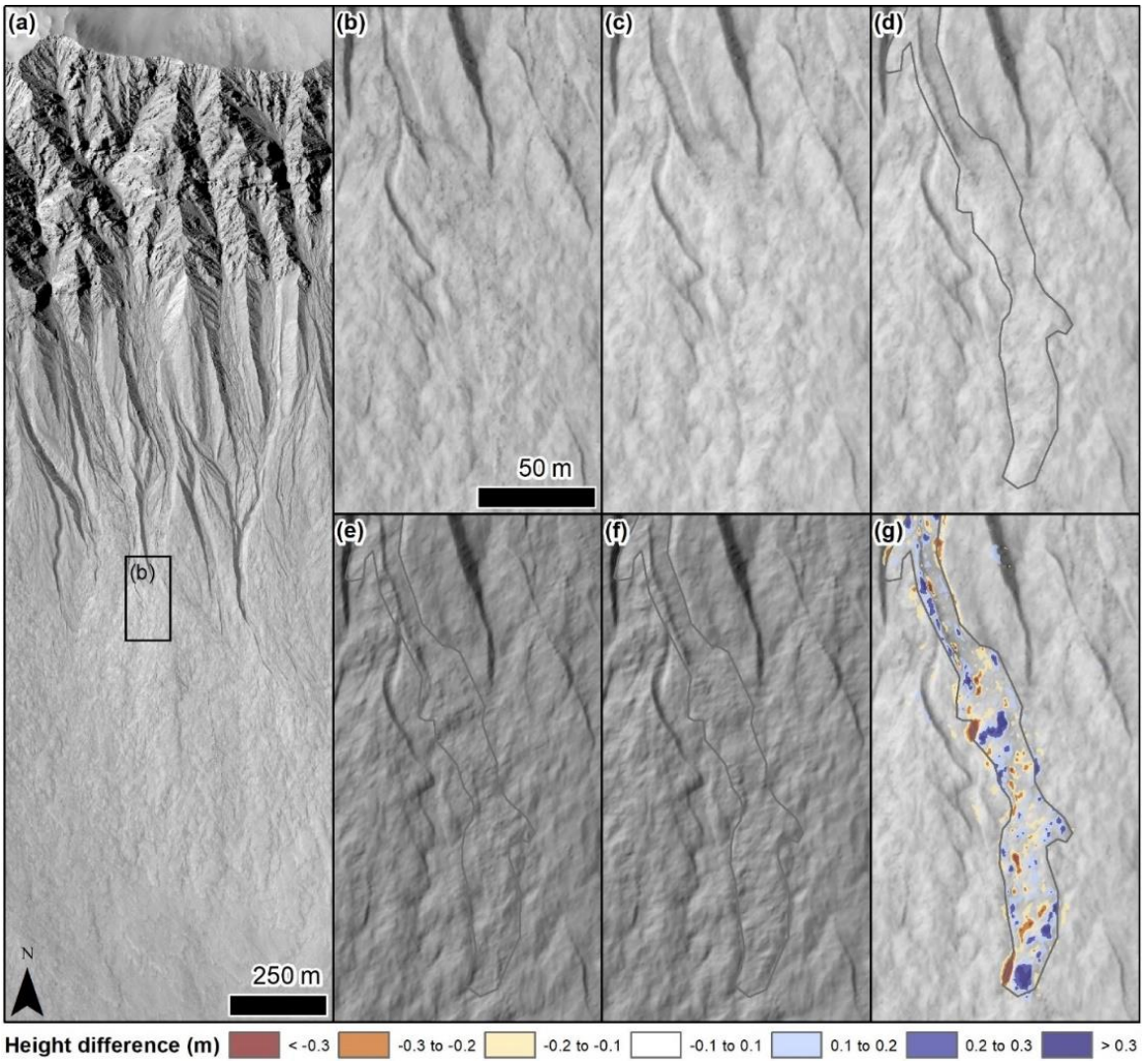

Figure 7.1: Pilot work demonstrating the potential of photoclinometry techniques developed at IPAG (Douté and Jiang, 2020; Jiang et al., 2017) to make volume change measurements in gullies. (a) Gullies in Galap Crater on Mars with area of interest outlined. B) image before change, c) image after change, d) same as c with change outlined, e and f) hillshaded relief of the photoclinometry

reconstructed topography before and after the change, respectively and g) estimated height difference between the two reconstructions. Note that this method is still under development, so areas marked as erosion (brown) are artifacts that we aim to eliminate through better tuning the model to take into account the reflectance properties of the surface.

The second project was submitted for an ERC consolidator grant in March 2021, its title is "Planetary Science informing hazard on Earth" (PSIHazE). It did not get to the second step. This project would use data and knowledge from planetary bodies to better understand gravitational mass movements on Earth. Events such as rockfalls or rock avalanches are stochastic and therefore rarely instrumented. Researchers instead rely on traces left by the event, such as deposits, or impact marks. On Earth these can rapidly be altered or removed by secondary processes e.g., rainfall, plant growth. On other planetary bodies surface process are much less active meaning that pristine morphologies related to gravitational mass movements are better preserved. This presents two advantages : i) pristine morphologies can he more readily studied and ii) many more examples can be studied as even morphologies related to ancient events are well-presumed. This project would focus on three processes where planetary data have the potential to unlock key insights:

1. **Rockfalls**. Rockfalls that have occurred in recent decades on Mars and the Moon leave behind them bounce-marks and furrows in the substrate which are surrounded by albedo markings representing the fallout of the dust cloud ejected by the passage of the rock fragment(s) (Grindrod et al., 2021; Vijayan et al., 2021). These ejecta give information on the energy of the impacts (speed + direction). Such ejecta are visible during rockfalls on Earth, but are not preserved. Hence, the project would use lunar and Martian rockfall ejecta to improve models of rockfall propagation on Earth (Figure 7.2).
2. **Landslides**. The project would use landslides on Mars with a similar size to those on Earth – although many are much bigger (McEwen, 1989; Quantin et al., 2004a). The project would to study both debris avalanches and rock avalanches, of which hundreds of examples exist in the relevant size-range (Crosta et al., 2018), to improve our understanding of how such mass movements propagate over complex 3D surfaces, without the added complication of the involvement of water on Mars. This would be the first time so many landslides could be used, providing an excellent test for existing models.
3. **Pyroclastic density flows** and potentially dry snow avalanches. For this workpackage we would take inspiration from studying sublimation-driven flows on Mars (Dundas et al., 2019a) in order to perform laboratory experiments to understand gas supported flows on Earth. Pyroclastic flows are usually simulated in the laboratory by providing gas from a porous bed (because natural conditions are hard to reproduce, with temperatures generally exceeding 200°C). We would instead use sublimation which supplies gas from the particles involved in the flow as would be the case in nature. Our initial experiments in simulating flows in martian gullies have already revealed some key similarities with pyroclastic flows.

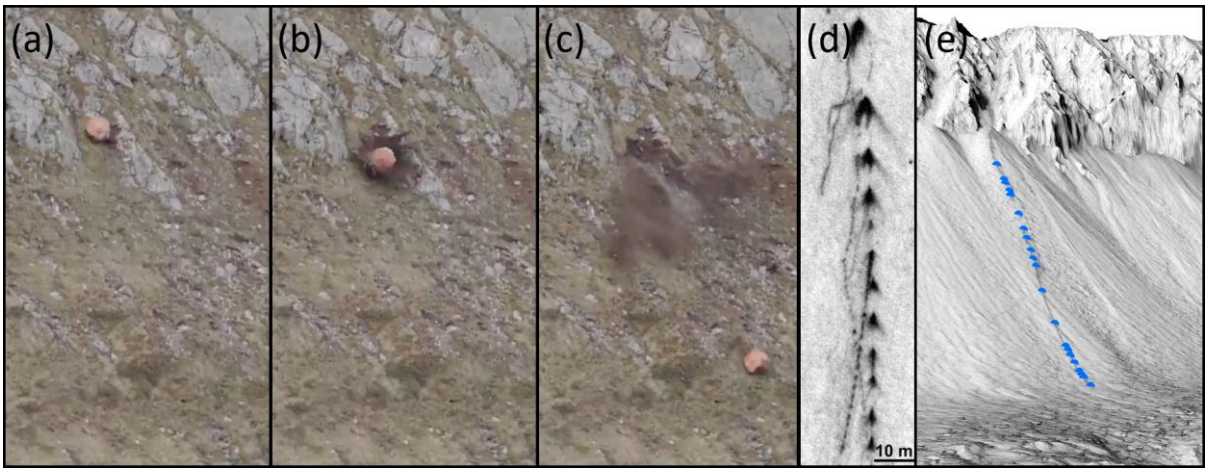

Figure 7.2: (a-c) Images captured from a video of a field-experiment involving a smart-rock (painted orange) from https://twitter.com/SLFDavos_RAMMS/status/1276515021913231360 *showing the "splash" in panel c that is not preserved on Earth. (d) A rockfall path on Mars where downslope is down-image showing the preserved splash marks. (e) A 3D view of a martian slope using a 1 m/pixel HiRISE DTM showing in blue the positions of splash marks on the slope – this project would map these in detail.*

The PERMOLARDS project concerned mass movements that mobilised ice-cemented sediments. Some of these mass movements were caused by the collapse of rock-glaciers (Milana, 2015). Since the start of this project in 2019 there has been a growing interest in mass movements triggered by the catastrophic detachment of glaciers (Kääb et al., 2021), particularly brought into focus by the Kolka event in 2002 in the Caucasus (Haeberli et al., 2004) and most recently the Chamoli slide in India that caused widespread destruction and loss of life (Shugar et al., 2021). These phenomena are linked by the involvement of the warming cryosphere in triggering these events. The precise mechanisms of detachment, however, remain unknown and we intend this to be the focus for a future project. This project would leverage the network of collaborators we have established during the PERMOLARDS project (~10 researchers from ~8 countries). We envisage an ERC Synergy Project or similar, where we would deploy networks of thermal monitoring stations to establish baseline data to do permafrost modelling (Magnin et al., 2015), geophysical investigation and geochemical/isotope analysis (Lacelle and Vasil'chuk, 2013) to study the types/origin/nature/age (e.g. lenses/intergranular) of the ground ice and permafrost in the source areas of molard-generating landslides and secondly infer the modes of ice detachment via analogue modelling.

The discovery of widespread glacial erosion on Mars that I reported in Conway et al. (2018a), left many open questions, regarding the exact mechanism and duration of the erosional event. In future work, therefore, we plan to leverage CTX DTMs to enable the exploration of the erosion intensity with latitude evaluated along the walls of valleys and fossae which traverse different latitude bands, including Mamers, Dao, Harmakhis and Reull Valles, and fossae on Elysium and the Tharsis Montes. In addition, analysis of HiRISE DTMs will be performed in locations where evidence for glaciation is weak, yet disrupted bedrock is still present in order to evaluate the potential role of periglacial rather than glacial processes in bedrock breakdown.

I am working closely with Giulia Magnarini (currently a postdoc at the Natural History Museum, London) to prepare a project concerning landslides in Iceland for submission to the European Research Council Marie Skłodowska-Curie Fellowhsip programme in September 2022. The project would date and characterise the morphology of landslides in Iceland that have longitudinal ridges. These ridges are found in martian landslides and have been linked to fluidisation by water (De Blasio, 2011) or hydrated minerals (Watkins et al., 2015), because of their close resemblance to supraglacial

landslides on Earth (Lucchitta, 1987). However, the landslides with these ridges in Iceland were paragalcial and not supraglacial in origin (Coquin et al., 2015; Feuillet et al., 2014; Mercier et al., 2017). Hence, the origin of these longitudinal ridges in Iceland is unknown. It is possible that these landslides contained significant ice and there are reports of landslide bodies continuing to move post-emplacement similarly to rock glaciers (Owen et al., 2010). In fact many landslide deposits in Iceland have been interpreted by certain workers as rock glaciers (Lilleøren et al., 2013). However, periodic longitudinal ridges is not a deformation feature usually associated with rock glaciers, so even if these deposits were formed in this context the presence of longitudinal ridges remains enigmatic. The project would have important implications for understanding the dynamics of long runout landslides in general and specifcally whether glacial retreat is an important triggering factor – particularly important considering that most of Earth's glaciers are currently retreating.

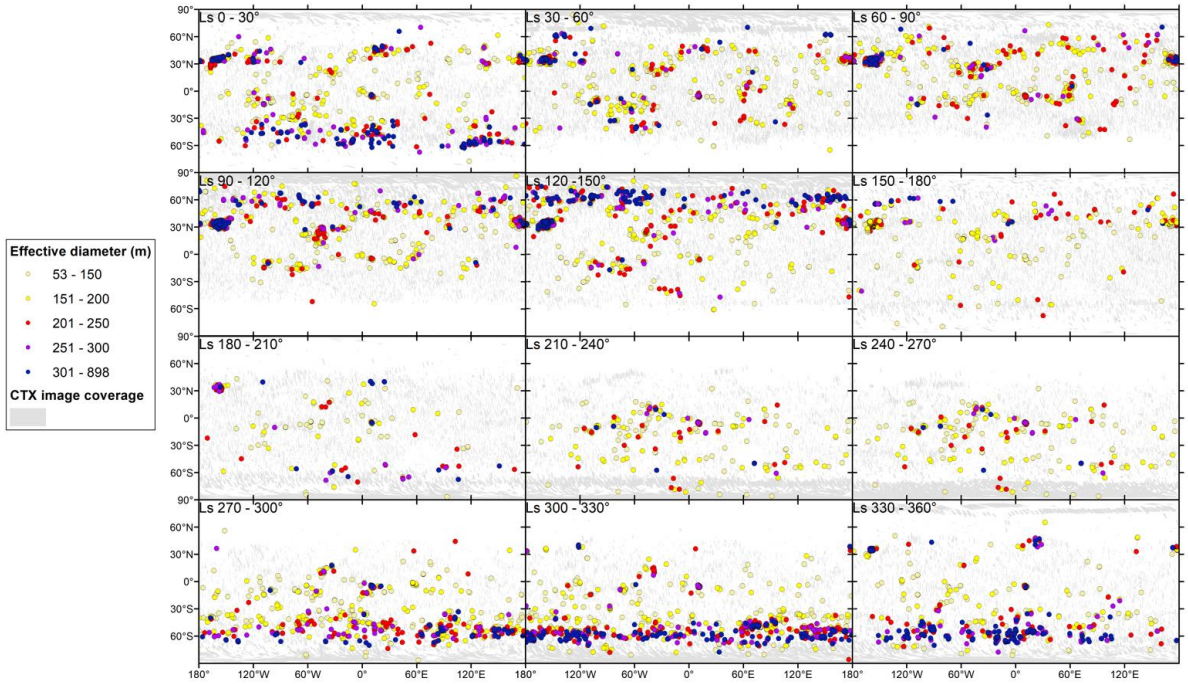

Figure 7.3. Dust devil locations and CTX image coverage for all Mars Years at different seasons (denoted by Ls ranges) showing concentrations of large dust devils around 60° latitude, north and south. Effective diameter is estimated from the bounding box size and is subject to error.

In terms of collaborative projects, I am involved in two machine learning based projects with Valentin Bickel (postdoc at ETH Zurich). The first has been accepted for funding by a NASA Mars Data Analysis Programme funding call 2022, led by Ingrid Daubar, entitled "Rockfalls on Mars - Indicators of Seismicity, Impacts, Volatiles, or Thermal Fatigue?". It concerns the automatic detection of rockfall tracks with associated boulders in all HiRISE images (greatly expanding the inital work of Bickel et al., 2020b), we will then analyse the data to determine the role of volatiles, seismicity, or other relevant triggers. The second project involves the detection of dust devil vortices in the global CTX dataset, where the detection and validation work has been done producing preliminary results (Figure 7.3), but the scientific analysis is ongoing (Conway et al., 2022). An undergrad intern in spring 2022 used the Zooniverse platform to make initial measurements on the detected dust devil dataset, including diameter, shadow-length, and relative opacity. Collaboration with Derek Jackson is completing this data collection with further undergard interns during summer 2022. This is the first global scale dataset spanning multiple Mars Years and we will compare the results on dust devil frequency, diameter, height and opacity with climatological parameters such as wind-speed, surface

temperature and atmospheric vorticity. Next steps include expanding the study to other imaging sensors, such as HRSC, THEMIS, HiRISE and CaSSIS, enabling a wide temporal and spatial-scale sampling as well as access to different times of day. Dust devils are important for understanding Mars' current climate, specifically atmospheric dust loading, which plays a pivotal role in modulating atmospheric circulation. Dust loading can indirectly influence CO_2 and H_2O seasonal/diurnal ice distributions at the surface and their phase transitions.

I will continue collaborating with members of the the CaSSIS and HiRISE science teams, including programming observations and joint observations between instruments. The science focusses include investigation of low latitude frost occurrences with Colin Dundas which is enabled by the colour channels of these instruments – (Figure 7.4). I will also continue to monitor gully locations, with the CaSSIS side driven by a PhD student Vidhya Rangarajan who I co-supervise with Livio Tornabene at Western University in Canada. Future monitoring will be driven by the sites mapped by my former engineer Axel Noblet (Noblet and Conway, 2022). Joint CaSSIS-HiRISE observations will continue to be focussed on active processes, such as defrosting features on dunes, gullies and spiders, icy scarps, RSL and isolated frost occurrences. These observations are exploratory to some degree, but have the common aim of understanding the diurnal influence on volatile-driven surface activity on Mars.

For Mercury the arrival of BepiColombo has the potential to revolutionise our understanding of surface processes on planetary bodies. Even with relatively low-resolution images at 50-100 m/pix we have been able to reveal kilometre scale features, such as spur and gully morphology and slope lineae, which were not expected prior to NASA's MESSENGER mission. The geological mapping using MESSENGER data in which I have been involved is on track to finish before BepiColombo starts imaging the surface and the whole surface will therefore have been scoured for any unusual remaining surface features at this resolution. I anticipate this strand of my research will have a short quiescent period until a critical mass of public data have been acquired and released by the BepiColombo team (~2027).

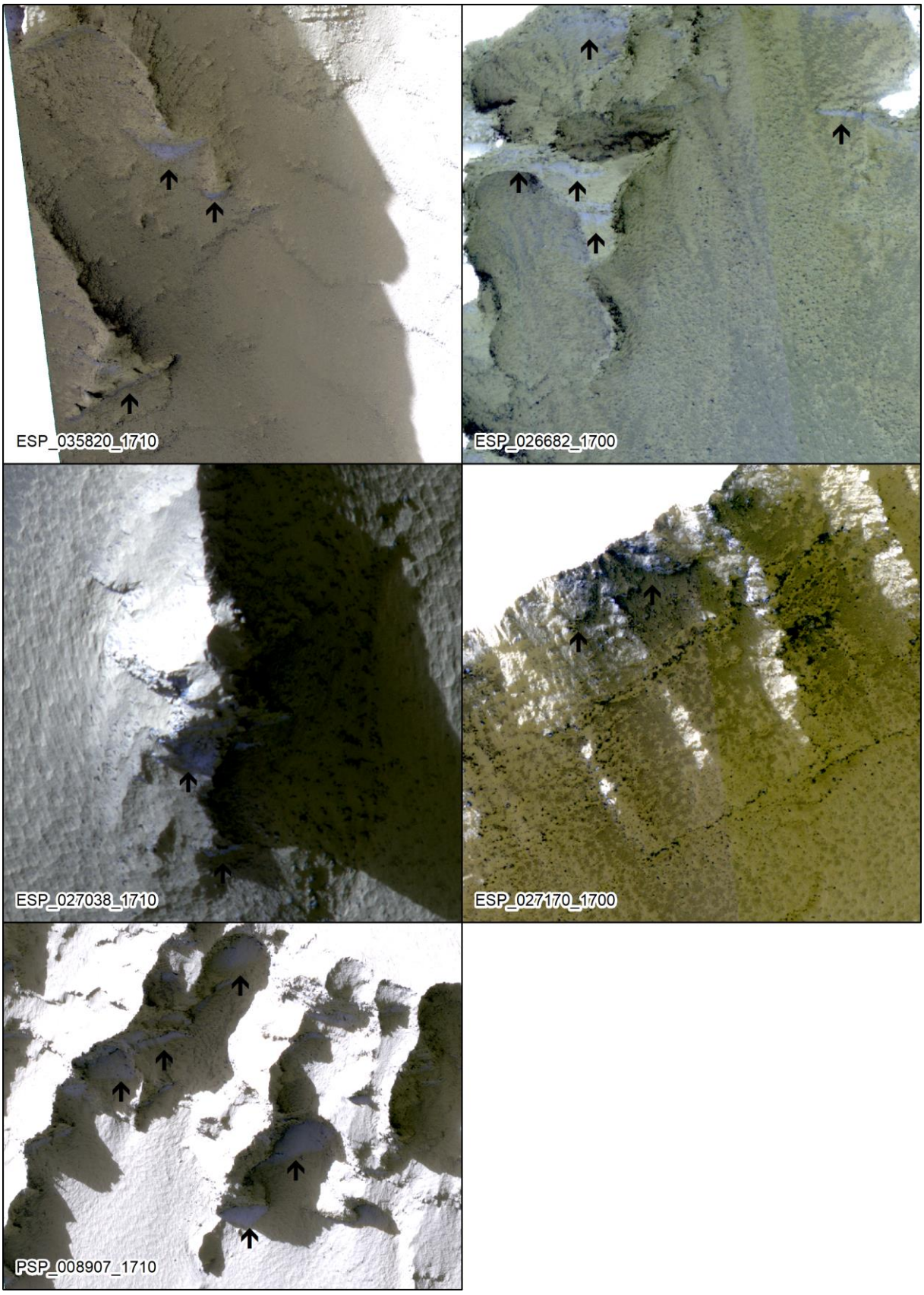

Figure 7.4: Low latitude frost patches (black arrows) visible in the pole-facing shadows as bluish coloration in the COLOR IRB products of HiRISE stretched linearly to "see into" the shadowed portions. ESP_035820_1710 at 9°S and Ls=104°, ESP_026682_1700 at 10°S and Ls=93°, ESP_027038_1710 at 9°S and Ls=105°, ESP_027170_1700 at 10°S and Ls 110°, PSP_008907_1710 at 9°S and Ls=88°.

7 References cited

Abotalib, A.Z., Heggy, E., 2019. A deep groundwater origin for recurring slope lineae on Mars. Nat. Geosci. 12, 235–241. https://doi.org/10.1038/s41561-019-0327-5

Abramov, O., Kring, D.A., 2005. Impact-induced hydrothermal activity on early Mars. J Geophys Res 110, doi:10.1029/2005je002453. https://doi.org/10.1029/2005je002453

Abrevaya, X.C., Anderson, R., Arney, G., Atri, D., Azúa-Bustos, A., Bowman, J.S., Brazelton, W.J., Brennecka, G.A., Carns, R., Chopra, A., Colangelo-Lillis, J., Crockett, C.J., DeMarines, J., Frank, E.A., Frantz, C., de la Fuente, E., Galante, D., Glass, J., Gleeson, D., Glein, C.R., Goldblatt, C., Horak, R., Horodyskyj, L., Kaçar, B., Kereszturi, A., Knowles, E., Mayeur, P., McGlynn, S., Miguel, Y., Montgomery, M., Neish, C., Noack, L., Petryshyn, V., Rugheimer, S., Stüeken, E.E., Tamez-Hidalgo, P., Walker, S.I., Wong, T., 2016. The Astrobiology Primer v2.0. Astrobiology 16, 561–653. https://doi.org/10.1089/ast.2015.1460

Ackiss, S.E., Wray, J.J., 2014. Occurrences of possible hydrated sulfates in the southern high latitudes of Mars. Icarus 243, 311–324. https://doi.org/10.1016/j.icarus.2014.08.016

Adeli, S., Hauber, E., Kleinhans, M., Le Deit, L., Platz, T., Fawdon, P., Jaumann, R., 2016. Amazonian-aged fluvial system and associated ice-related features in Terra Cimmeria, Mars. Icarus 277, 286–299. https://doi.org/10.1016/j.icarus.2016.05.020

Aharonson, O., Schorghofer, N., 2006. Subsurface ice on Mars with rough topography. J Geophys Res-Planets 111, 10. https://doi.org/E11007 Artn e11007

Aharonson, O., Schorghofer, N., Gerstell, M.F., 2003. Slope streak formation and dust deposition rates on Mars. J. Geophys. Res. Planets 108, 5138.

Ahrens, C.J., 2020. Modeling cryogenic mud volcanism on Pluto. J. Volcanol. Geotherm. Res. 406, 107070. https://doi.org/10.1016/j.jvolgeores.2020.107070

Albarede, F., 2009. Volatile accretion history of the terrestrial planets and dynamic implications. Nature 461, 1227–1233. https://doi.org/10.1038/nature08477

Allen, C.C., Oehler, D.Z., Etiope, G., Rensbergen, P.V., Baciu, C., Feyzullayev, A., Martinelli, G., Tanaka, K., Rooij, D.V., 2013. Fluid expulsion in terrestrial sedimentary basins: A process providing potential analogs for giant polygons and mounds in the martian lowlands. Icarus 224, 424–432. https://doi.org/10.1016/j.icarus.2012.09.018

Ancey, C., 2007. Plasticity and geophysical flows: A review. J. Non-Newton. Fluid Mech. 142, 4–35.

Andrews-Hanna, J.C., Phillips, R.J., 2007. Hydrological modeling of outflow channels and chaos regions on Mars. J. Geophys. Res. Planets 112, doi: 10.1029/2006JE002881.

Ansan, V., Mangold, N., Masson, P., Gailhardis, E., Neukum, G., 2008. Topography of valley networks on Mars from Mars Express High Resolution Stereo Camera digital elevation models. J. Geophys. Res. 113, E07006. https://doi.org/10.1029/2007JE002986

Appéré, T., Schmitt, B., Langevin, Y., Douté, S., Pommerol, A., Forget, F., Spiga, A., Gondet, B., Bibring, J.-P., 2011. Winter and spring evolution of northern seasonal deposits on Mars from OMEGA on Mars Express. J Geophys Res 116, E05001. https://doi.org/doi:10.1029/2010JE003762

Arfstrom, J., Hartmann, W.K., 2005. Martian flow features, moraine-like ridges, and gullies: Terrestrial analogs and interrelationships. Icarus 174, 321–335. https://doi.org/10.1016/j.icarus.2004.05.026

Arnold, N.S., Conway, S.J., Butcher, F.E.G., Balme, M.R., 2019. Modeled Subglacial Water Flow Routing Supports Localized Intrusive Heating as a Possible Cause of Basal Melting of Mars' South Polar Ice Cap. J. Geophys. Res. Planets 124, 2101–2116. https://doi.org/10.1029/2019JE006061

Arvidson, R., Drozd, R.J., Hohenberg, C.M., Morgan, C.J., Poupeau, G., 1975. Horizontal transport of the regolith, modification of features, and erosion rates on the lunar surface. The moon 13, 67–79. https://doi.org/10.1007/BF00567508

Aubry, C., Conway, S., Malliband, C., Galluzzi, V., Giacomini, L., 2021. A survey of landforms indicating slope processes in the mid-latitudes of Mercury. Presented at the Europlanet Science Congress 2021, oral, Online. https://doi.org/10.5194/epsc2021-490

Auld, K.C., Dixon, J.C., 2016. A Classification of Martian Gullies from HiRISE Imagery. Planet. Space Sci. 131, 88–101. https://doi.org/10.1016/j.pss.2016.08.002

Baioni, D., Sgavetti, M., 2013. Karst terrains as possible lithologic and stratigraphic markers in northern Sinus Meridiani, Mars. Planet. Space Sci. 75, 173–181. https://doi.org/10.1016/j.pss.2012.08.011

Baker, D.M.H., Carter, L.M., 2019a. Probing supraglacial debris on Mars 1: Sources, thickness, and stratigraphy. Icarus 319, 745–769. https://doi.org/10.1016/j.icarus.2018.09.001

Baker, D.M.H., Carter, L.M., 2019b. Probing supraglacial debris on Mars 2: Crater morphology. Icarus 319, 264–280. https://doi.org/10.1016/j.icarus.2018.09.009

Baker, D.M.H., Head, J.W., Marchant, D.R., 2010. Flow patterns of lobate debris aprons and lineated valley fill north of Ismeniae Fossae, Mars: Evidence for extensive mid-latitude glaciation in the Late Amazonian. Icarus 207, 186–209. https://doi.org/10.1016/j.icarus.2009.11.017

Baker, V.R., 2014. Terrestrial analogs, planetary geology, and the nature of geological reasoning. Planet. Geol. Field Symp. Kitakyushu Jpn. 2011 Planet. Geol. Terr. Analogs 95, 5–10. https://doi.org/10.1016/j.pss.2012.10.008

Baker, V.R., 1993. Extraterrestrial geomorphology: science and philosophy of Earthlike planetary landscapes, in: Geomorphology: The Research Frontier and Beyond. Elsevier, pp. 9–35. https://doi.org/10.1016/B978-0-444-89971-2.50006-7

Baker, V.R., 1979. Erosional processes in channelized water flows on Mars. J. Geophys. Res. 84, 7985. https://doi.org/10.1029/JB084iB14p07985

Baker, V.R., Kochel, R.C., 1979. Martian channel morphology: Maja and Kasei Valles. J. Geophys. Res. 84, 7961. https://doi.org/10.1029/JB084iB14p07961

Baker, V.R., Milton, D.J., 1974. Erosion by catastrophic floods on Mars and Earth. Icarus 23, 27–41. https://doi.org/10.1016/0019-1035(74)90101-8

Baker, V.R., Strom, R.G., Gulick, V.C., Kargel, J.S., Komatsu, G., Kale, V.S., 1991. Ancient oceans, ice sheets and the hydrological cycle on Mars. Nature 352, 589–594. https://doi.org/10.1038/352589a0

Bakker, M., Antoniazza, G., Odermatt, E., Lane, S.N., 2019. Morphological Response of an Alpine Braided Reach to Sediment-Laden Flow Events. J. Geophys. Res. Earth Surf. 124, 1310–1328. https://doi.org/10.1029/2018JF004811

Ballantyne, C.K., 2002. Paraglacial geomorphology. Quat Sci Rev 21, 1935–2017.

Balme, M., Greeley, R., 2006. Dust devils on Earth and Mars. Rev. Geophys. 44, RG3003. https://doi.org/10.1029/2005RG000188

Balme, M., Mangold, N., Baratoux, D., Costard, F., Gosselin, M., Masson, P., Pinet, P., Neukum, G., 2006. Orientation and distribution of recent gullies in the southern hemisphere of Mars: Observations from High Resolution Stereo Camera/Mars Express (HRSC/MEX) and Mars Orbiter Camera/Mars Global Surveyor (MOC/MGS) data. J. Geophys. Res. Planets 111, doi:10.1029/2005JE002607.

Balme, M.R., Gallagher, C., 2009. An equatorial periglacial landscape on Mars. Earth Planet. Sci. Lett. 285, 1–15.

Balme, M.R., Gallagher, C.J., Gupta, S., Murray, J.B., 2011. Fill and spill in Lethe Vallis: a recent flood-routing system in Elysium Planitia, Mars. Geol. Soc. Lond. Spec. Publ. 356, 203–227. https://doi.org/10.1144/SP356.11

Balme, M.R., Gallagher, C.J., Hauber, E., 2013. Morphological evidence for geologically young thaw of ice on Mars: A review of recent studies using high-resolution imaging data. Prog. Phys. Geogr. 37, 289–324. https://doi.org/10.1177/0309133313477123

Balme, M.R., Pathare, A., Metzger, S.M., Towner, M.C., Lewis, S.R., Spiga, A., Fenton, L.K., Renno, N.O., Elliott, H.M., Saca, F.A., Michaels, T.I., Russell, P., Verdasca, J., 2012. Field measurements of horizontal forward motion velocities of terrestrial dust devils: Towards a proxy for ambient winds on Mars and Earth. Icarus 221, 632–645. https://doi.org/10.1016/j.icarus.2012.08.021

Bapst, J., Byrne, S., Brown, A.J., 2018. On the icy edge at Louth and Korolev craters. Icarus 308, 15–26. https://doi.org/10.1016/j.icarus.2017.10.004

Baratoux, D., Delacourt, C., Allemand, P., 2002. An instability mechanism in the formation of the Martian lobate craters and the implications for the rheology of ejecta: EJECTA RHELOGY FROM AN INSTABILITY MECHANISM. Geophys. Res. Lett. 29, 51-1-51–4. https://doi.org/10.1029/2001GL013779

Baratoux, D., Mangold, N., Forget, F., Cord, A., Pinet, P., Daydou, Y., Jehl, A., Masson, P., Neukum, G., Thehrsccoinvestigatorteam, 2006. The role of the wind-transported dust in slope streaks activity: Evidence from the HRSC data. Icarus 183, 30–45. https://doi.org/10.1016/j.icarus.2006.01.023

Bargery, A.S., Gilbert, J.S., 2008. Aqueous eruption and channel flow on Mars during the Amazonian epoch. University of Lancaster, Department of Environmental Science, Lancaster, UK.

Barlow, N.G., 2006. Impact craters in the northern hemisphere of Mars: Layered ejecta and central pit characteristics. Meteorit Planet Sci 41, 1425–1436.

Barlow, N.G., 2005. A review of Martian impact crater ejecta structures and their implications for target properties. Geol. Soc. Am. Spec. Pap. 384, 433–442. https://doi.org/10.1130/0-8137-2384-1.433

Barlow, N.G., Perez, C.B., 2003. Martian impact crater ejecta morphologies as indicators of the distribution of subsurface volatiles. J Geophys Res-Planets 108, doi:10.1029/2002JE002036.

Barnhart, C.J., Nimmo, F., Travis, B.J., 2010. Martian post-impact hydrothermal systems incorporating freezing. Icarus 208, 101–117. https://doi.org/10.1016/j.icarus.2010.01.013

Barraud, O., Besse, S., Doressoundiram, A., Cornet, T., Muñoz, C., 2021. Spectral investigation of Mercury's pits' surroundings: Constraints on the planet's explosive activity. Icarus 370, 114652. https://doi.org/10.1016/j.icarus.2021.114652

Barraud, O., Doressoundiram, A., Besse, S., Sunshine, J.M., 2020. Near-Ultraviolet to Near-Infrared Spectral Properties of Hollows on Mercury: Implications for Origin and Formation Process. J. Geophys. Res. Planets 125. https://doi.org/10.1029/2020JE006497

Barrett, A.M., Balme, M.R., Patel, M.R., Hagermann, A., 2018. The distribution of putative periglacial landforms on the martian northern plains. Icarus 314, 133–148. https://doi.org/10.1016/j.icarus.2018.05.032

Barrett, A.M., Balme, M.R., Patel, M.R., Hagermann, A., 2017. Clastic patterned ground in Lomonosov crater, Mars: examining fracture controlled formation mechanisms. Icarus 295, 125–139. https://doi.org/10.1016/j.icarus.2017.06.008

Bartelt, P., Lehning, M., 2002. A physical SNOWPACK model for the Swiss avalanche warning. Cold Reg. Sci. Technol. 35, 123–145. https://doi.org/10.1016/S0165-232X(02)00074-5

Basilevsky, A.T., Shalygin, E.V., Titov, D.V., Markiewicz, W.J., Scholten, F., Roatsch, Th., Kreslavsky, M.A., Moroz, L.V., Ignatiev, N.I., Fiethe, B., Osterloh, B., Michalik, H., 2012. Geologic interpretation of the near-infrared images of the surface taken by the Venus Monitoring Camera, Venus Express. Icarus 217, 434–450. https://doi.org/10.1016/j.icarus.2011.11.003

Becerra, P., Sori, M.M., Byrne, S., 2017. Signals of astronomical climate forcing in the exposure topography of the North Polar Layered Deposits of Mars: Astronomical Forcing of Mars' NPLD. Geophys. Res. Lett. 44, 62–70. https://doi.org/10.1002/2016GL071197

Beddingfield, C.B., Beyer, R.A., Singer, K.N., McKinnon, W.B., Runyon, K., Grundy, W., Stern, S.A., Bray, V., Dhingra, R., Moore, J.M., Ennico, K., Olkin, C.B., Schenk, P., Spencer, J.R., Weaver, H.A., Young, L.A., 2020. Landslides on Charon. Icarus 335, 113383. https://doi.org/10.1016/j.icarus.2019.07.017

Benn, D.I., Evans, D.J.A., 2010. Glaciers & Glaciation, Second Edition. ed. Hodder Education, London.

Benz, W., Slattery, W.L., Cameron, A.G.W., 1988. Collisional stripping of Mercury's mantle. Icarus 74, 516–528. https://doi.org/10.1016/0019-1035(88)90118-2

Berman, D.C., Crown, D.A., Bleamaster, L.F., 2008. Degradation of Mid-Latitude Craters on Mars: Gullies, Arcuate Ridges, and Small Flow Lobes. Workshop on Martian Gullies 2008.

Berman, D.C., Crown, D.A., Joseph, E.C.S., 2015. Formation and mantling ages of lobate debris aprons on Mars: Insights from categorized crater counts. Planet. Space Sci. 111, 83–99. https://doi.org/10.1016/j.pss.2015.03.013

Berman, D.C., Hartmann, W.K., Crown, D.A., Baker, V.R., 2005. The role of arcuate ridges and gullies in the degradation of craters in the Newton Basin region of Mars. Icarus 178, 465–486. https://doi.org/10.1016/j.icarus.2005.05.011

Bernhardt, H., Reiss, D., Hiesinger, H., Ivanov, M.A., 2016. The honeycomb terrain on the Hellas basin floor, Mars: A case for salt or ice diapirism: Hellas' Honeycombs as Salt/Ice Diapirs. J. Geophys. Res. Planets 121, 714–738. https://doi.org/10.1002/2016JE005007

Besse, S., Doressoundiram, A., Barraud, O., Griton, L., Cornet, T., Muñoz Crego, C., Varatharajan, I., Helbert, J., 2020. Spectral properties and physical extent of pyroclastic deposits on Mercury: variability within selected deposits and implications for explosive volcanism. J. Geophys. Res. Planets. https://doi.org/10.1029/2018JE005879

Bhardwaj, A., Sam, L., Martín-Torres, F.J., Zorzano, M., 2019a. Are Slope Streaks Indicative of Global-Scale Aqueous Processes on Contemporary Mars? Rev. Geophys. 57, 48–77. https://doi.org/10.1029/2018RG000617

Bhardwaj, A., Sam, L., Martín-Torres, F.J., Zorzano, M.-P., 2019b. Discovery of recurring slope lineae candidates in Mawrth Vallis, Mars. Sci. Rep. 9, 2040. https://doi.org/10.1038/s41598-019-39599-z

Bhardwaj, A., Sam, L., Martín-Torres, F.J., Zorzano, M.-P., Fonseca, R.M., 2017. Martian slope streaks as plausible indicators of transient water activity. Sci. Rep. 7. https://doi.org/10.1038/s41598-017-07453-9

Bickel, V.T., Aaron, J., Manconi, A., Loew, S., Mall, U., 2020a. Impacts drive lunar rockfalls over billions of years. Nat. Commun. 11, 2862. https://doi.org/10.1038/s41467-020-16653-3

Bickel, V.T., Conway, S.J., Tesson, P.-A., Manconi, A., Loew, S., Mall, U., 2020b. Deep Learning-driven Detection and Mapping of Rockfalls on Mars. IEEE J. Sel. Top. Appl. Earth Obs. Remote Sens. 1–1. https://doi.org/10.1109/JSTARS.2020.2991588

Bickel, V.T., Kring, D.A., 2020. Lunar south pole boulders and boulder tracks: Implications for crew and rover traverses. Icarus 348, 113850. https://doi.org/10.1016/j.icarus.2020.113850

Bierson, C.J., Phillips, R.J., Smith, I.B., Wood, S.E., Putzig, N.E., Nunes, D., Byrne, S., 2016. Stratigraphy and evolution of the buried CO_2 deposit in the Martian south polar cap: MARS SPLD HISTORY. Geophys. Res. Lett. 43, 4172–4179. https://doi.org/10.1002/2016GL068457

Bishop, J.L., Murad, E., Lane, M.D., Mancinelli, R.L., 2004. Multiple techniques for mineral identification on Mars: Icarus 169, 311–323. https://doi.org/10.1016/j.icarus.2003.12.025

Blair, T.C., 1999. Cause of dominance by sheetflood vs. debris-flow processes on two adjoining alluvial fans, Death Valley, California. Sedimentology 46, 1015–1028.

Blair, T.C., McPherson, J.G., 2009. Processes and Forms of Alluvial Fans, in: Parsons, A.J., Abrahams, A.D. (Eds.), Geomorphology of Desert Environments. Springer Netherlands, Dordrecht, pp. 413–467. https://doi.org/10.1007/978-1-4020-5719-9_14

Blais-Stevens, A., Behnia, P., 2016. Debris flow susceptibility mapping using a qualitative heuristic method and Flow-R along the Yukon Alaska Highway Corridor, Canada. Nat. Hazards Earth Syst. Sci. 16, 449–462. https://doi.org/10.5194/nhess-16-449-2016

Blasius, K.R., Cutts, J.A., Howard, A.D., 1982. Topography and stratigraphy of Martian polar layered deposits. Icarus 50, 140–160. https://doi.org/10.1016/0019-1035(82)90122-1

Blewett, D.T., Chabot, N.L., Denevi, B.W., Ernst, C.M., Head, J.W., Izenberg, N.R., Murchie, S.L., Solomon, S.C., Nittler, L.R., McCoy, T.J., Xiao, Z., Baker, D.M.H., Fassett, C.I., Braden, S.E., Oberst, J., Scholten, F., Preusker, F., Hurwitz, D.M., 2011. Hollows on Mercury: MESSENGER Evidence for Geologically Recent Volatile-Related Activity. Science 333, 1856–1859. https://doi.org/10.1126/science.1211681

Blewett, D.T., Ernst, C.M., Murchie, S.L., Vilas, F., 2018. Mercury's Hollows, in: Solomon, S.C., Nittler, L.R., Anderson, B.J. (Eds.), Mercury. Cambridge University Press, pp. 324–345. https://doi.org/10.1017/9781316650684.013

Blewett, D.T., Stadermann, A.C., Susorney, H.C., Ernst, C.M., Xiao, Z., Chabot, N.L., Denevi, B.W., Murchie, S.L., McCubbin, F.M., Kinczyk, M.J., Gillis-Davis, J.J., Solomon, S.C., 2016. Analysis of MESSENGER high-resolution images of Mercury's hollows and implications for hollow formation: MERCURY's HOLLOWS AT HIGH RESOLUTION. J. Geophys. Res. Planets 121, 1798–1813. https://doi.org/10.1002/2016JE005070

Bordiec, M., Carpy, S., Bourgeois, O., Herny, C., Massé, M., Perret, L., Claudin, P., Pochat, S., Douté, S., 2020. Sublimation waves: Geomorphic markers of interactions between icy planetary surfaces and winds. Earth-Sci. Rev. 211, 103350. https://doi.org/10.1016/j.earscirev.2020.103350

Bottino, G., Chiarle, M., Joly, A., Mortara, G., 2002. Modelling rock avalanches and their relation to permafrost degradation in glacial environments. Permafr. Periglac. Process. 13, 283–288. https://doi.org/10.1002/ppp.432

Bourke, M.C., 2010. Barchan dune asymmetry: Observations from Mars and Earth. Icarus 205, 183–197. https://doi.org/10.1016/j.icarus.2009.08.023

Bourke, M.C., Balme, M., Lewis, S., Lorenz, R.D., Parteli, E., 2019. Planetary Aeolian Geomorphology. Aeolian Geomorphol. New Introd. 261–286.

Boxe, C.S., Hand, K.P., Nealson, K.H., Yung, Y.L., Yen, A.S., Saiz-Lopez, A., 2012. Adsorbed water and thin liquid films on Mars. Int. J. Astrobiol. 11, 169–175. https://doi.org/10.1017/S1473550412000080

Boyce, J., Barlow, N., Mouginis-Mark, P., Stewart, S., 2010. Rampart craters on Ganymede: Their implications for fluidized ejecta emplacement. Meteorit. Planet. Sci. 45, 638–661. https://doi.org/10.1111/j.1945-5100.2010.01044.x

Boyce, J.M., Mouginis-Mark, P., Robinson, M., 2020. The Tsiolkovskiy crater landslide, the moon: An LROC view. Icarus 337, 113464. https://doi.org/10.1016/j.icarus.2019.113464

Boyce, J.M., Wilson, L., Mouginis-Mark, P.J., Hamilton, C.W., Tornabene, L.L., 2012. Origin of small pits in martian impact craters. Icarus 221, 262–275. https://doi.org/10.1016/j.icarus.2012.07.027

Boynton, W.V., Feldman, W.C., Squyres, S.W., Prettyman, T.H., Brückner, J., Evans, L.G., Reedy, R.C., Starr, R., Arnold, J.R., Drake, D.M., Englert, P.A.J., Metzger, A.E., Mitrofanov, I., Trombka, J.I., d'Uston, C., Wänke, H., Gasnault, O., Hamara, D.K., Janes, D.M., Marcialis, R.L., Maurice, S., Mikheeva, I., Taylor, G.J., Tokar, R., Shinohara, C., 2002. Distribution of Hydrogen in the Near Surface of Mars: Evidence for Subsurface Ice Deposits. Science 297, 81–85. https://doi.org/10.1126/science.1073722

Bramson, A.M., Byrne, S., Bapst, J., 2017. Preservation of Midlatitude Ice Sheets on Mars: Mars Midlatitude Ice Sheet Preservation. J. Geophys. Res. Planets 122, 2250–2266. https://doi.org/10.1002/2017JE005357

Bramson, A.M., Byrne, S., Bapst, J., Smith, I.B., McClintock, T., 2019. A Migration Model for the Polar Spiral Troughs of Mars. J. Geophys. Res. Planets 124, 1020–1043. https://doi.org/10.1029/2018JE005806

Bramson, A.M., Byrne, S., Putzig, N.E., Sutton, S., Plaut, J.J., Brothers, T.C., Holt, J.W., 2015. Widespread excess ice in Arcadia Planitia, Mars. Geophys. Res. Lett. 42, 6566–6574. https://doi.org/10.1002/2015GL064844

Brideau, M.-A., Stead, D., Lipovsky, P., Jaboyedoff, M., Hopkinson, C., Demuth, M., Barlow, J., Evans, S., Delaney, K., 2009. Preliminary description and slope stability analyses of the 2008 Little Salmon Lake and 2007 Mt. Steele landslides, Yukon. Yukon Explor. Geol. 119–133.

Bridges, J.C., Catling, D.C., Saxton, J.M., Swindle, T.D., Lyon, I.C., Grady, M.M., 2001. Alteration Assemblages in Martian Meteorites: Implications for Near-Surface Processes. Space Sci. Rev. 96, 365–392. https://doi.org/10.1023/A:1011965826553

Bridges, N.T., Greeley, R., Haldemann, A.F.C., Herkenhoff, K.E., Kraft, M., Parker, T.J., Ward, A.W., 1999. Ventifacts at the Pathfinder landing site. J. Geophys. Res. Planets 104, 8595–8615. https://doi.org/10.1029/98JE02550

Bridges, N.T., Lackner, C.N., 2006. Northern hemisphere Martian gullies and mantled terrain: Implications for near-surface water migration in Mars' recent past. J. Geophys. Res. Planets 111, 09014. https://doi.org/10.1029/2006JE002702

Brooker, L.M., Balme, M.R., Conway, S.J., Hagermann, A., Barrett, A.M., Collins, G.S., Soare, R.J., 2018. Clastic polygonal networks around Lyot crater, Mars: Possible formation mechanisms from morphometric analysis. Icarus 302, 386–406. https://doi.org/10.1016/j.icarus.2017.11.022

Brosch, E., Lube, G., Cerminara, M., Esposti-Ongaro, T., Breard, E.C.P., Dufek, J., Sovilla, B., Fullard, L., 2021. Destructiveness of pyroclastic surges controlled by turbulent fluctuations. Nat. Commun. 12, 7306. https://doi.org/10.1038/s41467-021-27517-9

Brothers, T.C., Holt, J.W., 2016. Three-dimensional structure and origin of a 1.8 km thick ice dome within Korolev Crater, Mars: STRUCTURE AND ORIGIN OF KOROLEV ICE DOME. Geophys. Res. Lett. 43, 1443–1449. https://doi.org/10.1002/2015GL066440

Brothers, T.C., Holt, J.W., Spiga, A., 2013. Orbital radar, imagery, and atmospheric modeling reveal an aeolian origin for Abalos Mensa, Mars: AEOLIAN ORIGIN FOR ABALOS MENSA, MARS. Geophys. Res. Lett. 40, 1334–1339. https://doi.org/10.1002/grl.50293

Brough, S., Hubbard, B., Hubbard, A., 2016. Former extent of glacier-like forms on Mars. Icarus 274, 37–49. https://doi.org/10.1016/j.icarus.2016.03.006

Brown, A.J., Byrne, S., Tornabene, L.L., Roush, T., 2008. Louth crater: Evolution of a layered water ice mound. Icarus 196, 433–445.

Brown, A.J., Calvin, W.M., McGuire, P.C., Murchie, S.L., 2010. Compact Reconnaissance Imaging Spectrometer for Mars (CRISM) south polar mapping: First Mars year of observations. J Geophys Res 115, E00D13.

Brown, A.J., Calvin, W.M., Murchie, S.L., 2012. Compact Reconnaissance Imaging Spectrometer for Mars (CRISM) north polar springtime recession mapping: First 3 Mars years of observations. J Geophys Res 117, E00J20. https://doi.org/10.1029/2012JE004113

Brož, P., Čadek, O., Wright, J., Rothery, D.A., 2018. The Apparent Absence of Kilometer-Sized Pyroclastic Volcanoes on Mercury: Are We Looking Right? Geophys. Res. Lett. 45, 12,171-12,179. https://doi.org/10.1029/2018GL079902

Brož, P., Hauber, E., 2012. A unique volcanic field in Tharsis, Mars: Pyroclastic cones as evidence for explosive eruptions. Icarus 218, 88–99. https://doi.org/10.1016/j.icarus.2011.11.030

Brož, P., Hauber, E., Burgt, I., Špillar, V., Michael, G., 2019. Subsurface Sediment Mobilization in the Southern Chryse Planitia on Mars. J. Geophys. Res. Planets 124, 703–720. https://doi.org/10.1029/2018JE005868

Brož, P., Hauber, E., Conway, S.J., Luzzi, E., Mazzini, A., Noblet, A., Jaroš, J., Fawdon, P., Markonis, Y., 2022. New evidence for sedimentary volcanism on Chryse Planitia, Mars. Icarus 382, 115038. https://doi.org/10.1016/j.icarus.2022.115038

Brož, P., Krýza, O., Conway, S.J., Mueller, N.T., Hauber, E., Mazzini, A., Raack, J., Patel, M.R., Balme, M.R., Sylvest, M.E., 2020a. Mud Flow Levitation on Mars: Insights from Laboratory Simulations. Earth Planet. Sci. Lett. accepted.

Brož, P., Krýza, O., Wilson, L., Conway, S.J., Hauber, E., Mazzini, A., Raack, J., Balme, M.R., Sylvest, M.E., Patel, M.R., 2020b. Experimental evidence for lava-like mud flows under Martian surface conditions. Nat. Geosci. 13, 403–407. https://doi.org/10.1038/s41561-020-0577-2

Brunetti, M.T., Xiao, Z., Komatsu, G., Peruccacci, S., Guzzetti, F., 2015. Large rock slides in impact craters on the Moon and Mercury. Icarus 260, 289–300. https://doi.org/10.1016/j.icarus.2015.07.014

Bruno, B.C., Fagents, S.A., Hamilton, C.W., Burr, D.M., Baloga, S.M., 2006. Identification of volcanic rootless cones, ice mounds, and impact craters on Earth and Mars: Using spatial distribution as a remote sensing tool. J Geophys Res 111, E06017. https://doi.org/10.1029/2005JE002510

Brusnikin, E.S., Kreslavsky, M.A., Zubarev, A.E., Patratiy, V.D., Krasilnikov, S.S., Head, J.W., Karachevtseva, I.P., 2016. Topographic measurements of slope streaks on Mars. Icarus 278, 52–61. https://doi.org/10.1016/j.icarus.2016.06.005

Buhler, P.B., Ingersoll, A.P., Ehlmann, B.L., Fassett, C.I., Head, J.W., 2017. How the martian residual south polar cap develops quasi-circular and heart-shaped pits, troughs, and moats. Icarus 286, 69–93. https://doi.org/10.1016/j.icarus.2017.01.012

Buhler, P.B., Ingersoll, A.P., Piqueux, S., Ehlmann, B.L., Hayne, P.O., 2019. Coevolution of Mars's atmosphere and massive south polar CO2 ice deposit. Nat. Astron. https://doi.org/10.1038/s41550-019-0976-8

Buldovicz, S.N., Khilimonyuk, V.Z., Bychkov, A.Y., Ospennikov, E.N., Vorobyev, S.A., Gunar, A.Y., Gorshkov, E.I., Chuvilin, E.M., Cherbunina, M.Y., Kotov, P.I., Lubnina, N.V., Motenko, R.G., Amanzhurov, R.M., 2018. Cryovolcanism on the Earth: Origin of a Spectacular Crater in the Yamal Peninsula (Russia). Sci. Rep. 8, 13534. https://doi.org/10.1038/s41598-018-31858-9

Burke, M.J., Brennand, T.A., Perkins, A.J., 2012. Transient subglacial hydrology of a thin ice sheet: insights from the Chasm esker, British Columbia, Canada. Quat. Sci. Rev. 58, 30–55. https://doi.org/10.1016/j.quascirev.2012.09.004

Burn, C.R., Friele, P.A., 1989. Geomorphology, Vegetation Succession, Soil Characteristics and Permafrost in Retrogressive Thaw Slumps near Mayo, Yukon Territory. ARCTIC 42, 31–40. https://doi.org/10.14430/arctic1637

Burns, J.A., 2010. The four hundred years of planetary science since Galileo and Kepler. Nature 466, 575–584. https://doi.org/10.1038/nature09215

Burr, D.M., 2002. Recent aqueous floods from the Cerberus Fossae, Mars. Geophys. Res. Lett. 29. https://doi.org/10.1029/2001GL013345

Burr, D.M., Bruno, B.C., Lanagan, P.D., Glaze, L.S., Jaeger, W.L., Soare, R.J., Wan Bun Tseung, J.-M., Skinner, J.A., Baloga, S.M., 2009a. Mesoscale raised rim depressions (MRRDs) on Earth: A review of the characteristics, processes, and spatial distributions of analogs for Mars. Planet. Space Sci. 57, 579–596. https://doi.org/10.1016/j.pss.2008.11.011

Burr, D.M., Tanaka, K.L., Yoshikawa, K., 2009b. Pingos on Earth and Mars. Planet. Space Sci. 57, 541–555. https://doi.org/10.1016/j.pss.2008.11.003

Butcher, Frances E. G., Arnold, N.S., Berman, D.C., Conway, S.J., Davis, J.M., Balme, M.R., 2020. Possible Transport of Basal Debris to the Surface of a Mid-Latitude Glacier on Mars., in: EGU General Assembly Conference Abstracts, EGU General Assembly Conference Abstracts. p. 11628. https://doi.org/10.5194/egusphere-egu2020-11628

Butcher, F. E. G., Balme, M.R., Conway, S.J., Gallagher, C.J., Arnold, N.S., Storrar, R.D., Lewis, S.R., Hagermann, A., 2020. Morphometry of a Glacier-Linked Esker in NW Tempe Terra, Mars, and Implications for Sediment-Discharge Dynamics of Subglacial Drainage. Earth Planet. Sci. Lett. 542, 116325. https://doi.org/10.1016/j.epsl.2020.116325

Butcher, F.E.G., Balme, M.R., Gallagher, C., Arnold, N.S., Conway, S.J., Hagermann, A., Lewis, S.R., 2017. Recent Basal Melting of a Mid-Latitude Glacier on Mars. J. Geophys. Res. Planets. https://doi.org/10.1002/2017JE005434

Butcher, F.E.G., Conway, S.J., Arnold, N.S., 2016. Are the Dorsa Argentea on Mars eskers? Icarus 275, 65–84. https://doi.org/10.1016/j.icarus.2016.03.028

Byrne, P.K., Ghail, R.C., Şengör, A.M.C., James, P.B., Klimczak, C., Solomon, S.C., 2021. A globally fragmented and mobile lithosphere on Venus. Proc. Natl. Acad. Sci. 118, e2025919118. https://doi.org/10.1073/pnas.2025919118

Byrne, P.K., Klimczak, C., Celâl Şengör, A.M., Solomon, S.C., Watters, T.R., Hauck, II, S.A., 2014. Mercury's global contraction much greater than earlier estimates. Nat. Geosci. 7, 301–307. https://doi.org/10.1038/ngeo2097

Byrne, P.K., Klimczak, C., Williams, D.A., Hurwitz, D.M., Solomon, S.C., Head, J.W., Preusker, F., Oberst, J., 2013. An assemblage of lava flow features on Mercury: LAVA FLOW FEATURES ON MERCURY. J. Geophys. Res. Planets 118, 1303–1322. https://doi.org/10.1002/jgre.20052

Byrne, S., 2003. A Sublimation Model for Martian South Polar Ice Features. Science 299, 1051–1053. https://doi.org/10.1126/science.1080148

Byrne, S., Dundas, C.M., Kennedy, M.R., Mellon, M.T., McEwen, A.S., Cull, S.C., Daubar, I.J., Shean, D.E., Seelos, K.D., Murchie, S.L., Cantor, B.A., Arvidson, R.E., Edgett, K.S., Reufer, A., Thomas,

N., Harrison, T.N., Posiolova, L.V., Seelos, F.P., 2009. Distribution of mid-latitude ground ice on mars from new impact craters. Science 325, 1674–1676. https://doi.org/10.1126/science.1175307

Cabrol, N., Grin, E.A., 1999. Distribution, Classification, and Ages of Martian Impact Crater Lakes. Icarus 142, 160–172. https://doi.org/10.1006/icar.1999.6191

Calligaris, C., Boniello, M.A., Zini, L., 2008. Debris flow modelling in Julian Alps using FLO-2D, in: Monitoring, Simulation, Prevention and Remediation of Dense Debris Flows II. Presented at the DEBRIS FLOW 08, WIT Press, The New Forest, UK, pp. 81–88. https://doi.org/10.2495/DEB080091

Cameron, A.G.W., 1985. The partial volatilization of Mercury. Icarus 64, 285–294. https://doi.org/10.1016/0019-1035(85)90091-0

Carr, M., Head, J., 2019. Mars: Formation and fate of a frozen Hesperian ocean. Icarus 319, 433–443. https://doi.org/10.1016/j.icarus.2018.08.021

Carr, M.H., 1996. Channels and valleys on Mars: cold climate features formed as a result of a thickening cryosphere. Planet. Space Sci. 44, 1411–1417. https://doi.org/10.1016/S0032-0633(96)00053-0

Carr, M.H., 1979. Formation of Martian flood features by release of water from confined aquifers. J. Geophys. Res. 84, 2995–3007.

Carter, J., Loizeau, D., Mangold, N., Poulet, F., Bibring, J.-P., 2015. Widespread surface weathering on early Mars: A case for a warmer and wetter climate. Icarus 248, 373–382. https://doi.org/10.1016/j.icarus.2014.11.011

Cassanelli, J.P., Head, J.W., 2015. Firn densification in a Late Noachian “icy highlands” Mars: Implications for ice sheet evolution and thermal response. Icarus 253, 243–255. https://doi.org/10.1016/j.icarus.2015.03.004

Catling, D.C., Claire, M.W., Zahnle, K.J., Quinn, R.C., Clark, B.C., Hecht, M.H., Kounaves, S., 2010. Atmospheric origins of perchlorate on Mars and in the Atacama. J. Geophys. Res. 115, E00E11. https://doi.org/10.1029/2009JE003425

Cavalli, M., Trevisani, S., Comiti, F., Marchi, L., 2013. Geomorphometric assessment of spatial sediment connectivity in small Alpine catchments. Sediment Sources Source--Sink Fluxes Sediment. Budg. 188, 31–41. https://doi.org/10.1016/j.geomorph.2012.05.007

Cedillo-Flores, Y., Treiman, A.H., Lasue, J., Clifford, S.M., 2011. CO2 gas fluidization in the initiation and formation of Martian polar gullies. Geophys. Res. Lett. 38, doi:10.1029/2011GL049403. https://doi.org/10.1029/2011GL049403

Chabot, N.L., Ernst, C.M., Denevi, B.W., Nair, H., Deutsch, A.N., Blewett, D.T., Murchie, S.L., Neumann, G.A., Mazarico, E., Paige, D.A., Harmon, J.K., Head, J.W., Solomon, S.C., 2014. Images of surface volatiles in Mercury’s polar craters acquired by the MESSENGER spacecraft. Geology 42, 1051–1054. https://doi.org/10.1130/G35916.1

Chabot, N.L., Ernst, C.M., Harmon, J.K., Murchie, S.L., Solomon, S.C., Blewett, D.T., Denevi, B.W., 2013. Craters hosting radar-bright deposits in Mercury’s north polar region: Areas of persistent shadow determined from MESSENGER images. J. Geophys. Res. Planets 118, 26–36. https://doi.org/10.1029/2012JE004172

Chabot, N.L., Ernst, C.M., Paige, D.A., Nair, H., Denevi, B.W., Blewett, D.T., Murchie, S.L., Deutsch, A.N., Head, J.W., Solomon, S.C., 2016. Imaging Mercury’s polar deposits during MESSENGER’s low-altitude campaign: Imaging of Mercury’s Polar Deposits. Geophys. Res. Lett. 43, 9461–9468. https://doi.org/10.1002/2016GL070403

Chabot, N.L., Shread, E.E., Harmon, J.K., 2018. Investigating Mercury’s South Polar Deposits: Arecibo Radar Observations and High-Resolution Determination of Illumination Conditions. J. Geophys. Res. Planets 123, 666–681. https://doi.org/10.1002/2017JE005500

Chan, M.A., Beitler, B., Parry, W.T., Ormö, J., Komatsu, G., 2004. A possible terrestrial analogue for haematite concretions on Mars. Nature 429, 731–734. https://doi.org/10.1038/nature02600

Chen, S.-A., Michaelides, K., Grieve, S.W.D., Singer, M.B., 2019. Aridity is expressed in river topography globally. Nature 573, 573–577. https://doi.org/10.1038/s41586-019-1558-8

Chevrier, V.F., Hanley, J., Altheide, T.S., 2009. Stability of perchlorate hydrates and their liquid solutions at the Phoenix landing site, Mars. Geophys. Res. Lett. 36, 10202.

Chevrier, V.F., Rivera-Valentin, E.G., 2012. Formation of recurring slope lineae by liquid brines on present-day Mars. Geophys Res Lett 39, L21202. https://doi.org/10.1029/2012GL054119

Chojnacki, M., McEwen, A., Dundas, C., Ojha, L., Urso, A., Sutton, S., 2016. Geologic context of recurring slope lineae in Melas and Coprates Chasmata, Mars: GEOLOGY OF MELAS AND COPRATES RSL. J. Geophys. Res. Planets 121, 1204–1231. https://doi.org/10.1002/2015JE004991

Christen, M., Bartelt, P., Gruber, U., 2007. RAMMS-a Modeling System for Snow Avalanches, Debris Flows and Rockfalls based on IDL. Photogramm. Fernerkund. GEOINFORMATION 2007, 289.

Christensen, P.R., 2003. Formation of recent martian gullies through melting of extensive water-rich snow deposits. Nature 422, 45–48. https://doi.org/10.1038/nature01436

Christiansen, H.H., 1995. Observations of Open System Pingos in a Marsh Environment, Mellemfjord, Disko, Central West Greenland. Geogr. Tidsskr.-Dan. J. Geogr. 95, 42–48. https://doi.org/10.1080/00167223.1995.10649362

Chuang, F.C., Beyer, R.A., McEwen, A.S., Thomson, B.J., 2007. HiRISE observations of slope streaks on Mars. Geophys. Res. Lett. 34, doi:10.1029/2007GL031111. https://doi.org/L20204 Artn l20204

Citron, R.I., Manga, M., Hemingway, D.J., 2018. Timing of oceans on Mars from shoreline deformation. Nature 555, 643–646. https://doi.org/10.1038/nature26144

Clark, B., 1981. The salts of Mars. Icarus 45, 370–378. https://doi.org/10.1016/0019-1035(81)90041-5

Clifford, S.M., Lasue, J., Heggy, E., Boisson, J., McGovern, P., Max, M.D., 2010. Depth of the Martian cryosphere: Revised estimates and implications for the existence and detection of subpermafrost groundwater. J Geophys Res 115, doi:10.1029/2009JE003462. https://doi.org/10.1029/2009je003462

Clifford, S.M., Parker, T.J., 2001. The evolution of the Martian hydrosphere: Implications for the fate of a primordial ocean and the current state of the northern plains. Icarus 154, 40–79.

Cockell, C.S., Balme, M., Bridges, J.C., Davila, A., Schwenzer, S.P., 2012. Uninhabited habitats on Mars. Icarus 217, 184–193. https://doi.org/10.1016/j.icarus.2011.10.025

Coleman, N.M., 2005. Martian megaflood-triggered chaos formation, revealing groundwater depth, cryosphere thickness, and crustal heat flux. J. Geophys. Res. 110, E12S20. https://doi.org/10.1029/2005JE002419

Collins, G.C., McKinnon, W.B., Moore, J.M., Nimmo, F., Pappalardo, R.T., Prockter, L.M., Schenk, P.M., 2009. Tectonics of the outer planet satellites. Planet. Tecton. 11, 229.

Collins, G.S., Melosh, H.J., 2003. Acoustic fluidization and the extraordinary mobility of sturzstroms. J. Geophys. Res.-Solid Earth 108, doi:10.1029/2003JB002465. https://doi.org/10.1029/2003jb002465

Collins-May, J.L., Carr, J.R., Balme, M.R., Ross, N., Russell, A.J., Brough, S., Gallagher, C., 2020. Postimpact Evolution of the Southern Hale Crater Ejecta, Mars. J. Geophys. Res. Planets 125. https://doi.org/10.1029/2019JE006302

Conway, S., Peignaux, C., Morino, C., Philippe, M., Collins-May, J., Butcher, F., Roberti, G., 2020. Evidence for ice in the ejecta flows of Hale Crater, Mars. Presented at the Europlanet Science Congress 2020, oral, Online. https://doi.org/10.5194/epsc2020-347

Conway, S., Wright, J., Morino, C., 2019. Conical landforms on Mercury and Mars - indicators of volatile release, in: EPSC-DPS Joint Meeting 2019. p. EPSC-DPS2019-1827.

Conway, S.J., 2022. Planetary geomorphology, in: The History of the Study of Landforms or the Development of Geomorphology, Geological Society, London, Memoirs. Geological Society of London, London, pp. M58-2021–33.

Conway, S.J., Balme, M.R., 2016. A novel topographic parameterization scheme indicates that martian gullies display the signature of liquid water. Earth Planet. Sci. Lett. 454, 36–45. https://doi.org/10.1016/j.epsl.2016.08.031

Conway, S.J., Balme, M.R., 2014. Decametre-thick remnant glacial ice deposits on Mars. Geophys. Res. Lett. 41, 5402–5409. https://doi.org/10.1002/2014GL060314

Conway, S.J., Balme, M.R., Kreslavsky, M.A., Murray, J.B., Towner, M.C., 2015. The comparison of topographic long profiles of gullies on Earth to gullies on Mars: A signal of water on Mars. Icarus 253, 189–204. https://doi.org/10.1016/j.icarus.2015.03.009

Conway, S.J., Balme, M.R., Lamb, M.P., Towner, M.C., Murray, J.B., 2011a. Enhanced runout and erosion by overland flow under subfreezing and low pressure conditions: experiments and application to Mars. Icarus 211, 443–457. https://doi.org/10.1016/j.icarus.2010.08.026

Conway, S.J., Balme, M.R., Murray, J.B., Towner, M.C., Okubo, C.H., Grindrod, P.M., 2011b. The indication of Martian gully formation processes by slope–area analysis. Geol. Soc. Lond. Spec. Publ. 356, 171–201. https://doi.org/10.1144/SP356.10

Conway, S.J., Bickel, V.T., Patel, M.R., Fenton, L., Carson, H., 2022. Global Survey of Dust Devils in CTX Data Using Neural Networks, in: LPI Contributions, LPI Contributions. p. 1874.

Conway, S.J., Butcher, F.E.G., de Haas, T., Deijns, A.J., Grindrod, P.M., Davis, J.M., 2018a. Glacial and gully erosion on Mars: A terrestrial perspective. Geomorphology 318, 26–57. https://doi.org/10.1016/j.geomorph.2018.05.019

Conway, S.J., de Haas, T., Harrison, T.N., 2019. Martian gullies: a comprehensive review of observations, mechanisms and the insights from Earth analogues. Geol. Soc. Lond. Spec. Publ. 467. https://doi.org/10.1144/SP467.14

Conway, S.J., Decaulne, A., Balme, M.R., Murray, J.B., Towner, M.C., 2010. A new Approach to Estimating Hazard posed by Debris Flows in the Westfjords of Iceland. Geomorphology 114, 556–572. https://doi.org/10.1016/j.geomorph.2009.08.015

Conway, S.J., Harrison, T.N., Lewis, S.R., 2018b. Chapter 3: Martian gullies and their connection with the martian climate, in: Soare, R.J., Conway, Susan J., Clifford, S.M. (Eds.), Dynamic Mars: Recent and Current Landscape Evolution of the Red Planet. Elsevier.

Conway, S.J., Harrison, T.N., Soare, R.J., Britton, A., Steele, L., 2017. New Slope-Normalised Global Gully Density and Orientation Maps for Mars. Geol. Soc. Lond. Spec. Publ. 467. https://doi.org/10.1144/SP467.3

Conway, S.J., Hovius, N., Barnie, T., Besserer, J., Le Mouélic, S., Orosei, R., Read, N.A., 2012. Climate-driven deposition of water ice and the formation of mounds in craters in Mars' north polar region. Icarus 220, 174–193. https://doi.org/10.1016/j.icarus.2012.04.021

Conway, S.J., Stillman, D.E., 2021. The role of liquid water in recent surface processes on Mars, in: Mars Geological Enigmas. Elsevier, pp. 207–261. https://doi.org/10.1016/B978-0-12-820245-6.00009-4

Coquin, J., Mercier, D., Bourgeois, O., Cossart, E., Decaulne, A., 2015. Gravitational spreading of mountain ridges coeval with Late Weichselian deglaciation: impact on glacial landscapes in Tröllaskagi, northern Iceland. Quat. Sci. Rev. 107, 197–213. https://doi.org/10.1016/j.quascirev.2014.10.023

Corbel, J., Gallo, G., 1970. Cryokarsts et chimie des neiges en zone polaire. Rev. Géographique Pyrén. Sud-Ouest Sud-Ouest Eur. 41, 123–138.

Costard, F., 2007. Vallées de débâcle et processus cryokarstiques sur Mars et en Sibérie. Géographie Phys. Quat. 44, 97–104. https://doi.org/10.7202/032802ar

Costard, F., Forget, F., Jomelli, V., Mangold, N., 2007. Debris flows in Greenland and on Mars, in: Chapman, M. (Ed.), The Geology of Mars: Evidence from Earth-Based Analogs. Cambridge University Press, Cambridge, pp. 265–278.

Costard, F., Forget, F., Mangold, N., Peulvast, J.P., 2002. Formation of recent Martian debris flows by melting of near-surface ground ice at high obliquity. Science 295, 110–113. https://doi.org/10.1126/science.1066698

Costard, F., Sejourne, A., Kargel, J., Godin, E., 2016. Modeling and observational occurrences of near-surface drainage in Utopia Planitia, Mars. Geomorphology 275, 80–89. https://doi.org/10.1016/j.geomorph.2016.09.034

Costard, F., Séjourné, A., Kelfoun, K., Clifford, S., Lavigne, F., Di Pietro, I., Bouley, S., 2017. Modeling tsunami propagation and the emplacement of thumbprint terrain in an early Mars ocean: TSUNAMIS ON MARS. J. Geophys. Res. Planets 122, 633–649. https://doi.org/10.1002/2016JE005230

Costard, FrançoisM., 1989. The spatial distribution of volatiles in the Martian hydrolithosphere. Earth Moon Planets 45, 265–290. https://doi.org/10.1007/BF00057747

Costello, E.S., Ghent, R.R., Hirabayashi, M., Lucey, P.G., 2020. Impact Gardening as a Constraint on the Age, Source, and Evolution of Ice on Mercury and the Moon. J. Geophys. Res. Planets 125. https://doi.org/10.1029/2019JE006172

Craddock, R.A., Howard, A.D., 2002. The case for rainfall on a warm, wet early Mars. J Geophys Res 107, 5111.

Crane, K., 2020. Structural interpretation of thrust fault-related landforms on Mercury using Earth analogue fault models. Geomorphology 369, 107366. https://doi.org/10.1016/j.geomorph.2020.107366

Crane, K.T., Klimczak, C., 2017. Timing and rate of global contraction on Mercury: TIMING AND RATE OF GLOBAL CONTRACTION. Geophys. Res. Lett. 44, 3082–3089. https://doi.org/10.1002/2017GL072711

Crosta, G.B., Frattini, P., Valbuzzi, E., De Blasio, F.V., 2018. Introducing a New Inventory of Large Martian Landslides. Earth Space Sci. 5, 89–119. https://doi.org/10.1002/2017EA000324

Cull, S., Kennedy, E., Clark, A., 2014. Aqueous and non-aqueous soil processes on the northern plains of Mars: Insights from the distribution of perchlorate salts at the Phoenix landing site and in Earth analog environments. Planet. Space Sci. 96, 29–34. https://doi.org/10.1016/j.pss.2014.02.011

Davis, J.M., Balme, M., Grindrod, P.M., Williams, R.M.E., Gupta, S., 2016. Extensive Noachian fluvial systems in Arabia Terra: Implications for early Martian climate. Geology 44, 847–850. https://doi.org/10.1130/G38247.1

Davis, R.M., Collom, B., Viotti, M., Kelley, M., 2021. International Mars Ice Mapper Mission: A Reconnaissance Mission for the Human Exploration of Mars. Presented at the Lunar and Planetary Science Conference, p. 5071.

Day, M., Kocurek, G., 2016. Observations of an aeolian landscape: From surface to orbit in Gale Crater. Icarus 280, 37–71. https://doi.org/10.1016/j.icarus.2015.09.042

De Blasio, F.V., 2011. Landslides in Valles Marineris (Mars): A possible role of basal lubrication by sub-surface ice. Explor. Phobos 59, 1384–1392. https://doi.org/10.1016/j.pss.2011.04.015

de Haas, T., Conway, S.J., Butcher, F.E.G., Levy, J.S., Grindrod, P.M., Balme, M.R., Goudge, T.A., 2019. Time will tell: temporal evolution of Martian gullies and paleoclimatic implications. Geol. Soc. Lond. Spec. Publ. 467. https://doi.org/10.1144/SP467.1

de Haas, T., Hauber, E., Conway, S.J., van Steijn, H., Johnsson, A., Kleinhans, M.G., 2015a. Earth-like aqueous debris-flow activity on Mars at high orbital obliquity in the last million years. Nat. Commun. 6. https://doi.org/10.1038/ncomms8543

de Haas, T., Hauber, E., Kleinhans, M.G., 2013. Local late Amazonian boulder breakdown and denudation rate on Mars. Geophys. Res. Lett. https://doi.org/10.1002/grl.50726

de Haas, T., Kleinhans, M.G., Carbonneau, P.E., Rubensdotter, L., Hauber, E., 2015b. Surface morphology of fans in the high-arctic periglacial environment of Svalbard: Controls and processes. Earth-Sci. Rev. https://doi.org/10.1016/j.earscirev.2015.04.004

de Haas, T., Kruijt, A., Densmore, A.L., 2018. Effects of debris-flow magnitude-frequency distribution on avulsions and fan development: Effects of debris-flow magnitude-frequency distribution on avulsions and fan development. Earth Surf. Process. Landf. 43, 2779–2793. https://doi.org/10.1002/esp.4432

de Haas, T., McArdell, B.W., Nijland, W., Åberg, A.S., Hirschberg, J., Huguenin, P., 2022. Flow and Bed Conditions Jointly Control Debris-Flow Erosion and Bulking. Geophys. Res. Lett. 49. https://doi.org/10.1029/2021GL097611

de Haas, T., van den Berg, W., Braat, L., Kleinhans, M.G., 2016. Autogenic avulsion, channelization and backfilling dynamics of debris-flow fans. Sedimentology 63, 1596–1619. https://doi.org/10.1111/sed.12275

de Haas, T., Ventra, D., Hauber, E., Conway, S.J., Kleinhans, M.G., 2015c. Sedimentological analyses of martian gullies: The subsurface as the key to the surface. Icarus 258, 92–108. https://doi.org/10.1016/j.icarus.2015.06.017

de Scally, F.A., Owens, I.F., 2004. Morphometric controls and geomorphic responses on fans in the Southern Alps, New Zealand. Earth Surf. Process. Landf. 29, 311–322.

De Toffoli, B., Pozzobon, R., Massironi, M., Mazzarini, F., Conway, S., Cremonese, G., 2019. Surface Expressions of Subsurface Sediment Mobilization Rooted into a Gas Hydrate-Rich Cryosphere on Mars. Sci. Rep. 9, 8603. https://doi.org/10.1038/s41598-019-45057-7

De Toffoli, B., Pozzobon, R., Mazzarini, F., Orgel, C., Massironi, M., Giacomini, L., Mangold, N., Cremonese, G., 2018. Estimate of depths of source fluids related to mound fields on Mars. Planet. Space Sci. https://doi.org/10.1016/j.pss.2018.07.005

de Haas, T., McArdell, B.W., Conway, S.J., McElwaine, J.N., Kleinhans, M.G., Salese, F., Grindrod, P.M., 2019. Initiation and Flow Conditions of Contemporary Flows in Martian Gullies. J. Geophys. Res. Planets 124, 2018JE005899. https://doi.org/10.1029/2018JE005899

Dehouck, E., Mangold, N., Le Mouélic, S., Ansan, V., Poulet, F., 2010. Ismenius Cavus, Mars: A deep paleolake with phyllosilicate deposits. Planet. Space Sci. 58, 941–946. https://doi.org/10.1016/j.pss.2010.02.005

Deline, P., 2009. Interactions between rock avalanches and glaciers in the Mont Blanc massif during the late Holocene. Quat. Sci. Rev. 28, 1070–1083. https://doi.org/10.1016/j.quascirev.2008.09.025

Deline, P., Broccolato, M., Noetzli, J., Ravanel, L., Tamburini, A., 2013. The December 2008 Crammont Rock Avalanche, Mont Blanc Massif Area, Italy, in: Margottini, C., Canuti, P., Sassa, K. (Eds.), Landslide Science and Practice: Volume 4: Global Environmental Change. Springer Berlin Heidelberg, Berlin, Heidelberg, pp. 403–408. https://doi.org/10.1007/978-3-642-31337-0_52

Denevi, B.W., Blewett, D.T., Buczkowski, D.L., Capaccioni, F., Capria, M.T., De Sanctis, M.C., Garry, W.B., Gaskell, R.W., Le Corre, L., Li, J.-Y., Marchi, S., McCoy, T.J., Nathues, A., O'Brien, D.P., Petro, N.E., Pieters, C.M., Preusker, F., Raymond, C.A., Reddy, V., Russell, C.T., Schenk, P., Scully, J.E.C., Sunshine, J.M., Tosi, F., Williams, D.A., Wyrick, D., 2012. Pitted Terrain on Vesta and Implications for the Presence of Volatiles. Science 338, 246–249. https://doi.org/10.1126/science.1225374

Denevi, B.W., Ernst, C.M., Meyer, H.M., Robinson, M.S., Murchie, S.L., Whitten, J.L., Head, J.W., Watters, T.R., Solomon, S.C., Ostrach, L.R., Chapman, C.R., Byrne, P.K., Klimczak, C., Peplowski, P.N., 2013. The distribution and origin of smooth plains on Mercury: SMOOTH PLAINS ON MERCURY. J. Geophys. Res. Planets 118, 891–907. https://doi.org/10.1002/jgre.20075

Di Achille, G., Hynek, B.M., 2010. Ancient ocean on Mars supported by global distribution of deltas and valleys. Nat. Geosci. 3, 459–463. https://doi.org/10.1038/ngeo891

Dickson, J.L., Fassett, C.I., Head, J.W., 2009. Amazonian-aged fluvial valley systems in a climatic microenvironment on Mars: Melting of ice deposits on the interior of Lyot Crater. Geophys. Res. Lett. 36, 08201.

Dickson, J.L., Head III, J.W., Levy, J.S., Morgan, G.A., Marchant, D., 2018. Gully Formation in the McMurdo Dry Valleys, Antarctica: Multiple Sources of Water, Temporal Sequence and Relative Importance in Gully Erosion and Deposition Processes. Geol. Soc. Lond. Spec. Publ. accepted.

Dickson, J.L., Head, J.W., Goudge, T.A., Barbieri, L., 2015. Recent climate cycles on Mars: Stratigraphic relationships between multiple generations of gullies and the latitude dependent mantle. Icarus 252, 83–94. https://doi.org/10.1016/j.icarus.2014.12.035

Dickson, J.L., Head, J.W., Kreslavsky, M., 2007. Martian gullies in the southern mid-latitudes of Mars: Evidence for climate-controlled formation of young fluvial features based upon local and global topography. Icarus 188, 315–323.

Dickson, J.L., Head, J.W., Levy, J.S., Marchant, D.R., 2013. Don Juan Pond, Antarctica: Near-surface CaCl2-brine feeding Earth's most saline lake and implications for Mars. Sci. Rep. 3, 1166. https://doi.org/10.1038/srep01166

Diniega, S., 2021. Linear Gullies (Mars), in: Hargitai, H., Kereszturi, Á. (Eds.), Encyclopedia of Planetary Landforms. Springer New York, New York, NY, pp. 1–5. https://doi.org/10.1007/978-1-4614-9213-9_582-1

Diniega, S., Byrne, S., Bridges, N.T., Dundas, C.M., McEwen, A.S., 2010. Seasonality of present-day Martian dune-gully activity. Geology 38, 1047–1050. https://doi.org/10.1130/G31287.1

Diniega, S., Hansen, C.J., McElwaine, J.N., Hugenholtz, C.H., Dundas, C.M., McEwen, A.S., Bourke, M.C., 2013. A new dry hypothesis for the formation of martian linear gullies. Icarus 225, 526–537. https://doi.org/10.1016/j.icarus.2013.04.006

Dohm, J.M., Anderson, R.C., Baker, V.R., Ferris, J.C., Rudd, L.P., Hare, T.M., Rice, J.W., Casavant, R.R., Strom, R.G., Zimbelman, J.R., Scott, D.H., 2001. Latent outflow activity for western Tharsis, Mars: Significant flood record exposed. J. Geophys. Res. Planets 106, 12301–12314. https://doi.org/10.1029/2000JE001352

Draebing, D., Krautblatter, M., Hoffmann, T., 2017. Thermo-cryogenic controls of fracture kinematics in permafrost rockwalls. Geophys. Res. Lett. 44, 3535–3544. https://doi.org/10.1002/2016GL072050

Duarte, K.D., Schmidt, B.E., Chilton, H.T., Hughson, K.H.G., Sizemore, H.G., Ferrier, K.L., Buffo, J.J., Scully, J.E.C., Nathues, A., Platz, T., Landis, M., Byrne, S., Bland, M., Russell, C.T., Raymond, C.A., 2019. Landslides on Ceres: Diversity and Geologic Context. J. Geophys. Res. Planets 2018JE005673. https://doi.org/10.1029/2018JE005673

Dufresne, A., Wolken, G.J., Hibert, C., Bessette-Kirton, E.K., Coe, J.A., Geertsema, M., Ekström, G., 2019. The 2016 Lamplugh rock avalanche, Alaska: deposit structures and emplacement dynamics. Landslides 16, 2301–2319. https://doi.org/10.1007/s10346-019-01225-4

Dundas, C.M., 2021. Chapter 10 - Dry formation of recent Martian slope features, in: Soare, R.J., Conway, S.J., Williams, J.-P., Oehler, D.Z. (Eds.), Mars Geological Enigmas. Elsevier, pp. 263–288. https://doi.org/10.1016/B978-0-12-820245-6.00010-0

Dundas, C.M., 2020. Geomorphological evidence for a dry dust avalanche origin of slope streaks on Mars. Nat. Geosci. 13, 473–476. https://doi.org/10.1038/s41561-020-0598-x

Dundas, C.M., Bramson, A.M., Ojha, L., Wray, J.J., Mellon, M.T., Byrne, S., McEwen, A.S., Putzig, N.E., Viola, D., Sutton, S., Clark, E., Holt, J.W., 2018. Exposed subsurface ice sheets in the Martian mid-latitudes. Science 359, 199–201. https://doi.org/10.1126/science.aao1619

Dundas, C.M., Byrne, S., McEwen, A.S., 2015a. Modeling the development of martian sublimation thermokarst landforms. Icarus 262, 154–169. https://doi.org/10.1016/j.icarus.2015.07.033

Dundas, C.M., Byrne, S., McEwen, A.S., Mellon, M.T., Kennedy, M.R., Daubar, I.J., Saper, L., 2014. HiRISE observations of new impact craters exposing Martian ground ice. J. Geophys. Res. Planets 119, 2013JE004482. https://doi.org/10.1002/2013JE004482

Dundas, C.M., Conway, S.J., Cushing, G.E., 2022. Martian gully activity and the gully sediment transport system. Icarus 386, 115133. https://doi.org/10.1016/j.icarus.2022.115133

Dundas, C.M., Diniega, S., Hansen, C.J., Byrne, S., McEwen, A.S., 2012. Seasonal activity and morphological changes in martian gullies. Icarus 220, 124–143. https://doi.org/10.1016/j.icarus.2012.04.005

Dundas, C.M., Diniega, S., McEwen, A.S., 2015b. Long-Term Monitoring of Martian Gully Formation and Evolution with MRO/HiRISE. Icarus 251, 244–263. https://doi.org/10.1016/j.icarus.2014.05.013

Dundas, C.M., McEwen, A.S., 2010. An assessment of evidence for pingos on Mars using HiRISE. Icarus 205, 244–258. https://doi.org/doi: 10.1016/j.icarus.2009.02.020

Dundas, C.M., McEwen, A.S., Chojnacki, M., Milazzo, M.P., Byrne, S., McElwaine, J.N., Urso, A., 2017. Granular flows at recurring slope lineae on Mars indicate a limited role for liquid water. Nat. Geosci. 10, 903–907. https://doi.org/10.1038/s41561-017-0012-5

Dundas, C.M., McEwen, A.S., Diniega, S., Hansen, C.J., Byrne, S., McElwaine, J.N., 2019a. The Formation of Gullies on Mars Today. Geol. Soc. Lond. Spec. Publ. Martian Gullies and their Earth Analogues. https://doi.org/10.1144/SP467.5

Dundas, C.M., Mellon, M.T., Conway, S.J., Daubar, I.J., Williams, K.E., Ojha, L., Wray, J.J., Bramson, A.M., McEwen, A.S., Viola, D., Landis, M., 2020. Distribution and Properties of Ice-Exposing Scarps and Craters on Mars. Icarus submitted.

Dundas, C.M., Mellon, M.T., Conway, S.J., Gastineau, R., 2019b. Active Boulder Movement at High Martian Latitudes. Geophys. Res. Lett. 2019GL082293. https://doi.org/10.1029/2019GL082293

Dundas, C.M., Mellon, M.T., McEwen, A.S., Lefort, A., Keszthelyi, L.P., Thomas, N., 2008. HiRISE observations of fractured mounds: Possible Martian pingos. Geophys. Res. Lett. 35, L04201. https://doi.org/10.1029/2007GL031798

Dunning, S.A., Rosser, N.J., McColl, S.T., Reznichenko, N.V., 2015. Rapid sequestration of rock avalanche deposits within glaciers. Nat. Commun. 6, 7964.

Ehlmann, B.L., Mustard, J.F., Clark, R.N., Swayze, G.A., Murchie, S.L., 2011a. Evidence for low-grade metamorphism, hydrothermal alteration, and diagenesis on Mars from phyllosilicate mineral assemblages. Clays Clay Miner. 59, 359–377. https://doi.org/10.1346/CCMN.2011.0590402

Ehlmann, B.L., Mustard, J.F., Murchie, S.L., Bibring, J.-P., Meunier, A., Fraeman, A.A., Langevin, Y., 2011b. Subsurface water and clay mineral formation during the early history of Mars. Nature 479, 53–60. https://doi.org/10.1038/nature10582

El Mir, C., Ramesh, K.T., Delbo, M., 2019. The efficiency of thermal fatigue in regolith generation on small airless bodies. Icarus 333, 356–370. https://doi.org/10.1016/j.icarus.2019.06.001

El-Maarry, M.R., Dohm, J.M., Michael, G., Thomas, N., Maruyama, S., 2013. Morphology and evolution of the ejecta of Hale crater in Argyre basin, Mars: Results from high resolution mapping. Icarus 226, 905–922. https://doi.org/10.1016/j.icarus.2013.07.014

El-Maarry, M.R., Thomas, N., Gracia-Berná, A., Marschall, R., Auger, A.-T., Groussin, O., Mottola, S., Pajola, M., Massironi, M., Marchi, S., Höfner, S., Preusker, F., Scholten, F., Jorda, L., Kührt, E., Keller, H.U., Sierks, H., A'Hearn, M.F., Barbieri, C., Barucci, M.A., Bertaux, J.-L., Bertini, I., Cremonese, G., Da Deppo, V., Davidsson, B., Debei, S., De Cecco, M., Deller, J., Güttler, C., Fornasier, S., Fulle, M., Gutierrez, P.J., Hofmann, M., Hviid, S.F., Ip, W.-H., Knollenberg, J., Koschny, D., Kovacs, G., Kramm, J.-R., Küppers, M., Lamy, P.L., Lara, L.M., Lazzarin, M., Lopez Moreno, J.J., Marzari, F., Michalik, H., Naletto, G., Oklay, N., Pommerol, A., Rickman, H., Rodrigo, R., Tubiana, C., Vincent, J.-B., 2015. Fractures on comet 67P/Churyumov-Gerasimenko observed by Rosetta/OSIRIS: FRACTURES ON COMET 67P. Geophys. Res. Lett. 42, 5170–5178. https://doi.org/10.1002/2015GL064500

Eppes, M.-C., Willis, A., Molaro, J., Abernathy, S., Zhou, B., 2015. Cracks in Martian boulders exhibit preferred orientations that point to solar-induced thermal stress. Nat. Commun. 6, 6712. https://doi.org/10.1038/ncomms7712

Ewing, R.C., Lapotre, M.G.A., Lewis, K.W., Day, M., Stein, N., Rubin, D.M., Sullivan, R., Banham, S., Lamb, M.P., Bridges, N.T., Gupta, S., Fischer, W.W., 2017. "Sedimentary processes of the Bagnold Dunes: Implications for the eolian rock record of Mars": Bagnold Dune Field sedimentary processes. J. Geophys. Res. Planets. https://doi.org/10.1002/2017JE005324

Fagents, S.A., Lanagan, P., Greeley, R., 2002. Rootless cones on Mars: a consequence of lava-ground ice interaction. Geol. Soc. Lond. Spec. Publ. 202, 295–317. https://doi.org/10.1144/GSL.SP.2002.202.01.15

Fannin, R.J., Wise, M.P., 2001. An empirical-statistical model for debris flow travel distance. Can. Geotech. J. 38, 982–994.

Farrell, W.M., Plaut, J.J., Cummer, S.A., Gurnett, D.A., Picardi, G., Watters, T.R., Safaeinili, A., 2009. Is the Martian water table hidden from radar view?: MARTIAN WATER TABLE. Geophys. Res. Lett. 36, n/a-n/a. https://doi.org/10.1029/2009GL038945

Fassett, C.I., 2016. Ames stereo pipeline-derived digital terrain models of Mercury from MESSENGER stereo imaging. Planet. Space Sci. 134, 19–28. https://doi.org/10.1016/j.pss.2016.10.001

Fassett, C.I., Crowley, M.C., Leight, C., Dyar, M.D., Minton, D.A., Hirabayashi, M., Thomson, B.J., Watters, W.A., 2017. Evidence for rapid topographic evolution and crater degradation on Mercury from simple crater morphometry: Rapid Crater Degradation on Mercury. Geophys. Res. Lett. https://doi.org/10.1002/2017GL073769

Fassett, C.I., Dickson, J.L., Head, J.W., Levy, J.S., Marchant, D.R., 2010. Supraglacial and proglacial valleys on Amazonian Mars. Icarus 208, 86–100. https://doi.org/10.1016/j.icarus.2010.02.021

Fassett, C.I., Head III, J.W., 2008. The timing of martian valley network activity: Constraints from buffered crater counting. Icarus 195, 61–89. https://doi.org/10.1016/j.icarus.2007.12.009

Fastook, J.L., Head, J.W., 2015. Glaciation in the Late Noachian Icy Highlands: Ice accumulation, distribution, flow rates, basal melting, and top-down melting rates and patterns. Planet. Space Sci. 106, 82–98. https://doi.org/10.1016/j.pss.2014.11.028

Fastook, J.L., Head, J.W., 2014. Amazonian mid- to high-latitude glaciation on Mars: Supply-limited ice sources, ice accumulation patterns, and concentric crater fill glacial flow and ice sequestration. Planet. Space Sci. 91, 60–76. https://doi.org/10.1016/j.pss.2013.12.002

Fastook, J.L., Head, J.W., Marchant, D.R., Forget, F., Madeleine, J.-B., 2012. Early Mars climate near the Noachian–Hesperian boundary: Independent evidence for cold conditions from basal melting of the south polar ice sheet (Dorsa Argentea Formation) and implications for valley network formation. Icarus 219, 25–40. https://doi.org/10.1016/j.icarus.2012.02.013

Feldman, W.C., Bandfield, J.L., Diez, B., Elphic, R.C., Maurice, S., Nelli, S.M., 2008. North to south asymmetries in the water-equivalent hydrogen distribution at high latitudes on Mars. J. Geophys. Res. 113, E08006. https://doi.org/10.1029/2007JE003020

Feldman, W.C., Maurice, S., Binder, A.B., Barraclough, B.L., Elphic, R.C., Lawrence, D.J., 1998. Fluxes of Fast and Epithermal Neutrons from Lunar Prospector: Evidence for Water Ice at the Lunar Poles. Science 281, 1496–1500. https://doi.org/10.1126/science.281.5382.1496

Feldman, W.C., Mellon, M.T., Gasnault, O., Diez, B., Elphic, R.C., Hagerty, J.J., Lawrence, D.J., Maurice, S., Prettyman, T.H., 2007. Vertical distribution of hydrogen at high northern latitudes on Mars: The Mars Odyssey Neutron Spectrometer: MARS ODYSSEY NEUTRON SPECTROMETER. Geophys. Res. Lett. 34. https://doi.org/10.1029/2006GL028936

Feldman, W.C., Pathare, A., Maurice, S., Prettyman, T.H., Lawrence, D.J., Milliken, R.E., Travis, B.J., 2011. Mars Odyssey neutron data: 2. Search for buried excess water ice deposits at nonpolar latitudes on Mars. J Geophys Res 116, E11009. https://doi.org/10.1029/2011JE003806

Feldman, W.C., Prettyman, T.H., Maurice, S., Plaut, J.J., Bish, D.L., Vaniman, D.T., Mellon, M.T., Metzger, A.E., Squyres, S.W., Karunatillake, S., Boynton, W.V., Elphic, R.C., Funsten, H.O., Lawrence, D.J., Tokar, R.L., 2004. Global distribution of near-surface hydrogen on Mars. J Geophys Res 109. https://doi.org/10.1029/2003je002160

Ferri, F., Smith, P.H., Lemmon, M., Rennó, N.O., 2003. Dust devils as observed by Mars Pathfinder: DUST DEVILS AS OBSERVED BY MARS PATHFINDER. J. Geophys. Res. Planets 108. https://doi.org/10.1029/2000JE001421

Ferrill, D.A., Wyrick, D.Y., Morris, A.P., Sims, D.W., Franklin, N.M., 2004. Dilational fault slip and pit chain formation on Mars. GSA Today 14, 4. https://doi.org/10.1130/1052-5173(2004)014<4:DFSAPC>2.0.CO;2

Ferrill, D.A., Wyrick, D.Y., Smart, K.J., 2011. Coseismic, dilational-fault and extension-fracture related pit chain formation in Iceland: Analog for pit chains on Mars. Lithosphere 3, 133–142. https://doi.org/10.1130/L123.1

Feuillet, T., Coquin, J., Mercier, D., Cossart, E., Decaulne, A., Jónsson, H.P., Sæmundsson, Þorsteinn, 2014. Focusing on the spatial non-stationarity of landslide predisposing factors in northern

Iceland: Do paraglacial factors vary over space? Prog. Phys. Geogr. Earth Environ. 38, 354–377. https://doi.org/10.1177/0309133314528944

Fishbaugh, K.E., Hvidberg, C.S., 2006. Martian north polar layered deposits stratigraphy: Implications for accumulation rates and flow. J Geophys Res 111, doi:10.1029/2005je002571. https://doi.org/10.1029/2005je002571

Fisher, D.A., 2005. A process to make massive ice in the martian regolith using long-term diffusion and thermal cracking. Icarus 179, 387–397. https://doi.org/10.1016/j.icarus.2005.07.024

Fitzsimons, S., Howarth, J., 2020. Development of push moraines in deeply frozen sediment adjacent to a cold-based glacier in the McMurdo Dry Valleys, Antarctica. Earth Surf. Process. Landf. 45, 622–637. https://doi.org/10.1002/esp.4759

Flemal, R.C., 1976. Pingos and Pingo Scars: Their Characteristics, Distribution, and Utility in Reconstructing Former Permafrost Environments. Quat. Res. 6, 37–53. https://doi.org/10.1016/0033-5894(76)90039-9

French, H.M., 2013. The periglacial environment, 3rd ed. John Wiley & Sons, Chichester, England.

Frey, H., Jarosewich, M., 1982. Subkilometer Martian volcanoes: Properties and possible terrestrial analogs. J. Geophys. Res. 87, 9867. https://doi.org/10.1029/JB087iB12p09867

Gaidos, E.J., 2001. Cryovolcanism and the recent flow of liquid water on Mars. Icarus 153, 218–223.

Gallagher, C., Balme, M., 2015. Eskers in a complete, wet-based glacial system in the Phlegra Montes region, Mars. Earth Planet. Sci. Lett. 431, 96–109. https://doi.org/10.1016/j.epsl.2015.09.023

Gallagher, C., Balme, M., Soare, R., Conway, S.J., 2018. Formation and degradation of chaotic terrain in the Galaxias regions of Mars; implications for near-surface storage of ice. Icarus. https://doi.org/10.1016/j.icarus.2018.03.002

Gallagher, C., Balme, M.R., Conway, S.J., Grindrod, P.M., 2011. Sorted clastic stripes, lobes and associated gullies in high-latitude craters on Mars: Landforms indicative of very recent, polycyclic ground-ice thaw and liquid flows. Icarus 211, 458–471. https://doi.org/10.1016/j.icarus.2010.09.010

Gallagher, C.J., Bahia, R., 2021. Chapter 2 - Outflow channels on Mars, in: Soare, R.J., Conway, S.J., Williams, J.-P., Oehler, D.Z. (Eds.), Mars Geological Enigmas. Elsevier, pp. 13–40. https://doi.org/10.1016/B978-0-12-820245-6.00002-1

Gallagher, C.J., Balme, M.R., 2011. Landforms indicative of ground-ice thaw in the northern high latitudes of Mars. Geol. Soc. Lond. Spec. Publ. 356, 87–110. https://doi.org/10.1144/SP356.6

Gardin, E., Allemand, P., Quantin, C., Thollot, P., 2010. Defrosting, dark flow features, and dune activity on Mars: Example in Russell crater. J Geophys Res 115, doi:10.1029/2009JE003515. https://doi.org/10.1029/2009je003515

Gastineau, R., Conway, S.J., Johnsson, A., Eichel, J., Mangold, N., Grindrod, P.M., Izquierdo, T., 2020. Small-scale lobate hillslope features on Mars: A comparative 3D morphological study with terrestrial solifluction lobes and zebra stripe lobes. Icarus accepted.

Gellert, R., 2004. Chemistry of Rocks and Soils in Gusev Crater from the Alpha Particle X-ray Spectrometer. Science 305, 829–832. https://doi.org/10.1126/science.1099913

Ghatan, G., Zimbelman, J., 2006. Paucity of candidate coastal constructional landforms along proposed shorelines on Mars: Implications for a northern lowlands-filling ocean. Icarus 185, 171–196. https://doi.org/10.1016/j.icarus.2006.06.007

Ghatan, G.J., Head III, J.W., 2002. Candidate subglacial volcanoes in the south polar region of Mars: Morphology, morphometry, and eruption conditions. J. Geophys. Res. 107. https://doi.org/10.1029/2001JE001519

Ghent, R.R., Anderson, S.W., Pithawala, T.M., 2012. The formation of small cones in Isidis Planitia, Mars through mobilization of pyroclastic surge deposits. Icarus 217, 169–183. https://doi.org/10.1016/j.icarus.2011.10.018

Gillet, Ph., Barrat, J.A., Deloule, E., Wadhwa, M., Jambon, A., Sautter, V., Devouard, B., Neuville, D., Benzerara, K., Lesourd, M., 2002. Aqueous alteration in the Northwest Africa 817 (NWA 817) Martian meteorite. Earth Planet. Sci. Lett. 203, 431–444. https://doi.org/10.1016/S0012-821X(02)00835-X

Giuranna, M., Grassi, D., Formisano, V., Montabone, L., Forget, F., Zasova, L., 2008. PFS/MEX observations of the condensing CO2 south polar cap of Mars. Icarus 197, 386–402. https://doi.org/10.1016/j.icarus.2008.05.019

Glavin, D.P., Freissinet, C., Miller, K.E., Eigenbrode, J.L., Brunner, A.E., Buch, A., Sutter, B., Archer, P.D., Atreya, S.K., Brinckerhoff, W.B., Cabane, M., Coll, P., Conrad, P.G., Coscia, D., Dworkin, J.P., Franz, H.B., Grotzinger, J.P., Leshin, L.A., Martin, M.G., McKay, C., Ming, D.W., Navarro-González, R., Pavlov, A., Steele, A., Summons, R.E., Szopa, C., Teinturier, S., Mahaffy, P.R., 2013a. Evidence for perchlorates and the origin of chlorinated hydrocarbons detected by SAM at the Rocknest aeolian deposit in Gale Crater: EVIDENCE FOR PERCHLORATES AT ROCKNEST. J. Geophys. Res. Planets 118, 1955–1973. https://doi.org/10.1002/jgre.20144

Glavin, D.P., Freissinet, C., Miller, K.E., Eigenbrode, J.L., Brunner, A.E., Buch, A., Sutter, B., Archer, P.D., Atreya, S.K., Brinckerhoff, W.B., Cabane, M., Coll, P., Conrad, P.G., Coscia, D., Dworkin, J.P., Franz, H.B., Grotzinger, J.P., Leshin, L.A., Martin, M.G., McKay, C., Ming, D.W., Navarro-González, R., Pavlov, A., Steele, A., Summons, R.E., Szopa, C., Teinturier, S., Mahaffy, P.R., 2013b. Evidence for perchlorates and the origin of chlorinated hydrocarbons detected by SAM at the Rocknest aeolian deposit in Gale Crater: EVIDENCE FOR PERCHLORATES AT ROCKNEST. J. Geophys. Res. Planets 118, 1955–1973. https://doi.org/10.1002/jgre.20144

Goddard, K., Warner, N.H., Gupta, S., Kim, J.-R., 2014. Mechanisms and Timescales of Fluvial Activity at Mojave and other Young Martian Craters. J. Geophys. Res. Planets 2013JE004564. https://doi.org/10.1002/2013JE004564

Goldspiel, J.M., Squyres, S.W., 2011. Groundwater discharge and gully formation on martian slopes. Icarus 211, 238–258. https://doi.org/doi: 10.1016/j.icarus.2010.10.008

Gosse, G., Jones, B.M., 2011. Spatial distribution of pingos in northern Asia. The Cryosphere 5, 13–33. https://doi.org/10.5194/tc-5-13-2011

Goudge, T.A., Aureli, K.L., Head, J.W., Fassett, C.I., Mustard, J.F., 2015. Classification and analysis of candidate impact crater-hosted closed-basin lakes on Mars. Icarus 260, 346–367. https://doi.org/10.1016/j.icarus.2015.07.026

Goudge, T.A., Fassett, C.I., Head, J.W., Mustard, J.F., Aureli, K.L., 2016. Insights into surface runoff on early Mars from paleolake basin morphology and stratigraphy. Geology 44, 419–422. https://doi.org/10.1130/G37734.1

Goudge, T.A., Head, J.W., Kerber, L., Blewett, D.T., Denevi, B.W., Domingue, D.L., Gillis-Davis, J.J., Gwinner, K., Helbert, J., Holsclaw, G.M., Izenberg, N.R., Klima, R.L., McClintock, W.E., Murchie, S.L., Neumann, G.A., Smith, D.E., Strom, R.G., Xiao, Z., Zuber, M.T., Solomon, S.C., 2014. Global inventory and characterization of pyroclastic deposits on Mercury: New insights into pyroclastic activity from MESSENGER orbital data. J. Geophys. Res. Planets 119, 635–658. https://doi.org/10.1002/2013JE004480

Goudie, A.S., 2007. Mega-Yardangs: A Global Analysis: Mega-yardangs: A global analysis. Geogr. Compass 1, 65–81. https://doi.org/10.1111/j.1749-8198.2006.00003.x

Gough, R.V., Chevrier, V.F., Baustian, K.J., Wise, M.E., Tolbert, M.A., 2011. Laboratory studies of perchlorate phase transitions: Support for metastable aqueous perchlorate solutions on Mars. Earth Planet. Sci. Lett. 312, 371–377. https://doi.org/10.1016/j.epsl.2011.10.026

Gough, R.V., Chevrier, V.F., Tolbert, M.A., 2016. Formation of liquid water at low temperatures via the deliquescence of calcium chloride: Implications for Antarctica and Mars. Planet. Space Sci. 131, 79–87. https://doi.org/10.1016/j.pss.2016.07.006

Grant, J.A., Wilson, S.A., 2011. Late alluvial fan formation in southern Margaritifer Terra, Mars. Geophys Res Lett 38, L08201.

Grasby, S.E., Proemse, B.C., Beauchamp, B., 2014. Deep groundwater circulation through the High Arctic cryosphere forms Mars-like gullies. Geology 42, 651–654. https://doi.org/10.1130/G35599.1

Grau Galofre, A., Jellinek, A.M., Osinski, G.R., 2020. Valley formation on early Mars by subglacial and fluvial erosion. Nat. Geosci. https://doi.org/10.1038/s41561-020-0618-x

Greeley, R., Arvidson, R.E., Barlett, P.W., Blaney, D., Cabrol, N.A., Christensen, P.R., Fergason, R.L., Golombek, M.P., Landis, G.A., Lemmon, M.T., McLennan, S.M., Maki, J.N., Michaels, T., Moersch, J.E., Neakrase, L.D.V., Rafkin, S.C.R., Richter, L., Squyres, S.W., de Souza, P.A., Sullivan, R.J., Thompson, S.D., Whelley, P.L., 2006a. Gusev crater: Wind-related features and processes observed by the Mars Exploration Rover Spirit: GUSEV CRATER OBSERVED BY SPIRIT. J. Geophys. Res. Planets 111, n/a-n/a. https://doi.org/10.1029/2005JE002491

Greeley, R., Bender, K., Thomas, P.E., Schubert, G., Limonadi, D., Weitz, C.M., 1995. Wind-Related Features and Processes on Venus: Summary of Magellan Results. Icarus 115, 399–420. https://doi.org/10.1006/icar.1995.1107

Greeley, R., Whelley, P.L., Arvidson, R.E., Cabrol, N.A., Foley, D.J., Franklin, B.J., Geissler, P.G., Golombek, M.P., Kuzmin, R.O., Landis, G.A., Lemmon, M.T., Neakrase, L.D.V., Squyres, S.W., Thompson, S.D., 2006b. Active dust devils in Gusev crater, Mars: Observations from the Mars Exploration Rover Spirit: ACTIVE DUST DEVILS IN GUSEV CRATER, MARS. J. Geophys. Res. Planets 111, n/a-n/a. https://doi.org/10.1029/2006JE002743

Grimm, R.E., 2002. Low-frequency electromagnetic exploration for groundwater on Mars. J. Geophys. Res. 107. https://doi.org/10.1029/2001JE001504

Grimm, R.E., Delory, G.T., Espley, J.R., Stillman, D.E., 2020. A Magnetotelluric Sounder to Probe Terrestrial Planet and Satellite Interiors, in: Lunar and Planetary Science Conference. p. 1568.

Grimm, R.E., Harrison, K.P., Stillman, D.E., 2014. Water budgets of martian recurring slope lineae. Icarus 233, 316–327. https://doi.org/10.1016/j.icarus.2013.11.013

Grimm, R.E., Harrison, K.P., Stillman, D.E., Kirchoff, M.R., 2017. On the secular retention of ground water and ice on Mars. J. Geophys. Res. Planets 122, 94–109. https://doi.org/10.1002/2016JE005132

Grimm, R.E., Stillman, D.E., 2015. Field Test of Detection and Characterisation of Subsurface Ice using Broadband Spectral-Induced Polarisation: Subsurface Ice Characterisation using Spectral-Induced Polarisation. Permafr. Periglac. Process. 26, 28–38. https://doi.org/10.1002/ppp.1833

Grindrod, P.M., Balme, M.R., 2010. Groundwater processes in Hebes Chasma, Mars: GROUNDWATER AND HYDRATES ON MARS. Geophys. Res. Lett. 37, n/a-n/a. https://doi.org/10.1029/2010GL044122

Grindrod, P.M., Davis, J.M., Conway, S.J., de Haas, T., 2021. Active Boulder Falls in Terra Sirenum, Mars: Constraints on Timing and Causes. Geophys. Res. Lett. Accepted.

Guidat, T., Pochat, S., Bourgeois, O., Souček, O., 2015. Landform assemblage in Isidis Planitia, Mars: Evidence for a 3 Ga old polythermal ice sheet. Earth Planet. Sci. Lett. 411, 253–267. https://doi.org/10.1016/j.epsl.2014.12.002

Guimpier, A., Conway, S.J., Mangeney, A., Lucas, A., Mangold, N., Peruzzetto, M., Pajola, M., Lucchetti, A., Munaretto, G., Sæmundsson, T., Johnsson, A., Le Deit, L., Grindrod, P., Davis, J., Thomas, N., Cremonese, G., 2021. Dynamics of recent landslides (<20 My) on Mars: Insights from high-resolution topography on Earth and Mars and numerical modelling. Planet. Space Sci. 206, 105303. https://doi.org/10.1016/j.pss.2021.105303

Gulick, V.C., Glines, N., Hart, S., Freeman, P., 2019. Geomorphological analysis of gullies on the central peak of Lyot Crater, Mars. Geol. Soc. Lond. Spec. Publ. 467, 233–265. https://doi.org/10.1144/SP467.17

Gustafson, J.O., Bell, J.F., Gaddis, L.R., Hawke, B.R., Giguere, T.A., 2012. Characterization of previously unidentified lunar pyroclastic deposits using Lunar Reconnaissance Orbiter Camera data: NEW PYROCLASTIC DEPOSITS. J. Geophys. Res. Planets 117, n/a-n/a. https://doi.org/10.1029/2011JE003893

Haberle, R.M., Clancy, R.T., Forget, F., Smith, M.D., Zurek, R.W. (Eds.), 2017. The Atmosphere and Climate of Mars. Cambridge University Press, Cambridge. https://doi.org/10.1017/9781139060172

Haeberli, W., Huggel, C., Kääb, A., Zgraggen-Oswald, S., Polkvoj, A., Galushkin, I., Zotikov, I., Osokin, N., 2004. The Kolka-Karmadon rock/ice slide of 20 September 2002: an extraordinary event

of historical dimensions in North Ossetia, Russian Caucasus. J. Glaciol. 50, 533–546. https://doi.org/10.3189/172756504781829710

Hallet, B., 1990. Self-organization in freezing soils: from microscopic ice lenses to patterned ground. Can. J. Phys. 68, 842–852. https://doi.org/10.1139/p90-122

Hanna, J.C., Phillips, R.J., 2006. Tectonic pressurization of aquifers in the formation of Mangala and Athabasca Valles, Mars. J. Geophys. Res. 111. https://doi.org/10.1029/2005JE002546

Hansen, C.J., Byrne, S., Portyankina, G., Bourke, M., Dundas, C., McEwen, A., Mellon, M., Pommerol, A., Thomas, N., 2013. Observations of the northern seasonal polar cap on Mars: I. Spring sublimation activity and processes. Mars Polar Sci. V 225, 881–897. https://doi.org/10.1016/j.icarus.2012.09.024

Hansen, G., Giuranna, M., Formisano, V., Fonti, S., Grassi, D., Hirsh, H., Ignatiev, N., Maturilli, A., Orleanski, P., Piccioni, G., Rataj, M., Saggin, B., Zasova, L., 2005. PFS-MEX observation of ices in the residual south polar cap of Mars. Planet. Space Sci. 53, 1089–1095. https://doi.org/10.1016/j.pss.2004.12.011

Hargitai, H., Kereszturi, Á. (Eds.), 2015. Encyclopedia of Planetary Landforms, Springer reference. Springer, New York.

Harmon, J.K., Perillat, P.J., Slade, M.A., 2001. High-Resolution Radar Imaging of Mercury's North Pole. Icarus 149, 1–15. https://doi.org/10.1006/icar.2000.6544

Harrison, K.P., Grimm, R.E., 2008. Multiple flooding events in Martian outflow channels. J. Geophys. Res. 113, E02002. https://doi.org/10.1029/2007JE002951

Harrison, K.P., Grimm, R.E., 2003. Rheological constraints on martian landslides. Icarus 163, 347–362. https://doi.org/10.1016/S0019-1035(03)00045-9

Harrison, T.N., Malin, M.C., Edgett, K.S., Shean, D.E., Kennedy, M.R., Lipkaman, L.J., Cantor, B.A., Posiolova, L.V., 2010. Impact-induced overland fluid flow and channelized erosion at Lyot Crater, Mars. Geophys. Res. Lett. 37. https://doi.org/10.1029/2010gl045074

Harrison, T.N., Osinski, G.R., Tornabene, L.L., Jones, E., 2015. Global Documentation of Gullies with the Mars Reconnaissance Orbiter Context Camera and Implications for Their Formation. Icarus 252, 236–254. https://doi.org/10.1016/j.icarus.2015.01.022

Hartmann, W.K., Neukum, G., 2001. Cratering Chronology and the Evolution of Mars. Space Sci. Rev. 96, 165–194. https://doi.org/10.1023/A:1011945222010

Hartmann, W.K., Thorsteinsson, T., Sigurdsson, F., 2003. Martian hillside gullies and Icelandic analogs. Icarus 162, 259–277. https://doi.org/10.1016/S0019-1035(02)00065-9

Hartmann, W.K., Werner, S.C., 2010. Martian Cratering 10. Progress in use of crater counts to interpret geological processes: Examples from two debris aprons. Earth Planet. Sci. Lett. 294, 230–237. https://doi.org/10.1016/j.epsl.2009.10.001

Hauber, E., Platz, T., Reiss, D., Le Deit, L., Kleinhans, M.G., Marra, W.A., de Haas, T., Carbonneau, P., 2013. Asynchronous formation of Hesperian and Amazonian-aged deltas on Mars and implications for climate. J. Geophys. Res. Planets 118, 1529–1544. https://doi.org/10.1002/jgre.20107

Hauber, E., Reiss, D., Ulrich, M., Preusker, F., Trauthan, F., Zanetti, M., Hiesinger, H., Jaumann, R., Johansson, L., Johnsson, A., Olvmo, M., Carlsson, E., Johansson, H.A.B., McDaniel, S., 2011a. Periglacial landscapes on Svalbard: Terrestrial analogs for cold-climate landforms on Mars. Geol. Soc. Am. Spec. Pap. 483, 177–201. https://doi.org/10.1130/2011.2483(12)

Hauber, E., Reiss, D., Ulrich, M., Preusker, F., Trauthan, F., Zanetti, M., Hiesinger, H., Jaumann, R., Johansson, L., Johnsson, A., Van Gasselt, S., Olvmo, M., 2011b. Landscape evolution in Martian mid-latitude regions: insights from analogous periglacial landforms in Svalbard. Geol. Soc. Lond. Spec. Publ. 356, 111–131. https://doi.org/10.1144/SP356.7

Hauber, E., Sassenroth, C., de Vera, J.-P.P., Schmitz, N., Jaumann, R., Reiss, D., Hiesinger, H., Johnsson, A., 2018. Debris Flows and Water Tracks in Northern Victoria Land, Continental East Antarctica: A New Terrestrial Analogue Site for Gullies and Recurrent Slope Lineae on Mars. Geol. Soc. Lond. Spec. Publ. in review.

Hayne, P.O., Paige, D.A., Heavens, N.G., 2014. The role of snowfall in forming the seasonal ice caps of Mars: Models and constraints from the Mars Climate Sounder. Icarus 231, 122–130. https://doi.org/10.1016/j.icarus.2013.10.020

Head, J.W., Crumpler, L.S., Aubele, J.C., Guest, J.E., Saunders, R.S., 1992. Venus volcanism: Classification of volcanic features and structures, associations, and global distribution from Magellan data. J. Geophys. Res. 97, 13153. https://doi.org/10.1029/92JE01273

Head, J.W., Kreslavsky, M.A., Marchant, D.R., 2011. Pitted rock surfaces on Mars: A mechanism of formation by transient melting of snow and ice. J. Geophys. Res. 116, E09007. https://doi.org/10.1029/2011JE003826

Head, J.W., Marchant, D.R., 2003. Cold-based mountain glaciers on Mars: Western Arsia Mons. Geology 31, 641–644. https://doi.org/10.1130/0091-7613(2003)031<0641:CMGOMW>2.0.CO;2

Head, J.W., Marchant, D.R., Dickson, J.L., Kress, A.M., Baker, D.M., 2010. Northern mid-latitude glaciation in the Late Amazonian period of Mars: Criteria for the recognition of debris-covered glacier and valley glacier landsystem deposits. Earth Planet. Sci. Lett. 294, 306–320. https://doi.org/10.1016/j.epsl.2009.06.041

Head, J.W., Marchant, D.R., Kreslavsky, M.A., 2008a. Formation of gullies on Mars: Link to recent climate history and insolation microenvironments implicate surface water flow origin. Proc. Natl. Acad. Sci. U. S. A. 105, 13258–13263. https://doi.org/10.1073/pnas.0803760105

Head, J.W., Murchie, S.L., Prockter, L.M., Robinson, M.S., Solomon, S.C., Strom, R.G., Chapman, C.R., Watters, T.R., McClintock, W.E., Blewett, D.T., Gillis-Davis, J.J., 2008b. Volcanism on Mercury: Evidence from the First MESSENGER Flyby. Science 321, 69–72. https://doi.org/10.1126/science.1159256

Head, J.W., Mustard, J.F., Kreslavsky, M.A., Milliken, R.E., Marchant, D.R., 2003. Recent ice ages on Mars. Nature 426, 797–802. https://doi.org/10.1038/nature02114

Head, J.W., Pratt, S., 2001. Extensive Hesperian-aged south polar ice sheet on Mars: Evidence for massive melting and retreat, and lateral flow and ponding of meltwater. J. Geophys. Res. Planets 106, 12275–12299. https://doi.org/10.1029/2000JE001359

Hecht, M.H., 2002. Metastability of liquid water on Mars. Icarus 156, 373–386. https://doi.org/10.1006/icar.2001.6794

Hecht, M.H., Kounaves, S.P., Quinn, R.C., West, S.J., Young, S.M.M., Ming, D.W., Catling, D.C., Clark, B.C., Boynton, W.V., Hoffman, J., DeFlores, L.P., Gospodinova, K., Kapit, J., Smith, P.H., 2009. Detection of Perchlorate and the Soluble Chemistry of Martian Soil at the Phoenix Lander Site. Science 325, 64. https://doi.org/10.1126/science.1172466

Heckmann, T., Schwanghart, W., 2013. Geomorphic coupling and sediment connectivity in an alpine catchment — Exploring sediment cascades using graph theory. Geomorphology 182, 89–103. https://doi.org/10.1016/j.geomorph.2012.10.033

Heinz, J., Schulze-Makuch, D., Kounaves, S.P., 2016. Deliquescence-induced wetting and RSL-like darkening of a Mars analogue soil containing various perchlorate and chloride salts. Geophys. Res. Lett. 43, 4880–4884. https://doi.org/10.1002/2016GL068919

Heldmann, J.L., Carlsson, E., Johansson, H., Mellon, M.T., Toon, O.B., 2007. Observations of martian gullies and constraints on potential formation mechanisms II. The northern hemisphere. Icarus 188, 324–344.

Heldmann, J.L., Conley, C., Brown, A.J., Fletcher, L., Bishop, J.L., McKay, C.P., 2010. Possible Liquid Water Origin for Atacama Desert Mudflow and Recent Gully Deposits on Mars. Icarus 206, 685–690.

Heldmann, J.L., Mellon, M.T., 2004. Observations of martian gullies and constraints on potential formation mechanisms. Icarus 168, 285–304.

Heldmann, J.L., Schurmeier, L., McKay, C., Davila, A., Stoker, C., Marinova, M., Wilhelm, M.B., 2014. Midlatitude Ice-Rich Ground on Mars as a Target in the Search for Evidence of Life and for in situ Resource Utilization on Human Missions. Astrobiology 102–118. https://doi.org/10.1089/ast.2013.1103

Heldmann, J.L., Toon, O.B., Pollard, W.H., Mellon, M.T., Pitlick, J., McKay, C.P., Andersen, D.T., 2005. Formation of Martian gullies by the action of liquid water flowing under current Martian environmental conditions. J Geophys Res-Planets 110, doi:10.1029/2004JE002261.

Hemmi, R., Miyamoto, H., 2018. High-Resolution Topographic Analyses of Mounds in Southern Acidalia Planitia, Mars: Implications for Possible Mud Volcanism in Submarine and Subaerial Environments. Geosciences 8, 152. https://doi.org/10.3390/geosciences8050152

Hemmi, R., Miyamoto, H., 2017. Distribution, morphology, and morphometry of circular mounds in the elongated basin of northern Terra Sirenum, Mars. Prog. Earth Planet. Sci. 4. https://doi.org/10.1186/s40645-017-0141-x

Hepburn, A.J., Ng, F.S.L., Livingstone, S.J., Holt, T.O., Hubbard, B., 2019. Polyphase mid-latitude glaciation on Mars: chronology of the formation of superposed glacier-like forms from crater-count dating. J. Geophys. Res. Planets 2019JE006102. https://doi.org/10.1029/2019JE006102

Herkenhoff, K., 2001. Geologic map of the MTM-85000 Quadrangle, Planum Australe region of Mars, Geologic Investigations Series. The US Geological Survey.

Herkenhoff, K.E., Plaut, J.J., 2000. Surface Ages and Resurfacing Rates of the Polar Layered Deposits on Mars. Icarus 144, 243–253. https://doi.org/10.1006/icar.1999.6287

Herny, C., Conway, S.J., Raack, J., Carpy, S., Patel, M.R., Colle-Banse, T., 2019. Unstable liquid water as a geomorphological agent in martian gullies: experimental investigation of the effect of boiling intensity on downslope sediment transport. Geol. Soc. Lond. Spec. Publ., Martian Gullies and their Earth Analogues 467. https://doi.org/10.1144/SP467.10

Herrero-Gil, A., Egea-González, I., Ruiz, J., Romeo, I., 2019. Structural modeling of lobate scarps in the NW margin of Argyre impact basin, Mars. Icarus 319, 367–380. https://doi.org/10.1016/j.icarus.2018.09.027

Herschel, W., 1784. On the Remarkable Appearances at the Polar Regions of the Planet Mars, the Inclination of Its Axis, the Position of Its Poles, and Its Spheroidical Figure; With a Few Hints Relating to Its Real Diameter and Atmosphere. By William Herschel, Esq. F. R. S. Philos. Trans. R. Soc. Lond. 74, 233–273.

Hess, S.L., Ryan, J.A., Tillman, J.E., Henry, R.M., Leovy, C.B., 1980. The annual cycle of pressure on Mars measured by Viking Landers 1 and 2. Geophys. Res. Lett. 7, 197–200. https://doi.org/10.1029/GL007i003p00197

Hewitt, K., 2009. Rock avalanches that travel onto glaciers and related developments, Karakoram Himalaya, Inner Asia. Geomorphology 103, 66–79. https://doi.org/10.1016/j.geomorph.2007.10.017

Heyer, T., Kreslavsky, M., Hiesinger, H., Reiss, D., Bernhardt, H., Jaumann, R., 2019. Seasonal formation rates of martian slope streaks. Icarus 323, 76–86. https://doi.org/10.1016/j.icarus.2019.01.010

Hiesinger, H., Marchi, S., Schmedemann, N., Schenk, P., Pasckert, J.H., Neesemann, A., O'Brien, D.P., Kneissl, T., Ermakov, A.I., Fu, R.R., Bland, M.T., Nathues, A., Platz, T., Williams, D.A., Jaumann, R., Castillo-Rogez, J.C., Ruesch, O., Schmidt, B., Park, R.S., Preusker, F., Buczkowski, D.L., Russell, C.T., Raymond, C.A., 2016. Cratering on Ceres: Implications for its crust and evolution. Science 353, aaf4759. https://doi.org/10.1126/science.aaf4759

Hirata, N., Miyamoto, H., Showman, A.P., 2014. Particle deposition on the saturnian satellites from ephemeral cryovolcanism on Enceladus. Geophys. Res. Lett. 41, 4135–4141. https://doi.org/10.1002/2014GL060470

Hobbs, S.W., Paull, D.J., Clarke, J.D.A., 2017. Testing the water hypothesis: Quantitative morphological analysis of terrestrial and martian mid-latitude gullies. Geomorphology 295, 705–721. https://doi.org/10.1016/j.geomorph.2017.08.021

Hoffman, N., 2002. Active Polar Gullies on Mars and the Role of Carbon Dioxide. Astrobiology 2, 313–323. https://doi.org/10.1089/153110702762027899

Holt, J.W., Safaeinili, A., Plaut, J.J., Head, J.W., Phillips, R.J., Seu, R., Kempf, S.D., Choudhary, P., Young, D.A., Putzig, N.E., Biccari, D., Gim, Y., 2008. Radar Sounding Evidence for Buried

Glaciers in the Southern Mid-Latitudes of Mars. Science 322, 1235–1238. https://doi.org/10.1126/science.1164246

Horvath, A., Kereszturi, A., Berczi, S., Sik, A., Pocs, T., Ganti, T., Szathmary, E., 2009. Analysis of Dark Albedo Features on a Southern Polar Dune Field of Mars. Astrobiology 9, 90–103. https://doi.org/10.1089/ast.2007.0212

Hörz, F., Cintala, M.J., Rochelle, W.C., Kirk, B., 1999. Collisionally Processed Rocks on Mars. Science 285, 2105–2107. https://doi.org/10.1126/science.285.5436.2105

Hovius, N., Lea-Cox, A., Turowski, J.M., 2008. Recent volcano-ice interaction and outburst flooding in a Mars polar cap re-entrant. Icarus 197, 24–38.

Howard, A.D., Moore, J.M., 2011. Late Hesperian to early Amazonian midlatitude Martian valleys: Evidence from Newton and Gorgonum basins. J Geophys Res 116, E05003. https://doi.org/10.1029/2010JE003782

Howard, A.D., Moore, J.M., Umurhan, O.M., White, O.L., Anderson, R.S., McKinnon, W.B., Spencer, J.R., Schenk, P.M., Beyer, R.A., Stern, S.A., Ennico, K., Olkin, C.B., Weaver, H.A., Young, L.A., 2017a. Present and past glaciation on Pluto. Spec. Issue Pluto Syst. 287, 287–300. https://doi.org/10.1016/j.icarus.2016.07.006

Howard, A.D., Moore, J.M., White, O.L., Umurhan, O.M., Schenk, P.M., Grundy, W.M., Schmitt, B., Philippe, S., McKinnon, W.B., Spencer, J.R., Beyer, R.A., Stern, S.A., Ennico, K., Olkin, C.B., Weaver, H.A., Young, L.A., 2017b. Pluto: Pits and mantles on uplands north and east of Sputnik Planitia. Icarus 293, 218–230. https://doi.org/10.1016/j.icarus.2017.02.027

Hubbard, G.S., Naderi, F.M., Garvin, J.B., 2002. Following the water, the new program for Mars exploration. Acta Astronaut. 51, 337–350. https://doi.org/10.1016/S0094-5765(02)00067-X

Huber, C., Ojha, L., Lark, L., Head, J.W., 2020. Physical models and predictions for recurring slope lineae formed by wet and dry processes. Icarus 335, 113385. https://doi.org/10.1016/j.icarus.2019.07.019

Hungr, O., Leroueil, S., Picarelli, L., 2014. The Varnes classification of landslide types, an update. Landslides 11, 167–194. https://doi.org/10.1007/s10346-013-0436-y

Hurwitz, D.M., Head, J.W., Hiesinger, H., 2013. Lunar sinuous rilles: Distribution, characteristics, and implications for their origin. Planet. Space Sci. 79–80, 1–38. https://doi.org/10.1016/j.pss.2012.10.019

Hynek, B.M., Beach, M., Hoke, M.R.T., 2010. Updated global map of Martian valley networks and implications for climate and hydrologic processes. J Geophys Res 115, doi:10.1029/2009JE003548. https://doi.org/10.1029/2009je003548

Hynek, B.M., Phillips, R.J., 2003. New data reveal mature, integrated drainage systems on Mars indicative of past precipitation. Geology 31, 757. https://doi.org/10.1130/G19607.1

Ielpi, A., Lapôtre, M.G.A., 2020. A tenfold slowdown in river meander migration driven by plant life. Nat. Geosci. 13, 82–86. https://doi.org/10.1038/s41561-019-0491-7

Ivanov, M.A., Hiesinger, H., Erkeling, G., Reiss, D., 2014. Mud volcanism and morphology of impact craters in Utopia Planitia on Mars: Evidence for the ancient ocean. Icarus 228, 121–140. https://doi.org/10.1016/j.icarus.2013.09.018

Iverson, R.M., 2014. Debris flows: behaviour and hazard assessment. Geol. Today 30, 15–20. https://doi.org/10.1111/gto.12037

Iverson, R.M., 1997. The physics of debris flows. Rev Geophys 35, 245–296.

Jakosky, B.M., 1983. The role of seasonal reservoirs in the Mars water cycle. Icarus 55, 1–18. https://doi.org/10.1016/0019-1035(83)90046-5

Jakosky, B.M., Carr, M.H., 1985. Possible precipitation of ice at low latitudes of Mars during periods of high obliquity. Nature 315, 559–561. https://doi.org/10.1038/315559a0

Jakosky, B.M., Henderson, B.G., Mellon, M.T., 1995. Chaotic obliquity and the nature of the Martian climate. J. Geophys. Res. 100, 1579. https://doi.org/10.1029/94JE02801

Jakosky, B.M., Phillips, R.J., 2001. Mars' volatile and climate history. Nature 412, 237–244.

Jawin, E.R., Head, J.W., Marchant, D.R., 2018. Transient post-glacial processes on Mars: Geomorphologic evidence for a paraglacial period. Icarus 309, 187–206. https://doi.org/10.1016/j.icarus.2018.01.026

Jia, P., Andreotti, B., Claudin, P., 2017. Giant ripples on comet 67P/Churyumov–Gerasimenko sculpted by sunset thermal wind. Proc. Natl. Acad. Sci. 114, 2509–2514. https://doi.org/10.1073/pnas.1612176114

Johnson, B.C., Campbell, C.S., 2017. Drop Height and Volume Control the Mobility of Long-Runout Landslides on the Earth and Mars: The Mobility of Long-Runout Landslides on the Earth and Mars. Geophys. Res. Lett. https://doi.org/10.1002/2017GL076113

Johnson, B.C., Sori, M.M., 2020. Landslide Morphology and Mobility on Ceres Controlled by Topography. J. Geophys. Res. Planets 125. https://doi.org/10.1029/2020JE006640

Johnsson, A., Conway, S.J., Reiss, D., Hiesinger, H., Hauber, E., 2018. Slow periglacial mass wasting (solifluction) on Mars, in: Soare, R.J., Conway, S.J., Clifford, S.M. (Eds.), Dynamic Mars. Elsevier.

Johnsson, A., Reiss, D., Hauber, E., Hiesinger, H., Zanetti, M., 2014. Evidence for very recent melt-water and debris flow activity in gullies in a young mid-latitude crater on Mars. Icarus 235, 37–54. https://doi.org/10.1016/j.icarus.2014.03.005

Johnsson, A., Reiss, D., Hauber, E., Zanetti, M., Hiesinger, H., Johansson, L., Olvmo, M., 2012. Periglacial mass-wasting landforms on Mars suggestive of transient liquid water in the recent past: Insights from solifluction lobes on Svalbard. Icarus 218, 489–505. https://doi.org/10.1016/j.icarus.2011.12.021

Jones, A.P., McEwen, A.S., Tornabene, L.L., Baker, V.R., Melosh, H.J., Berman, D.C., 2011. A geomorphic analysis of Hale crater, Mars: The effects of impact into ice-rich crust. Icarus 211, 259–272. https://doi.org/10.1016/j.icarus.2010.10.014

Jones, A.P., Pickering, K.T., 2003. Evidence for aqueous fluid–sediment transport and erosional processes on Venus. J. Geol. Soc. 160, 319–327. https://doi.org/10.1144/0016-764902-111

Jones, B.M., Grosse, G., Hinkel, K.M., Arp, C.D., Walker, S., Beck, R.A., Galloway, J.P., 2012. Assessment of pingo distribution and morphometry using an IfSAR derived digital surface model, western Arctic Coastal Plain, Northern Alaska. Geomorphology 138, 1–14. https://doi.org/10.1016/j.geomorph.2011.08.007

Jones, E.G., Lineweaver, C.H., 2012. Using the phase diagram of liquid water to search for life. Aust. J. Earth Sci. 59, 253–262. https://doi.org/10.1080/08120099.2011.591430

Jónsson, Ó.B., Pétursson, H.G., Sigvaldason, J., 1957. Skriðuföll og snjóflóð. Skjaldborg.

Jouannic, G., Gargani, J., Conway, S.J., Costard, F., Balme, M.R., Patel, M.R., Massé, M., Marmo, C., Jomelli, V., Ori, G.G., 2015. Laboratory simulation of debris flows over sand dunes: Insights into gully-formation (Mars). Geomorphology 231, 101–115. https://doi.org/10.1016/j.geomorph.2014.12.007

Jouannic, G., Gargani, J., Conway, S.J., Costard, F., Massé, M., Bourgeois, O., Carter, J., Schmidt, F., Marmo, C., Ori, G.G., Nachon, M., Pasquon, K., 2019. Morphological characterization of landforms produced by springtime seasonal activity on Russell dune (Mars). Geol. Soc. Lond. Spec. Publ., Martian Gullies and their Earth Analogues 467. https://doi.org/10.1144/SP467.16

Jouglet, D., Poulet, F., Milliken, R.E., Mustard, J.F., Bibring, J.-P., Langevin, Y., Gondet, B., Gomez, C., 2007. Hydration state of the Martian surface as seen by Mars Express OMEGA: 1. Analysis of the 3 μ m hydration feature: HYDRATION STATE OF THE MARTIAN SURFACE, 1. J. Geophys. Res. Planets 112. https://doi.org/10.1029/2006JE002846

Kääb, A., Jacquemart, M., Gilbert, A., Leinss, S., Girod, L., Huggel, C., Falaschi, D., Ugalde, F., Petrakov, D., Chernomorets, S., Dokukin, M., Paul, F., Gascoin, S., Berthier, E., Kargel, J.S., 2021. Sudden large-volume detachments of low-angle mountain glaciers – more frequent than thought? The Cryosphere 15, 1751–1785. https://doi.org/10.5194/tc-15-1751-2021

Karatekin, Ö., Van Hoolst, T., Dehant, V., 2006. Martian global-scale CO_2 exchange from time-variable gravity measurements. J. Geophys. Res. 111, E06003. https://doi.org/10.1029/2005JE002591

Kargel, J.S., 1995. Cryovolcanism on the Icy Satellites, in: Chahine, M.T., A'Hearn, M.F., Rahe, J., Solomon, P., Nickle, N.L. (Eds.), Comparative Planetology with an Earth Perspective. Springer Netherlands, Dordrecht, pp. 101–113. https://doi.org/10.1007/978-94-017-1092-3_12

Kargel, J.S., Baker, V.R., Begét, J.E., Lockwood, J.F., Péwé, T.L., Shaw, J.S., Strom, R.G., 1995. Evidence of ancient continental glaciation in the Martian northern plains. J. Geophys. Res. 100, 5351. https://doi.org/10.1029/94JE02447

Kargel, J.S., Kirk, R.L., Fegley, B., Treiman, A.H., 1994. Carbonate-Sulfate Volcanism on Venus? Icarus 112, 219–252. https://doi.org/10.1006/icar.1994.1179

Karlsson, N.B., Schmidt, L.S., Hvidberg, C.S., 2015. Volume of Martian midlatitude glaciers from radar observations and ice flow modeling. Geophys. Res. Lett. 42, 2627–2633. https://doi.org/10.1002/2015GL063219

Kattenhorn, S.A., Prockter, L.M., 2014. Evidence for subduction in the ice shell of Europa. Nat. Geosci. 7, 762–767. https://doi.org/10.1038/ngeo2245

Keller, J.M., Boynton, W.V., Karunatillake, S., Baker, V.R., Dohm, J.M., Evans, L.G., Finch, M.J., Hahn, B.C., Hamara, D.K., Janes, D.M., Kerry, K.E., Newsom, H.E., Reedy, R.C., Sprague, A.L., Squyres, S.W., Starr, R.D., Taylor, G.J., Williams, R.M.S., 2007. Equatorial and midlatitude distribution of chlorine measured by Mars Odyssey GRS. J. Geophys. Res. 112, E03S08. https://doi.org/10.1029/2006JE002679

Kenkmann, T., Poelchau, M.H., Wulf, G., 2014. Structural geology of impact craters. J. Struct. Geol. 62, 156–182. https://doi.org/10.1016/j.jsg.2014.01.015

Kerber, L., Head, J.W., Blewett, D.T., Solomon, S.C., Wilson, L., Murchie, S.L., Robinson, M.S., Denevi, B.W., Domingue, D.L., 2011. The global distribution of pyroclastic deposits on Mercury: The view from MESSENGER flybys 1–3. Planet. Space Sci. 59, 1895–1909. https://doi.org/10.1016/j.pss.2011.03.020

Kerber, L., Head, J.W., Solomon, S.C., Murchie, S.L., Blewett, D.T., Wilson, L., 2009. Explosive volcanic eruptions on Mercury: Eruption conditions, magma volatile content, and implications for interior volatile abundances. Earth Planet. Sci. Lett. 285, 263–271. https://doi.org/10.1016/j.epsl.2009.04.037

Kereszturi, A., Appéré, T., 2014. Searching for springtime zonal liquid interfacial water on Mars. Icarus 238, 66–76. https://doi.org/10.1016/j.icarus.2014.05.001

Kereszturi, A., Bradak, B., Chatzitheodoridis, E., Ujvari, G., 2016. Indicators and Methods to Understand Past Environments from ExoMars Rover Drills. Orig. Life Evol. Biospheres 46, 435–454. https://doi.org/10.1007/s11084-016-9492-3

Kereszturi, A., Möhlmann, D., Berczi, S., Ganti, T., Horvath, A., Kuti, A., Sik, A., Szathmary, E., 2010. Indications of brine related local seepage phenomena on the northern hemisphere of Mars. Icarus 207, 149–164.

Kereszturi, A., Möhlmann, D., Berczi, S., Ganti, T., Kuti, A., Sik, A., Horvath, A., 2009. Recent rheologic processes on dark polar dunes of Mars: Driven by interfacial water? Icarus 201, 492–503.

Kereszturi, A., Möhlmann, D., Berczi, Sz., Horvath, A., Sik, A., Szathmary, E., 2011a. Possible role of brines in the darkening and flow-like features on the Martian polar dunes based on HiRISE images. Planet. Space Sci. 59, 1413–1427. https://doi.org/10.1016/j.pss.2011.05.012

Kereszturi, A., Petrik, A., 2020. Age determination for valley networks on Mars using tectonic-fluvial interaction. Planet. Space Sci. 180, 104754. https://doi.org/10.1016/j.pss.2019.104754

Kereszturi, A., Rivera-Valentin, E.G., 2016. Possible water lubricated grain movement in the circumpolar region of Mars. Planet. Space Sci. 125, 130–146. https://doi.org/10.1016/j.pss.2016.03.015

Kereszturi, A., Rivera-Valentin, E.G., 2012. Locations of thin liquid water layers on present-day Mars. Icarus 221, 289–295. https://doi.org/10.1016/j.icarus.2012.08.004

Kereszturi, A., Vincendon, M., Schmidt, F., 2011b. Water ice in the dark dune spots of Richardson crater on Mars. Planet. Space Sci. 59, 26–42. https://doi.org/10.1016/j.pss.2010.10.015

Kessler, M.A., Werner, B.T., 2003. Self-Organization of Sorted Patterned Ground. Science 299, 380–383. https://doi.org/10.1126/science.1077309

Khuller, A., Christensen, P., 2021. Evidence of Exposed Dusty Water Ice within Martian Gullies. J. Geophys. Res. Planets 126. https://doi.org/10.1029/2020JE006539

Kieffer, H.H., 1990. H2O grain size and the amount of dust in Mars' residual north polar CAP. J. Geophys. Res. 95, 1481–1493.

Kieffer, H.H., Christensen, P.R., Titus, T.N., 2006. CO2 jets formed by sublimation beneath translucent slab ice in Mars' seasonal south polar ice cap. Nature 442, 793–796. https://doi.org/10.1038/nature04945

Kite, E.S., Mayer, D.P., Wilson, S.A., Davis, J.M., Lucas, A.S., Stucky de Quay, G., 2019. Persistence of intense, climate-driven runoff late in Mars history. Sci. Adv. 5, eaav7710. https://doi.org/10.1126/sciadv.aav7710

Kite, E.S., Michaels, T.I., Rafkin, S., Manga, M., Dietrich, W.E., 2011. Localized precipitation and runoff on Mars. J Geophys Res 116, E07002. https://doi.org/10.1029/2010JE003783

Kite, E.S., Sneed, J., Mayer, D.P., Wilson, S.A., 2017. Persistent or repeated surface habitability on Mars during the late Hesperian - Amazonian: Mars Alluvial Fan Aggradation Took >20 Ma. Geophys. Res. Lett. 44, 3991–3999. https://doi.org/10.1002/2017GL072660

Kminek, G., Rummel, J.D., Cockell, C.S., Atlas, R., Barlow, N., Beaty, D., Boynton, W., Carr, M., Clifford, S., Conley, C.A., Davila, A.F., Debus, A., Doran, P., Hecht, M., Heldmann, J., Helbert, J., Hipkin, V., Horneck, G., Kieft, T.L., Klingelhoefer, G., Meyer, M., Newsom, H., Ori, G.G., Parnell, J., Prieur, D., Raulin, F., Schulze-Makuch, D., Spry, J.A., Stabekis, P.E., Stackebrandt, E., Vago, J., Viso, M., Voytek, M., Wells, L., Westall, F., 2010. Report of the COSPAR mars special regions colloquium. Life Sci. Space 46, 811–829. https://doi.org/10.1016/j.asr.2010.04.039

Kneisel, C., Rothenbühler, C., Keller, F., Haeberli, W., 2007. Hazard assessment of potential periglacial debris flows based on GIS-based spatial modelling and geophysical field surveys: A case study in the Swiss Alps. Permafr. Periglac. Process. 18, 259–268.

Kneissl, T., Reiss, D., van Gasselt, S., Neukum, G., 2010. Distribution and orientation of northern-hemisphere gullies on Mars from the evaluation of HRSC and MOC-NA data. Earth Planet. Sci. Lett. 294, 357–367. https://doi.org/j.epsl.2009.05.018

Knight, J., 2008. The environmental significance of ventifacts: A critical review. Earth-Sci. Rev. 86, 89–105. https://doi.org/10.1016/j.earscirev.2007.08.003

Kok, J.F., Parteli, E.J.R., Michaels, T.I., Karam, D.B., 2012. The physics of wind-blown sand and dust. Rep. Prog. Phys. 75, 106901. https://doi.org/10.1088/0034-4885/75/10/106901

Kokelj, S.V., Jorgenson, M.T., 2013. Advances in Thermokarst Research: Recent Advances in Research Investigating Thermokarst Processes. Permafr. Periglac. Process. 24, 108–119. https://doi.org/10.1002/ppp.1779

Kolb, K.J., Pelletier, J.D., McEwen, A.S., 2010. Modeling the formation of bright slope deposits associated with gullies in Hale Crater, Mars: Implications for recent liquid water. Icarus 205, 113–137.

Komar, P.D., 1979. Comparisons of the hydraulics of water flows in Martian outflow channels with flows of similar scale on earth. Icarus 37, 156–181. https://doi.org/10.1016/0019-1035(79)90123-4

Komatsu, G., Baker, V.R., 1994. Meander properties of Venusian channels. Geology 22, 67. https://doi.org/10.1130/0091-7613(1994)022<0067:MPOVC>2.3.CO;2

Komatsu, G., Okubo, C.H., Wray, J.J., Ojha, L., Cardinale, M., Murana, A., Orosei, R., Chan, M.A., Ormö, J., Gallagher, R., 2016. Small edifice features in Chryse Planitia, Mars: Assessment of a mud volcano hypothesis. Icarus 268, 56–75. https://doi.org/10.1016/j.icarus.2015.12.032

Kossacki, K.J., Markiewicz, W.J., 2010. Interfacial liquid water on Mars and its potential role in formation of hill and dune gullies. Icarus 210, 83–91.

Kossacki, K.J., Markiewicz, W.J., 2004. Seasonal melting of surface water ice condensing in martian gullies. Icarus 171, 272–283.

Kounaves, S.P., Hecht, M.H., Kapit, J., Quinn, R.C., Catling, D.C., Clark, B.C., Ming, D.W., Gospodinova, K., Hredzak, P., McElhoney, K., Shusterman, J., 2010. Soluble sulfate in the martian soil at the Phoenix landing site: SULFATE AT THE PHOENIX LANDING SITE. Geophys. Res. Lett. 37, n/a-n/a. https://doi.org/10.1029/2010GL042613

Kreslavsky, M.A., Head, J.W., 2009. Slope streaks on Mars: A new "wet" mechanism. Icarus 201, 517–527.

Kreslavsky, M.A., Head, J.W., 2003. North-south topographic slope asymmetry on Mars: Evidence for insolation-related erosion at high obliquity. Geophys Res Lett 30, doi:10.1029/2003GL017795.

Kreslavsky, M.A., Head, J.W., 2002. Mars: Nature and evolution of young latitude-dependent water-ice-rich mantle. Geophys. Res. Lett. 29, 14–1. https://doi.org/10.1029/2002GL015392

Kreslavsky, M.A., Head, J.W., 2000. Kilometer-scale roughness of Mars: Results from MOLA data analysis. J. Geophys. Res. 105, 26695–26712. https://doi.org/10.1029/2000JE001259

Kreslavsky, M.A., Head, J.W., Neumann, G.A., Zuber, M.T., Smith, D.E., 2014. Kilometer-scale topographic roughness of Mercury: Correlation with geologic features and units. Geophys. Res. Lett. 41, 8245–8251. https://doi.org/10.1002/2014GL062162

Kress, A.M., Head, J.W., 2015. Late Noachian and early Hesperian ridge systems in the south circumpolar Dorsa Argentea Formation, Mars: Evidence for two stages of melting of an extensive late Noachian ice sheet. Planet. Space Sci. 109–110, 1–20. https://doi.org/10.1016/j.pss.2014.11.025

Kritikos, T., Davies, T., 2015. Assessment of rainfall-generated shallow landslide/debris-flow susceptibility and runout using a GIS-based approach: application to western Southern Alps of New Zealand. Landslides 12, 1051–1075. https://doi.org/10.1007/s10346-014-0533-6

Lacelle, D., Bjornson, J., Lauriol, B., 2010. Climatic and geomorphic factors affecting contemporary (1950-2004) activity of retrogressive thaw slumps on the Aklavik Plateau, Richardson Mountains, NWT, Canada: Climatic and Geomorphic Factors affecting Thaw Slump Activity. Permafr. Periglac. Process. 21, 1–15. https://doi.org/10.1002/ppp.666

Lacelle, D., Vasil'chuk, Y.K., 2013. Recent Progress (2007-2012) in Permafrost Isotope Geochemistry: Recent Progress in Permafrost Isotope Geochemistry. Permafr. Periglac. Process. 24, 138–145. https://doi.org/10.1002/ppp.1768

Lague, D., Davy, P., 2003. Constraints on the long-term colluvial erosion law by analyzing slope-area relationships at various uplift rates in the Siwaliks Hills (Nepal). J. Geophys. Res. B Solid Earth 108, doi:10.1029/2002JB001893.

Laity, J.E., Bridges, N.T., 2009. Ventifacts on Earth and Mars: Analytical, field, and laboratory studies supporting sand abrasion and windward feature development. Geomorphology 105, 202–217. https://doi.org/10.1016/j.geomorph.2008.09.014

Landis, M.E., Byrne, S., Daubar, I.J., Herkenhoff, K.E., Dundas, C.M., 2016. A revised surface age for the North Polar Layered Deposits of Mars. Geophys. Res. Lett. 43, 3060–3068. https://doi.org/10.1002/2016GL068434

Langston, G., Bentley, L.R., Hayashi, M., McClymont, A., Pidlisecky, A., 2011. Internal structure and hydrological functions of an alpine proglacial moraine. Hydrol. Process. n/a-n/a. https://doi.org/10.1002/hyp.8144

Lantz, T.C., Kokelj, S.V., 2008. Increasing rates of retrogressive thaw slump activity in the Mackenzie Delta region, N.W.T., Canada. Geophys. Res. Lett. 35, L06502. https://doi.org/10.1029/2007GL032433

Lanza, N.L., Meyer, G.A., Okubo, C.H., Newsom, H.E., Wiens, R.C., 2010. Evidence for debris flow gully formation initiated by shallow subsurface water on Mars. Icarus 205, 103–112.

Lapôtre, M.G.A., O'Rourke, J.G., Schaefer, L.K., Siebach, K.L., Spalding, C., Tikoo, S.M., Wordsworth, R.D., 2020. Probing space to understand Earth. Nat. Rev. Earth Environ. 1, 170–181. https://doi.org/10.1038/s43017-020-0029-y

Laskar, J., Correia, A.C.M., Gastineau, M., Joutel, F., Levrard, B., Robutel, P., 2004. Long term evolution and chaotic diffusion of the insolation quantities of Mars. Icarus 170, 343–364. https://doi.org/10.1016/j.icarus.2004.04.005

Laskar, J., Levrard, B., Mustard, J.F., 2002. Orbital forcing of the martian polar layered deposits. Nature 419, 375–377.

Lasue, J., Clifford, S.M., Conway, S.J., Mangold, N., Butcher, F.E.G., 2019. The Hydrology of Mars Including a Potential Cryosphere, in: Volatiles in the Martian Crust. Elsevier, pp. 185–246. https://doi.org/10.1016/B978-0-12-804191-8.00007-6

Lauretta, D.S., Hergenrother, C.W., Chesley, S.R., Leonard, J.M., Pelgrift, J.Y., Adam, C.D., Al Asad, M., Antreasian, P.G., Ballouz, R.-L., Becker, K.J., Bennett, C.A., Bos, B.J., Bottke, W.F., Brozović, M., Campins, H., Connolly, H.C., Daly, M.G., Davis, A.B., de León, J., DellaGiustina, D.N., Drouet d'Aubigny, C.Y., Dworkin, J.P., Emery, J.P., Farnocchia, D., Glavin, D.P., Golish, D.R., Hartzell, C.M., Jacobson, R.A., Jawin, E.R., Jenniskens, P., Kidd, J.N., Lessac-Chenen, E.J., Li, J.-Y., Libourel, G., Licandro, J., Liounis, A.J., Maleszewski, C.K., Manzoni, C., May, B., McCarthy, L.K., McMahon, J.W., Michel, P., Molaro, J.L., Moreau, M.C., Nelson, D.S., Owen, W.M., Rizk, B., Roper, H.L., Rozitis, B., Sahr, E.M., Scheeres, D.J., Seabrook, J.A., Selznick, S.H., Takahashi, Y., Thuillet, F., Tricarico, P., Vokrouhlický, D., Wolner, C.W.V., 2019. Episodes of particle ejection from the surface of the active asteroid (101955) Bennu. Science 366, eaay3544. https://doi.org/10.1126/science.aay3544

Lauro, S.E., Pettinelli, E., Caprarelli, G., Guallini, L., Rossi, A.P., Mattei, E., Cosciotti, B., Cicchetti, A., Soldovieri, F., Cartacci, M., Di Paolo, F., Noschese, R., Orosei, R., 2020. Multiple subglacial water bodies below the south pole of Mars unveiled by new MARSIS data. Nat. Astron. https://doi.org/10.1038/s41550-020-1200-6

Lawrence, D.J., Feldman, W.C., Goldsten, J.O., Maurice, S., Peplowski, P.N., Anderson, B.J., Bazell, D., McNutt, R.L., Nittler, L.R., Prettyman, T.H., Rodgers, D.J., Solomon, S.C., Weider, S.Z., 2013. Evidence for Water Ice Near Mercury's North Pole from MESSENGER Neutron Spectrometer Measurements. Science 339, 292–296. https://doi.org/10.1126/science.1229953

Leask, E.K., Ehlmann, B.L., Dundar, M.M., Murchie, S.L., Seelos, F.P., 2018. Challenges in the Search for Perchlorate and Other Hydrated Minerals With 2.1-μm Absorptions on Mars. Geophys. Res. Lett. 45. https://doi.org/10.1029/2018GL080077

Leask, H.J., Wilson, L., Mitchell, K.L., 2007. Formation of Mangala Valles outflow channel, Mars: Morphological development and water discharge and duration estimates. J. Geophys. Res. Planets 112, doi: 10.1029/2006JE002851.

Lefort, A., Russell, P.S., Thomas, N., 2010. Scalloped terrains in the Peneus and Amphitrites Paterae region of Mars as observed by HiRISE. Icarus 205, 259–268. https://doi.org/10.1016/j.icarus.2009.06.005

Legros, F., 2002. The mobility of long-runout landslides. Eng. Geol. 63, 301–331.

Leung, C.W.S., McEwen, A.S., Kahre, M.A., Stillman, D.E., 2020. Atmospheric Water Budgets for Recurring Slope Lineae Activity. J. Geophys. Res. in review.

Leverington, D.W., 2021. Chapter 4 - Dry megafloods on Mars: formation of the outflow channels by voluminous effusions of low viscosity lava, in: Soare, R.J., Conway, S.J., Williams, J.-P., Oehler, D.Z. (Eds.), Mars Geological Enigmas. Elsevier, pp. 61–93. https://doi.org/10.1016/B978-0-12-820245-6.00004-5

Leverington, D.W., 2011. A volcanic origin for the outflow channels of Mars: Key evidence and major implications. Geomorphology 132, 51–75. https://doi.org/10.1016/j.geomorph.2011.05.022

Leverington, D.W., 2009. Reconciling channel formation processes with the nature of elevated outflow systems at Ophir and Aurorae Plana, Mars. J. Geophys. Res. Planets 114, 10005.

Levin, J.N., Dickson, J.L., Lamb, M.P., 2022. Evaluating the Role of Volatiles in Bedrock Chute Formation on the Moon and Mars. Icarus 373, 114774. https://doi.org/10.1016/j.icarus.2021.114774

Levrard, B., Forget, F., Montmessin, F., Laskar, J., 2007. Recent formation and evolution of northern Martian polar layered deposits as inferred from a Global Climate Model. J. Geophys. Res. Planets 112. https://doi.org/10.1029/2006JE002772

Levy, J.S., Fassett, C.I., Head, J.W., Schwartz, C., Watters, J.L., 2014. Sequestered glacial ice contribution to the global Martian water budget: Geometric constraints on the volume of remnant, midlatitude debris-covered glaciers. J. Geophys. Res. Planets 119, 2014JE004685. https://doi.org/10.1002/2014JE004685

Levy, J.S., Head, J., Marchant, D., 2009a. Thermal contraction crack polygons on Mars: Classification, distribution, and climate implications from HiRISE observations. J. Geophys. Res. Planets 114, 01007.

Levy, J.S., Head, J.W., Dickson, J.L., Fassett, C.I., Morgan, G.A., Schon, S.C., 2010a. Identification of gully debris flow deposits in Protonilus Mensae, Mars: Characterization of a water-bearing, energetic gully-forming process. Earth Planet. Sci. Lett., Mars Express after 6 Years in Orbit: Mars Geology from Three-Dimensional Mapping by the High Resolution Stereo Camera (HRSC) Experiment 294, 368–377. https://doi.org/10.1016/j.epsl.2009.08.002

Levy, J.S., Head, J.W., Marchant, D.R., 2009b. Concentric crater fill in Utopia Planitia: History and interaction between glacial “brain terrain” and periglacial mantle processes. Icarus 202, 462–476. https://doi.org/10.1016/j.icarus.2009.02.018

Levy, J.S., Head, J.W., Marchant, D.R., Dickson, J.L., Morgan, G.A., 2009c. Geologically recent gully-polygon relationships on Mars: Insights from the Antarctic dry valleys on the roles of permafrost, microclimates, and water sources for surface flow. Icarus 201, 113–126. https://doi.org/10.1016/j.icarus.2008.12.043

Levy, J.S., Marchant, D.R., Head, J.W., 2010b. Thermal contraction crack polygons on Mars: A synthesis from HiRISE, Phoenix, and terrestrial analog studies. Sol. Wind Interact. Mars 206, 229–252. https://doi.org/10.1016/j.icarus.2009.09.005

L’Haridon, J., Mangold, N., Meslin, P.-Y., Johnson, J.R., Rapin, W., Forni, O., Cousin, A., Payré, V., Dehouck, E., Nachon, M., Le Deit, L., Gasnault, O., Maurice, S., Wiens, R.C., 2018. Chemical variability in mineralized veins observed by ChemCam on the lower slopes of Mount Sharp in Gale crater, Mars. Icarus 311, 69–86. https://doi.org/10.1016/j.icarus.2018.01.028

Lilleøren, K.S., Etzelmüller, B., Gärtner-Roer, I., Kääb, A., Westermann, S., Guðmundsson, Á., 2013. The Distribution, Thermal Characteristics and Dynamics of Permafrost in Tröllaskagi, Northern Iceland, as Inferred from the Distribution of Rock Glaciers and Ice-Cored Moraines: Rock Glaciers and Ice-Cored Moraines, Northern Iceland. Permafr. Periglac. Process. 24, 322–335. https://doi.org/10.1002/ppp.1792

Lillis, R.J., Frey, H.V., Manga, M., 2008. Rapid decrease in Martian crustal magnetization in the Noachian era: Implications for the dynamo and climate of early Mars. Geophys Res Lett 35, L14203. https://doi.org/10.1029/2008GL034338

Loizeau, D., Mangold, N., Poulet, F., Bibring, J.-P., Gendrin, A., Ansan, V., Gomez, C., Gondet, B., Langevin, Y., Masson, P., Neukum, G., 2007. Phyllosilicates in the Mawrth Vallis region of Mars. J Geophys Res 112, E08S08. https://doi.org/10.1029/2006JE002877

Lorenz, R., Zimbelman, J.R., 2014. Dune worlds: how windblown sand shapes planetary landscapes, Springer Praxis books. Geophysical sciences. Springer ; Published in association with Praxis Publishing, Berlin ; New York ; London : Chichester, UK.

Lowe, D.R., Bishop, J.L., Loizeau, D., Wray, J.J., Beyer, R.A., 2020. Deposition of >3.7 Ga clay-rich strata of the Mawrth Vallis Group, Mars, in lacustrine, alluvial, and aeolian environments. GSA Bull. 132, 17–30. https://doi.org/10.1130/B35185.1

Lucchetti, A., Pajola, M., Poggiali, G., Semenzato, A., Munaretto, G., Cremonese, G., Brucato, J.R., Massironi, M., 2021. Volatiles on Mercury: The case of hollows and the pyroclastic vent of Tyagaraja crater. Icarus 370, 114694. https://doi.org/10.1016/j.icarus.2021.114694

Lucchetti, A., Penasa, L., Pajola, M., Massironi, M., Brunetti, M.T., Cremonese, G., Oklay, N., Vincent, J., Mottola, S., Fornasier, S., Sierks, H., Naletto, G., Lamy, P.L., Rodrigo, R., Koschny, D., Davidsson, B., Barbieri, C., Barucci, M.A., Bertaux, J., Bertini, I., Bodewits, D., Cambianica, P.,

Da Deppo, V., Debei, S., De Cecco, M., Deller, J., Ferrari, S., Ferri, F., Franceschi, M., Fulle, M., Gutiérrez, P., Güttler, C., Ip, W., Keller, U., Lara, L., Lazzarin, M., Moreno, J.L., Marzari, F., Tubiana, C., 2019. The Rocky-Like Behavior of Cometary Landslides on 67P/Churyumov-Gerasimenko. Geophys. Res. Lett. 46, 14336–14346. https://doi.org/10.1029/2019GL085132

Lucchitta, B.K., 1987. Valles Marineris, Mars: Wet debris flows and ground ice. Icarus 72, 411–429. https://doi.org/10.1016/0019-1035(87)90183-7

Lucchitta, B.K., 1978. A large landslide on Mars. Geol. Soc. Am. Bull. 89, 1601. https://doi.org/10.1130/0016-7606(1978)89<1601:ALLOM>2.0.CO;2

Luo, W., Cang, X., Howard, A.D., 2017. New Martian valley network volume estimate consistent with ancient ocean and warm and wet climate. Nat. Commun. 8, 15766. https://doi.org/10.1038/ncomms15766

Luo, W., Howard, A.D., 2008. Computer simulation of the role of groundwater seepage in forming Martian valley networks. J. Geophys. Res. Planets 113, E05002. https://doi.org/10.1029/2007JE002981

Mackay, J.R., 2002. Pingo Growth and collapse, Tuktoyaktuk Peninsula Area, Western Arctic Coast, Canada: a long-term field study. Géographie Phys. Quat. 52, 271–323. https://doi.org/10.7202/004847ar

MacKay, J.R., 2002. Thermally induced movements in ice-wedge polygons, western arctic coast: a long-term study. Géographie Phys. Quat. 54, 41–68. https://doi.org/10.7202/004846ar

Mackay, J.R., 1987. Some mechanical aspects of pingo growth and failure, western Arctic coast, Canada. Can. J. Earth Sci. 24, 1108–1119. https://doi.org/10.1139/e87-108

MacKenzie, S.M., Barnes, J.W., Sotin, C., Soderblom, J.M., Le Mouélic, S., Rodriguez, S., Baines, K.H., Buratti, B.J., Clark, R.N., Nicholson, P.D., McCord, T.B., 2014. Evidence of Titan's climate history from evaporite distribution. Icarus 243, 191–207. https://doi.org/10.1016/j.icarus.2014.08.022

Madeleine, J.B., Forget, F., Head, J.W., Levrard, B., Montmessin, F., Millour, E., 2009. Amazonian northern mid-latitude glaciation on Mars: A proposed climate scenario. Icarus 203, 390–405. https://doi.org/10.1016/j.icarus.2009.04.037

Madeleine, J.-B., Forget, F., Millour, E., Montabone, L., Wolff, M.J., 2011. Revisiting the radiative impact of dust on Mars using the LMD Global Climate Model. J. Geophys. Res. 116, E11010. https://doi.org/10.1029/2011JE003855

Madeleine, J.-B., Head, J.W., Forget, F., Navarro, T., Millour, E., Spiga, A., Colaïtis, A., Määttänen, A., Montmessin, F., Dickson, J.L., 2014. Recent Ice Ages on Mars: The role of radiatively active clouds and cloud microphysics. Geophys. Res. Lett. https://doi.org/10.1002/2014GL059861

Magnarini, G., Mitchell, T.M., Grindrod, P.M., Schmitt, H.H., Petro, N.E., 2021. Scaling Relationship Between the Wavelength of Longitudinal Ridges and the Thickness of Long Runout Landslides on the Moon. J. Geophys. Res. Planets 126. https://doi.org/10.1029/2021JE006922

Magnin, F., Krautblatter, M., Deline, P., Ravanel, L., Malet, E., Bevington, A., 2015. Determination of warm, sensitive permafrost areas in near-vertical rockwalls and evaluation of distributed models by electrical resistivity tomography: ERT IN NEAR-VERTICAL ROCK FACES. J. Geophys. Res. Earth Surf. 120, 745–762. https://doi.org/10.1002/2014JF003351

Malin, M.C., Edgett, K.S., 2000. Evidence for recent groundwater seepage and surface runoff on Mars. Science 288, 2330–2335. https://doi.org/10.1126/science.288.5475.2330

Malin, M.C., Edgett, K.S., 1999. Oceans or seas in the Martian northern lowlands: High resolution imaging tests of proposed coastlines. Geophys. Res. Lett. 26, 3049–3052. https://doi.org/10.1029/1999GL002342

Malin, M.C., Edgett, K.S., Posiolova, L.V., McColley, S.M., Dobrea, E.Z.N., 2006. Present-day impact cratering rate and contemporary gully activity on Mars. Science 314, 1573–1577. https://doi.org/10.1126/science.1135156

Malliband, C.C., Conway, S.J., Rothery, D.A., Balme, M.R., 2019. Potential Identification of Downslope Mass Movements on Mercury Driven by Volatile-Loss, in: Lunar and Planetary Science Conference. p. #1804.

Maltagliati, L., Montmessin, F., Fedorova, A., Korablev, O., Forget, F., Bertaux, J.-L., 2011. Evidence of Water Vapor in Excess of Saturation in the Atmosphere of Mars. Science 333, 1868–1871. https://doi.org/10.1126/science.1207957

Mangold, N., 2012. Fluvial landforms on fresh impact ejecta on Mars. Planet. Space Sci. 62, 69–85. https://doi.org/10.1016/j.pss.2011.12.009

Mangold, N., 2011. Ice sublimation as a geomorphic process: A planetary perspective. Geomorphology 126, 1–17. https://doi.org/10.1016/j.geomorph.2010.11.009

Mangold, N., 2005. High latitude patterned grounds on Mars: Classification, distribution and climatic control. Mars Polar Sci. III 174, 336–359. https://doi.org/10.1016/j.icarus.2004.07.030

Mangold, N., 2003. Geomorphic analysis of lobate debris aprons on Mars at Mars Orbiter Camera scale: Evidence for ice sublimation initiated by fractures. J Geophys Res 108, 8021. https://doi.org/10.1029/2002JE001885

Mangold, Nicolas, Adeli, S., Conway, S.J., Ansan, V., Langlais, B., 2012. A chronology of early Mars climatic evolution from impact crater degradation. J. Geophys. Res. Planets 117, E04003. https://doi.org/10.1029/2011JE004005

Mangold, N., Kite, E.S., Kleinhans, M.G., Newsom, H., Ansan, V., Hauber, E., Kraal, E., Quantin, C., Tanaka, K., 2012. The origin and timing of fluvial activity at Eberswalde crater, Mars. Icarus 220, 530–551. https://doi.org/10.1016/j.icarus.2012.05.026

Manning, C., Mckay, C., Zahnle, K., 2006. Thick and thin models of the evolution of carbon dioxide on Mars. Icarus 180, 38–59. https://doi.org/10.1016/j.icarus.2005.08.014

Manning, C.V., Bierson, C., Putzig, N.E., McKay, C.P., 2019. The formation and stability of buried polar CO2 deposits on Mars. Icarus 317, 509–517. https://doi.org/10.1016/j.icarus.2018.07.021

Marchant, D.R., Lewis, A.R., Phillips, W.M., Moore, E.J., Souchez, R.A., Denton, G.H., Sugden, D.E., Potter Jr., N., Landis, G.P., 2002. Formation of patterned ground and sublimation till over Miocene glacier ice in Beacon Valley, southern Victoria Land, Antarctica. Geol. Soc. Am. Bull. 114, 718–730. https://doi.org/10.1130/0016-7606(2002)114<0718:FOPGAS>2.0.CO;2

Marquez, A., de Pablo, M.A., Oyarzun, R., Viedma, C., 2005. Evidence of gully formation by regional groundwater flow in the Gorgonum-Newton region (Mars). Icarus 179, 398–414.

Marra, W.A., Braat, L., Baar, A.W., Kleinhans, M.G., 2014. Valley formation by groundwater seepage, pressurized groundwater outbursts and crater-lake overflow in flume experiments with implications for Mars. Icarus 232, 97–117. https://doi.org/10.1016/j.icarus.2013.12.026

Marra, Wouter A., Hauber, E., de Jong, S.M., Kleinhans, M.G., 2015. Pressurized groundwater systems in Lunae and Ophir Plana (Mars): Insights from small-scale morphology and experiments. GeoResJ 8, 1–13. https://doi.org/10.1016/j.grj.2015.08.001

Marra, W. A., McLelland, S.J., Parsons, D.R., Murphy, B.J., Hauber, E., Kleinhans, M.G., 2015. Groundwater seepage landscapes from distant and local sources in experiments and on Mars. Earth Surf Dynam 3, 389–408. https://doi.org/10.5194/esurf-3-389-2015

Martínez-Alonso, S., Mellon, M.T., Banks, M.E., Keszthelyi, L.P., McEwen, A.S., 2011. Evidence of volcanic and glacial activity in Chryse and Acidalia Planitiae, Mars. Icarus 212, 597–621. https://doi.org/10.1016/j.icarus.2011.01.004

Martín-Torres, F.J., Zorzano, M.-P., Valentín-Serrano, P., Harri, A.-M., Genzer, M., Kemppinen, O., Rivera-Valentin, E.G., Jun, I., Wray, J., Bo Madsen, M., Goetz, W., McEwen, A.S., Hardgrove, C., Renno, N., Chevrier, V.F., Mischna, M., Navarro-González, R., Martínez-Frías, J., Conrad, P., McConnochie, T., Cockell, C., Berger, G., R. Vasavada, A., Sumner, D., Vaniman, D., 2015. Transient liquid water and water activity at Gale crater on Mars. Nat. Geosci. 8, 357–361. https://doi.org/10.1038/ngeo2412

Massé, M., Beck, P., Schmitt, B., Pommerol, A., McEwen, A., Chevrier, V., Brissaud, O., Séjourné, A., 2014. Spectroscopy and detectability of liquid brines on mars. Planet. Space Sci. 92, 136–149. https://doi.org/10.1016/j.pss.2014.01.018

Massé, M., Conway, S.J., Gargani, J., Patel, M.R., Pasquon, K., McEwen, A.S., Carpy, S., Chevrier, V., Balme, M.R., Ojha, L., Vincendon, M., Poulet, F., Jouannic, G., 2016. Transport processes

induced by metastable boiling water under Martian surface conditions. Nat. Geosci. 9, 425–428. https://doi.org/10.1038/ngeo2706

Mastrogiuseppe, M., Poggiali, V., Hayes, A.G., Lunine, J.I., Seu, R., Mitri, G., Lorenz, R.D., 2019. Deep and methane-rich lakes on Titan. Nat. Astron. 3, 535–542. https://doi.org/10.1038/s41550-019-0714-2

Masursky, H., 1973. An overview of geological results from Mariner 9. J. Geophys. Res. 78, 4009–4030. https://doi.org/10.1029/JB078i020p04009

Matsuoka, N., 2001. Solifluction rates, processes and landforms: a global review. Earth-Sci. Rev. 55, 107–134. https://doi.org/10.1016/S0012-8252(01)00057-5

Maurice, S., Feldman, W., Diez, B., Gasnault, O., Lawrence, D.J., Pathare, A., Prettyman, T., 2011. Mars Odyssey neutron data: 1. Data processing and models of water-equivalent-hydrogen distribution. J Geophys Res 116, E11008. https://doi.org/10.1029/2011JE003810

Max, M.D., Clifford, S.M., 2001. Initiation of Martian outflow channels: Related to the dissociation of gas hydrate? Geophys. Res. Lett. 28, 1787–1790. https://doi.org/10.1029/2000GL011606

May, C.L., Gresswell, R.E., 2004. Spatial and temporal patterns of debris-flow deposition in the Oregon Coast Range, USA. Geomorphology 57, 135–149. https://doi.org/10.1016/S0169-555X(03)00086-2

Mc Keown, L.E., Bourke, M.C., McElwaine, J.N., 2017. Experiments On Sublimating Carbon Dioxide Ice And Implications For Contemporary Surface Processes On Mars. Sci. Rep. 7, 14181. https://doi.org/10.1038/s41598-017-14132-2

McColl, S.T., 2012. Paraglacial rock-slope stability. Geomorphology 153–154, 1–16. https://doi.org/10.1016/j.geomorph.2012.02.015

McColl, S.T., Cook, S.J., Stahl, T., Davies, T.R.H., 2019. Origin and age of The Hillocks and implications for post-glacial landscape development in the upper Lake Wakatipu catchment, New Zealand. J. Quat. Sci. 34, 685–696. https://doi.org/10.1002/jqs.3168

McColl, S.T., Davies, T.R., 2011. Evidence for a rock-avalanche origin for 'The Hillocks' "moraine", Otago, New Zealand. Geomorphology 127, 216–224. https://doi.org/10.1016/j.geomorph.2010.12.017

McEwen, A., Byrne, S., Chevrier, V., Dundas, C., Hansen, C., Masse, M., Mattson, S., Murchie, S., Ojha, L., Paige, D., Schaefer, E., Thomas, N., Wray, J., 2012. Future Orbital Measurements Needed to Understand Present-Day Liquid H2O on Mars, in: Concepts and Approaches for Mars Exploration. p. 4284.

McEwen, A.S., 1998. High-Temperature Silicate Volcanism on Jupiter's Moon Io. Science 281, 87–90. https://doi.org/10.1126/science.281.5373.87

McEwen, A.S., 1989. Mobility of large rock avalanches: Evidence from Valles Marineris, Mars. Geology 17, 1111–1114. https://doi.org/10.1130/0091-7613(1989)017<1111:MOLRAE>2.3.CO;2

McEwen, A.S., Dundas, C.M., Mattson, S.S., Toigo, A.D., Ojha, L., Wray, J.J., Chojnacki, M., Byrne, S., Murchie, S.L., Thomas, N., 2014. Recurring slope lineae in equatorial regions of Mars. Nat. Geosci 7, 53–58. https://doi.org/10.1038/ngeo2014

McEwen, A.S., Hansen, C.J., Delamere, W.A., Eliason, E.M., Herkenhoff, K.E., Keszthelyi, L., Gulick, V.C., Kirk, R.L., Mellon, M.T., Grant, J.A., Thomas, N., Weitz, C.M., Squyres, S.W., Bridges, N.T., Murchie, S.L., Seelos, F., Seelos, K., Okubo, C.H., Milazzo, M.P., Tornabene, L.L., Jaeger, W.L., Byrne, S., Russell, P.S., Griffes, J.L., Martínez-Alonso, S., Davatzes, A., Chuang, F.C., Thomson, B.J., Fishbaugh, K.E., Dundas, C.M., Kolb, K.J., Banks, M.E., Wray, J.J., 2007. A Closer Look at Water-Related Geologic Activity on Mars. Science 317, 1706–1709. https://doi.org/10.1126/science.1143987

McEwen, A.S., Ojha, L., Dundas, C.M., Mattson, S.S., Byrne, S., Wray, J.J., Cull, S.C., Murchie, S.L., Thomas, N., Gulick, V.C., 2011. Seasonal Flows on Warm Martian Slopes. Science 333, 740–743. https://doi.org/10.1126/science.1204816

McEwen, A.S., Schafer, E., Sutton, S., Chojnacki, M., 2019. Abundant Recurring Slope Lineae (RSL) Following the 2018 Planet-Encircling Dust Event (PEDE). Presented at the Lunar and Planetary Science Conference, p. 1376.

McGill, G.E., 1986. The giant polygons of Utopia, northern Martian Plains. Geophys. Res. Lett. 13, 705–708. https://doi.org/10.1029/GL013i008p00705

McGowan, E.M., 2011. The Utopia/Isidis overlap: Possible conduit for mud volcanism on Mars. Icarus 212, 622–628. https://doi.org/10.1016/j.icarus.2011.01.025

McSween, H.Y., Keil, K., 2000. Mixing relationships in the Martian regolith and the composition of globally homogeneous dust. Geochim. Cosmochim. Acta 64, 2155–2166. https://doi.org/10.1016/S0016-7037(99)00401-9

Mège, D., 2003. Volcanic rifting at Martian grabens. J. Geophys. Res. 108, 5044. https://doi.org/10.1029/2002JE001852

Mellon, M.T., 1997. Small-scale polygonal features on Mars: Seasonal thermal contraction cracks in permafrost. J. Geophys. Res. Planets 102, 25617–25628. https://doi.org/10.1029/97JE02582

Mellon, M.T., Arvidson, R.E., Sizemore, H.G., Searls, M.L., Blaney, D.L., Cull, S., Hecht, M.H., Heet, T.L., Keller, H.U., Lemmon, M.T., Markiewicz, W.J., Ming, D.W., Morris, R.V., Pike, W.T., Zent, A.P., 2009. Ground ice at the Phoenix Landing Site: Stability state and origin. J. Geophys. Res. Planets 114, E00E07. https://doi.org/10.1029/2009JE003417

Mellon, M.T., Jakosky, B.M., 1995. The distribution and behavior of Martian ground ice during past and present epochs. J. Geophys. Res. 100, 3367. https://doi.org/10.1029/95JE01027

Mellon, M.T., Jakosky, B.M., 1993. Geographic variations in the thermal and diffusive stability of ground ice on Mars. J. Geophys. Res. 98, 3345. https://doi.org/10.1029/92JE02355

Mellon, M.T., Phillips, R.J., 2001. Recent gullies on Mars and the source of liquid water. J Geophys Res-Planets 106, 23165–23179.

Melosh, H.J., 1989. Impact cratering: a geologic process, Oxford monographs on geology and geophysics ; no. 11. Oxford University Press.

Melosh, H.J., 1979. Acoustic Fluidization - New Geologic Process. J. Geophys. Res. 84, 7513–7520.

Melosh, H.J., Schenk, P., 1993. Split comets and the origin of crater chains on Ganymede and Callisto. Nature 365, 731–733. https://doi.org/10.1038/365731a0

Mercier, D., Coquin, J., Feuillet, T., Decaulne, A., Cossart, E., Jónsson, H.P., Sæmundsson, Þ., 2017. Are Icelandic rock-slope failures paraglacial? Age evaluation of seventeen rock-slope failures in the Skagafjörður area, based on geomorphological stacking, radiocarbon dating and tephrochronology. Geomorphology 296, 45–58. https://doi.org/10.1016/j.geomorph.2017.08.011

Michael, G.G., Neukum, G., 2010. Planetary surface dating from crater size–frequency distribution measurements: Partial resurfacing events and statistical age uncertainty. Earth Planet. Sci. Lett. 294, 223–229. https://doi.org/10.1016/j.epsl.2009.12.041

Milana, J.P., 2015. Molards and Their Relation to Landslides Involving Permafrost Failure. Permafr. Periglac. Process. 27, 271–284. https://doi.org/10.1002/ppp.1878

Milbury, C., Schubert, G., Raymond, C.A., Smrekar, S.E., Langlais, B., 2012. The history of Mars' dynamo as revealed by modeling magnetic anomalies near Tyrrhenus Mons and Syrtis Major: MARS' DYNAMO HISTORY. J. Geophys. Res. Planets 117. https://doi.org/10.1029/2012JE004099

Milliken, R.E., Bish, D.L., 2010. Sources and sinks of clay minerals on Mars. Philos. Mag. 90, 2293–2308. https://doi.org/10.1080/14786430903575132

Milliken, R.E., Mustard, J.F., Goldsby, D.L., 2003. Viscous flow features on the surface of Mars: Observations from high-resolution Mars Orbiter Camera (MOC) images. J. Geophys. Res.-Planets 108, 5057. https://doi.org/10.1029/2002JE002005

Milliken, R.E., Mustard, J.F., Poulet, F., Jouglet, D., Bibring, J.-P., Gondet, B., Langevin, Y., 2007. Hydration state of the Martian surface as seen by Mars Express OMEGA: 2. H_2O content of the surface: HYDRATION STATE OF THE MARTIAN SURFACE. J. Geophys. Res. Planets 112. https://doi.org/10.1029/2006JE002853

Mitchell, J.L., Christensen, P.R., 2016. Recurring slope lineae and chlorides on the surface of Mars: RSL and Chlorides on Mars Surface. J. Geophys. Res. Planets 121, 1411–1428. https://doi.org/10.1002/2016JE005012

Miyamoto, H., 2004. Fluid dynamical implications of anastomosing slope streaks on Mars. J. Geophys. Res. 109. https://doi.org/10.1029/2003JE002234

Möhlmann, D., Kereszturi, A., 2010. Viscous liquid film flow on dune slopes of Mars. Icarus 207, 654–658. https://doi.org/10.1016/j.icarus.2010.01.002

Möhlmann, D.T.F., 2010. Temporary liquid water in upper snow/ice sub-surfaces on Mars? Icarus 207, 140–148.

Möhlmann, D.T.F., 2008. The influence of van der Waals forces on the state of water in the shallow subsurface of Mars. Icarus 195, 131–139. https://doi.org/10.1016/j.icarus.2007.11.026

Möhlmann, D.T.F., 2004. Water in the upper martian surface at mid- and low-latitudes: presence, state, and consequences. Icarus 168, 318–323. https://doi.org/10.1016/j.icarus.2003.11.008

Molaro, J., Byrne, S., 2012. Rates of temperature change of airless landscapes and implications for thermal stress weathering. J Geophys Res 117, E10011. https://doi.org/10.1029/2012JE004138

Montgomery, D.R., Gillespie, A., 2005. Formation of Martian outflow channels by catastrophic dewatering of evaporite deposits. Geology 33, 625–628. https://doi.org/10.1130/G21270AR.1

Moore, J.M., Asphaug, E., Morrison, D., Spencer, J.R., Chapman, C.R., Bierhaus, B., Sullivan, R.J., Chuang, F.C., Klemaszewski, J.E., Greeley, R., Bender, K.C., Geissler, P.E., Helfenstein, P., Pilcher, C.B., 1999. Mass Movement and Landform Degradation on the Icy Galilean Satellites: Results of the Galileo Nominal Mission. Icarus 140, 294–312. https://doi.org/10.1006/icar.1999.6132

Moore, J.M., Howard, A.D., 2010. Are the basins of Titan's Hotei Regio and Tui Regio sites of former low latitude seas?: FORMER LOW LATITUDE SEAS OF TITAN. Geophys. Res. Lett. 37, n/a-n/a. https://doi.org/10.1029/2010GL045234

Moore, J.M., Howard, A.D., Umurhan, O.M., White, O.L., Schenk, P.M., Beyer, R.A., McKinnon, W.B., Spencer, J.R., Singer, K.N., Grundy, W.M., Earle, A.M., Schmitt, B., Protopapa, S., Nimmo, F., Cruikshank, D.P., Hinson, D.P., Young, L.A., Stern, S.A., Weaver, H.A., Olkin, C.B., Ennico, K., Collins, G., Bertrand, T., Forget, F., Scipioni, F., 2018. Bladed Terrain on Pluto: Possible origins and evolution. Icarus 300, 129–144. https://doi.org/10.1016/j.icarus.2017.08.031

Morgan, G.A., Head, J.W., Marchant, D.R., 2009. Lineated valley fill (LVF) and lobate debris aprons (LDA) in the Deuteronilus Mensae northern dichotomy boundary region, Mars: Constraints on the extent, age and episodicity of Amazonian glacial events. Icarus 202, 22–38. https://doi.org/10.1016/j.icarus.2009.02.017

Morino, C., Conway, S.J., Balme, M.R., Hillier, J., Jordan, C., Saemundsson, Þ., Argles, T., 2018. Debris-flow release processes investigated through the analysis of multi-temporal LiDAR datasets in north-western Iceland: Debris-flow processes investigated by multi-temporal LiDAR datasets. Earth Surf. Process. Landf. https://doi.org/10.1002/esp.4488

Morino, C., Conway, S.J., Sæmundsson, Þ., Kristinn Helgason, J., Hillier, J., Butcher, F.E.G., Balme, M.R., Jordan, C., Argles, T., 2019. Molards as an indicator of permafrost degradation and landslide processes. Earth Planet. Sci. Lett. 516, 136–147. https://doi.org/10.1016/j.epsl.2019.03.040

Morris, A.R., Mouginis-Mark, P.J., Garbeil, H., 2010. Possible impact melt and debris flows at Tooting Crater, Mars. Icarus 209, 369–389. https://doi.org/10.1016/j.icarus.2010.05.029

Morris, E.C., 1982. Aureole deposits of the Martian volcano Olympus Mons. J. Geophys. Res. 87, 1164–1178.

Mottola, S., Arnold, G., Grothues, H.-G., Jaumann, R., Michaelis, H., Neukum, G., Bibring, J.-P., Schroder, S.E., Hamm, M., Otto, K.A., Pelivan, I., Proffe, G., Scholten, F., Tirsch, D., Kreslavsky, M., Remetean, E., Souvannavong, F., Dolives, B., 2015. The structure of the regolith on

67P/Churyumov-Gerasimenko from ROLIS descent imaging. Science 349, aab0232–aab0232. https://doi.org/10.1126/science.aab0232

Mouginis-Mark, P., 1981. Ejecta emplacement and modes of formation of martian fluidized ejecta craters. Icarus 45, 60–76. https://doi.org/10.1016/0019-1035(81)90006-3

Mouginis-Mark, P., 1979. Martian fluidized crater morphology: Variations with crater size, latitude, altitude, and target material. J. Geophys. Res. 84, 8011. https://doi.org/10.1029/JB084iB14p08011

Mouginis-Mark, P.J., Boyce, J.M., 2012. Tooting crater: Geology and geomorphology of the archetype large, fresh, impact crater on Mars. Chem. Erde - Geochem. 72, 1–23. https://doi.org/10.1016/j.chemer.2011.12.001

Munaretto, G., Pajola, M., Cremonese, G., Re, C., Lucchetti, A., McEwen, A.S., Pommerol, A., Becerra, P., Conway, S.J., Thomas, N., Massironi, M., 2020. Implications for the origin and evolution of Martian Recurring Slope Lineae at Hale crater from CaSSIS observations. Planet. Space Sci. 187, 104947. https://doi.org/10.1016/j.pss.2020.104947

Murton, J.B., Worsley, P., Gozdzik, J., 2000. Sand veins and wedges in cold aeolian environments. Quat. Sci. Rev. 19, 899–922. https://doi.org/10.1016/S0277-3791(99)00045-1

Mustard, J.F., Cooper, C.D., Rifkin, M.K., 2001. Evidence for recent climate change on Mars from the identification of youthful near-surface ground ice. Nature 412, 411–414. https://doi.org/10.1038/35086515

Nahm, A.L., Schultz, R.A., 2011. Magnitude of global contraction on Mars from analysis of surface faults: Implications for martian thermal history. Icarus 211, 389–400. https://doi.org/10.1016/j.icarus.2010.11.003

Nathues, A., Schmedemann, N., Thangjam, G., Pasckert, J.H., Mengel, K., Castillo-Rogez, J., Cloutis, E.A., Hiesinger, H., Hoffmann, M., Le Corre, L., Li, J.-Y., Pieters, C., Raymond, C.A., Reddy, V., Ruesch, O., Williams, D.A., 2020. Recent cryovolcanic activity at Occator crater on Ceres. Nat. Astron. 4, 794–801. https://doi.org/10.1038/s41550-020-1146-8

National Aeronautics and Space Administration, 2005. Planetary Protection Provisions for Roboti c Extraterrestrial Missions. (No. NPR 8020.12C). Washington, D.C.

Navarro-González, R., Vargas, E., de la Rosa, J., Raga, A.C., McKay, C.P., 2010. Reanalysis of the Viking results suggests perchlorate and organics at midlatitudes on Mars. J. Geophys. Res. 115. https://doi.org/10.1029/2010JE003599

Newsom, H.E., 1980. Hydrothermal alteration of impact melt sheets with implications for Mars. Icarus 44, 207–216. https://doi.org/10.1016/0019-1035(80)90066-4

Nittler, L.R., Chabot, N.L., Grove, T.L., Peplowski, P.N., 2018. The Chemical Composition of Mercury, in: Solomon, S.C., Nittler, L.R., Anderson, B.J. (Eds.), Mercury. Cambridge University Press, pp. 30–51. https://doi.org/10.1017/9781316650684.003

Nittler, L.R., Weider, S.Z., 2019. The Surface Composition of Mercury. Elements 15, 33–38. https://doi.org/10.2138/gselements.15.1.33

Noblet, A., Conway, S.J., 2022. A Global Map of Gullied Hillslopes. Presented at the 53rd Lunar and Planetary Science Conference, The Woodlands, Texas.

Nuding, D.L., Davis, R.D., Gough, R.V., Tolbert, M.A., 2015. The aqueous stability of a Mars salt analog: Instant Mars. J. Geophys. Res. Planets 120, 588–598. https://doi.org/10.1002/2014JE004722

Nunes, D.C., Smrekar, S.E., Safaeinili, A., Holt, J., Phillips, R.J., Seu, R., Campbell, B., 2010. Examination of gully sites on Mars with the shallow radar. J Geophys Res 115, doi:10.1029/2009JE003509. https://doi.org/10.1029/2009je003509

Oberbeck, V.R., 2009. Layered ejecta craters and the early water/ice aquifer on Mars. Meteorit. Planet. Sci. 44, 43–54. https://doi.org/10.1111/j.1945-5100.2009.tb00716.x

Obleitner, F., Spötl, C., 2011. The mass and energy balance of ice within the Eisriesenwelt cave, Austria. The Cryosphere 5, 245–257. https://doi.org/10.5194/tc-5-245-2011

Obu, J., Westermann, S., Bartsch, A., Berdnikov, N., Christiansen, H.H., Dashtseren, A., Delaloye, R., Elberling, B., Etzelmüller, B., Kholodov, A., Khomutov, A., Kääb, A., Leibman, M.O.,

Lewkowicz, A.G., Panda, S.K., Romanovsky, V., Way, R.G., Westergaard-Nielsen, A., Wu, T., Yamkhin, J., Zou, D., 2019. Northern Hemisphere permafrost map based on TTOP modelling for 2000–2016 at 1 km2 scale. Earth-Sci. Rev. 193, 299–316. https://doi.org/10.1016/j.earscirev.2019.04.023

Oehler, D.Z., Allen, C.C., 2010. Evidence for pervasive mud volcanism in Acidalia Planitia, Mars. Icarus 208, 636–657. https://doi.org/10.1016/j.icarus.2010.03.031

Ojha, L., Chojnacki, M., McDonald, G.D., Shumway, A., Wolff, M.J., Smith, M.D., McEwen, A.S., Ferrier, K., Huber, C., Wray, J.J., Toigo, A., 2017. Seasonal Slumps in Juventae Chasma, Mars: Seasonal Slumps in Juventae Chasma, Mars. J. Geophys. Res. Planets. https://doi.org/10.1002/2017JE005375

Ojha, L., McEwen, A., Dundas, C., Byrne, S., Mattson, S., Wray, J., Masse, M., Schaefer, E., 2014. HiRISE observations of Recurring Slope Lineae (RSL) during southern summer on Mars. Icarus 231, 365–376. https://doi.org/10.1016/j.icarus.2013.12.021

Ojha, L., Wilhelm, M.B., Murchie, S.L., McEwen, A.S., Wray, J.J., Hanley, J., Masse, M., Chojnacki, M., 2015. Spectral evidence for hydrated salts in recurring slope lineae on Mars. Nat. Geosci 8, 829–832.

Okubo, C.H., 2016. Morphologic evidence of subsurface sediment mobilization and mud volcanism in Candor and Coprates Chasmata, Valles Marineris, Mars. Icarus 269, 23–37. https://doi.org/10.1016/j.icarus.2015.12.051

Ordonez-Etxeberria, I., Hueso, R., Sánchez-Lavega, A., Millour, E., Forget, F., 2019. Meteorological pressure at Gale crater from a comparison of REMS/MSL data and MCD modelling: Effect of dust storms. Icarus 317, 591–609. https://doi.org/10.1016/j.icarus.2018.09.003

Orgel, C., Hauber, E., van Gasselt, S., Reiss, D., Johnsson, A., Ramsdale, J.D., Smith, I., Swirad, Z.M., Séjourné, A., Wilson, J.T., Balme, M.R., Conway, S.J., Costard, F., Eke, V.R., Gallagher, C., Kereszturi, Á., Łosiak, A., Massey, R.J., Platz, T., Skinner, J.A., Teodoro, L.F.A., 2018. Gridmapping the Northern Plains of Mars: A New Overview of Recent Water- and Ice-Related Landforms in Acidalia Planitia. J. Geophys. Res. Planets. https://doi.org/10.1029/2018JE005664

Orloff, T., Kreslavsky, M., Asphaug, E., Korteniemi, J., 2011. Boulder movement at high northern latitudes of Mars. J. Geophys. Res. 116. https://doi.org/10.1029/2011JE003811

Orloff, T.C., Kreslavsky, M.A., Asphaug, E.I., 2013. Possible mechanism of boulder clustering on Mars. Icarus 225, 992–999. https://doi.org/10.1016/j.icarus.2013.01.002

Orosei, R., Lauro, S.E., Pettinelli, E., Cicchetti, A., Coradini, M., Cosciotti, B., Di Paolo, F., Flamini, E., Mattei, E., Pajola, M., Soldovieri, F., Cartacci, M., Cassenti, F., Frigeri, A., Giuppi, S., Martufi, R., Masdea, A., Mitri, G., Nenna, C., Noschese, R., Restano, M., Seu, R., 2018. Radar evidence of subglacial liquid water on Mars. Science eaar7268. https://doi.org/10.1126/science.aar7268

Osinski, G.R., Tornabene, L.L., Banerjee, N.R., Cockell, C.S., Flemming, R., Izawa, M.R.M., McCutcheon, J., Parnell, J., Preston, L.J., Pickersgill, A.E., Pontefract, A., Sapers, H.M., Southam, G., 2013. Impact-generated hydrothermal systems on Earth and Mars. Icarus 224, 347–363. https://doi.org/10.1016/j.icarus.2012.08.030

Owen, G., Hiemstra, J.F., Matthews, J.A., Mcewen, L.J., 2010. Landslide-glacier interaction in a neoparaglacial setting at tverrbytnede, jotunheimen, southern norway. Geogr. Ann. Ser. Phys. Geogr. 92, 421–436. https://doi.org/10.1111/j.1468-0459.2010.00405.x

Paillou, P., Seignovert, B., Radebaugh, J., Wall, S., 2016. Radar scattering of linear dunes and mega-yardangs: Application to Titan. Icarus 270, 211–221. https://doi.org/10.1016/j.icarus.2015.07.038

Pajola, M., Mergili, M., Cambianica, P., Lucchetti, A., Brunetti, M.T., Guimpier, A., Mastropietro, M., Munaretto, G., Conway, S., Beccarelli, J., Cremonese, G., 2022. Modelling reconstruction and boulder size-frequency distribution of a young (<5 Myr) landslide located in Simud Vallis floor, Mars. Icarus 375, 114850. https://doi.org/10.1016/j.icarus.2021.114850

Pál, B., Kereszturi, Á., 2017. Possibility of microscopic liquid water formation at landing sites on Mars and their observational potential. Icarus 282, 84–92. https://doi.org/10.1016/j.icarus.2016.09.006

Palumbo, A.M., Head, J.W., 2019. Oceans on Mars: The possibility of a Noachian groundwater-fed ocean in a sub-freezing martian climate. Icarus 331, 209–225. https://doi.org/10.1016/j.icarus.2019.04.022

Pankine, A.A., Tamppari, L.K., 2019. MGS TES observations of the water vapor in the martian southern polar atmosphere during spring and summer. Icarus 331, 26–48. https://doi.org/10.1016/j.icarus.2019.05.010

Pankine, A.A., Tamppari, L.K., Smith, M.D., 2010. MGS TES observations of the water vapor above the seasonal and perennial ice caps during northern spring and summer. Icarus 210, 58–71. https://doi.org/10.1016/j.icarus.2010.06.043

Paola, C., Straub, K., Mohrig, D., Reinhardt, L., 2009. The “unreasonable effectiveness” of stratigraphic and geomorphic experiments. Earth-Sci. Rev. 97, 1–43. https://doi.org/10.1016/j.earscirev.2009.05.003

Parker, T.J., Gorsline, D.S., Saunders, R.S., Pieri, D.C., Schneeberger, D.M., 1993. Coastal geomorphology of the Martian northern plains. J. Geophys. Res. 98, 11061. https://doi.org/10.1029/93JE00618

Parsons, R.A., Nimmo, F., 2010. Numerical modeling of Martian gully sediment transport: Testing the fluvial hypothesis. J Geophys Res 115, doi:10.1029/2009JE003517. https://doi.org/10.1029/2009je003517

Parsons, R.A., Nimmo, F., Miyamoto, H., 2011. Constraints on martian lobate debris apron evolution and rheology from numerical modeling of ice flow. Icarus 214, 246–257. https://doi.org/10.1016/j.icarus.2011.04.014

Pasquon, K., Gargani, J., Massé, M., Conway, S.J., 2016. Present-day formation and seasonal evolution of linear dune gullies on Mars. Icarus 274, 195–210. https://doi.org/10.1016/j.icarus.2016.03.024

Pasquon, K., Gargani, J., Massé, M., Vincendon, M., Conway, S.J., Séjourné, A., Jomelli, V., Balme, M.R., Lopez, S., Guimpier, A., 2019a. Present-day development of gully-channel sinuosity by carbon dioxide gas supported flows on Mars. Icarus 329, 296–313. https://doi.org/10.1016/j.icarus.2019.03.034

Pasquon, K., Gargani, J., Nachon, M., Conway, S.J., Massé, M., Jouannic, G., Balme, M.R., Costard, F., Vincendon, M., 2019b. Are different Martian gully morphologies due to different processes on the Kaiser dune field? Geol. Soc. Lond. Spec. Publ. 467. https://doi.org/10.1144/SP467.13

Pathare, A.V., Feldman, W.C., Prettyman, T.H., Maurice, S., 2018. Driven by excess? Climatic implications of new global mapping of near-surface water-equivalent hydrogen on Mars. Icarus 301, 97–116. https://doi.org/10.1016/j.icarus.2017.09.031

Peale, S.J., Schubert, G., Lingenfelter, R.E., 1968. Distribution of Sinuous Rilles and Water on the Moon. Nature 220, 1222–1225. https://doi.org/10.1038/2201222a0

Peel, S.E., Fassett, C.I., 2013. Valleys in pit craters on Mars: Characteristics, distribution, and formation mechanisms. Icarus 225, 272–282. https://doi.org/10.1016/j.icarus.2013.03.031

Pegg, D.L., Rothery, D.A., Balme, M.R., Conway, S.J., 2021a. Explosive vent sites on mercury: Commonplace multiple eruptions and their implications. Icarus 365, 114510. https://doi.org/10.1016/j.icarus.2021.114510

Pegg, D.L., Rothery, D.A., Conway, S.J., Balme, M.R., 2021b. A fault surface exposed on Mercury. Planet. Space Sci. 201, 105223. https://doi.org/10.1016/j.pss.2021.105223

Pelletier, J.D., Kolb, K.J., McEwen, A.S., Kirk, R.L., 2008. Recent bright gully deposits on Mars: Wet or dry flow? Geology 36, 211–214.

Penido, J.C., Fassett, C.I., Som, S.M., 2013. Scaling relationships and concavity of small valley networks on Mars. Planet. Space Sci. 75, 105–116. https://doi.org/10.1016/j.pss.2012.09.009

Peplowski, P.N., Klima, R.L., Lawrence, D.J., Ernst, C.M., Denevi, B.W., Frank, E.A., Goldsten, J.O., Murchie, S.L., Nittler, L.R., Solomon, S.C., 2016. Remote sensing evidence for an ancient

carbon-bearing crust on Mercury. Nat. Geosci. 9, 273–276. https://doi.org/10.1038/ngeo2669

Perron, J.T., Lamb, M.P., Koven, C.D., Fung, I.Y., Yager, E., Ádámkovics, M., 2006. Valley formation and methane precipitation rates on Titan. J. Geophys. Res. 111, E11001. https://doi.org/10.1029/2005JE002602

Perry, M.R., Bain, Z.M., Putzig, N.E., Morgan, G.A., Bramson, A.M., Petersen, E.I., Mastrogiuseppe, M., Baker, D.M.H., Hoover, R.H., Sizemore, H.G., Smith, I.B., Campbell, B.A., 2019. Mars Subsurface Water Ice Mapping (SWIM): The SWIM Equation and Project Infrastructure. Presented at the Lunar and Planetary Science Conference, p. 3083.

Petersen, E.I., Holt, J.W., Levy, J.S., 2018. High Ice Purity of Martian Lobate Debris Aprons at the Regional Scale: Evidence From an Orbital Radar Sounding Survey in Deuteronilus and Protonilus Mensae. Geophys. Res. Lett. 45, 11,595-11,604. https://doi.org/10.1029/2018GL079759

Pewe, T.L., 1959. Sand-wedge polygons (tesselations) in the McMurdo Sound region, Antarctica; a progress report. Am. J. Sci. 257, 545–552. https://doi.org/10.2475/ajs.257.8.545

Phillips, C.B., Burr, D.M., Beyer, R.A., 2007. Mass movement within a slope streak on Mars. Geophys. Res. Lett. 34, doi:10.1029/2007GL031577. https://doi.org/L21202 Artn l21202

Phillips, M.S., Moersch, J.E., Viviano, C.E., Emery, J.P., 2021. The lifecycle of hollows on mercury: An evaluation of candidate volatile phases and a novel model of formation. Icarus 114306. https://doi.org/10.1016/j.icarus.2021.114306

Phillips, R.J., Davis, B.J., Tanaka, K.L., Byrne, S., Mellon, M.T., Putzig, N.E., Haberle, R.M., Kahre, M.A., Campbell, B.A., Carter, L.M., Smith, I.B., Holt, J.W., Smrekar, S.E., Nunes, D.C., Plaut, J.J., Egan, A.F., Titus, T.N., Seu, R., 2011. Massive CO2 Ice Deposits Sequestered in the South Polar Layered Deposits of Mars. Science 332, 838–841. https://doi.org/10.1126/science.1203091

Pilorget, C., Forget, F., 2016. Formation of gullies on Mars by debris flows triggered by CO2 sublimation. Nat. Geosci 9, 65–69. https://doi.org/10.1038/ngeo2619

Piqueux, S., Buz, J., Edwards, C.S., Bandfield, J.L., Kleinböhl, A., Kass, D.M., Hayne, P.O., The MCS, THEMIS Teams, 2019. Widespread Shallow Water Ice on Mars at High Latitudesand Midlatitudes. Geophys. Res. Lett. 2019GL083947. https://doi.org/10.1029/2019GL083947

Piqueux, S., Kleinböhl, A., Hayne, P.O., Kass, D.M., Schofield, J.T., McCleese, D.J., 2015. Variability of the martian seasonal CO2 cap extent over eight Mars Years. Dyn. Mars 251, 164–180. https://doi.org/10.1016/j.icarus.2014.10.045

Plaut, J.J., Picardi, G., Safaeinili, A., Ivanov, A.B., Milkovich, S.M., Cicchetti, A., Kofman, W., Mouginot, J., Farrell, W.M., Phillips, R.J., Clifford, S.M., Frigeri, A., Orosei, R., Federico, C., Williams, I.P., Gurnett, D.A., Nielsen, E., Hagfors, T., Heggy, E., Stofan, E.R., Plettemeier, D., Watters, T.R., Leuschen, C.J., Edenhofer, P., 2007. Subsurface Radar Sounding of the South Polar Layered Deposits of Mars. Science 316, 92. https://doi.org/10.1126/science.1139672

Plaut, J.J., Safaeinili, A., Holt, J.W., Phillips, R.J., Head, J.W., Seu, R., Putzig, N.E., Frigeri, A., 2009. Radar evidence for ice in lobate debris aprons in the mid-northern latitudes of Mars. Geophys. Res. Lett. 36, 02203. https://doi.org/10.1029/2008GL036379

Pollack, J.B., Kasting, J.F., Richardson, S.M., Poliakoff, K., 1987. The case for a wet, warm climate on early Mars. Icarus 71, 203–224. https://doi.org/10.1016/0019-1035(87)90147-3

Porco, Carolyn C., Baker, E., Barbara, J., Beurle, K., Brahic, A., Burns, J.A., Charnoz, S., Cooper, N., Dawson, D.D., Del Genio, A.D., Denk, T., Dones, L., Dyudina, U., Evans, M.W., Fussner, S., Giese, B., Grazier, K., Helfenstein, P., Ingersoll, A.P., Jacobson, R.A., Johnson, T.V., McEwen, A., Murray, C.D., Neukum, G., Owen, W.M., Perry, J., Roatsch, T., Spitale, J., Squyres, S., Thomas, P., Tiscareno, M., Turtle, E.P., Vasavada, A.R., Veverka, J., Wagner, R., West, R., 2005. Imaging of Titan from the Cassini spacecraft. Nature 434, 159–168. https://doi.org/10.1038/nature03436

Porco, C. C., Baker, E., Barbara, J., Beurle, K., Brahic, A., Burns, J.A., Charnoz, S., Cooper, N., Dawson, D.D., Del Genio, A.D., Denk, T., Dones, L., Dyudina, U., Evans, M.W., Giese, B., Grazier, K., Helfenstein, P., Ingersoll, A.P., Jacobson, R.A., Johnson, T.V., McEwen, A., Murray, C.D.,

Neukum, G., Owen, W.M., Perry, J., Roatsch, T., Spitale, J., Squyres, S., Thomas, P.C., Tiscareno, M., Turtle, E., Vasavada, A.R., Veverka, J., Wagner, R., West, R., 2005. Cassini Imaging Science: Initial Results on Phoebe and Iapetus. Science 307, 1237–1242. https://doi.org/10.1126/science.1107981

Portyankina, G., Markiewicz, W.J., Thomas, N., Hansen, C.J., Milazzo, M., 2010. HiRISE observations of gas sublimation-driven activity in Mars' southern polar regions: III. Models of processes involving translucent ice. MROHiRISE Stud. Mars 205, 311–320. https://doi.org/10.1016/j.icarus.2009.08.029

Poulet, F., Bibring, J.-P., Mustard, J.F., Gendrin, A., Mangold, N., Langevin, Y., Arvidson, R.E., Gondet, B., Gomez, C., 2005. Phyllosilicates on Mars and implications for early martian climate. Nature 438, 623–627. https://doi.org/10.1038/nature04274

Poulos, M.J., Pierce, J.L., Flores, A.N., Benner, S.G., 2012. Hillslope asymmetry maps reveal widespread, multi-scale organization: MAPPING HILLSLOPE ASYMMETRY. Geophys. Res. Lett. 39, n/a-n/a. https://doi.org/10.1029/2012GL051283

Primm, K.M., 2018. Exploring the water uptake and release of Mars-relevant salt and surface analogs through Raman microscopy. University of Colorado at Boulder.

Primm, K.M., Gough, R.V., Chevrier, V.F., Tolbert, M.A., 2017. Freezing of perchlorate and chloride brines under Mars-relevant conditions. Geochim. Cosmochim. Acta 212, 211–220. https://doi.org/10.1016/j.gca.2017.06.012

Primm, K.M., Gough, R.V., Wong, J., Rivera-Valentin, E.G., Martinez, G.M., Hogancamp, J.V., Archer, P.D., Ming, D.W., Tolbert, M.A., 2018. The Effect of Mars-Relevant Soil Analogs on the Water Uptake of Magnesium Perchlorate and Implications for the Near-Surface of Mars. J. Geophys. Res. Planets 123, 2076–2088. https://doi.org/10.1029/2018JE005540

Primm, K.M., Stillman, D.E., Michaels, T.I., 2019. Investigating the hysteretic behavior of Mars-relevant chlorides. Icarus. https://doi.org/10.1016/j.icarus.2019.06.003

Pudasaini, S.P., 2012. A general two-phase debris flow model: A GENERAL TWO-PHASE DEBRIS FLOW MODEL. J. Geophys. Res. Earth Surf. 117, n/a-n/a. https://doi.org/10.1029/2011JF002186

Quantin, C., Allemand, P., Delacourt, C., 2004a. Morphology and geometry of Valles Marineris landslides. Planet Mars Spons. Cent. Natl. Etudes Spatiales CNES Cent. Natl. Rech. Sci. CNRS Obs. Paris 52, 1011–1022. https://doi.org/10.1016/j.pss.2004.07.016

Quantin, C., Allemand, P., Mangold, N., Delacourt, C., 2004b. Ages of Valles Marineris (Mars) landslides and implications for canyon history. Icarus 172, 555–572. https://doi.org/10.1016/j.icarus.2004.06.013

Quantin, C., Flahaut, J., Clenet, H., Allemand, P., Thomas, P., 2012. Composition and structures of the subsurface in the vicinity of Valles Marineris as revealed by central uplifts of impact craters. Icarus 221, 436–452. https://doi.org/10.1016/j.icarus.2012.07.031

Raack, J., Conway, S.J., Herny, C., Balme, M.R., Carpy, S., Patel, M.R., 2017. Water induced sediment levitation enhances down-slope transport on Mars. Nat. Commun. 8, 1151. https://doi.org/10.1038/s41467-017-01213-z

Raack, J., Conway, S.J., Heyer, T., Bickel, V.T., Philippe, M., Hiesinger, H., Johnsson, A., Massé, M., 2020. Present-day gully activity in Sisyphi Cavi, Mars – Flow-like features and block movements. Icarus 350, 113899. https://doi.org/10.1016/j.icarus.2020.113899

Raack, J., Reiss, D., Appéré, T., Vincendon, M., Ruesch, O., Hiesinger, H., 2015. Present-Day Seasonal Gully Activity in a South Polar Pit (Sisyphi Cavi) on Mars. Icarus 251, 226–243. https://doi.org/j.icarus.2014.03.040

Rager, A.H., Smith, E.I., Scheu, B., Dingwell, D.B., 2014. The effects of water vaporization on rock fragmentation during rapid decompression: Implications for the formation of fluidized ejecta on Mars. Earth Planet. Sci. Lett. 385, 68–78. https://doi.org/10.1016/j.epsl.2013.10.029

Ramsdale, J.D., Balme, M.R., Gallagher, C., Conway, S.J., Smith, I.B., Hauber, E., Orgel, C., Séjourné, A., Costard, F., Eke, V.R., van Gasseltg, S.A., Johnsson, A., Kereszturi, A., Losiak, A., Massey, R.J., Platz, T., Reiss, D., Swirad, Z.M., Teodoro, L.F.A., Wilson, J.T., 2018. Gridmapping the

northern plains of Mars: Geomorphological, Radar and Water-Equivalent Hydrogen results from Arcadia Plantia. J. Geophys. Res. Planets. https://doi.org/10.1029/2018JE005663

Rathbun, J.A., Squyres, S.W., 2002. Hydrothermal Systems Associated with Martian Impact Craters. Icarus 157, 362–372.

Ravanel, L., 2009. Évolution géomorphologique de la haute montagne alpine dans le contexte actuel de réchauffement climatique. Collect. EDYTEM Cah. Géographie 8, 113–124. https://doi.org/10.3406/edyte.2009.1078

Reiss, D., Jaumann, R., 2003. Recent debris flows on Mars: Seasonal observations of the Russell Crater dune field. Geophys Res Lett 30, doi:10.1029/2002GL016704.

Reiss, D., Raack, J., Rossi, A.P., Di Achille, G., Hiesinger, H., 2010. First in-situ analysis of dust devil tracks on Earth and their comparison with tracks on Mars: DARK DUST DEVIL TRACKS ON EARTH. Geophys. Res. Lett. 37, n/a-n/a. https://doi.org/10.1029/2010GL044016

Reiss, D., van Gasselt, S., Neukum, G., Jaumann, R., 2004. Absolute dune ages and implications for the time of formation of gullies in Nirgal Vallis, Mars. J Geophys Res-Planets 109, doi:10.1029/2004JE002251.

Rempel, A.W., 2012. Hydromechanical Processes in Freezing Soils. Vadose Zone J. 11, vzj2012.0045. https://doi.org/10.2136/vzj2012.0045

Rempel, A.W., 2007. Formation of ice lenses and frost heave. J. Geophys. Res. 112. https://doi.org/10.1029/2006JF000525

Richardson, M.I., Mischna, M.A., 2005. Long-term evolution of transient liquid water on Mars. J. Geophys. Res. Planets 110, 03003. https://doi.org/10.1029/2004JE002367

Rivera-Valentin, E.G., Barr, A.C., 2014. Impact-induced compositional variations on Mercury. Earth Planet. Sci. Lett. 391, 234–242. https://doi.org/10.1016/j.epsl.2014.02.003

Roback, K.P., Ehlmann, B.L., 2021. Controls on the Global Distribution of Martian Landslides. J. Geophys. Res. Planets 126. https://doi.org/10.1029/2020JE006675

Roberts, G.P., Matthews, B., Bristow, C., Guerrieri, L., Vetterlein, J., 2012. Possible evidence of paleomarsquakes from fallen boulder populations, Cerberus Fossae, Mars. J. Geophys. Res. Planets 117, E02009. https://doi.org/10.1029/2011JE003816

Rodriguez, J.A.P., Fairén, A.G., Tanaka, K.L., Zarroca, M., Linares, R., Platz, T., Komatsu, G., Miyamoto, H., Kargel, J.S., Yan, J., Gulick, V., Higuchi, K., Baker, V.R., Glines, N., 2016. Tsunami waves extensively resurfaced the shorelines of an early Martian ocean. Sci. Rep. 6, 25106. https://doi.org/10.1038/srep25106

Rodriguez, J.A.P., Leonard, G.J., Kargel, J.S., Domingue, D., Berman, D.C., Banks, M., Zarroca, M., Linares, R., Marchi, S., Baker, V.R., Webster, K.D., Sykes, M., 2020. The Chaotic Terrains of Mercury Reveal a History of Planetary Volatile Retention and Loss in the Innermost Solar System. Sci. Rep. 10, 4737. https://doi.org/10.1038/s41598-020-59885-5

Rodriguez, J.A.P., Platz, T., Gulick, V., Baker, V.R., Fairén, A.G., Kargel, J., Yan, J., Miyamoto, H., Glines, N., 2015. Did the martian outflow channels mostly form during the Amazonian Period? Icarus 257, 387–395. https://doi.org/10.1016/j.icarus.2015.04.024

Rossbacher, L.A., Judson, S., 1981. Ground ice on Mars: Inventory, distribution, and resulting landforms. Icarus 45, 39–59. https://doi.org/10.1016/0019-1035(81)90005-1

Rothery, D.A., Thomas, R.J., Kerber, L., 2014. Prolonged eruptive history of a compound volcano on Mercury: Volcanic and tectonic implications. Earth Planet. Sci. Lett. 385, 59–67. https://doi.org/10.1016/j.epsl.2013.10.023

Ruesch, O., Sefton-Nash, E., Vago, J.L., Küppers, M., Pasckert, J.H., Krohn, K., Otto, K., 2020. In situ fragmentation of lunar blocks and implications for impacts and solar-induced thermal stresses. Icarus 336, 113431. https://doi.org/10.1016/j.icarus.2019.113431

Rummel, J.D., Beaty, D.W., Jones, M.A., Bakermans, C., Barlow, N.G., Boston, P.J., Chevrier, V.F., Clark, B.C., de Vera, J.-P.P., Gough, R.V., Hallsworth, J.E., Head, J.W., Hipkin, V.J., Kieft, T.L., McEwen, A.S., Mellon, M.T., Mikucki, J.A., Nicholson, W.L., Omelon, C.R., Peterson, R., Roden, E.E., Sherwood Lollar, B., Tanaka, K.L., Viola, D., Wray, J.J., 2014. A New Analysis of

Mars “Special Regions”: Findings of the Second MEPAG Special Regions Science Analysis Group (SR-SAG2). Astrobiology 14, 887–968. https://doi.org/10.1089/ast.2014.1227

Ryan, J.A., Lucich, R.D., 1983. Possible dust devils, vortices on Mars. J. Geophys. Res. 88, 11005. https://doi.org/10.1029/JC088iC15p11005

Salese, F., Pondrelli, M., Neeseman, A., Schmidt, G., Ori, G.G., 2019. Geological Evidence of Planet-Wide Groundwater System on Mars. J. Geophys. Res. Planets 124, 374–395. https://doi.org/10.1029/2018JE005802

Salvatore, M.R., Christensen, P.R., 2014. On the origin of the Vastitas Borealis Formation in Chryse and Acidalia Planitiae, Mars: Vastitas Borealis Formation, Mars. J. Geophys. Res. Planets 119, 2437–2456. https://doi.org/10.1002/2014JE004682

Sam, L., Bhardwaj, A., 2022. A Remote Sensing Perspective on Mass Wasting in Contrasting Planetary Environments: Cases of the Moon and Ceres. Remote Sens. 14, 1049. https://doi.org/10.3390/rs14041049

Santi, P.M., deWolfe, V.G., Higgins, J.D., Cannon, S.H., Gartner, J.E., 2008. Sources of debris flow material in burned areas. Geomorphology 96, 310–321.

Sarafian, A.R., Nielsen, S.G., Marschall, H.R., McCubbin, F.M., Monteleone, B.D., 2014. Early accretion of water in the inner solar system from a carbonaceous chondrite–like source. Science 346, 623–626. https://doi.org/10.1126/science.1256717

Sasaki, S., Honda, C., Sugita, S., Miyammoto, H., Michikami, T., Morota, T., Kanda, S., Kikuchi, H., 2021. Crack orientations of boulders and thermal fatigue on (162173) Ryugu. 43rd COSPAR Sci. Assem. Held 28 January-4 Febr. 43, 270.

Sauro, F., Pozzobon, R., Massironi, M., De Berardinis, P., Santagata, T., De Waele, J., 2020. Lava tubes on Earth, Moon and Mars: A review on their size and morphology revealed by comparative planetology. Earth-Sci. Rev. 209, 103288. https://doi.org/10.1016/j.earscirev.2020.103288

Scanlon, K.E., Head, J.W., Fastook, J.L., Wordsworth, R.D., 2018. The Dorsa Argentea Formation and the Noachian-Hesperian climate transition. Icarus 299, 339–363. https://doi.org/10.1016/j.icarus.2017.07.031

Scanlon, K.E., Head, J.W., Marchant, D.R., 2015. Volcanism-induced, local wet-based glacial conditions recorded in the Late Amazonian Arsia Mons tropical mountain glacier deposits. Icarus 250, 18–31. https://doi.org/10.1016/j.icarus.2014.11.016

Scapozza, C., Lambiel, C., Baron, L., Marescot, L., Reynard, E., 2011. Internal structure and permafrost distribution in two alpine periglacial talus slopes, Valais, Swiss Alps. Geomorphology 132, 208–221. https://doi.org/doi: 10.1016/j.geomorph.2011.05.010

Schaefer, E.I., McEwen, A.S., Sutton, S.S., 2019. A case study of recurring slope lineae (RSL) at Tivat crater: Implications for RSL origins. Icarus 317, 621–648. https://doi.org/10.1016/j.icarus.2018.07.014

Schenk, P., Jackson, M.P.A., 1993. Diapirism on Triton: A record of crustal layering and instability. Geology 21, 299–302.

Schleicher, L.S., Watters, T.R., Martin, A.J., Banks, M.E., 2019. Wrinkle ridges on Mercury and the Moon within and outside of mascons. Icarus 331, 226–237. https://doi.org/10.1016/j.icarus.2019.04.013

Schmidt, B.E., Hughson, K.H.G., Chilton, H.T., Scully, J.E.C., Platz, T., Nathues, A., Sizemore, H., Bland, M.T., Byrne, S., Marchi, S., O’Brien, D.P., Schorghofer, N., Hiesinger, H., Jaumann, R., Pasckert, J.H., Lawrence, J.D., Buzckowski, D., Castillo-Rogez, J.C., Sykes, M.V., Schenk, P.M., DeSanctis, M.-C., Mitri, G., Formisano, M., Li, J.-Y., Reddy, V., LeCorre, L., Russell, C.T., Raymond, C.A., 2017. Geomorphological evidence for ground ice on dwarf planet Ceres. Nat. Geosci. 10, 338–343. https://doi.org/10.1038/ngeo2936

Schmidt, F., Andrieu, F., Costard, F., Kocifaj, M., Meresescu, A.G., 2017. Formation of recurring slope lineae on Mars by rarefied gas-triggered granular flows. Nat. Geosci 10, 270–273.

Schon, S.C., Head, J.W., Fassett, C.I., 2009a. Unique chronostratigraphic marker in depositional fan stratigraphy on Mars: Evidence for ca. 1.25 Ma gully activity and surficial meltwater origin. Geology 37, 207–210. https://doi.org/10.1130/g25398a.1

Schon, S.C., Head, J.W., Milliken, R.E., 2009b. A recent ice age on Mars: Evidence for climate oscillations from regional layering in mid-latitude mantling deposits. Geophys Res Lett 36. https://doi.org/10.1029/2009GL038554

Schorghofer, N., Aharonson, O., 2005. Stability and exchange of subsurface ice on Mars. J Geophys Res-Planets 110, doi:10.1029/2004JE002350.

Schorghofer, N., Aharonson, O., Gerstell, M.F., Tatsumi, L., 2007. Three decades of slope streak activity on Mars. Icarus 191, 132–140. https://doi.org/10.1016/j.icarus.2007.04.026

Schorghofer, N., Aharonson, O., Khatiwala, S., 2002. Slope streaks on Mars: Correlations with surface properties and the potential role of water. Geophys. Res. Lett. 29, 2126. https://doi.org/10.1029/2002GL015889

Schultz, P.H., Gault, D.E., 1975. Seismic effects from major basin formations on the moon and mercury. The Moon 12, 159–177. https://doi.org/10.1007/BF00577875

Schwenzer, S.P., Bridges, J.C., Wiens, R.C., Conrad, P.G., Kelley, S.P., Leveille, R., Mangold, N., Martín-Torres, J., McAdam, A., Newsom, H., Zorzano, M.P., Rapin, W., Spray, J., Treiman, A.H., Westall, F., Fairén, A.G., Meslin, P.-Y., 2016. Fluids during diagenesis and sulfate vein formation in sediments at Gale crater, Mars. Meteorit. Planet. Sci. 51, 2175–2202. https://doi.org/10.1111/maps.12668

Scott, D.H., Tanaka, K.L., 1987. Geologic map of the polar regions of Mars. U.S. Geological Survey.

Scully, J.E.C., Buczkowski, D.L., Schmedemann, N., Raymond, C.A., Castillo-Rogez, J.C., King, S.D., Bland, M.T., Ermakov, A.I., O'Brien, D.P., Marchi, S., Longobardo, A., Russell, C.T., Fu, R.R., Neveu, M., 2017. Evidence for the Interior Evolution of Ceres from Geologic Analysis of Fractures. Geophys. Res. Lett. 44, 9564–9572. https://doi.org/10.1002/2017GL075086

Scully, J.E.C., Russell, C.T., Yin, A., Jaumann, R., Carey, E., Castillo-Rogez, J., McSween, H.Y., Raymond, C.A., Reddy, V., Le Corre, L., 2015. Geomorphological evidence for transient water flow on Vesta. Earth Planet. Sci. Lett. 411, 151–163. https://doi.org/10.1016/j.epsl.2014.12.004

Sefton-Nash, E., Catling, D.C., Wood, S.E., Grindrod, P.M., Teanby, N.A., 2012. Topographic, spectral and thermal inertia analysis of interior layered deposits in Iani Chaos, Mars. Icarus 221, 20–42. https://doi.org/10.1016/j.icarus.2012.06.036

Segura, T.L., 2002. Environmental Effects of Large Impacts on Mars. Science 298, 1977–1980. https://doi.org/10.1126/science.1073586

Segura, T.L., Toon, O.B., Colaprete, A., 2008. Modeling the environmental effects of moderate-sized impacts on Mars. J. Geophys. Res. 113. https://doi.org/10.1029/2008JE003147

Séjourné, A., Costard, F., Gargani, J., Soare, R.J., Fedorov, A., Marmo, C., 2011. Scalloped depressions and small-sized polygons in western Utopia Planitia, Mars: A new formation hypothesis. Planet. Space Sci. 59, 412–422. https://doi.org/10.1016/j.pss.2011.01.007

Séjourné, A., Costard, F., Swirad, Z.M., Łosiak, A., Bouley, S., Smith, I., Balme, M.R., Orgel, C., Ramsdale, J.D., Hauber, E., Conway, S.J., van Gasselt, S., Reiss, D., Johnsson, A., Gallagher, C., Skinner, J.A., Kereszturi, Á., Platz, T., 2018. Grid-mapping the northern plains of Mars: using morphotype and distribution of ice-related landforms to understand multiple ice-rich deposits in Utopia Planitia. J. Geophys. Res. Planets. https://doi.org/10.1029/2018JE005665

Selvans, M.M., Plaut, J.J., Aharonson, O., Safaeinili, A., 2010. Internal structure of Planum Boreum, from Mars advanced radar for subsurface and ionospheric sounding data. J Geophys Res 115, doi:10.1029/2009JE003537. https://doi.org/10.1029/2009je003537

Senthil Kumar, P., Keerthi, V., Senthil Kumar, A., Mustard, J., Gopala Krishna, B., Amitabh, Ostrach, L.R., Kring, David.A., Kiran Kumar, A.S., Goswami, J.N., 2013. Gullies and landslides on the Moon: Evidence for dry-granular flows. J. Geophys. Res. Planets 118, 206–223. https://doi.org/10.1002/jgre.20043

Senthil Kumar, P., Krishna, N., Prasanna Lakshmi, K.J., Raghukanth, S.T.G., Dhabu, A., Platz, T., 2019. Recent seismicity in Valles Marineris, Mars: Insights from young faults, landslides, boulder falls and possible mud volcanoes. Earth Planet. Sci. Lett. 505, 51–64. https://doi.org/10.1016/j.epsl.2018.10.008

Senthil Kumar, P., Sruthi, U., Krishna, N., Lakshmi, K.J.P., Menon, R., Amitabh, Gopala Krishna, B., Kring, D.A., Head, J.W., Goswami, J.N., Kiran Kumar, A.S., 2016. Recent shallow moonquake and impact-triggered boulder falls on the Moon: New insights from the Schrödinger basin: Recent Seismotectonics of the Moon. J. Geophys. Res. Planets. https://doi.org/10.1002/2015JE004850

Sharp, R.P., 1980. Geomorphological Processes on Terrestrial Planetary Surfaces. Annu. Rev. Earth Planet. Sci. 8, 231–261. https://doi.org/10.1146/annurev.ea.08.050180.001311

Shelef, E., Hilley, G.E., 2016. A Unified Framework for Modeling Landscape Evolution by Discrete Flows: LANDSCAPE FORMATION BY DISCRETE FLOWS. J. Geophys. Res. Earth Surf. https://doi.org/10.1002/2015JF003693

Shi, X., Oberst, J., Willner, K., 2016. Mass wasting on Phobos triggered by an evolving tidal environment. Geophys. Res. Lett. 43. https://doi.org/10.1002/2016GL071650

Shoji, D., Imamura, S., Nakamura, M., Noguchi, R., 2019. Angle of repose of Martian wet sand using discrete element method: Implication for the seasonal cycle of recurring slope lineae(RSL) by relative humidity. https://arxiv.org/abs/1909.06144.

Sholes, S.F., Dickeson, Z.I., Montgomery, D.R., Catling, D.C., 2021. Where are Mars' Hypothesized Ocean Shorelines? Large Lateral and Topographic Offsets Between Different Versions of Paleoshoreline Maps. J. Geophys. Res. Planets 126. https://doi.org/10.1029/2020JE006486

Shugar, D.H., Jacquemart, M., Shean, D., Bhushan, S., Upadhyay, K., Sattar, A., Schwanghart, W., McBride, S., de Vries, M.V.W., Mergili, M., Emmer, A., Deschamps-Berger, C., McDonnell, M., Bhambri, R., Allen, S., Berthier, E., Carrivick, J.L., Clague, J.J., Dokukin, M., Dunning, S.A., Frey, H., Gascoin, S., Haritashya, U.K., Huggel, C., Kääb, A., Kargel, J.S., Kavanaugh, J.L., Lacroix, P., Petley, D., Rupper, S., Azam, M.F., Cook, S.J., Dimri, A.P., Eriksson, M., Farinotti, D., Fiddes, J., Gnyawali, K.R., Harrison, S., Jha, M., Koppes, M., Kumar, A., Leinss, S., Majeed, U., Mal, S., Muhuri, A., Noetzli, J., Paul, F., Rashid, I., Sain, K., Steiner, J., Ugalde, F., Watson, C.S., Westoby, M.J., 2021. A massive rock and ice avalanche caused the 2021 disaster at Chamoli, Indian Himalaya. Science 373, 300–306. https://doi.org/10.1126/science.abh4455

Singer, K.N., McKinnon, W.B., Schenk, P.M., Moore, J.M., 2012. Massive ice avalanches on Iapetus mobilized by friction reduction during flash heating. Nat. Geosci. 5, 574–578. https://doi.org/10.1038/ngeo1526

Sinha, R.K., Ray, D., de Haas, T., Conway, Susan J., 2020. Global documentation of overlapping lobate deposits in Martian gullies. Icarus in review.

Sinha, R.K., Sivaprahasam, V., Shukla, A.D., Das, P., Bhattacharya, F., 2018. Gullies and Debris-flows in Ladakh Himalaya, India: a potential Martian analogue. Geol. Soc. Lond. Spec. Publ. accepted.

Sizemore, H.G., Zent, A.P., Rempel, A.W., 2015. Initiation and Growth of Martian Ice Lenses. Icarus 251, 191–210. https://doi.org/10.1016/j.icarus.2014.04.013

Skinner, J.A., Mazzini, A., 2009. Martian mud volcanism: Terrestrial analogs and implications for formational scenarios. Mar. Pet. Geol. 26, 1866–1878. https://doi.org/10.1016/j.marpetgeo.2009.02.006

Skinner, J.A., Tanaka, K.L., 2007. Evidence for and implications of sedimentary diapirism and mud volcanism in the southern Utopia highland–lowland boundary plain, Mars. Icarus 186, 41–59. https://doi.org/10.1016/j.icarus.2006.08.013

Skjetne, H.L., Singer, K.N., Hynek, B.M., Knight, K.I., Schenk, P.M., Olkin, C.B., White, O.L., Bertrand, T., Runyon, K.D., McKinnon, W.B., Moore, J.M., Stern, S.A., Weaver, H.A., Young, L.A., Ennico, K., 2021. Morphological comparison of blocks in chaos terrains on Pluto, Europa, and Mars. Icarus 356, 113866. https://doi.org/10.1016/j.icarus.2020.113866

Smith, D.E., Zuber, M.T., Neumann, G.A., 2001. Seasonal Variations of Snow Depth on Mars. Science 294, 2141–2146. https://doi.org/10.1126/science.1066556

Smith, I.B., Holt, J.W., 2010. Onset and migration of spiral troughs on Mars revealed by orbital radar. Nature 465, 450–453.

Smith, I.B., Holt, J.W., Spiga, A., Howard, A.D., Parker, G., 2013. The spiral troughs of Mars as cyclic steps: THE SPIRAL TROUGHS OF MARS. J. Geophys. Res. Planets 118, 1835–1857. https://doi.org/10.1002/jgre.20142

Smith, M.D., 2002. The annual cycle of water vapor on Mars as observed by the Thermal Emission Spectrometer. J Geophys Res 107, 5115. https://doi.org/10.1029/2001je001522

Smith, M.L., Claire, M.W., Catling, D.C., Zahnle, K.J., 2014. The formation of sulfate, nitrate and perchlorate salts in the martian atmosphere. Icarus 231, 51–64. https://doi.org/10.1016/j.icarus.2013.11.031

Soare, R.J., Burr, D.M., Wan Bun Tseung, J.M., 2005. Possible pingos and a periglacial landscape in northwest Utopia Planitia. Icarus 174, 373–382. https://doi.org/10.1016/j.icarus.2004.11.013

Soare, R.J., Conway, S.J., Dohm, J.M., 2014a. Possible ice-wedge polygons and recent landscape modification by “wet” periglacial processes in and around the Argyre impact basin, Mars. Icarus 233, 214–228. https://doi.org/10.1016/j.icarus.2014.01.034

Soare, R.J., Conway, S.J., Dohm, J.M., El-Maarry, M.R., 2014b. Possible open-system (hydraulic) pingos in and around the Argyre impact region of Mars. Earth Planet. Sci. Lett. 398, 25–36. https://doi.org/10.1016/j.epsl.2014.04.044

Soare, R.J., Conway, S.J., Gallagher, C., Dohm, J.M., 2016. Sorted (clastic) polygons in the Argyre region, Mars, and possible evidence of pre- and post-glacial periglaciation in the Late Amazonian Epoch. Icarus 264, 184–197. https://doi.org/10.1016/j.icarus.2015.09.019

Soare, R.J., Conway, S.J., Gallagher, C., Dohm, J.M., Reiss, D., 2018a. Periglacial complexes and the deductive evidence of “wet”-flows at the Hale impact-crater, Mars. Geol. Soc. Lond. Spec. Publ. 467. https://doi.org/10.1144/SP467.7

Soare, R.J., Conway, S.J., Gallagher, C.J., Williams, J.-P., Osinski, G.R., 2018b. Paleo-Periglacial and “Ice-Rich” Complexes in Utopia Planitia, in: Dynamic Mars. Elsevier, pp. 209–237. https://doi.org/10.1016/B978-0-12-813018-6.00007-8

Soare, R.J., Conway, S.J., Pearce, G.D., Costard, F., Séjourné, A., 2013a. Sub-kilometre (intra-crater) mounds in Utopia Planitia, Mars: character, occurrence and possible formation hypotheses. Mars Polar Sci. V 225, 982–991. https://doi.org/10.1016/j.icarus.2012.06.003

Soare, R.J., Conway, S.J., Pearce, G.D., Dohm, J.M., Grindrod, P.M., 2013b. Possible crater-based pingos, paleolakes and periglacial landscapes at the high latitudes of Utopia Planitia, Mars. Mars Polar Sci. V 225, 971–981. https://doi.org/10.1016/j.icarus.2012.08.041

Soare, R. J., Conway, S.J., Williams, J.-P., Hepburn, A.J., 2021a. Possible polyphase periglaciation and glaciation adjacent to the Moreux impact-crater, Mars. Icarus 362, 114401. https://doi.org/10.1016/j.icarus.2021.114401

Soare, R.J., Conway, S.J., Williams, J.-P., Philippe, M., Mc Keown, L.E., Godin, E., Hawkswell, J., 2021. Possible ice-wedge polygonisation in Utopia Planitia, Mars and its latitudinal gradient of distribution. Icarus 358, 114208. https://doi.org/10.1016/j.icarus.2020.114208

Soare, R.J., Costard, F., Pearce, G.D., Séjourné, A., 2012. A re-interpretation of the recent stratigraphical history of Utopia Planitia, Mars: Implications for late-Amazonian periglacial and ice-rich terrain. Planet. Space Sci. 60, 131–139. https://doi.org/10.1016/j.pss.2011.07.007

Soare, R.J., Horgan, B., Conway, S.J., Souness, C., El-Maarry, M.R., 2015. Volcanic terrain and the possible periglacial formation of “excess ice” at the mid-latitudes of Utopia Planitia, Mars. Earth Planet. Sci. Lett. 423, 182–192. https://doi.org/10.1016/j.epsl.2015.04.033

Soare, R.J., Kargel, J.S., Osinski, G.R., Costard, F., 2007. Thermokarst processes and the origin of crater-rim gullies in Utopia and western Elysium Planitia. Icarus 191, 95–112.

Soare, R.J., Osinski, G.R., Roehm, C.L., 2008. Thermokarst lakes and ponds on Mars in the very recent (late Amazonian) past. Earth Planet. Sci. Lett. 272, 382–393. https://doi.org/10.1016/j.epsl.2008.05.010

Soare, R.J., Séjourné, A., Pearce, G., Costard, F., Osinski, G.R., 2011. The Tuktoyaktuk Coastlands of northern Canada: A possible “wet” periglacial analog of Utopia Planitia, Mars. Geol. Soc. Am. Spec. Pap. 483, 203–218. https://doi.org/10.1130/2011.2483(13)

Soare, R. J., Williams, J.-P., Conway, S.J., El-Maarry, M.R., 2021b. Chapter 14 - Pingo-like mounds and possible polyphase periglaciation/glaciation at/adjacent to the Moreux impact crater, in: Soare, Richard J., Conway, S.J., Williams, J.-P., Oehler, D.Z. (Eds.), Mars Geological Enigmas. Elsevier, pp. 407–435. https://doi.org/10.1016/B978-0-12-820245-6.00014-8

Soderblom, L.A., 1970. A model for small-impact erosion applied to the lunar surface. J. Geophys. Res. 75, 2655–2661. https://doi.org/10.1029/JB075i014p02655

Sori, M.M., Bapst, J., Becerra, P., Byrne, S., 2019. Islands of ice on Mars and Pluto. J. Geophys. Res. Planets 124, 2522–2542. https://doi.org/10.1029/2018JE005861

Sosio, R., Crosta, G.B., Chen, J.H., Hungr, O., 2012. Modelling rock avalanche propagation onto glaciers. Quat. Sci. Rev. 47, 23–40. https://doi.org/10.1016/j.quascirev.2012.05.010

Spudis, P.D., Bussey, D.B.J., Baloga, S.M., Cahill, J.T.S., Glaze, L.S., Patterson, G.W., Raney, R.K., Thompson, T.W., Thomson, B.J., Ustinov, E.A., 2013. Evidence for water ice on the moon: results for anomalous polar craters from the LRO Mini-RF imaging radar. J. Geophys. Res. Planets 118, doi: 10.1002/jgre.20156. https://doi.org/10.1002/jgre.20156

Stack, K.M., Grotzinger, J.P., Kah, L.C., Schmidt, M.E., Mangold, N., Edgett, K.S., Sumner, D.Y., Siebach, K.L., Nachon, M., Lee, R., Blaney, D.L., Deflores, L.P., Edgar, L.A., Fairén, A.G., Leshin, L.A., Maurice, S., Oehler, D.Z., Rice, M.S., Wiens, R.C., 2014. Diagenetic origin of nodules in the Sheepbed member, Yellowknife Bay formation, Gale crater, Mars: Diagenetic Nodules in Gale Crater. J. Geophys. Res. Planets 119, 1637–1664. https://doi.org/10.1002/2014JE004617

Stamenkovic, V., Mischna, M., Lanza, N., Grimm, R.E., Mustard, J.F., Orphan, V., Rogers, K., Zacny, K., Sherwood Lollar, B., Menez, B., Spohn, T., Plesa, A.-C., Michalski, J., Osburn, M., 2020. Probing the Modern-Day Martian Subsurface Habitability with VALKYRIE, in: Lunar and Planetary Science Conference. p. 1812.

Steakley, K., Murphy, J., Kahre, M., Haberle, R., Kling, A., 2019. Testing the impact heating hypothesis for early Mars with a 3-D global climate model. Icarus 330, 169–188. https://doi.org/10.1016/j.icarus.2019.04.005

Stein, N., Grotzinger, J.P., Schieber, J., Mangold, N., Hallet, B., Newsom, H., Stack, K.M., Berger, J.A., Thompson, L., Siebach, K.L., Cousin, A., Le Mouélic, S., Minitti, M., Sumner, D.Y., Fedo, C., House, C.H., Gupta, S., Vasavada, A.R., Gellert, R., Wiens, R.C., Frydenvang, J., Forni, O., Meslin, P.Y., Payré, V., Dehouck, E., 2018. Desiccation cracks provide evidence of lake drying on Mars, Sutton Island member, Murray formation, Gale Crater. Geology 46, 515–518. https://doi.org/10.1130/G40005.1

Stern, S.A., Binzel, R.P., Earle, A.M., Singer, K.N., Young, L.A., Weaver, H.A., Olkin, C.B., Ennico, K., Moore, J.M., McKinnon, W.B., Spencer, J.R., 2017. Past epochs of significantly higher pressure atmospheres on Pluto. Icarus 287, 47–53. https://doi.org/10.1016/j.icarus.2016.11.022

Stillman, D.E., Bue, B.D., Wagstaff, K.L., Primm, K.M., Michaels, T.I., Grimm, R.E., 2020. Evaluation of wet and dry recurring slope lineae (RSL) formation mechanisms based on quantitative mapping of RSL in Garni Crater, Valles Marineris, Mars. Icarus 335, 113420. https://doi.org/10.1016/j.icarus.2019.113420

Stillman, D.E., Grimm, R.E., 2018. Two pulses of seasonal activity in martian southern mid-latitude recurring slope lineae (RSL). Icarus 302, 126–133. https://doi.org/10.1016/j.icarus.2017.10.026

Stillman, D.E., Grimm, R.E., 2011. Radar penetrates only the youngest geological units on Mars. J. Geophys. Res. 116. https://doi.org/10.1029/2010JE003661

Stillman, D.E., Michaels, T.I., Grimm, R.E., 2017. Characteristics of the numerous and widespread recurring slope lineae (RSL) in Valles Marineris, Mars. Icarus 285, 195–210. https://doi.org/10.1016/j.icarus.2016.10.025

Stillman, D.E., Michaels, T.I., Grimm, R.E., Hanley, J., 2016. Observations and modeling of northern mid-latitude recurring slope lineae (RSL) suggest recharge by a present-day martian briny aquifer. Icarus 265, 125–138. https://doi.org/10.1016/j.icarus.2015.10.007

Stillman, D.E., Michaels, T.I., Grimm, R.E., Harrison, K.P., 2014. New observations of martian southern mid-latitude recurring slope lineae (RSL) imply formation by freshwater subsurface flows. Icarus 233, 328–341. https://doi.org/10.1016/j.icarus.2014.01.017

Stuart-Alexander, D.E., Howard, K.A., 1970. Lunar Maria and circular basins—a review. Icarus 12, 440–456. https://doi.org/10.1016/0019-1035(70)90013-8

Stuurman, C.M., Osinski, G.R., Holt, J.W., Levy, J.S., Brothers, T.C., Kerrigan, M., Campbell, B.A., 2016. SHARAD detection and characterization of subsurface water ice deposits in Utopia Planitia, Mars: SHARAD DETECTION OF ICE UTOPIA PLANITIA. Geophys. Res. Lett. 43, 9484–9491. https://doi.org/10.1002/2016GL070138

Sullivan, R., Kok, J.F., Katra, I., Yizhaq, H., 2020. A Broad Continuum of Aeolian Impact Ripple Morphologies on Mars is Enabled by Low Wind Dynamic Pressures. J. Geophys. Res. Planets 125. https://doi.org/10.1029/2020JE006485

Sullivan, R., Thomas, P., Veverka, J., Malin, M., Edgett, K.S., 2001. Mass movement slope streaks imaged by the Mars Orbiter Camera. J Geophys Res-Planets 106, 23607–23633.

Sutter, B., Quinn, R.C., Archer, P.D., Glavin, D.P., Glotch, T.D., Kounaves, S.P., Osterloo, M.M., Rampe, E.B., Ming, D.W., 2017. Measurements of Oxychlorine species on Mars. Int. J. Astrobiol. 16, 203–217. https://doi.org/10.1017/S1473550416000057

Svitek, T., Murray, B., 1990. Winter frost at Viking Lander 2 site. J. Geophys. Res. 95, 1495. https://doi.org/10.1029/JB095iB02p01495

Swanson, D., Nolan, M., 2018. Growth of Retrogressive Thaw Slumps in the Noatak Valley, Alaska, 2010–2016, Measured by Airborne Photogrammetry. Remote Sens. 10, 983. https://doi.org/10.3390/rs10070983

Sylvest, M.E., Conway, S.J., Patel, M.R., Dixon, J.C., Barnes, A., 2016. Mass wasting triggered by seasonal CO_2 sublimation under Martian atmospheric conditions: Laboratory experiments. Geophys. Res. Lett. 43, 12,363-12,370. https://doi.org/10.1002/2016GL071022

Sylvest, M.E., Dixon, J.C., Conway, S.J., Patel, M.R., McElwaine, J.N., Hagermann, A., Barnes, A., 2019. CO_2sublimation in martian gullies: laboratory experiments at varied slope angle and regolith grain sizes. Geol. Soc. Lond. Spec. Publ. Martian Gullies and their Earth Analogues. https://doi.org/10.1144/SP467.11

Tanaka, K.L., Skinner Jr, J.A., Hare, T.M., 2005. Geologic map of the northern plains of Mars.

Tao, Y., Douté, S., Muller, J.-P., Conway, S.J., Thomas, N., Cremonese, G., 2021a. Ultra-High-Resolution 1 m/pixel CaSSIS DTM Using Super-Resolution Restoration and Shape-from-Shading: Demonstration over Oxia Planum on Mars. Remote Sens. 13, 2185. https://doi.org/10.3390/rs13112185

Tao, Y., Michael, G., Muller, J.-P., Conway, S.J., Putri, A.R.D., 2021b. Seamless 3D Image Mapping and Mosaicing of Valles Marineris on Mars Using Orbital HRSC Stereo and Panchromatic Images. Remote Sens. 13, 1385. https://doi.org/10.3390/rs13071385

Tao, Y., Muller, J.-P., Xiong, S., Conway, S.J., 2021c. MADNet 2.0: Pixel-Scale Topography Retrieval from Single-View Orbital Imagery of Mars Using Deep Learning. Remote Sens. 13, 4220. https://doi.org/10.3390/rs13214220

Tao, Y., Xiong, S., Conway, S.J., Muller, J.-P., Guimpier, A., Fawdon, P., Thomas, N., Cremonese, G., 2021d. Rapid Single Image-Based DTM Estimation from ExoMars TGO CaSSIS Images Using Generative Adversarial U-Nets. Remote Sens. 13, 2877. https://doi.org/10.3390/rs13152877

Tebolt, M., Levy, J., Goudge, T., Schorghofer, N., 2020. Slope, elevation, and thermal inertia trends of martian recurring slope lineae initiation and termination points: Multiple possible processes occurring on coarse, sandy slopes. Icarus 338, 113536. https://doi.org/10.1016/j.icarus.2019.113536

Telfer, M.W., Parteli, E.J.R., Radebaugh, J., Beyer, R.A., Bertrand, T., Forget, F., Nimmo, F., Grundy, W.M., Moore, J.M., Stern, S.A., Spencer, J., Lauer, T.R., Earle, A.M., Binzel, R.P., Weaver, H.A., Olkin, C.B., Young, L.A., Ennico, K., Runyon, K., The New Horizons Geology, Geophysics and Imaging Science Theme Team, Buie, M., Buratti, B., Cheng, A., Kavelaars, J.J., Linscott, I.,

McKinnon, W.B., Reitsema, H., Reuter, D., Schenk, P., Showalter, M., Tyler, L., 2018. Dunes on Pluto. Science 360, 992–997. https://doi.org/10.1126/science.aao2975

Teodoro, L., Davila, A., Elphic, R.C., Hamilton, D., McKay, C., Quinn, R., 2018. Habitability and Biomarker Preservation in the Martian Near-Surface Radiation Environment, in: From Habitability to Life on Mars. Elsevier, pp. 211–231. https://doi.org/10.1016/B978-0-12-809935-3.00012-8

Tesson, P.-A., Conway, S.J., Mangold, N., Ciazela, J., Lewis, S.R., Mège, D., 2020. Evidence for thermal-stress-induced rockfalls on Mars impact crater slopes. Icarus 342, 113503. https://doi.org/10.1016/j.icarus.2019.113503

Thapa, P., Martin, Y.E., Johnson, E.A., 2017. Quantification of controls on regional rockfall activity and talus deposition, Kananaskis, Canadian Rockies. Geomorphology 299, 107–123. https://doi.org/10.1016/j.geomorph.2017.09.039

Thomas, M.F., McEwen, A.S., Dundas, C.M., 2020. Present-day mass wasting in sulfate-rich sediments in the equatorial regions of Mars. Icarus 342, 113566. https://doi.org/10.1016/j.icarus.2019.113566

Thomas, N., Davidsson, B., El-Maarry, M.R., Fornasier, S., Giacomini, L., Gracia-Berná, A.G., Hviid, S.F., Ip, W.-H., Jorda, L., Keller, H.U., Knollenberg, J., Kührt, E., La Forgia, F., Lai, I.L., Liao, Y., Marschall, R., Massironi, M., Mottola, S., Pajola, M., Poch, O., Pommerol, A., Preusker, F., Scholten, F., Su, C.C., Wu, J.S., Vincent, J.-B., Sierks, H., Barbieri, C., Lamy, P.L., Rodrigo, R., Koschny, D., Rickman, H., A'Hearn, M.F., Barucci, M.A., Bertaux, J.-L., Bertini, I., Cremonese, G., Da Deppo, V., Debei, S., de Cecco, M., Fulle, M., Groussin, O., Gutierrez, P.J., Kramm, J.-R., Küppers, M., Lara, L.M., Lazzarin, M., Lopez Moreno, J.J., Marzari, F., Michalik, H., Naletto, G., Agarwal, J., Güttler, C., Oklay, N., Tubiana, C., 2015. Redistribution of particles across the nucleus of comet 67P/Churyumov-Gerasimenko. Astron. Astrophys. 583, A17. https://doi.org/10.1051/0004-6361/201526049

Thomas, N., Portyankina, G., Hansen, C.J., Pommerol, A., 2011. HiRISE observations of gas sublimation-driven activity in Mars' southern polar regions: IV. Fluid dynamics models of CO2 jets. Icarus 212, 66–85. https://doi.org/10.1016/j.icarus.2010.12.016

Thomas, P., Gierasch, P.J., 1985. Dust Devils on Mars. Science 230, 175–177. https://doi.org/10.1126/science.230.4722.175

Thomas, P.C., James, P.B., Calvin, W.M., Haberle, R., Malin, M.C., 2009. Residual south polar cap of Mars: Stratigraphy, history, and implications of recent changes. Icarus 203, 352–375. https://doi.org/10.1016/j.icarus.2009.05.014

Thomas, R.J., Hynek, B.M., Rothery, D.A., Conway, S.J., 2016. Mercury's low-reflectance material: Constraints from hollows. Icarus 277, 455–465. https://doi.org/10.1016/j.icarus.2016.05.036

Thomas, R.J., Rothery, D.A., Conway, S.J., Anand, M., 2014a. Long-lived explosive volcanism on Mercury. Geophys. Res. Lett. 41, 6084–6092. https://doi.org/10.1002/2014GL061224

Thomas, R.J., Rothery, D.A., Conway, S.J., Anand, M., 2014b. Hollows on Mercury: Materials and mechanisms involved in their formation. Icarus 229, 221–235. https://doi.org/10.1016/j.icarus.2013.11.018

Thomas, R.J., Rothery, D.A., Conway, S.J., Anand, M., 2014c. Mechanisms of explosive volcanism on Mercury: Implications from its global distribution and morphology: Explosive volcanism on Mercury. J. Geophys. Res. Planets 119, 2239–2254. https://doi.org/10.1002/2014JE004692

Thomson, B.J., Bridges, N.T., Greeley, R., 2008. Rock abrasion features in the Columbia Hills, Mars. J. Geophys. Res. 113, E08010. https://doi.org/10.1029/2007JE003018

Tomasko, M.G., Archinal, B., Becker, T., Bézard, B., Bushroe, M., Combes, M., Cook, D., Coustenis, A., de Bergh, C., Dafoe, L.E., Doose, L., Douté, S., Eibl, A., Engel, S., Gliem, F., Grieger, B., Holso, K., Howington-Kraus, E., Karkoschka, E., Keller, H.U., Kirk, R., Kramm, R., Küppers, M., Lanagan, P., Lellouch, E., Lemmon, M., Lunine, J., McFarlane, E., Moores, J., Prout, G.M., Rizk, B., Rosiek, M., Rueffer, P., Schröder, S.E., Schmitt, B., See, C., Smith, P., Soderblom, L., Thomas, N., West, R., 2005. Rain, winds and haze during the Huygens probe's descent to Titan's surface. Nature 438, 765–778. https://doi.org/10.1038/nature04126

Toner, J.D., Catling, D.C., Light, B., 2014a. The formation of supercooled brines, viscous liquids, and low-temperature perchlorate glasses in aqueous solutions relevant to Mars. Icarus 233, 36–47. https://doi.org/10.1016/j.icarus.2014.01.018

Toner, J.D., Catling, D.C., Light, B., 2014b. Soluble salts at the Phoenix Lander site, Mars: A reanalysis of the Wet Chemistry Laboratory data. Geochim. Cosmochim. Acta 136, 142–168. https://doi.org/10.1016/j.gca.2014.03.030

Tornabene, L.L., Osinski, G.R., McEwen, A.S., Boyce, J.M., Bray, V.J., Caudill, C.M., Grant, J.A., Hamilton, C.W., Mattson, S., Mouginis-Mark, P.J., 2012. Widespread crater-related pitted materials on Mars: Further evidence for the role of target volatiles during the impact process. Icarus 220, 348–368. https://doi.org/10.1016/j.icarus.2012.05.022

Treiman, A.H., 2003. Geologic settings of Martian gullies: Implications for their origins. J. Geophys. Res. Planets 108, doi:10.1029/2002JE001900. https://doi.org/10.1029/2002JE001900

Turner, S.M.R., Bridges, J.C., Grebby, S., Ehlmann, B.L., 2016. Hydrothermal Activity Recorded in Post Noachian-aged Impact Craters on Mars: Post-Noachian Impact Craters. J. Geophys. Res. Planets. https://doi.org/10.1002/2015JE004989

Ulrich, M., Hauber, E., Herzschuh, U., Härtel, S., Schirrmeister, L., 2011. Polygon pattern geomorphometry on Svalbard (Norway) and western Utopia Planitia (Mars) using high-resolution stereo remote-sensing data. Geomorphology 134, 197–216. https://doi.org/10.1016/j.geomorph.2011.07.002

Ulrich, M., Morgenstern, A., Günther, F., Reiss, D., Bauch, K.E., Hauber, E., Rössler, S., Schirrmeister, L., 2010. Thermokarst in Siberian ice-rich permafrost: Comparison to asymmetric scalloped depressions on Mars. J Geophys Res 115, doi:10.1029/2010JE003640. https://doi.org/10.1029/2010je003640

Vago, J.L., Westall, F., Pasteur Instrument Teams, Landing S, Coates, A.J., Jaumann, R., Korablev, O., Ciarletti, V., Mitrofanov, I., Josset, J.-L., De Sanctis, M.C., Bibring, J.-P., Rull, F., Goesmann, F., Steininger, H., Goetz, W., Brinckerhoff, W., Szopa, C., Raulin, F., Westall, F., Edwards, H.G.M., Whyte, L.G., Fairén, A.G., Bibring, J.-P., Bridges, J., Hauber, E., Ori, G.G., Werner, S., Loizeau, D., Kuzmin, R.O., Williams, R.M.E., Flahaut, J., Forget, F., Vago, J.L., Rodionov, D., Korablev, O., Svedhem, H., Sefton-Nash, E., Kminek, G., Lorenzoni, L., Joudrier, L., Mikhailov, V., Zashchirinskiy, A., Alexashkin, S., Calantropio, F., Merlo, A., Poulakis, P., Witasse, O., Bayle, O., Bayón, S., Meierhenrich, U., Carter, J., García-Ruiz, J.M., Baglioni, P., Haldemann, A., Ball, A.J., Debus, A., Lindner, R., Haessig, F., Monteiro, D., Trautner, R., Voland, C., Rebeyre, P., Goulty, D., Didot, F., Durrant, S., Zekri, E., Koschny, D., Toni, A., Visentin, G., Zwick, M., van Winnendael, M., Azkarate, M., Carreau, C., the ExoMars Project Team, 2017. Habitability on Early Mars and the Search for Biosignatures with the ExoMars Rover. Astrobiology 17, 471–510. https://doi.org/10.1089/ast.2016.1533

van den Broeke, M.R., Bintanja, R., 1995. Summertime atmospheric circulation in the vicinity of a blue ice area in Queen Maud Land, Antarctica. Bound.-Layer Meteorol. 72, 411–438. https://doi.org/10.1007/BF00709002

Veeder, G.J., Davies, A.G., Matson, D.L., Johnson, T.V., 2009. Io: Heat flow from dark volcanic fields. Icarus 204, 239–253. https://doi.org/10.1016/j.icarus.2009.06.027

Vijayan, S., Harish, Kimi, K., Tuhi, S., Vigneshwaran, K., Sinha, R., Conway, S.J., Sivaraman, B., Bhardwaj, A., 2021. Boulder Fall Ejecta: Present day activity on Mars. Geophys. Res. Lett. Accepted.

Vijayan, S., Sinha, R.K., 2017. Amazonian fluvial outflow channels in Jovis Tholus region, Mars: FLUVIAL CHANNELS IN JOVIS THOLUS REGION. J. Geophys. Res. Planets 122, 927–949. https://doi.org/10.1002/2016JE005237

Vincendon, M., 2015. Identification of Mars gully activity types associated with ice composition. J. Geophys. Res. Planets 120, 1859–1879. https://doi.org/10.1002/2015JE004909

Vincendon, M., Audouard, J., Altieri, F., Ody, A., 2015. Mars Express measurements of surface albedo changes over 2004–2010. Icarus 251, 145–163. https://doi.org/10.1016/j.icarus.2014.10.029

Vincendon, M., Forget, F., Mustard, J., 2010a. Water ice at low to midlatitudes on Mars. J Geophys Res 115, doi:10.1029/2010JE003584. https://doi.org/10.1029/2010je003584

Vincendon, M., Mustard, J., Forget, F., Kreslavsky, M., Spiga, A., Murchie, S., Bibring, J.-P., 2010b. Near-tropical subsurface ice on Mars. Geophys. Res. Lett. 37. https://doi.org/10.1029/2009gl041426

Vincendon, M., Pilorget, C., Carter, J., Stcherbinine, A., 2019. Observational evidence for a dry dust-wind origin of Mars seasonal dark flows. Icarus 325, 115–127. https://doi.org/10.1016/j.icarus.2019.02.024

Vincent, J.-B., Bodewits, D., Besse, S., Sierks, H., Barbieri, C., Lamy, P., Rodrigo, R., Koschny, D., Rickman, H., Keller, H.U., Agarwal, J., A'Hearn, M.F., Auger, A.-T., Barucci, M.A., Bertaux, J.-L., Bertini, I., Capanna, C., Cremonese, G., Da Deppo, V., Davidsson, B., Debei, S., De Cecco, M., El-Maarry, M.R., Ferri, F., Fornasier, S., Fulle, M., Gaskell, R., Giacomini, L., Groussin, O., Guilbert-Lepoutre, A., Gutierrez-Marques, P., Gutierrez, P.J., Guttler, C., Hoekzema, N., Hofner, S., Hviid, S.F., Ip, W.-H., Jorda, L., Knollenberg, J., Kovacs, G., Kramm, R., Kuhrt, E., Kuppers, M., La Forgia, F., Lara, L.M., Lazzarin, M., Lee, V., Leyrat, C., Lin, Z.-Y., Lopez Moreno, J.J., Lowry, S., Magrin, S., Maquet, L., Marchi, S., Marzari, F., Massironi, M., Michalik, H., Moissl, R., Mottola, S., Naletto, G., Oklay, N., Pajola, M., Preusker, F., Scholten, F., Thomas, N., Toth, I., Tubiana, C., 2015. Large heterogeneities in comet 67P as revealed by active pits from sinkhole collapse. Nature 523, 63–66. https://doi.org/10.1038/nature14564

Vincent, J.-B., Oklay, N., Pajola, M., Höfner, S., Sierks, H., Hu, X., Barbieri, C., Lamy, P.L., Rodrigo, R., Koschny, D., Rickman, H., Keller, H.U., A'Hearn, M.F., Barucci, M.A., Bertaux, J.-L., Bertini, I., Besse, S., Bodewits, D., Cremonese, G., Da Deppo, V., Davidsson, B., Debei, S., De Cecco, M., El-Maarry, M.R., Fornasier, S., Fulle, M., Groussin, O., Gutiérrez, P.J., Gutiérrez-Marquez, P., Güttler, C., Hofmann, M., Hviid, S.F., Ip, W.-H., Jorda, L., Knollenberg, J., Kovacs, G., Kramm, J.-R., Kührt, E., Küppers, M., Lara, L.M., Lazzarin, M., Lin, Z.-Y., Lopez Moreno, J.J., Lowry, S., Marzari, F., Massironi, M., Moreno, F., Mottola, S., Naletto, G., Preusker, F., Scholten, F., Shi, X., Thomas, N., Toth, I., Tubiana, C., 2016. Are fractured cliffs the source of cometary dust jets? Insights from OSIRIS/Rosetta at 67P/Churyumov-Gerasimenko. Astron. Astrophys. 587, A14. https://doi.org/10.1051/0004-6361/201527159

Viola, D., 2021. Chapter 15 - Thermokarst-like depressions on Mars: age constraints on ice degradation in Utopia Planitia, in: Soare, R.J., Conway, S.J., Williams, J.-P., Oehler, D.Z. (Eds.), Mars Geological Enigmas. Elsevier, pp. 437–472. https://doi.org/10.1016/B978-0-12-820245-6.00015-X

Viola, D., McEwen, A.S., 2018. Geomorphological Evidence for Shallow Ice in the Southern Hemisphere of Mars. J. Geophys. Res. Planets 123, 262–277. https://doi.org/10.1002/2017JE005366

Viola, D., McEwen, A.S., Dundas, C.M., Byrne, S., 2015. Expanded secondary craters in the Arcadia Planitia region, Mars: Evidence for tens of Myr-old shallow subsurface ice. Icarus 248, 190–204. https://doi.org/10.1016/j.icarus.2014.10.032

Viviano, C.E., Moersch, J.E., McSween, H.Y., 2013. Implications for early hydrothermal environments on Mars through the spectral evidence for carbonation and chloritization reactions in the Nili Fossae region: HYDROTHERMAL ENVIRONMENTS IN NILI FOSSAE. J. Geophys. Res. Planets 118, 1858–1872. https://doi.org/10.1002/jgre.20141

Voelker, M., Hauber, E., Schulzeck, F., Jaumann, R., 2017. Grid-mapping Hellas Planitia, Mars – Insights into distribution, evolution and geomorphology of (Peri)-glacial, fluvial and lacustrine landforms in Mars' deepest basin. Planet. Space Sci. 145, 49–70. https://doi.org/10.1016/j.pss.2017.07.012

Wada, K., Barnouin-Jha, O.S., 2006. The formation of fluidized ejecta on Mars by granular flows. Meteorit. Planet. Sci. 41, 1551–1569. https://doi.org/10.1111/j.1945-5100.2006.tb00435.x

Walsh, K.J., Jawin, E.R., Ballouz, R.-L., Barnouin, O.S., Bierhaus, E.B., Connolly, H.C., Molaro, J.L., McCoy, T.J., Delbo', M., Hartzell, C.M., Pajola, M., Schwartz, S.R., Trang, D., Asphaug, E., Becker, K.J., Beddingfield, C.B., Bennett, C.A., Bottke, W.F., Burke, K.N., Clark, B.C., Daly,

M.G., DellaGiustina, D.N., Dworkin, J.P., Elder, C.M., Golish, D.R., Hildebrand, A.R., Malhotra, R., Marshall, J., Michel, P., Nolan, M.C., Perry, M.E., Rizk, B., Ryan, A., Sandford, S.A., Scheeres, D.J., Susorney, H.C.M., Thuillet, F., Lauretta, D.S., The OSIRIS-REx Team, 2019. Craters, boulders and regolith of (101955) Bennu indicative of an old and dynamic surface. Nat. Geosci. 12, 242–246. https://doi.org/10.1038/s41561-019-0326-6

Wang, A., Ling, Z., Yan, Y., McEwen, A.S., Mellon, M.T., Smith, M.D., Jolliff, B.L., Head, J., 2019. Subsurface Cl-bearing salts as potential contributors to recurring slope lineae (RSL) on Mars. Icarus 333, 464–480. https://doi.org/10.1016/j.icarus.2019.06.024

Wang, Y., Xiao, Z., Chang, Y., Cui, J., 2020. Lost Volatiles During the Formation of Hollows on Mercury. J. Geophys. Res. Planets 125. https://doi.org/10.1029/2020JE006559

Ward, W.R., 1992. Long-term orbital and spin dynamics of Mars, in: Mars. University of Arizona Press, Tucson, AZ, United States, pp. 298–320.

Ward, W.R., 1979. Present obliquity oscillations of Mars: Fourth-order accuracy in orbital *e* and *I*. J. Geophys. Res. Solid Earth 84, 237–241. https://doi.org/10.1029/JB084iB01p00237

Ward, W.R., 1974. Climatic variations on Mars: 1. Astronomical theory of insolation. J. Geophys. Res. 79, 3375–3386. https://doi.org/10.1029/JC079i024p03375

Warner, N., Gupta, S., Muller, J.-P., Kim, J.-R., Lin, S.-Y., 2009. A refined chronology of catastrophic outflow events in Ares Vallis, Mars. Earth Planet. Sci. Lett. 288, 58–69.

Watkins, J.A., Ehlmann, B.L., Yin, A., 2015. Long-runout landslides and the long-lasting effects of early water activity on Mars. Geology 43, 107–110. https://doi.org/10.1130/G36215.1

Watters, T.R., 2021. A case for limited global contraction of Mercury. Commun. Earth Environ. 2, 9. https://doi.org/10.1038/s43247-020-00076-5

Watters, T.R., Robinson, M.S., Beyer, R.A., Banks, M.E., Bell, J.F., Pritchard, M.E., Hiesinger, H., van der Bogert, C.H., Thomas, P.C., Turtle, E.P., Williams, N.R., 2010. Evidence of Recent Thrust Faulting on the Moon Revealed by the Lunar Reconnaissance Orbiter Camera. Science 329, 936–940. https://doi.org/10.1126/science.1189590

Webster, C.R., Mahaffy, P.R., Atreya, S.K., Moores, J.E., Flesch, G.J., Malespin, C., McKay, C.P., Martinez, G., Smith, C.L., Martin-Torres, J., Gomez-Elvira, J., Zorzano, M.-P., Wong, M.H., Trainer, M.G., Steele, A., Archer, D., Sutter, B., Coll, P.J., Freissinet, C., Meslin, P.-Y., Gough, R.V., House, C.H., Pavlov, A., Eigenbrode, J.L., Glavin, D.P., Pearson, J.C., Keymeulen, D., Christensen, L.E., Schwenzer, S.P., Navarro-Gonzalez, R., Pla-García, J., Rafkin, S.C.R., Vicente-Retortillo, Á., Kahanpää, H., Viudez-Moreiras, D., Smith, M.D., Harri, A.-M., Genzer, M., Hassler, D.M., Lemmon, M., Crisp, J., Sander, S.P., Zurek, R.W., Vasavada, A.R., 2018. Background levels of methane in Mars' atmosphere show strong seasonal variations. Science 360, 1093–1096. https://doi.org/10.1126/science.aaq0131

Weiss, D.K., Head, J.W., 2016. Impact ejecta-induced melting of surface ice deposits on Mars. Icarus 280, 205–233. https://doi.org/10.1016/j.icarus.2016.07.007

Weiss, D.K., Head, J.W., 2015. Crater degradation in the Noachian highlands of Mars: Assessing the hypothesis of regional snow and ice deposits on a cold and icy early Mars. Planet. Space Sci. 117, 401–420. https://doi.org/10.1016/j.pss.2015.08.009

Weiss, D.K., Head, J.W., 2014. Ejecta mobility of layered ejecta craters on Mars: Assessing the influence of snow and ice deposits. Icarus 233, 131–146. https://doi.org/10.1016/j.icarus.2014.01.038

Weiss, D.K., Head, J.W., 2013. Formation of double-layered ejecta craters on Mars: A glacial substrate model. Geophys. Res. Lett. 40, 3819–3824. https://doi.org/10.1002/grl.50778

Weiss, D.K., Head, J.W., Palumbo, A.M., Cassanelli, J.P., 2017. Extensive Amazonian-aged fluvial channels on Mars: Evaluating the role of Lyot crater in their formation: Fluvial Channel Formation by Lyot Crater. Geophys. Res. Lett. 44, 5336–5344. https://doi.org/10.1002/2017GL073821

Weitz, N., Zanetti, M., Osinski, G.R., Fastook, J.L., 2018. Modeling concentric crater fill in Utopia Planitia, Mars, with an ice flow line model. Icarus 308, 209–220. https://doi.org/10.1016/j.icarus.2017.08.023

Wells, G.L., Zimbelman, J.R., 1997. Extraterrestrial arid surface processes. Arid Zone Geomorphol. Process Form Change Drylands.

Westbrook, O.W., 2009. Crater ice deposits near the south pole of Mars (Masters). Massachusetts Institute of Technology, Cambridge, MA.

Whalley, W.B., Azizi, F., 2003. Rock glaciers and protalus landforms: Analogous forms and ice sources on Earth and Mars. J Geophys Res-Planets 108, doi:10.1029/2002JE001864.

Wheatley, D.F., Chan, M.A., Okubo, C.H., 2019. Clastic pipes and mud volcanism across Mars: Terrestrial analog evidence of past martian groundwater and subsurface fluid mobilization. Icarus 328, 141–151. https://doi.org/10.1016/j.icarus.2019.02.002

White, O.L., Umurhan, O.M., Moore, J.M., Howard, A.D., 2016. Modeling of ice pinnacle formation on Callisto: Modeling of Callisto's Pinnacle Terrain. J. Geophys. Res. Planets 121, 21–45. https://doi.org/10.1002/2015JE004846

Wilford, D.J., Sakals, M.E., Innes, J.L., Sidle, R.C., Bergerud, W.A., 2004. Recognition of debris flow, debris flood and flood hazard through watershed morphometrics. Landslides 1, 61–66. https://doi.org/10.1007/s10346-003-0002-0

Williams, K.E., Toon, O.B., Heldmann, J.L., McKay, C., Mellon, M.T., 2008. Stability of mid-latitude snowpacks on Mars. Icarus 196, 565–577. https://doi.org/10.1016/j.icarus.2008.03.017

Williams, K.E., Toon, O.B., Heldmann, J.L., Mellon, M.T., 2009. Ancient melting of mid-latitude snowpacks on Mars as a water source for gullies. Icarus 200, 418–425. https://doi.org/10.1016/j.icarus.2008.12.013

Williams, R.M.E., Grotzinger, J.P., Dietrich, W.E., Gupta, S., Sumner, D.Y., Wiens, R.C., Mangold, N., Malin, M.C., Edgett, K.S., Maurice, S., Forni, O., Gasnault, O., Ollila, A., Newsom, H.E., Dromart, G., Palucis, M.C., Yingst, R.A., Anderson, R.B., Herkenhoff, K.E., Le Mouelic, S., Goetz, W., Madsen, M.B., Koefoed, A., Jensen, J.K., Bridges, J.C., Schwenzer, S.P., Lewis, K.W., Stack, K.M., Rubin, D., Kah, L.C., Bell, J.F., Farmer, J.D., Sullivan, R., Van Beek, T., Blaney, D.L., Pariser, O., Deen, R.G., MSL Science Team, Kemppinen, O., Bridges, N., Johnson, J.R., Minitti, M., Cremers, D., Edgar, L., Godber, A., Wadhwa, M., Wellington, D., McEwan, I., Newman, C., Richardson, M., Charpentier, A., Peret, L., King, P., Blank, J., Weigle, G., Schmidt, M., Li, S., Milliken, R., Robertson, K., Sun, V., Baker, M., Edwards, C., Ehlmann, B., Farley, K., Griffes, J., Miller, H., Newcombe, M., Pilorget, C., Rice, M., Siebach, K., Stolper, E., Brunet, C., Hipkin, V., Leveille, R., Marchand, G., Sobron Sanchez, P., Favot, L., Cody, G., Steele, A., Fluckiger, L., Lees, D., Nefian, A., Martin, M., Gailhanou, M., Westall, F., Israel, G., Agard, C., Baroukh, J., Donny, C., Gaboriaud, A., Guillemot, P., Lafaille, V., Lorigny, E., Paillet, A., Perez, R., Saccoccio, M., Yana, C., Aparicio, C.A., Caride Rodriguez, J., Carrasco Blazquez, I., Gomez Gomez, F., Elvira, J.G., Hettrich, S., Lepinette Malvitte, A., Marin Jimenez, M., Frias, J.M., Soler, J.M., Torres, F.J.M., Molina Jurado, A., Sotomayor, L.M., Munoz Caro, G., Navarro Lopez, S., Gonzalez, V.P., Garcia, J.P., Rodriguez Manfredi, J.A., Planello, J.J.R., Alejandra Sans Fuentes, S., Sebastian Martinez, E., Torres Redondo, J., O'Callaghan, R.U., Zorzano Mier, M.-P., Chipera, S., Lacour, J.-L., Mauchien, P., Sirven, J.-B., Manning, H., Fairen, A., Hayes, A., Joseph, J., Squyres, S., Thomas, P., Dupont, A., Lundberg, A., Melikechi, N., Mezzacappa, A., DeMarines, J., Grinspoon, D., Reitz, G., Prats, B., Atlaskin, E., Genzer, M., Harri, A.-M., Haukka, H., Kahanpaa, H., Kauhanen, J., Paton, M., Polkko, J., Schmidt, W., Siili, T., Fabre, C., Wray, J., Wilhelm, M.B., Poitrasson, F., Patel, K., Gorevan, S., Indyk, S., Paulsen, G., Bish, D., Schieber, J., Gondet, B., Langevin, Y., Geffroy, C., Baratoux, D., Berger, G., Cros, A., Uston, C. d., Lasue, J., Lee, Q.-M., Meslin, P.-Y., Pallier, E., Parot, Y., Pinet, P., Schroder, S., Toplis, M., Lewin, E., Brunner, W., Heydari, E., Achilles, C., Oehler, D., Sutter, B., Cabane, M., Coscia, D., Szopa, C., Robert, F., Sautter, V., Nachon, M., Buch, A., Stalport, F., Coll, P., Francois, P., Raulin, F., Teinturier, S., Cameron, J., Clegg, S., Cousin, A., DeLapp, D., Dingler, R., Jackson, R.S., Johnstone, S., Lanza, N., Little, C., Nelson, T., Williams, R.B., Jones, A., Kirkland, L., Treiman, A., Baker, B., Cantor, B., Caplinger, M., Davis, S., Duston, B., Fay, D., Hardgrove, C., Harker, D., Herrera, P., Jensen, E., Kennedy, M.R., Krezoski, G., Krysak, D., Lipkaman, L., McCartney, E., McNair, S., Nixon, B., Posiolova, L., Ravine, M., Salamon, A., Saper, L., Stoiber,

K., Supulver, K., Van Beek, J., Zimdar, R., French, K.L., Iagnemma, K., Miller, K., Summons, R., Goesmann, F., Hviid, S., Johnson, M., Lefavor, M., Lyness, E., Breves, E., Dyar, M.D., Fassett, C., Blake, D.F., Bristow, T., DesMarais, D., Edwards, L., Haberle, R., Hoehler, T., Hollingsworth, J., Kahre, M., Keely, L., McKay, C., Bleacher, L., Brinckerhoff, W., Choi, D., Conrad, P., Dworkin, J.P., Eigenbrode, J., Floyd, M., Freissinet, C., Garvin, J., Glavin, D., Harpold, D., Mahaffy, P., Martin, D.K., McAdam, A., Pavlov, A., Raaen, E., Smith, M.D., Stern, J., Tan, F., Trainer, M., Meyer, M., Posner, A., Voytek, M., Anderson, R.C., Aubrey, A., Beegle, L.W., Behar, A., Brinza, D., Calef, F., Christensen, L., Crisp, J.A., DeFlores, L., Feldman, J., Feldman, S., Flesch, G., Hurowitz, J., Jun, I., Keymeulen, D., Maki, J., Mischna, M., Morookian, J.M., Parker, T., Pavri, B., Schoppers, M., Sengstacken, A., Simmonds, J.J., Spanovich, N., de la Torre Juarez, M., Vasavada, A.R., Webster, C.R., Yen, A., Archer, P.D., Cucinotta, F., Jones, J.H., Ming, D., Morris, R.V., Niles, P., Rampe, E., Nolan, T., Fisk, M., Radziemski, L., Barraclough, B., Bender, S., Berman, D., Dobrea, E.N., Tokar, R., Vaniman, D., Leshin, L., Cleghorn, T., Huntress, W., Manhes, G., Hudgins, J., Olson, T., Stewart, N., Sarrazin, P., Grant, J., Vicenzi, E., Wilson, S.A., Bullock, M., Ehresmann, B., Hamilton, V., Hassler, D., Peterson, J., Rafkin, S., Zeitlin, C., Fedosov, F., Golovin, D., Karpushkina, N., Kozyrev, A., Litvak, M., Malakhov, A., Mitrofanov, I., Mokrousov, M., Nikiforov, S., Prokhorov, V., Sanin, A., Tretyakov, V., Varenikov, A., Vostrukhin, A., Kuzmin, R., Clark, B., Wolff, M., McLennan, S., Botta, O., Drake, D., Bean, K., Lemmon, M., Lee, E.M., Sucharski, R., Hernandez, M.A. d. P., Blanco Avalos, J.J., Ramos, M., Kim, M.-H., Malespin, C., Plante, I., Muller, J.-P., Gonzalez, R.N., Ewing, R., Boynton, W., Downs, R., Fitzgibbon, M., Harshman, K., Morrison, S., Kortmann, O., Williams, A., Lugmair, G., Wilson, M.A., Jakosky, B., Zunic, T.B., Frydenvang, J., Kinch, K., Stipp, S.L.S., Boyd, N., Campbell, J.L., Gellert, R., Perrett, G., Pradler, I., VanBommel, S., Jacob, S., Owen, T., Rowland, S., Savijarvi, H., Boehm, E., Bottcher, S., Burmeister, S., Guo, J., Kohler, J., Garcia, C.M., Mellin, R.M., Schweingruber, R.W., McConnochie, T., Benna, M., Franz, H., Bower, H., Brunner, A., Blau, H., Boucher, T., Carmosino, M., Atreya, S., Elliott, H., Halleaux, D., Renno, N., Wong, M., Pepin, R., Elliott, B., Spray, J., Thompson, L., Gordon, S., Williams, J., Vasconcelos, P., Bentz, J., Nealson, K., Popa, R., Moersch, J., Tate, C., Day, M., Kocurek, G., Hallet, B., Sletten, R., Francis, R., McCullough, E., Cloutis, E., ten Kate, I.L., Arvidson, R., Fraeman, A., Scholes, D., Slavney, S., Stein, T., Ward, J., Berger, J., Moores, J.E., 2013. Martian Fluvial Conglomerates at Gale Crater. Science 340, 1068–1072. https://doi.org/10.1126/science.1237317

Williams, R.M.E., Irwin, R.P., Zimbelman, J.R., 2009. Evaluation of paleohydrologic models for terrestrial inverted channels: Implications for application to martian sinuous ridges. Geomorphology 107, 300–315. https://doi.org/10.1016/j.geomorph.2008.12.015

Williams, R.M.E., Malin, M.C., 2008. Sub-kilometer fans in Mojave Crater, Mars. Icarus 198, 365–383.

Williams, R.M.E., Phillips, R.J., 2001. Morphometric measurements of martian valley networks from Mars Orbiter Laser Altimeter (MOLA) data. J. Geophys. Res. Planets 106, 23737–23751. https://doi.org/10.1029/2000JE001409

Willmes, M., Reiss, D., Hiesinger, H., Zanetti, M., 2012. Surface age of the ice–dust mantle deposit in Malea Planum, Mars. Planet. Space Sci. 60, 199–206. https://doi.org/10.1016/j.pss.2011.08.006

Wilson, J.T., Eke, V.R., Massey, R.J., Elphic, R.C., Feldman, W.C., Maurice, S., Teodoro, L.F.A., 2018. Equatorial locations of water on Mars: Improved resolution maps based on Mars Odyssey Neutron Spectrometer data. Icarus 299, 148–160. https://doi.org/10.1016/j.icarus.2017.07.028

Wilson, L., 2004. Mars outflow channels: A reappraisal of the estimation of water flow velocities from water depths, regional slopes, and channel floor properties. J. Geophys. Res. 109, E09003. https://doi.org/10.1029/2004JE002281

Wilson, L., Head, J.W., 2002. Tharsis-radial graben systems as the surface manifestation of plume-related dike intrusion complexes: Models and implications. J. Geophys. Res. 107. https://doi.org/10.1029/2001JE001593

Wilson, S.A., Howard, A.D., Moore, J.M., Grant, J.A., 2016. A Cold-Wet Mid-Latitude Environment on Mars during the Hesperian-Amazonian Transition: Evidence from Northern Arabia Valleys and Paleolakes: A Late, Cold and Wet Climate on Mars. J. Geophys. Res. Planets. https://doi.org/10.1002/2016JE005052

Wordsworth, R., Forget, F., Millour, E., Head, J.W., Madeleine, J.-B., Charnay, B., 2013. Global modelling of the early martian climate under a denser CO2 atmosphere: Water cycle and ice evolution. Icarus 222, 1–19. https://doi.org/10.1016/j.icarus.2012.09.036

Wray, J.J., Murchie, S.L., Squyres, S.W., Seelos, F.P., Tornabene, L.L., 2009. Diverse aqueous environments on ancient Mars revealed in the southern highlands. Geology 37, 1043–1046. https://doi.org/10.1130/G30331A.1

Wright, J., Conway, S.J., Morino, C., Rothery, D.A., Balme, M.R., Fassett, C.I., 2020. Modification of Caloris ejecta blocks by long-lived mass-wasting: A volatile-driven process? Earth Planet. Sci. Lett. 549, 116519. https://doi.org/10.1016/j.epsl.2020.116519

Wright, J., Rothery, D.A., Balme, M.R., Conway, S.J., 2019. Geology of the Hokusai quadrangle (H05), Mercury. J. Maps 15, 509–520. https://doi.org/10.1080/17445647.2019.1625821

Wright, J., Rothery, D.A., Balme, M.R., Conway, S.J., 2018. Constructional Volcanic Edifices on Mercury: Candidates and Hypotheses of Formation. J. Geophys. Res. Planets 123, 952–971. https://doi.org/10.1002/2017JE005450

Wyrick, D., 2004. Distribution, morphology, and origins of Martian pit crater chains. J. Geophys. Res. 109. https://doi.org/10.1029/2004JE002240

Xiao, Z., Komatsu, G., 2013. Impact craters with ejecta flows and central pits on Mercury. Planet. Space Sci. 82–83, 62–78. https://doi.org/10.1016/j.pss.2013.03.015

Xiao, Z., Zeng, Z., Ding, N., Molaro, J., 2013. Mass wasting features on the Moon – how active is the lunar surface? Earth Planet. Sci. Lett. 376, 1–11. https://doi.org/10.1016/j.epsl.2013.06.015

Xu, W., Yu, W., Jing, S., Zhang, G., Huang, J., 2013. Debris flow susceptibility assessment by GIS and information value model in a large-scale region, Sichuan Province (China). Nat. Hazards 65, 1379–1392. https://doi.org/10.1007/s11069-012-0414-z

Yoder, C.F., Konopliv, A.S., Yuan, D.N., Standish, E.M., Folkner, W.M., 2003. Fluid Core Size of Mars from Detection of the Solar Tide. Science 300, 299–303. https://doi.org/10.1126/science.1079645

Yue, Z., Hu, W., Liu, B., Liu, Y., Sun, X., Zhao, Q., Di, K., 2014. Quantitative analysis of the morphology of martian gullies and insights into their formation. Icarus 243, 208–221. https://doi.org/10.1016/j.icarus.2014.08.028

Zanetti, M., Hiesinger, H., Reiss, D., Hauber, E., Neukum, G., 2010. Distribution and evolution of scalloped terrain in the southern hemisphere, Mars. Icarus 206, 691–706. https://doi.org/10.1016/j.icarus.2009.09.010

Zent, A.P., Fanale, F.P., Salvail, J.R., Postawko, S.E., 1986. Distribution and state of H2O in the high-latitude shallow subsurface of mars. Icarus 67, 19–36. https://doi.org/10.1016/0019-1035(86)90171-5

Zharkova, A.Yu., Kreslavsky, M.A., Head, J.W., Kokhanov, A.A., 2020. Regolith textures on Mercury: Comparison with the Moon. Icarus 351, 113945. https://doi.org/10.1016/j.icarus.2020.113945

Zimbelman, J.R., Foroutan, M., 2020. Dingo Gap: Curiosity Went Up a Small Transverse Aeolian Ridge and Came Down a Megaripple. J. Geophys. Res. Planets 125. https://doi.org/10.1029/2020JE006489